Letter from the Editors

Dear readers of the 18th issue of *Acta Naturae*,

We are delighted to see you again! As usual, this issue begins with the Forum section containing two publications. The first article continues the discussion on the significance of scientometrics and the quantitative indicators used to determine the efficiency of a research paper. This is, in our view, a very interesting, albeit ambiguous, topic, and we consider the article to be interesting for readers. The second article discusses the international workshop held in Moscow and devoted to the methods used to select data from large data arrays. Such methods are extremely important for biologists, as they take into account the increasing and endless flow of information we are witnessing. Reading this article will expose you to a lot of interesting, new facts.

The research section of the issue consists of four reviews devoted to the recent achievements and hurdles in our field of science. Two reviews (Perevozchikova *et al.*, Popova *et al.*) are devoted to the fundamental problems of molecular biology, while the other two reviews (Nikitenko *et al.*, Khandanzhinskaya *et al.*) are related to the practical application of the results of fundamental studies. The scope of questions covered is rather broad. The 18th issue also contains seven full-size research articles and a short communication (by the way, short communications are highly welcomed by the editorial board).

Now the number of manuscripts in the backlog is enough for three issues, while the number of articles received continues to increase. So, we will tighten the manuscript selection policy.

We want to close this introduction on this optimistic note.

See you in the next issue of *Acta Naturae*. ●

Sincerely, Editorial Board

Metagenomic Analysis of Dynamic Changes in the Gut Microbiome of the Participants of the MARS-500 Experiment Simulating a Long-Term Space Flight

A. V. Mardanov, M. M. Babykin, A. V. Beletsky, A. I. Grigoriev, V. V. Zinchenko, V. V. Kadnikov, M. P. Kirpichnikov, A. M. Mazur, A. V. Nedoluzhko, N. D. Novikova, E. B. Prokhorchuk, N. V. Ravin, K. G. Skryabin, S. V. Shestakov

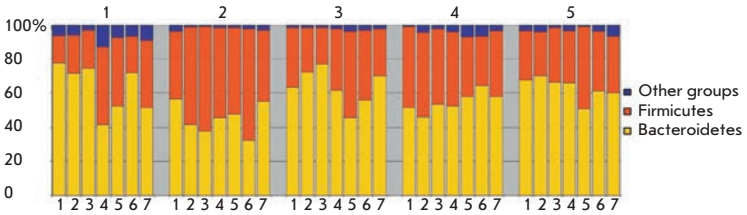

Dynamic changes in the gut microbiome of participants of the MARS-500 experiment

A metagenomic analysis of dynamic changes in the composition of intestinal microbiome of five participants of the MARS-500 experiment was carried out. The taxonomic composition of the intestinal ecosystem of each participant adaptively changed during the experiment in order to reflect the individual response to the experimental conditions. The new balanced taxonomic composition of microbiome was formed to ensure stable gene content of the community as a whole without any negative effects on participants' health.

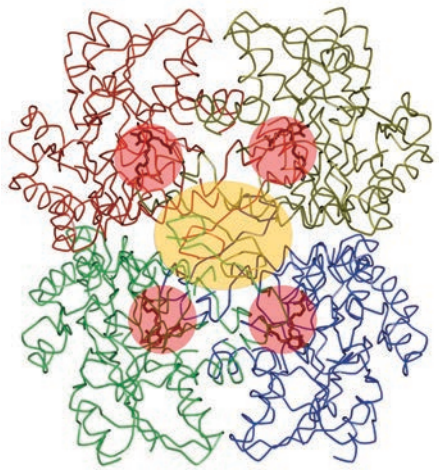

Tetramer of *C. freundii* methionine γ-lyase

Kinetic Parameters and Cytotoxic Activity of Recombinant Methionine γ-Lyase from *Clostridium tetani*, *Clostridium sporogenes*, *Porphyromonas gingivalis* and *Citrobacter freundii*

E. A. Morozova, V. V. Kulikova, D. V. Yashin, N. V. Anufrieva, N. Yu. Anisimova, S. V. Revtovich, M. I. Kotlov, Yu. F. Belyi, V. S. Pokrovsky, T. V. Demidkina

The steady-state kinetic parameters of the pyridoxal 5'-phosphate-dependent recombinant methionine γ-lyase from three pathogenic bacteria *Clostridium sporogenes*, *Clostridium tetani*, and *Porphyromonas gingivalis* were determined in β- and γ-elimination reactions. The cytotoxicity of methionine γ-lyase was evaluated using K562, PC-3, LnCap, MCF7, SKOV-3, and L5178y tumor cell lines.

Original Nerve Growth Factor Mimetic Dipeptide GK-2 Restores the Impaired Cognitive Functions in Rat Models of Alzheimer's Disease

P. Yu. Povarnina, O. N. Vorontsova, T. A. Gudasheva, R. U. Ostrovskaya, S. B. Seredenin

The mnemotropic effects of dipeptide mimetic of the nerve growth factor loop 4 (GK-2) were studied in rat models of Alzheimer's disease (AD). GK-2 is found to significantly reduce habituation deficits induced by septo-hippocampal pathway transsection. GK-2 is also shown to significantly prevent spatial memory impairments in the Morris water maze in a streptozotocin-induced model of AD.

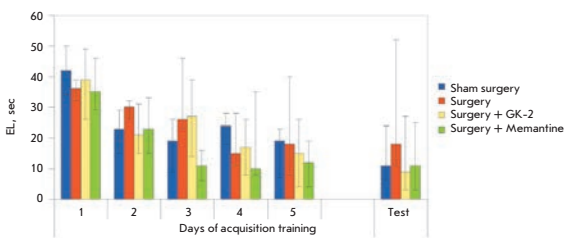

Spatial learning and skill retention test in the Morris water maze

ActaNaturae
JULY–SEPTEMBER 2013 VOL. 5 №3 (18)

Founders
Ministry of Education and
Science of the Russian Federation,
Lomonosov Moscow State University,
Park Media Ltd

Address: 119234 Moscow, Russia, Leninskiye Gory, Nauchny
Park MGU, vlad.1, stroeniye 75G.
Phone/Fax: +7 (495) 930 88 50
E-mail: vera.knorre@gmail.com, mmorozova@strf.ru,
actanaturae@gmail.com

Номер подписан в печать 17 сентября 2013 г.
Тираж 200 экз. Цена свободная.
Отпечатано в типографии «МЕДИА-ГРАНД»

CONTENTS

SHORT REPORTS

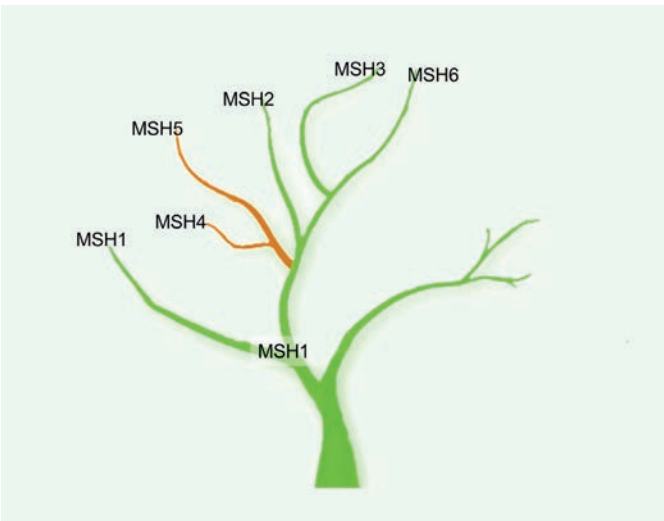

IMAGE ON THE COVER PAGE
Phylogenetic tree for the MutS family of proteins (article by Perevozchikova et al.)

Bibliometric Indicators of Russian Journals by JCR-Science Edition, 1995-2010

A.N. Libkind[1], V.A. Markusova[1], L.E. Mindeli[2]
[1]All-Russian Institute for Scientific and Technical Information, Russian Academy of Sciences, Usievicha Str., 20, Moscow, Russia, 125190
[2]Institute for the Study of Science, Russian Academy of Sciences, Butlerova Str., 12, p/o box 6, Moscow, Russia, 117485
E-mail: libkind@viniti.ru, valentina.markusova@gmail.com, L.Mindeli@issras.ru
Received 26.03.2013

ABSTRACT **A representative empirical bibliometric analysis of Russian journals included in the Journal Citation Reports-Science Edition (JCR-SE) for the time period 1995–2010 was conducted at the macro level (excluding the subject categories). It was found that the growth in the number of articles covered by JCR (a 1.8-fold increase compared to 1995) is ahead of the growth rates of Russian publications (1.2-fold increase). Hence, the share of Russian articles covered by JCR-SE was down from 2.5% in 1995 to 1.7% in 2010. It was determined that the number of articles published in an average Russian journal reduced by 20% as compared to the number of articles in an average journal of the full data set. These facts could partly shed light on the question why Russian research performance is staggering (approximately 30,000 articles per year), although the coverage of Russian journals has expanded to 150 titles. Over the past 15 years, a twofold increase in the impact factor of the Russian journals has been observed, which is higher than that for the full data set of journals (a 1.4-fold increase). Measures to improve the quality of Russian journals are proposed.**
KEYWORDS **article; impact factor; Russian journal; full data set; bibliometric indicators; expected citation rate; JCR.**

INTRODUCTION

It is a well-known fact that the development of scientometrics was triggered by the Science Citation Index (SCI) creation by Dr. E. Garfield of the Institute for Scientific Information (ISI)[1] in 1964. This event has become a revolutionary factor not only for the development of a novel unique information tool, but it has also led to the development of a new scientific discipline, scientometrics (or more commonly known today as bibliometrics). According to Dr. E. Garfield, "we are witnessing the transformation of bibliometric studies into a field of industry: the assessment of the output of the research carried out by universities and by scientific teams" [1]. Although there has been growing dissatisfaction among members of the scientific community with the passion of bureaucrats from various foundations and ministries for all kinds of ratings and evaluations, the effect of these indicators on the level of funding for basic research is becoming greater.

With the accumulation of a large collection of bibliographic data at the ISI and the simultaneous rapid development of computer technology in the United States, a new information product was developed based on the interrelationships between the journals the Journal Citation Reports (JCR), which is published annually. Since 1978, JCR Social Sciences Edition has been published. Beginning from 2009, both editions of the JCR have been available online as part of the Web of Knowledge (WoK). JCR shows the relationship between citing and cited journals and contains data on a journal's impact factor (IF). The concept of impact factor was proposed by Dr. E. Garfield in collaboration with Dr. Irving Sher in 1955 [2]. The introduction of this term contributed to an increase in the quality of libraries' acquisition. However, IF quickly became popular as a symbol of the scientific prestige of a journal, although its value significantly varies depending on the field of science and its relevance to the subject field. As Dr. Garfield has mentioned, "Many scholars and editors are currently making a terrible mistake thinking that SCI was created exclusively to produce its by-product, JCR. The major purpose of these resources was not only to aid information retrieval but also to use it as an alerting tool, i.e., for selective dissemination of information." [1]

One can say it is a bulk of literature considering the drawbacks and shortages of the IF, but it is impossible to receive a research grant at foreign universities, unless the grant applicant has publica-

[1] *K2001Kg. This institute belongs to the ThomsonReuters (TR) company.*

tions in journals with a high IF. It is impossible to list the number of bibliometric studies based on the use of JCR statistics and devoted to various aspects of IF application, including the analysis of growth rates in the scientific literature by a specific subject category, to the factors affecting the IF value within subject categories, as well as to the use of IF by funding organizations as a measure to assess scientific activity at the level of university departments and research groups.

In certain field of science, excessive passion for using the IF as an indicator of the research activity efficiency and decision-making regarding promotion within organizations (getting tenure), as well as for assessing the viability of faculties and colleges, results in negative consequences. Thus, it was noted in [3] that "the desire by research personnel at medical colleges in many countries to be published exclusively in journals with a high IF threatens the very existence of medical nursing journals and causes cessation of the publication of books and chapters in books for which the IF values are not calculated." In the Netherlands, the desire to be published exclusively in the journals listed in the JCR has led to cessation of the publication of Dutch journals on social sciences [4]. A significant contribution to the development of bibliometric studies related to the normalization of the IF in various fields of science has been made by Braun T. [5], Glanzel W., [6], and Leydesdorff L. [7].

The increasing amount of scientific literature and transformation of the industrial society into the knowledge economy have resulted in an expansion of the journals' coverage by JCR. While the first JCR edition contained statistics on 3,000 journals, the number of journals in the JCR-Science Edition increased up to 8,700 in 2010. According to German specialists [8], the reason behind the expansion of journals coverage processed by ThomsonReuters is due to its competition with Elsevier, which has been issuing the Scopus since 2005. Scopus is similar to SCI to a significant extent. It consists of over 18,000 journals. The criteria for the selection of journals to be included in the Thomson Information Resources were thoroughly discussed in [9]. The IF depends on the language of publication, research field, and sociocultural traditions of science. The first analysis of Soviet journals was performed by Dr. E. Garfield [10]. I. Marshakova's article devoted to a comparative analysis of the IF of Russian and Polish journals on mathematics should be mentioned among the papers that discussed the analysis of Russian journals IF [11].

No representative in-depth analysis of the bibliometric indicators of Russian journals has been performed within the past 20 years. The aim of this empirical study carried out at the macro level (regardless of the journal's subject category) was to identify the trends in the bibliometric indicators of Russian journals and to compare them to the global trends by analyzing the annual sets of the JCR-Science Edition (JCR-SE) for the time period 1995–2010. Since only four Russian journals have been included in the JCR-Social Science Edition during the past decade, the data on the comparative analysis of these journals against the trends in the full data set would not be statistically significant.

The choice of the subject of our research is directly related to the reform of the basic research and the higher education sectors being carried out in Russia. This reform is accompanied by growing attention by the President and the Government of the Russian Federation to bibliometric indicators as a tool for research efficiency evaluation. On May 7, 2012, Russian President Vladimir Putin signed a decree on "Measures for the Implementation of the State Policy in the Field of Education and Science." This decree, in particular, contains provisions regarding increasing competition among Russian universities. In accordance with the latter, "at least five Russian universities must be included in the list of the top 100 best universities in the world by 2020, according to one of three World University Rankings." [12] Accomplishing this task is largely associated with the IF of the journals in which the articles of the teachers of the higher education sector will be published. Our earlier studies have demonstrated that ~ 60% of Russian articles included in the Web of Science (WoS) were published in Russian journals [13]. Meanwhile, despite the expansion of Russian journals coverage by Web of Science, the number of Russian publications over recent years has remained stable and does not exceed 30,000 articles. Significant financial investments by the Russian Government in universities have resulted in the fact that universities pay authors a substantial amount of money for publication in journals covered by WoS. Furthermore, the amount of compensation depends on the IF value.

METHODS

Issues of the JCR-SE for the time period 1995–2010 were used as the source of bibliometric statistics data. During the period from 1995 to 2008, JCR was issued on CD-ROM, and since 2009 it has become available as a part of Web of Knowledge via the Internet. Unfortunately, the CD-ROM for 2001 was not available; therefore, the statistics were collected only for a 15-year period: 1995–2000 and 2002–2010.

Bibliometric statistics were collected from the JCR for each year for the following indicators:

- the number of Russian journals and the total number of journals;
- share of Russian journals in JCR;
- the annual number of articles in an average Russian journal and in an average journal of the full data set;
- the average number of articles published in a Russian journal and in an average journal of the full data set;
- the average IF of a Russian journal and the average IF of a journal of the full data set
- the expected response for a Russian journal.

To calculate the expected response (ER) to articles published in a specified journal (either Russian or one in the full data set) for a given year was estimated. The expected response is the number of articles published in the journal in a given year $_t$ multiplied by the IF of this journal over that year $_t$:

$$ER^t_j = f^t_j IF^t_j,$$

where f^t_j is the number of articles published by the journal $_j$ over the year ^{t}; IF^t_j is the IF of the journal $_j$ in the year ^{t}; and ER^t_j is the expected response to articles published in the journal $_j$ over the year ^{t}.

L_t is the list of journals (Russian or total journals set) in a given year ^{t}. The total estimated response S_ER^t to articles published in all journals from the list L_t over the year ^{t} was calculated according to the formula

$$S_t\_ER^t = \sum_{j=1}^{N_{L_t}} ER^t_j,$$

where N_{Lt} is the total number of journals in the list L_t.

The original information contained in each annual set of JCR-SE was uploaded into a special database based on the MS SQL Server 5. As a result, statistics were collected for each of the aforementioned indicators during each of the 15 years.

RESULTS AND DISCUSSION

The results of our study indicate that there is a steady increase in the number of journals indexed in WoS[2], and, correspondingly, JCR: 4,655 titles were covered by JCR-SE in 1995, and 8,073 titles were covered in 2010. In other words, there has been a 1.75-fold increase. In 1995, this database covered 108 Russian journals; this number increased to 148 titles in 2010; i.e., a 1.37-fold increase was observed (*Fig. 1*). The difference between the growth rates of the Russian and the full data set has a negative impact on Russian research output. *Figure 1* shows diagrams characterizing the growth rates of the Russian journals and the full data set.

A significant decline was observed in 1997 (96 titles). In 1998, the number of journals increased to 112. The relatively stable number of titles during the period between 2004 and 2008 rose to 130 and 148 in 2009 and 2010, respectively. The changes in the number of Russian journals during the studied period were partially associated with ThomsonReuters processing changes: from processing Russian-language versions to English-language ones. The increase in the coverage of the Russian journals is related both to the improvement in the quality of Russian journals and competition with the Scopus, which covers 230 Russian titles.

Our data regarding the growth of scientific literature virtually coincide with the data [7] obtained from WoS statistics (both versions of the SCI-Expanded and SSCI-Expanded) for the period 2000–2008. According to this publication, the number of journals has increased by 29%, with an average growth rate of 3.3%. The highest growth rate was recorded in 2007–2008. It is a known fact that a journal must have been listed in WoS for at least two years before it receives an IF. Hence, the IFs of journals published in 2008 could appear in the JCR only in 2010.

The growth in the global literature is attributed to several factors, including the development and globalization of science, emergence of a new research area, and appearance of new journals, as well as ThomsonReuters policy to expand journals coverage in WoS. As mentioned in [12], the number of publications in WoS is growing rapidly. Our results have shown that JCR-SE covered 607,049 articles in 1995, while the number of articles reached 1,080,209 in 2010 (i.e., a 1.78-fold increase was observed). The number of Russian articles covered by JCR-SE has also increased; however, only a 1.22-fold increase was observed. The proportion of Russian articles among the total number of publications covered by JCR-SE was down from 2.48% in 1995 to 1.7% in 2010.

Our goal was to find out to what extent the increase in the total number of Russian articles is associated with the expansion in the journal coverage by JCR-SE or whether the growth is attributed just to the increase in the number of articles per single average journal. So we investigated the trends of a single average Russian journal and a journal from the total journals' set over the studied period. *Fig. 2* shows two diagrams characterizing the trends of both types of journals.

The data presented in *Fig. 2* demonstrate the "ups" and "downs" in the average number of articles per single Russian journal. The sharp fall shown in the diagram for 2006 is obviously associated with the changes that were occurring at that time at the Nauka publishing house and at the company respon-

[2] *Only 93-95% of Russian publications covered by WoS are covered by JCR-SE (Science Citation Index-Expanded).*

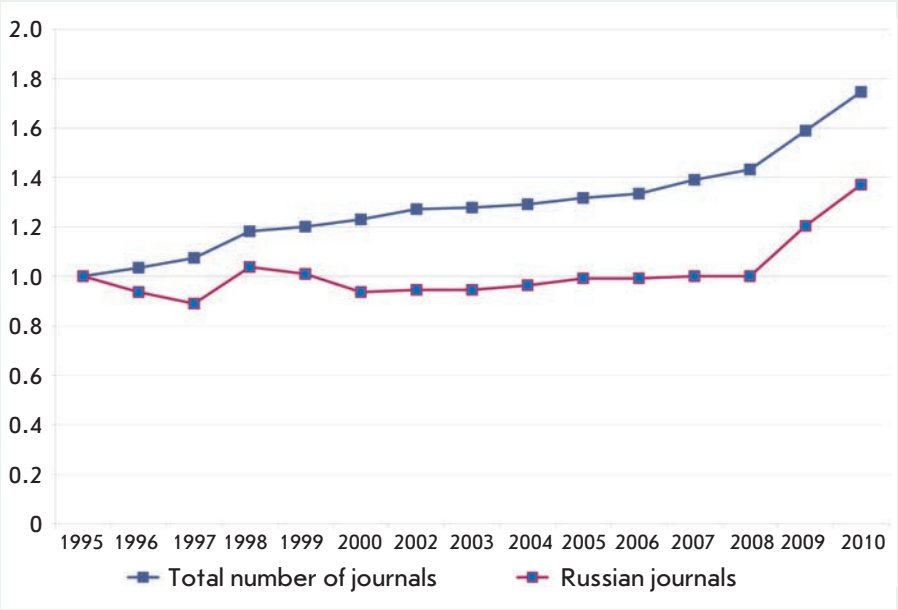

Fig. 1. Growth rate of the number of Russian journals and the total number of journals covered by JCR-SE as compared to that in 1995

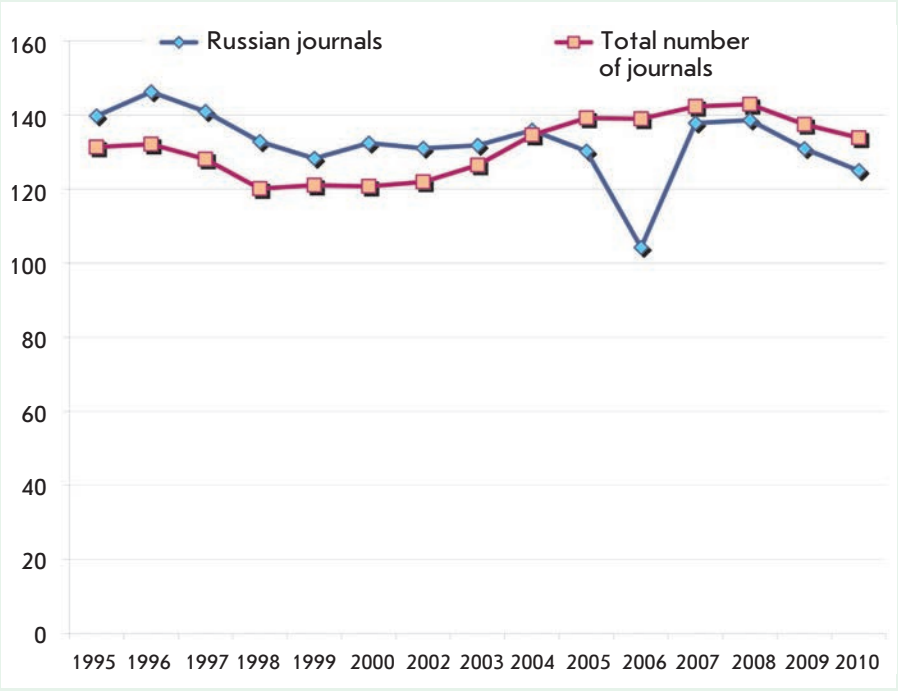

Fig. 2. Changes in the number of articles per single average Russian journal and per journal among the total number of journals covered by JCR-SE

sible for the translation of Russian journals. Over all, the number of articles per single average Russian journal fell by 18.3% (or 20 articles) as compared to 1996. An opposite trend was evident in the total journals set: a 1.9% growth rate was observed. A conclusion can be drawn that the significant decrease in the number of articles (by almost 20%) per single Russian journal that has occurred over the past 15 years is one of the main reasons for the lack of growth in Russian research output.

In order to assess all the causes of the stagnation in the number of Russian publications, one needs to collect statistics related to all the articles of Russian researchers published in foreign journals. We compared the number of Russian publications covered by WoS to that covered by JCR-SE between 2006 and 2010. These data are listed in Table 1.

It is clear from Table 1 that the number of articles published in Russian journals increased significantly during the period 2009–2010. The share of Russian publications in foreign journals remains high. This demonstrates that Russian science remains part of global science.

A journal's IF plays an important role in evaluating a scientist's performance (however, too much significance is often attached to it). In 2005, the average IF of a single Russian journal was 0.27 compared to 1.3 IF for a journal in the full data set and that of a journal among the full data set was 1.3; i.e., there was a 4.8-fold difference. During the survey period, a tendency toward increased IF values was observed for journals in both groups. These data are presented in *Fig. 3*.

The average IF of a Russian journal for the studied period has increased 1.75-fold, although it still remains relatively low. However, despite the obvious difference in the IF values between the two groups of

Table 1. Share of articles published in Russian journals, %

Year	Share of articles published in Russian journals, %
2006	44.6
2007	46.3
2008	43.7
2009	45.8
2010	53.6

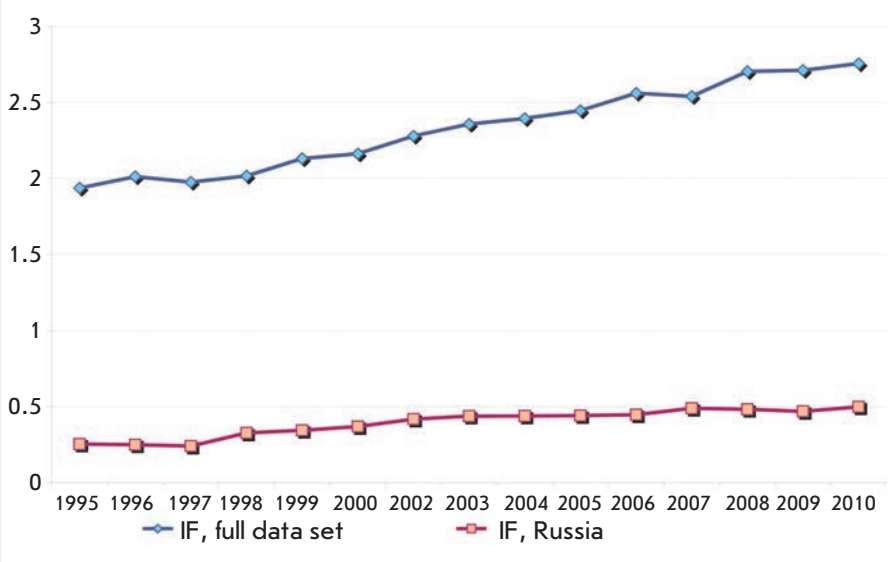

Fig. 3. Trends in the IF values of journals during the period 1995–2010 according to JCR-SE

journals this difference slightly narrowed in 2010: there was a 4.8-fold gap between the IF values in 1995, while in 2010 it had shrunk to 4.1 times. The period between submission of the manuscript to a Russian journal and its publication exceeds one year; hence, there is an almost zero probability that the publication will be cited during the same year. This is only one of the reasons why the IF of Russian journals is significantly lower than that of foreign ones. Among the full data set, the share of publications on life sciences and clinical medicine amounts to over 70%. These fields of science are characterized by high citation rates and the highest IFs. The pattern of distribution of Russian journals over the fields of science is completely different: sciences known as "hard science" (i.e., physics, chemistry, mathematics, materials science, Earth sciences) account for ~80%. The citation scores of these fields are significantly lower. This fact also considerably affects the relatively low average IF value.

As mentioned above, the IF of a journal is becoming increasingly important as Russian universities offer additional financial rewards to uthors, which depend on the journal's IF [13]. Certain universities are developing an evaluation methodology depending on the national identity of a journal: either Russian or foreign (htpp://urfu/fileadmin/user_upload/docs/science/Prikaz_122_2013.pdf).

The highest IF values among Russian journals have been conventionally assigned to the review journals *Physics-Uspekhi* and *Russian Chemistry Review*. In assessing the scientific productivity, a special weighted indicator is assigned not only to the IF, but also to which percentage group a journal belongs to in the subject category as was described by Dr. E. Garfield [14].

The journals assigned to a particular subject category and ranked by the highest value of the IF, which account for the first 25%, are considered to be the most important ones. This research has resulted in the widespread application of the 25% subject category journals both abroad and in Russia. For instance, the lecturers at Moscow State University receive an additional monthly financial reward for the publication of articles in the international journals included in the top 25% of subject category according to the Web of Science classification htpp://istina.imec.msu/statistics/journals/top.

As we have mentioned above, the IF strongly depends on the subject category, since the citation rate between immunology and mathematics differs by almost an order of magnitude. The list of Russian journals in the JCR-SE for 2010 contains only nine journals with IF higher than one. However, only a few of them have been listed in the top 25 or 50% most prestigious journals in the relevant subject category. *Table 2* contains data on these journals. It is noteworthy that among eight journals of this category, three are mathematics journals with IFs substantially lower than one.

A number of Russian journals with relatively high IFs were not included even in the top 75% of journals. This applies to *Biochemistry*, which ranks fourth among Russian

Table 2. Russian journals included in the top 25 and 50% of the corresponding subject category

Journal	Impact factor	Rank among the Russian journals with respect to IF	Rank in the JCR subject category	Subject category	Number of journals in the subject category	The size of the share in the JCR subject category, %
Laser Physics	1.362	5	34	Optics	79	50
Physics-Uspekhi	2.245	2	18	Interdisciplinary sciences, physics	80	25
Russian Chemistry Review	2.346	1	43	Interdisciplinary sciences, chemistry	154	50
JETP Letters	1.557	3	32	Interdisciplinary sciences, physics	80	50
Functional Analysis and Its Applications	0.688	25	103	Mathematics	279	50
Moscow Mathematical Journal	0.721	21	93	Mathematics	279	30
Journal of Mathematical Physics	1.131	6	28	Interdisciplinary sciences, physics	55	50
Journal of Experimental and Theoretical Physics	0.946	12	41	Interdisciplinary sciences, physics	80	50

journals, with an IF of 1.402. This journal belongs to the "Biochemistry and molecular biology" subject category, consisting of 286 journals. *Biochemistry* in this subject category ranks 234th, and it was not even included in the top 75%. Another example is *Astronomy Letters*, with an IF value of 1.091, which ranks 8th among Russian journals with respect to the IF and 36th among 55 journals in the "Astronomy and astrophysics" subject category. This journal belongs to the 75% group. The remaining Russian journals have relatively low rankings in their relevant subject categories. We consider it necessary to bolster the credibility of Russian journals in the eyes of the international scientific community. It would be reasonable to invite foreign colleagues to join editorial boards and to provide each issue of the journal with content in English. The authors have to provide an abstract and a list of keywords in the Russian and English languages. The articles should to be accompanied by a list of references. The establishment of language counseling centers for assistance in editing the articles written by Russian authors in the English language seems relevant. Publications by leading scientists in Russian journals contribute to the development of Russian science and could guide young researchers in their scientific endeavors. Since the Ministry of Education and Science of the Russian Federation attaches great importance to the bibliometric indicators of Russian science, it could use the experience of foreign universities and colleges, which have special training courses that teach how to prepare articles and reports, technical papers, and grant applications.

The expected response (*ER*) to journal articles is the number of articles multiplied by the journal IF in a specific year. In order to calculate the expected response of the aggregate of Russian journals (or that of the full data set), the sum of these products throughout the entire given set (Russian journals or the full data set) for the year under study is used. It can be noted that a maximum expected response is observed for the articles published in Russian journals twelve years ago. The falls on the curve are associated with the technological changes in the journals' processing as has been mentioned above.

It should be mentioned that these response data only apply to Russian articles published in Russian journals. Since over 45% of Russian articles are published in foreign journals, the total response to Russian articles is much higher.

CONCLUSIONS

A representative empirical bibliometric analysis of the Russian journals covered by Journal Citation Reports-Science Edition (JCR-SE) for the period 1995–2010 has been conducted for the first time at the macro level (excluding subject categories).

The growth of the total number of articles (1.8-fold increase) as compared to 1995 outpaces the growth rates of Russian publications (1.2-fold increase). As a result, the share of Russian articles among the total

number of publications decreased from 2.49% in 1995 to 1.71% in 2010.

It was determined that the number of journals among the full data set and that of Russian journals increased by factors of 1.75 and 1.37, respectively.

Over a 15-year period, the number of articles published in a single average Russian journal has decreased by 17.9% as compared to that in 1995. An increase by 1.9% was observed for the full data set. This fall is the reason behind the stagnation in the Russian research output for the period 2008–2010, despite the increase in the number of Russian journals covered by Web of Science. Another cause is the decline in the share of Russian journals in the total number of journals covered by Web of Science from 2.34% in 1995 to 1.83% in 2010.

Despite the fact that the weighted average IF of Russian journals remains significantly lower than that of the journals among the total number of journals, it increased 1.96-fold as compared to that in 1995. Meanwhile, the weighted average IF of the full data set is characterized by a 1.42-fold increase.

Our data provide reliable statistics for policy makers and editorial boards. In order to improve the bibliometric indicators of Russian science, it is necessary to improve the quality of Russian journals translation into English. Furthermore, a program for graduate and undergraduate students on "How to prepare a research paper" is required. The Ministry of Education and Science of the Russian Federation should play a key role in this preparation. ●

The authors are grateful to the Russian Foundation for the Humanities for financial support (grant № 12-70000) and to Thomson Reuters for the opportunity to use the data.

REFERENCES

1. Garfield E. // 12th COLLNET Meeting. September 20–23, 2011. Istanbul Bilgi University, 2011.
2. Garfield E. // J. Am. Med. Ass. 2006. V. 295. № 1. P. 90–93.
3. Johnstone M.J. // Intern. Nursing Rev. 2007. V. 54. № 1. P. 35–40.
4. Leydesdorff L., Wagner C. // Macro-level Indicators of the Relations between Research Funding and Research Output (http://www.leydesdorff.net/roadmap/roadmap.pdf).
5. Braun T., Glanzel W., Schubert A. // Scientometrics. 2006. V. 69. № 1. P. 169–173.
6. Glanzel W. // Scientometrics. 2006. V. 67. № 2. P. 121–129.
7. Halfman W., Leydesdorff L. Is inequality among universities increasing? Gini coefficients and the elusive rise of elite universities. www.loet@leydesdorff.net.
8. Michels C., Schmoch U. // Scientometrics. 2012. V. 93. № 3. P. 831–846. DOI 10.1007/s11192-012-0732-7 DEC 2012
9. Markusova V.A. // Acta Naturae. 2012. V. 4. № 2 (13). P. 6–13.
10. Garfield E. Citation Indexing. N. Y.: John Wiley & Sons, 1981. 274 p.
11. Marshakova-Shaikevich I. // Sociology of Science and Technology. 2012. V. 3. № 2. P. 79–100.
12. Decree of the President of the RF № 599 of May 7, 2012 "Measures to Implement State Policy in Education and Science" / Official website of the President of Russia. Moscow, 2012. URL: http://graph.document.kremlin.ru/page.aspx?1;1610850.
13. Markusova V.A., Ivanov V.V., Varshavskii A.E. // Herald Russ.Acad.Sci 2009. № 7. P. 483–491.
14. Garfield E., Pudovkin A. // 6th Intern. Conf. on Webometrics, Informetrics and Scientometrics & 11th COLLNET Meeting from 19–22 October 2010 in Mysore, South India, 2010.

Big Data in Biology and Medicine

Based on material from a joint workshop with representatives of the international Data-Enabled Life Science Alliance, July 4, 2013, Moscow, Russia

O. P. Trifonova[1]*, V. A. Il'in[2,3], E. V. Kolker[4,5], A. V. Lisitsa[1]

[1] Orekhovich Research Institute of Biomedical Chemistry, Russian Academy of Medical Sciences, Pogodinskaya Str. 10, Bld. 8, Moscow, Russia, 119121

[2] Scientific Research Center "Kurchatov Institute," Academician Kurchatov Sq. 1, Moscow, Russia 123182

[3] Skobel'tsyn Research Institute of Nuclear Physics, Lomonosov Moscow State University, Leninskie Gory 1, Bld. 58, Moscow, Russia, 119992

[4] DELSA Global, USA

[5] Seattle Children's Research Institute, 1900 9th Ave Seattle, WA 98101, USA

*E-mail: oxana.trifonova@gmail.com

The task of extracting new knowledge from large data sets is designated by the term "Big Data." To put it simply, the Big Data phenomenon is when the results of your experiments cannot be imported into an Excel file. Estimated, the volume of Twitter chats throughout a year is several orders of magnitude larger than the volume of a person's memory accumulated during his/her entire life. As compared to Twitter, all the data on human genomes constitute a negligibly small amount [1]. The problem of converting data sets into knowledge brought up by the U.S. National Institutes of Health in 2013 is the primary area of interest of the Data-Enabled Life Science Alliance (DELSA, www.delsaglobal.org) [2].

Why have the issues of computer-aided collection of Big Data created incentives for the formation of the DELSA community, which includes over 80 world-leading researchers focused on the areas of medicine, health care, and applied information science? This new trend was discussed by the participants of the workshop "Convergent Technologies: Big Data in Biology and Medicine."

The total number of workshop participants was 35, including representatives of research institutes dealing with the analysis of large experimental data sets and commercial companies developing information systems. The workshop participants delivered 16 short reports that were aimed at discussing how manipulating large data sets is related to the issues of medicine and health care.

The workshop was opened by Prof. Eugene Kolker, who presented a report on the behalf of the Data-Enabled Life Science Alliance (DELSA, www.delsaglobal.org). The alliance supports the globalization of bioinformatics approaches in life sciences and the establishment of scientific communities in the field of "omics." The main idea is to accelerate translation of the results of biomedical research to satisfy the needs of the community.

Large data sets that need to be stored, processed, and analyzed are accumulated in many scientific fields, in addition to biology; there is nothing surprising about this fact. Large data sets in the field of high-energy physics imply several dozen petabytes; in biology, this number is lower by an order of magnitude, although it also approaches petabyte scale. The question discussed during the workshop was what Russian researchers should focus on in the Big Data world: either molecular biology in the "omics" format, or integrative biology in brain modeling, or social sciences?

The tasks of working with large data sets can be subdivided into two groups: (1) when data are obtained interactively and need to be processed immediately and (2) when there is a large body of accumulated data requiring comprehensive interpretation. The former category of data is related to commercial systems, such as Google, Twitter, and Facebook. Repositories of genomic and proteomic data exemplify the latter type of data.

Systems for handling large data arrays are being developed at the Institute for System Programming, Russian Academy of Sciences, with special attention on poorly structured and ambiguous data that are typical of the medical and biological fields. Collections of software utilities and packages, as well as distributed programming frameworks running on clusters consisting of several hundreds and thousands of nodes, are employed to implement smart methods for data search, storage, and analysis. Such projects as Hadoop (http://hadoop.apache.org/), Data-Intensive Computing, and NoSQL are used to run searches and context mechanisms when

From problem to solution: the experts in the field of data processing, Data-Enabled Life Science Alliance-DELSA, are ready to beat back challenge of NIH

handling data sets on a number of modern web sites.

Prof. Konstantin Anokhin (Scientific Research Center "Kurchatov Institute"), talked on the fundamentally novel discipline of connectomics, which is focused on handling data sets by integrating data obtained at various organizational levels. Large bodies of data will accumulate in the field of neuroscience because of the merging of two fundamental factors. First, an enormous amount of results obtained using high-resolution analytical methods has been accumulated in the field of neurosciences. Second, the main concern of scientists is whole-brain functioning and how its function is projected onto the system (mind, thought, action), rather than the function of individual synapses. Obtaining data on the functioning of the brain as a system includes visualization techniques: high-resolution computed tomography, light microscopy, and electron microscopy. Megaprojects on brain simulation have already been launched (e.g., the Human Brain Project in Europe); the investments to obtaining new experimental data will be devalued with time, while the analysis of the resulting data will become the highest priority.

Extraction and interpretation of information from existing databases using novel analytical algorithms will play a key role in science in future. The existence of a large number of open information sources, including various databases and search systems, often impedes the search for the desired data. According to Andrey Lisitsa (Research Institute of Biomedical Chemistry, Russian Academy of Medical Sciences), existing interactomics databases coincide to no more than 55% [3]. The goal in handling large data sets is to obtain a noncontradictory picture when integrating data taken from different sources.

The concept of dynamic profiling of a person's health or the state of an underlying chronic disease using entire sets of high throughput data without reducing the dataset to the size of the diagnostic biomarker panels is being developed at the Research Center of Medical Genetics of the Russian Academy of Medical Sciences. The description of a normal human tissue requires one to integrate several thousand quantifiable variables that may be derived using genome, transcriptome and/or proteome profiling techniques; composite, integrative measures may be used to quantify the distance that separate any two samples. However, as each human organism has both individual genetic predispositions and a history of environmentalal exposure, the traditional concept of averaged norm would not be appropriate for personalized medicine applications in its true sense. Instead, Prof. Ancha Baranova introduced the concept of a multidimensional space occupied by set of normal sample tissue and the tissue-specific centers within this space ("the ideal state of the tissue"). The diseased tissues will be located at a greater distance from the center as compared to healthy ones. The proposed approach allows one to abandon binary (yes/no) predictions and to show the departure of a given tissue sample as a point in an easily understandable line graph that places each sample in the context of other samples collected from patients with the same condition and associated with survival and other post-hoc measures.

Prof. Vsevolod Makeev (Institute of General Genetics, Russian Acad-

emy of Sciences) asserted in his report that we will be dealing with large data sets more frequently in the near future. There will be two types of data: data pertaining to the individual genome (the 1000 Genomes Project), which are obtained once and subsequently stored in databases to be downloaded when required. The second type of data pertains to the transcriptome or proteome analysis, which is conducted on a regular basis in order to obtain an integrative personal omics profile [4]. There are several providers of such data in the case of genomes; Russian laboratories can use these repositories and employ their own bioinformatics approaches to arrive at new results [5].

The flow of dynamic data for individuals (results of monitoring the parameters of the organism) will increase as modern analytical methods are adopted. Researchers will face the need for rapid processing of continuously obtained data and for transferring the information to repositories for further annotation and automated decision-making. There emerges the need for modifying the technology of data storage and transfer to ensure a more rapid exchange of information. Cloud services for storing and transferring large sets of data exist already (e.g., AmazonS3).

The development of more rapid methods of mathematical analysis also plays a significant role. The report delivered by Ivan Oseledets (Institute of Computational Mathematics, Russian Academy of Sciences) focused on the mathematical apparatus for compact presentation of multidimensional arrays based on tensor trains (tensor train format, TT-format). Multidimensional tasks constantly emerge in biomedical applications; the TT-format allows one to identify the key variables that are sufficient to describe the system or process under study.

Medical data need to be processed interactively so that a preliminary diagnosis can be made no later than several minutes after the data have been obtained. The "Progress" company is currently developing a system for remote monitoring of medical indicators using mobile devices and the cellular network for data transfer (Telehealth, report by Oleg Gashnikov). This method allows one to provide 24-hour out-of-hospital monitoring of a patient, which is supposed to reduce medical services costs in future. At this stage, techniques for forming alarm patterns are to be developed based on accumulated data; algorithms are to be modified for each patient.

The report on the problem of collecting and processing the geo location data that are accumulated by mobile network operators and collected by aggregators, such as Google, Facebook, and AlterGeo, appeared to lie beyond the workshop's topic on the face of it. The lecturer, Artem Wolftrub (leading developer at Gramant Ltd.), reported that a number of papers have been published by a group led by Alex Pentland and David Laser (Massachusetts Institute of Technology) since 2009, where it has been substantiated that the analysis of geo data can be no less informative for predicting socially important diseases than the genome is. Environmental factors (the so-called exposome) play a significant role in the pathogenesis of multigene diseases. Data regarding the exposome can be obtained with a sufficient degree of detail by analyzing the relocations of a person, by comparing the general regularities of population migrations, and by identifying the patterns that correlate with health risks (e.g., development of cardiovascular diseases or obesity [6]).

In their discussions, the workshop participants mentioned the Watson supercomputer in various contexts. This supercomputer was designed by IBM to provide answers to questions (theoretically any questions!) formulated using the natural language. It is one of the first examples of expert systems utilizing the Big Data principle. In 2011, it was announced that the supercomputer will be used to process poorly structured data sets in order to solve medical and health care problems [7].

When analyzing the problem of Big Data in biology and medicine, one should note that the disciplines have been characterized by the accumulation of large data sets that describe the results of observations since the natural philosophy era. During the genomic era, the aim of data accumulation seemed to be understandable. However, as the technical aspect was solved and the genome deciphered, it turned out that the data was poorly related to the problems of health maintenance [8].

In the post-genomic era, biomedical science has returned back to the level of phenomenological description oriented towards data collection only, without an understanding of the prospect of its further interpretation. The Human Proteome Project is such an example: data for each protein are collected; however, it is not always a given that these data can be used in the applied problems of in-vitro diagnostics. Another example is the Human Connectome Project, which is aimed at accumulating data on signal transduction between neurons in expectation of the fact that having been accumulated to a certain critical level, these data will allow one to simulate human brain activity using a computer.

In summary, the workshop participants noted that the Big Data phenomenon is related to the newly available opportunity of modern technogenic media to generate

and store data; however, there is no clear understanding as to the reason and purpose for the accumulation of such data. Russian scientists should primarily focus on analyzing Big Data so that the data array can be converted into hypotheses applicable for verification using a point-wise biochemical experiment. The task of getting acquainted with the data accumulated within the "Connectome" Project is bound to be the main direction of development at the Russian subgroup of DELSA. ●

REFERENCES

1. Hesla L. Particle physics tames big data // Symmetry. August 01, 2012. (http://www.symmetrymagazine.org/article/august-2012/particle-physics-tames-big-data).
2. Kolker E., Stewart E., Ozdemir V. // OMICS. 2012. V. 3. № 16. P. 138–147.
3. Lehne B., Schlitt T. // Human Genomics. 2009. № 3. P. 291–297.
4. Li-Pook-Than J., Snyder M. // Chemistry & Biology. 2013. № 20. P. 660–666.
5. Tsoy O.V., Pyatnitskiy M.A., Kazanov M.D., Gelfand M.S. // BMC Evolutionary Biology. 2012. № 12. (doi: 10.1186/1471-2148-12-200).
6. Pentland A., Lazer D., Brewer D., Heibeck T. // Studies in Health Technology and Informatics. 2009. № 149. P. 93–102.
7. Wakeman N. // IBM's Watson heads to medical school. Washington Technology. February 17, 2011. (http://washingtontechnology.com/articles/2011/02/17/ibm-watson-next-steps.aspx).
8. Bentley D.R. // Nature. 2004. V. 429. № 6990. P. 440–445.

Modern Aspects of the Structural and Functional Organization of the DNA Mismatch Repair System

S. A. Perevoztchikova[1], E. A. Romanova[1], T. S. Oretskaya[1, 2], P. Friedhoff[3], E. A. Kubareva[1]*
[1] Belozersky Institute of Physico-Chemical Biology, Lomonosov Moscow State University, Leninskie Gory, 1, bld. 40, Moscow, Russia, 119991
[2] Chemistry Department, Lomonosov Moscow State University, Leninskie Gory, 1, bld. 3, Moscow, Russia, 119991
[3] Institute of Biochemistry, FB 08, Justus Liebig University, Heinrich-Buff-Ring 58, D-35392 Giessen, Germany
*E-mail: kubareva@belozersky.msu.ru
Received by the editor on 21 May 2013

ABSTRACT **This review is focused on the general aspects of the DNA mismatch repair (MMR) process. The key proteins of the DNA mismatch repair system are MutS and MutL. To date, their main structural and functional characteristics have been thoroughly studied. However, different opinions exist about the initial stages of the mismatch repair process with the participation of these proteins. This review aims to summarize the data on the relationship between the two MutS functions, ATPase and DNA-binding, and to systematize various models of coordination between the mismatch site and the strand discrimination site in DNA. To test these models, novel techniques for the trapping of short-living complexes that appear at different MMR stages are to be developed.**
KEYWORDS **DNA mismatch repair system, structure of proteins, protein-protein and protein-DNA interactions, MutS, MutL, MutH.**
ABBREVIATIONS **aa – amino acid residue, bp – base pair, HNPCC – hereditary nonpolyposis colon cancer (Lynch syndrome), HTH – helix-turn-helix, IDL – insertion-deletion loop, IRC– initial recognition complex, m^6A – N6-methyl-2'-deoxyadenosine, MMR – mismatch repair, PCNA – proliferating cell nuclear antigen, SSB protein – single-strand binding protein, URC – ultimate recognition complex, XRD – X-ray diffraction analysis.**

INTRODUCTION

The genome is the primary repository of the information necessary for the survival of any organism. Replication of the genetic material in unaltered form during the somatic and generative cell division is the most important condition for the existence and maintenance of the viability of organisms. A single nucleotide substitution in a single gene can lead to developmental disorders or even to a lethal outcome if the former occurs in germ cells [1] or to carcinogenesis if mutations occur in somatic cells [2]. Errors take place during replication regardless of the correcting activity of DNA polymerases. It is estimated that on average one nucleotide substitution occurs per 10^8–10^{10} nucleotides during the replication of DNA by bacterial DNA polymerase [3]. Not all eukaryotic DNA polymerases possess a 3'→5'-exonuclease activity, which leads to a large error rate [4], and, therefore, the need for systems repairing the incorrectly inserted nucleotides that could prevent the occurrence of mutations is evident. Currently, from five to nine systems involved in the damage repair can be identified, amongst which the mechanisms of direct repair, excision repair, post-replicative and SOS-repair are being extensively investigated [5, 6]. A DNA mismatch repair (MMR) also performs an important role in the maintenance of the genome's stability.

The need for research concerning maintenance of the genetic stability is supported by the large number of experimental and review articles on the subject. The most important achievement is discussed every year in the penultimate issue of the journal "Science." In 1994, the topic was DNA repair [7]. The first issue of "Biochemistry" (Moscow) in 2011 [8] was devoted to the mechanisms of DNA damage repair systems. In the present review we consider the DNA mismatch repair system. Over the past decade and a half, a significant number of review papers have been dedicated to the repair of mismatches [9–17]. We considered the experimental data, including those obtained during the last 5–6 years, and an attempt to systematize the understanding of the mechanisms by which the MMR system functions was made.

THE ROLE OF THE MMR SYSTEM IN BIOLOGICAL PROCESSES

Mismatches are considered to be any nucleotide pairs other than G/C and A/T. Their occurrence is caused by erroneous insertion of nucleotides by DNA polymerase during the copying of the template strand, as well as the influence of mutagenic factors (including free radicals and ionizing radiation). Insertion of modified nucleotides carried out by DNA polymerase or an unmodified nucleotide opposite the damaged base in the template strand is feasible [5, 18].

Another common error of the replication system is short insertion-deletion loops (IDL), which also occur during the formation of duplexes in the course of homologous recombination [19, 20]. The damages mentioned above are recognized and restored by the mismatch repair system (MMR), thereby reducing the likelihood of emergence of mutations by a factor of 50–1,000 [21, 22]. The MMR system is also involved in DNA restoration after the occurrence of certain chemical modifications. Repair of the following modifications has been demonstrated: O6-methylguanosine [23, 24], 8-oxoguanosine [25, 26], adducts formed during exposure of carcinogens on DNA [27], photo-induced compounds [28–30], and products of the reaction of DNA with cisplatin derivatives [31].

The role of the MMR system is not limited to the repair of the above-listed DNA lesions. The proteins of this system are involved in cell cycle regulation. In particular, during the G2 phase the DNA damage signal transmitted by the MutS protein triggers a cascade of processes that cause programmed cell death (apoptosis) [15, 32, 33]. Abnormality in this function leads to enhanced cell survival resulting in carcinogenesis, as well as resistance of these cells to chemotherapy [13, 25]. Likewise, defects in the mismatch repair system in prokaryotes lead to an increased rate of mutagenesis and to interspecies gene transfer, which can ensure adaptability of the bacteria to stressful conditions and to drug resistance [34].

The MMR system is vital for maintaining the length of microsatellite repeats, i.e. short repetitive DNA [13, 35, 36]. Replication of the repeated segments often leads to errors attributed to the slippage of the DNA polymerase to an analogous sequence. As most of the burden of the repair of these lesions lies with the MMR system, microsatellite instability is used as a biomarker for the abnormalities of the functioning of the proteins of this repair system. Dysfunctions within the MMR system result in various DNA rearrangements and telomerase-independent telomere lengthening [37, 38].

MMR system proteins are also important for the prevention of recombination between similar, but not identical, DNA sequences, as well as for chromosome pairing during meiosis and the segregation of chromosomes [39]. In somatic cells the MMR is involved in hypermutation during the formation of the repertoire of immunoglobulins in B lymphocytes [40, 41]. The wide variety of biological functions of the mismatch repair system draws interest regarding the details of its mechanisms.

The mismatch repair system has been discovered in all kingdoms of living organisms; its key proteins – MutS and MutL – are highly conserved across species, from bacteria to higher eukaryotes [42]. Given the structural similarity of the proteins, it is assumed that the principles of the mismatch repair mechanisms are similar in all organisms. Defects in the MMR system proteins in humans lead to the emergence of tumors, including malignant ones. The Lynch syndrome or hereditary nonpolyposis colon cancer (HNPCC) is the most common amongst them. Mortality rates associated with the latter ranks third amongst cancers [43–46]. Mutations in the genes encoding the proteins of the MMR system are identified in 85% of hereditary nonpolyposis colon cancer cases [44] and in 15–25% of cases of sporadic tumors of various tissues [47]. Detection of abnormalities in the MMR system plays an important role in the diagnosis of tumors [48]. The existence of a link between human cancers and the MMR determines the relevance of investigations of the DNA mismatch repair system.

In 1989 the MMR process was reconstituted *in vitro* using purified components [49], and currently the general scheme of how the MMR system works is well understood. However, many questions remain to be resolved in order to create an adequate model of the MMR process. The general views on the mechanism of MMR are presented below.

OVERVIEW OF THE MECHANISM AND ORDER OF EVENTS IN THE MMR PROCESS

The key proteins of the MMR system are MutS and MutL. The genes encoding these proteins were originally discovered in *Streptococcus pneumoniae* (*hexA* and *hexB* genes) [50]. Somewhat later, homologous genes were discovered in *Escherichia coli* (*mutS* gene, *hexA* homologue, and *mutL* gene, *hexB* homologue), as well as *mutH* and *mutU* genes [51]. MMR system proteins were named Mut (short for mutagenic) as their dysfunction leads to hypermutability in microorganisms. Genes encoding proteins that are homologous to MutS and MutL have been discovered in the majority of sequenced genomes. The names of MutS and MutL homologues are formed using the abbreviations MSH (from MutS homologue) and MLH (from MutL homologue), respectively.

MMR is a multicomponent system. Its function requires the coordinated action of over 10 proteins [52].

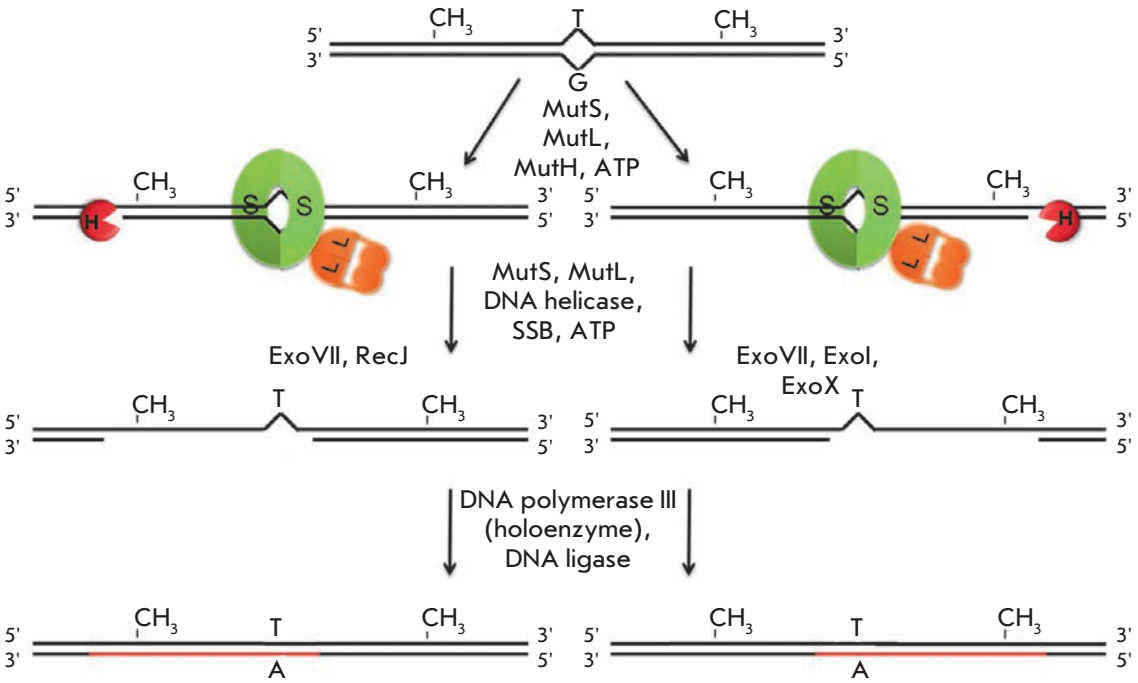

Fig. 1. The scheme showing the DNA mismatch repair process in *E. coli*

Table 1 shows the key proteins of the MMR system in *E. coli* and humans, and their functions are compared.

The general scheme of the mismatch repair in *E. coli* is shown in *Fig. 1*. MutS acts as a sensor scanning the DNA searching the mismatches: G/T, C/T, A/C, A/G, G/G, A/A, T/T (all but the C/C), and small insertion-deletion loops (IDL) [14]. Over the past years, it has been demonstrated that MutS also stimulates the cellular response to damaging agents in mammals such as cisplatin, ionizing radiation, antimetabolites, ultraviolet radiation, and alkylating and intercalating agents [24–31, 53, 54]. MutS forms specific contacts with a mismatch in the so-called initial recognition complex (IRC) characterized by bending of the DNA by 60° [13, 55]. The MutS protein then interacts with the MutL protein, forming a ternary complex which acts as a coordinator of subsequent processes, including distinguishing between the parent and the daughter (i.e., containing the error) DNA strands. MutS and MutL are ATPases: their functioning requires the presence of ADP and ATP [13, 14].

The absence of methylation in the newly synthesized strand plays an important role in distinguishing between the parental and the daughter DNA strands in enterobacteria. Hence, the MMR system in such bacteria is called a methyl-directed mismatch repair system. This relationship was discovered by Meselson *et al.* [56, 57], who investigated the repair of bacteriophage λ carrying one or several mismatches after its transfecting into *E. coli* strains. It was found that the repair of closely positioned mismatches occurs in the same DNA strand [56]. Involvement of the MutH protein, a DNA nicking enzyme responsible for recognizing the hemimethylated sequence 5'-Gm^{6}ATC-3'/3'-CTAG↓-5' (where m^{6}A is N6-methyl-2'-deoxyadenosine; the arrow indicates the position of hydrolysis), is important during the selection of the DNA strand in which to introduce a break and to start the subsequent excision repair. The emergence of MutH recognition sites is associated with the action of cellular Dam-methyltransferase. Before DNA replication is initiated, the adenosine residues of both strands of the 5'-GATC-3' sequences are methylated within the cell. However, for a certain period of time after replication, the cell contains a pool of DNA in which only one of the two strands is methylated [58]. MutH catalyzes the single-stranded break in the unmethylated, i.e. newly synthesized DNA strand [16, 59]. Fully methylated DNA in *E. coli* cells does not undergo a repair process [60], and in the absence of methylation (*dam*$^-$ strains) distinguishing between parent and daughter strands is impossible, which may lead to double-stranded DNA breaks. Therefore, *E. coli* strains with insufficiently and excessively active Dam methyltransferase demonstrate an increased rate of mutagenisis [61, 62]. The catalytic function of MutH is stimulated by a ternary complex consisting of the MutS and MutL proteins and DNA containing a mismatch. Typically, MutH bound to its recognition site and located in the nearest possible position to the mismatch on either side of the DNA relative to the mismatch is activated. The distance between

Table 1. Key proteins of the *E.coli* and human mismatch repair systems

E. coli	Function	Homologue in human cells	Function
MutS (homodimer)	Recognition of mismatches	MSH2–MSH6 (MutSα)	Repair of mismatch and insertion-deletion loops consisting of 1-2 nucleotides
		MSH2–MSH3 (MutSβ)	Repair of insertion-deletion loops consisting of 2 or more nucleotides
		MSH4–MSH5	Participation in the meiotic recombination and in the order of switching of immunoglobulin synthesis
MutL (homodimer)	Coordination of the MMR processes after recognition of a mismatch and before reparative biosynthesis of DNA	MLH1–PMS2 (MutLα)	As per MutL from *E. coli*
		MLH1–PMS1 (MutLβ)	Suppression of insertion-deletion mutagenesis in yeast homologues; the function of the human homologue in the MMR is unclear
		MLH1–MLH3 (MutLγ)	Suppression of insertion-deletion mutagenesis; participation in meiotic recombination
MutH	Recognition of 5'-Gm^{6}ATC-3'/ 3'-CTAG↓-5' and hydrolysis of the daughter unmethylated DNA strand	Not identified	

the mismatch and the site of strand discrimination can reach 2,000 bp [14, 63].

Mismatch repair is independent of DNA methylation in the cells of most other organisms. The question of how the repair system detects the daughter strand, i.e. the strand containing an error, remains open to discussion. Introduction of a break into the DNA in such organisms is attributed to MutL homologues in which an endonuclease motif was discovered [64]; however, this fact has not been confirmed experimentally. Another assumption is that single-stranded breaks occurring in the course of DNA replication may serve as signals of a newly synthesized DNA strand: from the 3'-end of the leading strand and the 3'- and 5'-ends of the lagging strand [65].

The single-stranded break serves as a signal for excision steps of the repair process in which a fragment of a DNA strand containing a mismatch is removed. The DNA helicase UvrD binds to the nick and unwinds the DNA until a non-canonical base pair is reached. It has been shown that the action of a DNA helicase is stimulated by the ternary MutS-MutL-DNA complex and directed towards the mismatch [66–68]. The latter indirectly indicates the ability of a ternary complex to coordinate the recognition of a mismatch and the subsequent occurrence of excision repair. The released single-stranded DNA is hydrolyzed by a specific set of exonucleases depending on whether the 5'- or 3'-end is accessible [69, 70]. The single-strand binding protein (SSB) interacts with the parent DNA strand covering its entire surface and preventing degradation [71, 72]. The single-stranded gap is rebuilt by DNA polymerase III. DNA ligase restores the integrity of the corrected strand.

MutS AS A KEY PROTEIN OF THE MMR SYSTEM

A substantial amount of structural and biochemical data regarding the protein MutS and its homologues has been accumulated. The MutS protein from *E. coli* is a polypeptide with a molecular weight of 95 kDa. The MutS quaternary structure in the solution is an equilibrium mixture of dimers and tetramers [73] formed by the equivalent subunits (with regards to the primary structure). In eukaryotes, MutS homologues forms dimers from two different subunits. Six human homologues of MutS (MSH1–MSH6) have been identified. Heterodimers, known as MutSα (MSH2–MSH6) and MutSβ (MSH2–MSH3), together perform the functions of the bacterial MutS protein, ensuring accuracy in mitotic replication (*Table 1*). MSH1 supports genetic stability in the mitochondria of eukaryotes [20]. The MSH4–MSH5 heterodimer is involved in the resolution of Holliday junctions during meiosis [74–76] and does not participate in the repair of replication errors. A bioinformatics analysis enables to construct a phylogenetic tree that reflects the functional specialization of MutS homologues [77] (*Fig. 2*).

Structure of the MutS protein from *E. coli* and functions of its individual domains

An important milestone in investigations of the MutS protein was the elucidation of its crystal structure. In 2000, the crystal structures of MutS–DNA complexes from *E. coli* [55] and *Thermus aquaticus* [78] containing a non-canonical pair were solved. Crystals of the MutS proteins and their mutant forms in complexes with DNA containing various mismatches were obtained later [79–83]. From amongst the eukaryotic MutS homologues, the structures of human MSHα and

MSHβ have been elucidated. To date the structures of over 20 MutS–DNA complexes [55, 78, 79, 81-86] have been determined; the corresponding data are openly available in the Protein Data Bank (PDB) (*Table 2*).

It should be noted that the structures of all MutS-DNA complexes obtained by X-ray diffraction analysis (XRD) are very similar. They represent the initial recognition complex (IRC) of the MutS with DNA containing a mismatch. In these structures the MutS protein forms specific contacts with a mismatch and is bound to a cofactor, ADP. The only structure of the MutS-DNA complex containing a G/T-mismatch and two molecules of ATP (code PDB 1W7A) was obtained by soaking of the crystals in an ATP solution. In this case the molecules remained firmly fixed in the crystal lattice, which prevented significant conformational rearrangements of the complex [85]. Data regarding the structure of the protein at the stage of scanning of the DNA in search of a mismatch or during the stage of signal transduction to other components of the MMR repair system cannot be obtained, which is attributed to the high dynamics of MutS-DNA complexes during these stages.

The primary structure of MutS is highly conserved across all living organisms. The secondary and tertiary structures of this protein in different organisms are highly conserved. In complex with the DNA, the protein is a dimer of elongated shape with two channels (each approximately 100 Å in length). Its shape resembles the Greek letter θ [87] (*Fig. 3A, B*). While the duplex with a mismatch is located in the larger channel, the function of the second channel remains unknown. However, its size and charge lead to conclude that it is capable of forming contacts with DNA [82].

XRD was used to obtain a high-resolution structure of the protein (less than 2 Å). Attempts to characterize the structures of four regions (aa 2–13, 57–66, 95–107 and 659–668) in the DNA-free protein (PDB-code 1EWR) have failed, indicating the conformational mobility of the protein in the absence of DNA. The positions of all amino acids, except for the loop formed by the aa 659–668, have been determined in MutS–DNA complexes containing a mismatch [55].

Each MutS monomer has seven structural domains (*Fig. 3B*). The N-terminal domain is a mismatch-binding (aa 2–115) one. This domain is formed by a mixed ß-sheet layer consisting of five strands and surrounding the latter three α-helices. The following adjacent domain, which is a connector domain (aa 116–266), is primarily composed of parallel ß-strands surrounded by four α-helices. The core domain (aa 267–443 and 540–567) comprises two bundles of α-helices. The lever domain (aa 504–567) consists of two α-helices protruding out of the core domain and surrounding the DNA

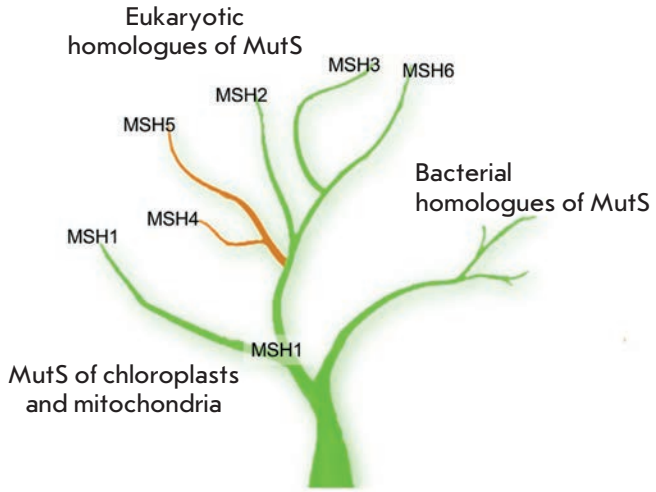

Fig. 2. The phylogenetic tree of MutS family proteins. Green branches represent MutS homologues involved in the maintenance of genetic material stability during vegetative cell division; the brown branches – during meiotic DNA recombination

but lacking direct contact with the latter. An important feature of the structures of prokaryotic and eukaryotic MutS homologues is a long α-helix consisting of 60 aa which connects the core domain to the clamp domain. The helix is likely to be involved in the signal transduction between the ATPase and the DNA-binding domains [86]. The clamp domain (aa 444–503) is an insertion into the upper part of the lever domain. It is formed by four antiparallel ß-strands. The nucleotide-binding (ATPase) domain (aa 568–765) and the HTH (helix-turn-helix) domain (aa 766–800) are located in the C-terminal region of the protein.

Within the structure of the complex of MutS with the DNA containing a mismatch the protein is a homodimer arranged asymmetrically. The subunit forming specific contacts with the mismatch is hereinafter referred to as subunit 1 (in *Fig. 3* its domains are shown in different colors). The second subunit that forms contacts only with the DNA sugar-phosphate backbone is hereinafter referred to as subunit 2 (in *Fig. 3* it is shown in green). The protein surrounds the DNA in the location of a mismatch, covering an area comprising 24–28 bp [88]. The MutS protein covers the DNA in the form of a clamp. The binding of the protein to the DNA requires the clamp to "open up." It is believed that the opening of the clamp is promoted by the flexible structure of the upper part of the domain that contains a large percentage of loops [89]. The flexibility of the DNA-binding domains is confirmed by the fact that the

Table 2. Crystal structures of the MutS protein

Organism	DNA[1]	ATP or ADP	Resolution, Å	PDB code	Reference	Substitution, aa
E. coli[2]	G/T	ADP	2.20	1E3M	[55]	—
	«	«	2.10	1WB9	[84]	E38T
	«	«	2.50	1WBB	[84]	E38A
	«	«	2.40	1WBD	[84]	E38Q
	«	«	2.20	3K0S	[83]	D693N
	«	ADP (2 molecules)	2.60	1NG9	[79]	R697A
	«	ATP (2 molecules)	2.27	1W7A	[85]	–
	A/A	ADP	2.40	1OH6	[81]	–
	A/A	«	3.40	2WTU	[83]	–
	G/G	«	2.50	1OH7	[81]	–
	C/A	«	2.90	1OH5	[81]	–
	extra T	«	2.90	1OH8	[81]	–
Thermus aquaticus[3]	–	–	3.19	1EWR	[78]	–
	extra T	–	2.20	1EWQ	[78]	–
	extra T	ADP (2 molecules)	2.70	1FW6	[79]	–
	extra T	ADP (2 molecules)·BeF_3	3.11	1NNE	[82]	–
Human (MSHα)	G/T	ADP	3.30	2O8E	[86]	–
	G/T	ADP (2 molecules)	2.75	2O8B	«	–
	G/dU	ADP	3.00	2O8D	«	–
	m^6G/T[4]	«	3.37	2O8C	«	–
	extra T	«	3.25	2O8F	«	–
Human (MSHβ)	loop 4 n.r.[5]	«	3.09	3THW	–	–
	loop 3 n.r.	«	2.70	3THX	–	–
	loop 2 n.r.	«	2.89	3THY	–	–
	loop 6 n.r.	«	4.30	3THZ	–	–

[1] Non-canonical pair of nucleotides in the DNA duplex used for crystallization is shown.
[2] In the case of MutS from *E. coli* deletion variants containing aa 1–800 were used.
[3] In the case of MutS from *T. aquaticus* deletion variants containing aa 1–782 were used.
[4] m^6G – O6-methyl-2′-deoxyguanosine.
[5] n.r. – nucleotide residues.

former are not structured in the crystals of the DNA-free MutS [78].

In a specific complex with MutS, the DNA is bent by 60° [78, 79] (*Fig. 3*). A mismatch is located at the apex of the corner. Bending results in expansion of the minor groove of the DNA in a manner that its width becomes approximately equal to the major groove width. Within the specific complex, the aa of both MutS subunits interact with the DNA; however, binding is asymmetrical – each subunit forms multiple contacts; however, they are all different. The total surface area of the DNA-protein contacts is ~ 1850 Å^2 [81]. The majority of the contacts between the protein and the DNA are hydrophilic (aa interact with the sugar-phosphate backbone of the DNA) and do not depend on the nucleotide sequence. Hence, MutS can function in various nucleotide contexts. Only amino acids from the subunit 1 (Phe-X-Glu motif) form specific contacts with a mismatch [86]. With respect to eukaryotic homologues, this motif is present in MSH6 but absent in MSH2 and MSH3. Even prior to the availability of XRD results, it was established that Phe36 (numbering for MutS from *E. coli*) performs an important role in the binding of MutS to DNA. Replacement of Phe36 with Ala disrupts the ability of MutS to engage in a specific interaction with DNA [90]. Perhaps, Phe36 is

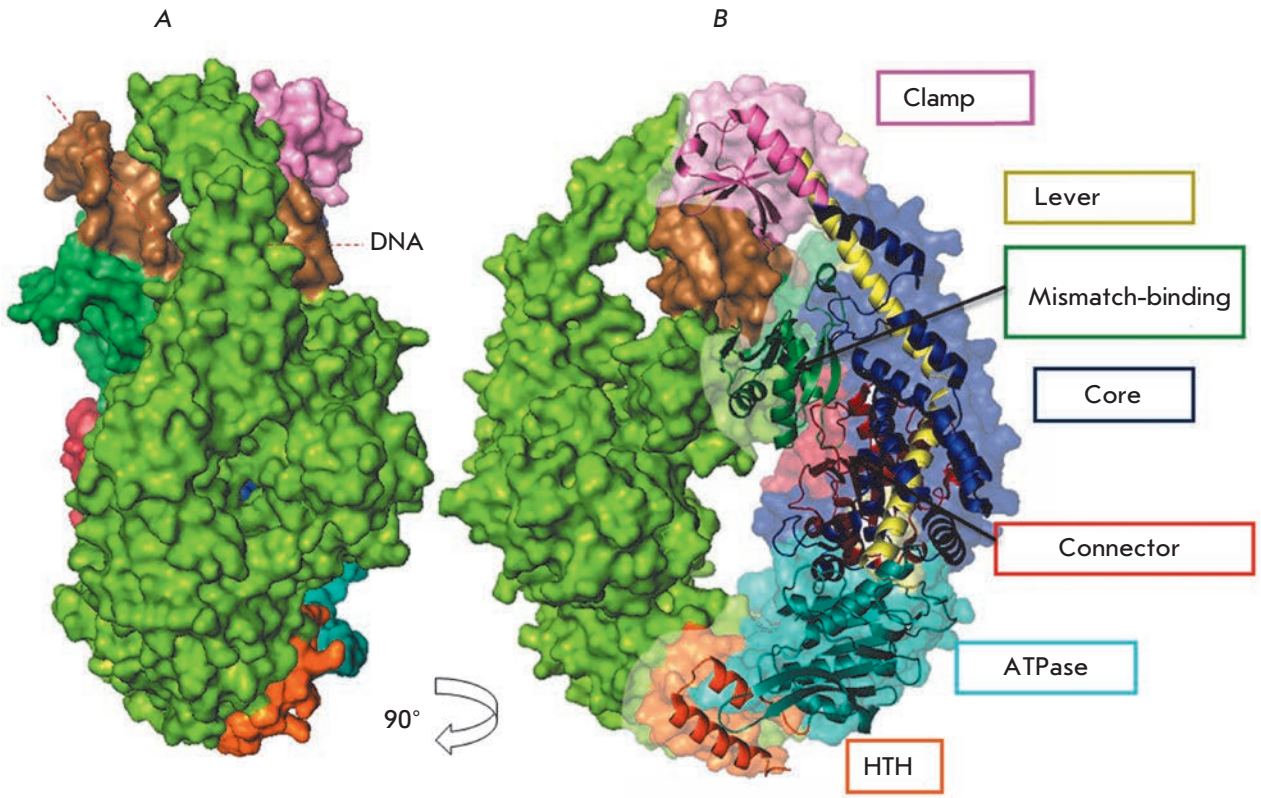

Fig. 3. The overall structure of the MutS from *E. coli* in complex with DNA containing a G/T-mismatch. Lateral view (**A**) and frontal view (**B**) are presented. DNA is colored in brown, MutS subunit 2 – in green. The domains of DNA-binding subunit 1 are shown in picture **B**: the mismatch-binding domain (aa 2–115) is colored in dark green; the connector domain (aa 116–266) – in red; the core domain (aa 267–443) – in blue; the lever domain (aa 504–567) – in yellow; the clamp domain (aa 444–503) – in pink; the ATPase domain (aa 568–765) – in cyan; and the HTH domain (aa 766–800) – in orange. The DNA kink is marked by a red dashed line (PDB code 1E3M)

important in the search for a mismatch. According to XRD data, phenylalanine from the Phe-X-Glu motif is involved in the stacking with one of the heterocyclic bases of a mismatch on the minor groove side of the DNA [55, 78]. In the specific binding of MutS to a DNA mismatch, an important role is also performed by Glu38 (numbering for MutS from *E. coli*), which, similar to Phe36, forms contacts with the same heterocyclic base. The results of this interaction include the formation of a hydrogen bond between the carbonyl oxygen of Glu38 and the base nitrogen atom. Glu38 forms a hydrogen bond with the N3-atom of the T in the structures of MutS with a duplex containing a G/T pair or an unpaired nucleotide T. Glu38 forms a hydrogen bond with the N7-atom of the purine during the interaction of MutS with duplexes containing C/A and A/A pairs; an analogous contact is also formed with a non-canonical G/G pair [81]. Specific contacts determine the direction of the bend in the DNA. It was demonstrated that the replacement of a conserved residue of Glu38 with glutamine completely disrupts the ability of the protein to distinguish between canonical and mismatch-containing duplexes [91].

Unfortunately, little is known about the structure of the non-specific complex of MutS with the canonical DNA (homoduplex) as crystals of MutS with this DNA fragment could not be obtained. Sixma [89] suggests that the protein searches for a mismatch using the bind-release mechanism attempting to insert Phe36 into the "stack" of bases at each stage and, as a result, kink the DNA. The mismatch does not typically distort the structure of a DNA duplex [92, 93] but destabilizes it [94]. Natrajan *et al.* [81] suggest that MutS is able to detect these local weakening in the structure of the DNA. Atomic force microscopy demonstrated that DNA of non-canonical content in complex with MutS can be found in one of two conformations: bent or unbent [95]. It is believed that in the search for a mismatch MutS continuously bends and straightens the DNA. Detection of a mismatch leads to ATP-dependent rearrangements of MutS domains and the formation of the activated DNA-protein complex.

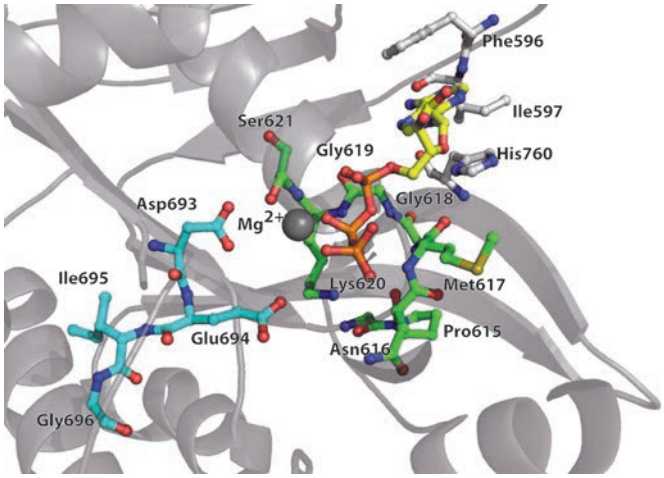

Fig. 4. MutS protein ATPase domain. ADP-contacting amino acid residues are shown in light-gray; amino acids of the Walker motif from subunit 1 are indicated in green; from subunit 2 – in cyan; the ADP molecule – in yellow-orange; and Mg^{2+} – in gray

The MutS protein belongs to ABC-family ATPases (ATP binding cassette). The proteins of this class, such as membrane transferases, bind to the substrate and hydrolyze ATP to regulate their activity. Certain members of this family demonstrate dimerization of the ATPase domains [96, 97]. The area of dimerization in the region of the ATPase domains in the MutS protein is significant and equal to 2922 $Å^2$ [85]. A characteristic feature of the proteins from ABC-family ATPases is a conservative loop protruding from one subunit and complementing the active site of the ATPase domain in another subunit. The binding of ATP or ADP occurs in a classic way characteristic of ATPases through the P-loop (phosphate-binding). The position of the adenine base is fixed from two sides by the aa His760 and Phe596 (in MutS from *E. coli*, *Fig. 4*). The conserved Ile597 forms two hydrogen bonds with the nucleotide. Ser621 coordinates complex formation consisting of a Mg^{2+} ion and β-phosphate of ADP with the involvement of the four water molecules [55]. The Walker motif (D-E-X-X, where X is any amino acid) in MutS from *E. coli* formed by the aa 693–696 stabilizes the water molecules associated with Mg^{2+} [55]. Substitutions of these aa result in loss of the ATPase activity of MutS and inactivation of the repair system [85].

The data obtained using biochemical methods are indicative of significant conformational rearrangements in the ATPase domains upon binding to ATP or its non-hydrolyzable analogs [98–100]. However, only certain aa (Ser668, Asn616 and His728) change their position in relation to the complex in the presence of ADP in the crystal of the MutS-DNA complex in which MutS is bound to two molecules of ATP [85]. According to biochemical data, the affinity of the two ATPase domains for each other is higher upon binding to ATP and lower in the presence of ADP. The general structure of the MutS protein is most compact upon binding to two molecules of ATP, whereas the most relaxed form is observed in the presence of ADP. The ATP- and ADP-free protein has an intermediate conformation [101]. Indirect observations also suggest modulation of protein conformation by nucleotides. For instance, the limited proteolysis patterns of MutS (from *E. coli*) in the presence of ADP, ATP and ATPγS are different from the latter in the absence of nucleotides [98, 99].

In addition, nonequivalence of the two domains of the protein upon binding to ADP (which is characteristic of ABC-family ATPases) was observed in MutS [55, 85]. ADP binds more efficiently to subunit 1 forming specific contacts with a mismatch. Asymmetry of domains is observed even in the absence of DNA [83, 102].

Structural and biochemical data suggest that the conformational changes in the ATPase domain stimulate the rearrangements in the DNA binding domains and vice versa. Transduction of a signal to a distance of ~60 Å and its amplification occurs through the α-helices connecting the two functional domains of the protein and the highly conserved mobile loops of the ATPase domains (*Fig. 4*). It is believed that Glu38, Glu694, Asp693, Asn616, His728 and Ser668 are the key amino acids involved in the signal transduction between the DNA-binding and ATPase domains [84]. Substitution of these aa results in loss of communication between the DNA-binding and ATPase functions of MutS, whereby the protein loses its function in the MMR.

The full-sized MutS protein forms tetramers and oligomers of higher order in solution. MutS tetramerization is important for the suppression of homologous recombination and repair of adducts of cisplatin with DNA [103]. It should be noted that the MutS tetramer is not simply a dimer of dimers as it can bind only one heteroduplex [73]. All crystal structures where MutS was a dimer were obtained using mutants lacking the ability for tetramerization (without C-terminal amino acids 53 aa in the MutS from *E. coli*).

The stages of MutS protein function in the MMR process

Several stages can be identified in the functioning of the MutS protein (*Fig. 5*). The protein binds nonspecifically to DNA and bends it in a search of a mismatch. Translocation of MutS along the DNA at this stage occurs during linear diffusion [104]. Specific binding to a non-canonical pair of nucleotides leads to confor-

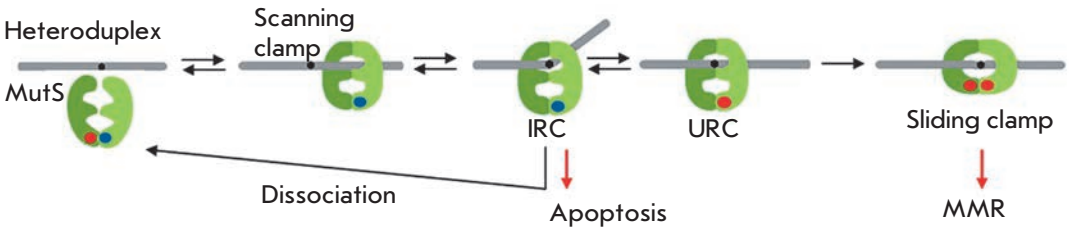

Fig. 5. Dynamic model of mismatch recognition by the MutS protein. Heteroduplex is a DNA duplex with a non-canonical pair, modified after [13]

mational rearrangements in the DNA and the protein with the formation of the initial recognition complex, IRC [13]. Within this complex, the DNA is bent by 60° [55]. Currently, only the crystal structure of this type of complexes with DNA has been established by XRD. The formation of an ultimate recognition complex, URC, has been proposed. In this complex the DNA is straightened and the non-canonical pair of nucleotides is located outside of the double helix. This assumption is based on analogy with other proteins, such as DNA methyltransferases, Tn10 transposase, etc., which, similarly to MutS, "wedge" recognizing amino acids into the DNA from the minor groove side [105, 106]. The protein bound to ATP forms an active conformation of a sliding clamp capable of activating the subsequent stages of mismatch repair.

The role of the ATPase cycle of MutS

Binding of ADP or ATP to the two subunits of MutS is necessary for the transition from one conformational state to another. It enables the protein to act as a molecular switch [104, 107, 108].

Two nucleotide-binding centers of MutS perform different functions in the MMR [79], which is in accordance with the structural asymmetry established through XRD [55, 78]. Both subunits can simultaneously bind to adenine nucleotides (ATP or ADP) [109]. The dissociation constants for the MutS-ATP or MutS-ADP complex are found in the range of 1–20 μM. Such affinity suggests that the state of MutS wherein one or both of the nucleotide-binding centers are free from nucleotides exists only temporarily. It was demonstrated that MutS exhibits different affinities for ATP, ADP and non-hydrolyzable analogs of ATP. However, there is no unanimity in views regarding the effectiveness of the interaction between these nucleotides and MutS. For instance, even at high concentrations of ADP (100 μM) only one equivalent of a nucleotide per protein dimer would bind to MutS homologues from *E. coli*, yeast, or a human [73, 109, 110]. On the other hand, the ratio of ADP- to ATP-bound nucleotides in MutSα in the absence of DNA equals 1.6. Hence, the protein binds nucleotides in various combinations – ATP/ADP or ADP/ADP, wherein the second combination emerges as a result of the hydrolysis of the ATP molecule from the first combination [13]. Currently, it is well established that MSH6 (and the corresponding subunit 1 of bacterial MutS) binds to ATP with a higher efficiency than MSH2 (subunit 2 of bacterial MutS) [111, 112]. The ATPase activity of all MutS homologues is stimulated by the presence of DNA (both canonical and non-canonical) [113]. However, the data regarding the impact of the non-canonical pair of nucleotides in the DNA on the ATPase activity of MutS are inconsistent. Several studies have described acceleration (approximately a 4-fold increase) of ATP hydrolysis in the presence of DNA containing a mismatch in comparison with a homoduplex [107]. Other studies [114] have demonstrated that DNA containing a mismatch stimulates the ATPase activity of MutS to a lesser extent in comparison to the DNA with a canonical structure. Both homo- and heteroduplexes accelerate the exchange of nucleotides in the ATPase domains [113]. However, only in the case of a heteroduplex does the cycle of hydrolysis of ATP itself and not the exchange of nucleotides (occurring after hydrolysis) become the rate-limiting step [107].

Coordination of DNA binding and the hydrolysis of ATP processes in the ATPase domains of both subunits of MutS can be described using two schemes. According to scheme 1 [83], the ATPase domain of subunit 1 contains a single molecule of ADP during scanning of the DNA by the MutS protein in search for a mismatch. If the DNA is a substrate of the MMR system, e.g. contains a G/T-pair, MutS forms a specific complex. In this case, the ADP is replaced with ATP in the ATPase domains. The ATPase domain of the second subunit also binds to ATP; the conformational changes then occur in the MutS leading to the formation of a sliding clamp structure. This sliding clamp serves as a signal and recruits the MutL protein which activates the subsequent stages of the repair process. Thereafter, dissociation of MutS from the DNA-containing complex and ATP hydrolysis occur. The MutS protein retains the bound ADP molecule in one of the ATPase domains after completion of the cycle and is ready for a new interaction with the DNA.

Scheme 2 [115] suggests a different approach to the understanding of the nucleotide-binding and ATPase

Table 3. Crystal structures of the MutL protein

Organism	Protein fragment	Cofactors and their analogs	Resolution, Å	PDB code	Reference
E. coli	N-terminal domain – ATPase domain fragment (LN40)	-	2.90	1BKN	[122]
	«	ADP, Mg^{2+}	2.10	1B62	[121]
	«	ADPnP[1], Mg^{2+}	1.90	1B63	[121]
	«	ADPnP, Mg^{2+}, Rb^{+}	2.40	1NHH	[123]
	«	ADPnP, Mg^{2+}, K^{+}	2.00	1NHI	[123]
	«	ADPnP, Mg^{2+}, Na^{+}	2.30	1NHJ	[123]
	C-terminal domain	Na^{+}	2.10	1X9Z	[124]
Bacillus subtilis	C-terminal domain	-	2.50	3GAB	[125]
	«	-	2.00	3KDG	[125]
	«	Zn^{2+}	2.26	3KDK	[125]
Neisseria gonorrhoeae	C-terminal domain	-	2.40	3NCV	[126]
Saccharomyces cerevisiae (MLH1/PMS1)	C-terminal domains of the heterodimer	-	2.50	4E4W	—
	C-terminal domains of the heterodimer with the N-terminal domain fragment	Zn^{2+}	2.69	4FMN	—
	C-terminal domains of the heterodimer with the exonuclease I fragment	Zn^{2+}, Mg^{2+}	3.04	4FMO	—
Human (MLH1)	N-terminal domain	ATP	2.50	3NA3	—
	C-terminal domain	-	2.16	3RBN	—

[1] 5′-adenylyl-β,γ-imidodiphosphate

functions of MutS. This scheme is based on XRD data supplemented by calculations using the normal-mode analysis. According to the developed model, subunit 1 binds to and immediately hydrolyzes ATP in the process of the scanning of DNA. ADP release is the rate-limiting step of the ATPase cycle. At this point, only ADP is located in subunit 2. After the formation of a specific complex with a mismatch, both subunits lose their affinity for ADP, then they bind and retain the ATP. Hydrolysis of ATP within the two subunits occurs only after the transition of MutS from the structure sliding clamp into the DNA scanning mode.

In our opinion, the schemes 1 and 2 have significant differences:

1. According to scheme 1 ATP and ADP are absent in subunit 2 during the process of DNA scanning, whereas scheme 2 suggests that subunit 2 at this stage has higher affinity for ADP.

2. According to scheme 1 during DNA mismatch scanning MutS does not hydrolyze ATP; hydrolysis occurs only during the release of MutS from the DNA-containing complex, while according to scheme 2 the hydrolysis of ATP occurs at the stage of DNA scanning and after the formation of a specific complex.

It can be concluded that there is no clear understanding of the function of the ATPase domains of MutS and of the coordination of their functions at the different stages of the MutS protein action. Hence, the debate over this topic continues.

MutL PROTEIN – MOLECULAR COORDINATOR OF THE MMR

One of the unique features of the mismatch repair process is the distance of the mismatch from the site of the hydrolysis of the daughter strand of DNA (distance approaching 2,000 bp). Therefore, there has to be a clear coordination in space and time of all the proteins involved in the MMR. A central role in coordinating various stages of the MMR is assigned to the MutL protein. MutL receives a signal regarding the detection of a mismatch and directs the excision repair in the daughter strand of the DNA and DNA repair synthesis. Functioning as a coordinator of mismatch repair processes, MutL interacts with MutS and with the majority of the proteins involved in the subsequent stages of the repair process: MutH, UvrD-helicase, polymerase III and polymerase processivity factors – β-clamp (in prokaryotes) or proliferating cell nuclear antigen (PCNA, in eukaryotes), exonuclease ExoI (in prokaryotes) or polymerase Polη (in eukaryotes) [116].

The role of MutL and its eukaryotic homologues is not limited to the MMR process. It was demonstrated

that MutL interacts with the proteins participating in processes involving DNA, such as double-stranded DNA break repair, maintenance of the cellular response to DNA damage, apoptosis, meiotic recombination, and somatic hypermutation [116-119]. All this makes MutL the main element in the coordination of DNA damage recognition and the cellular response to damage in one of the available ways: repair, delay in cell division, or apoptosis [116].

MutL (and its eukaryotic homologues) binds non-specifically to single- and double-stranded DNA [111, 120]. It is assumed that the interaction of MutL with DNA occurs in complex with MutS. Biochemical studies of the MutL protein are complicated. The latter is attributed to its conformational mobility. In addition, its effect can be evaluated only through a change in the function of its protein partners [116].

MutL, similarly to MutS, functions as a dimer: homodimer in *E. coli* and heterodimer in eukaryotes (MutLα = MLH1 and PMS2, MutLβ = MLH1 and PMS1, MutLγ = MLH1 and MLH3). The molecular weight of MutL from *E. coli* is 68 kDa [121]. The structure of a full-length protein has not yet been established; however, crystals of the C-terminal and N-terminal domains have been obtained separately [122–127]. All structures to date for MutL and its homologues are presented in *Table 3*.

The current model of the MutL structure (*Fig. 6*) was obtained on the basis of XRD data for the N- and C-terminal domains of the protein [128]. According to this model, the N-terminal (aa 1–349) and C-terminal (aa 432–615) domains are interconnected by an unstructured region (aa 350–431) [125, 129]. Interestingly, the primary structure of the C-terminal domain of MutL homologues is less conserved, whereas the secondary structure is conserved. Meanwhile, both the primary and secondary structures of the N-terminal domain are highly conserved.

The C-terminal domains in the MutL dimer are involved in the formation of the primary dimerization interface, and the N-terminal domains contain ATP-binding sites. MutL is an ATPase which belongs to a new family of ATPases containing a novel nucleotide-binding motif. This family also includes topoisomerases of the second type (gyrases), the Hsp90 chaperone protein, and histidine kinases [130]. ATP binding and hydrolysis lead to structural rearrangements in the entire N-terminal domain [122]. The N-terminal domains undergo dimerization in the presence of ADP and ATP. The variable activity of the two ATPase domains of the heterodimers in the ATPase cycle was demonstrated for eukaryotic MutL homologues [131]. The value of the ATPase cycle is significant for the functioning of MutL. Mutant forms of MutL with a lack of the ATPase activity are unable

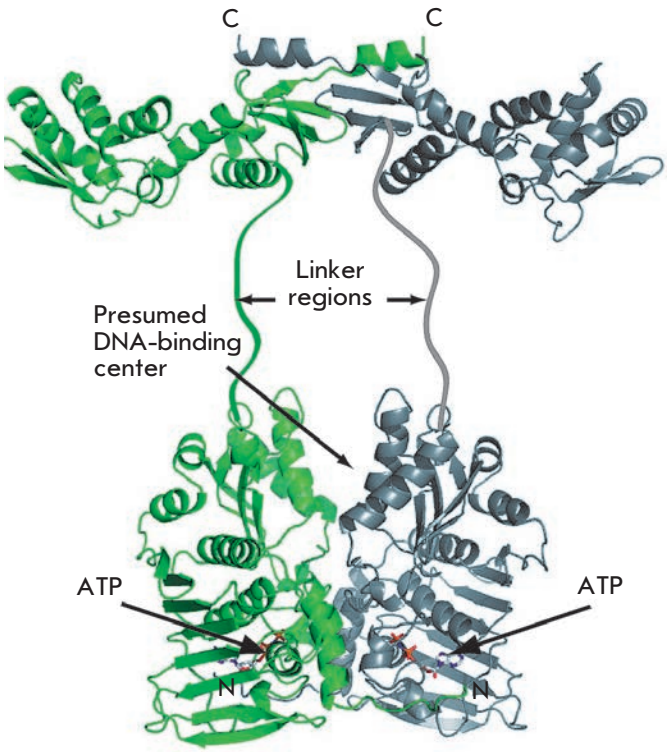

Fig. 6. The structural model of a full-length *E. coli* MutL homodimer based on the structures of the N-terminal (PDB code 1B63) and the C-terminal (PDB code 1X9Z) domains

to participate in the repair process and are unable to perform other protein functions [132]. It is believed that ATPase activity is necessary for the MutL protein to modulate protein-protein interactions [122].

Two loops of the MutL positioned in close proximity to the N-terminus are involved in the interaction with MutS, and the groove formed along the lateral surface of the N-terminal domain is involved in the binding to MutH [133] (*Fig. 6*). The saddle-shaped groove located on the surface of the N-terminal domain is most likely involved in the DNA binding. Mutations in the basic amino acids found in this segment, e.g. Arg266, lead to a decrease in the affinity of MutL for DNA and reduce its ATPase activity [134, 135]. However, the assumption regarding the DNA-binding surface in the MutL requires experimental confirmation. Interestingly, MutLα contains an endonuclease motif $DQHA(X)_2E(X)_4E$ (where X is any amino acid) which is localized in the PMS2 subunit [136]. This catalytic motif is found in all homologues of MutL, with the exception of some gamma-proteobacteria that are

characterized by site-directed hydrolysis of the DNA daughter strand performed by the MutH protein. However, regulation of the catalytic motif of MutL in the hydrolysis of the DNA daughter strand has not yet been confirmed.

MutH — PROTEIN DIRECTING THE MMR IN *E. coli*

The MutH protein, a 25-kDa monomeric site-specific nicking enzyme, exhibits similarities to the type II restriction endonuclease Sau3AI [137] and with respect to structure resembles PvuII and EcoRV [138]. The MutH protein binds specifically to a double-stranded sequence 5'-Gm^{6}ATC-3'/3'-CTAG↓-5' (location of hydrolysis is indicated by the arrow) and catalyzes the hydrolysis of only one unmethylated, i.e. the newly synthesized DNA strand [16]. Furthermore, MutH also hydrolyzes unmethylated sites, which may cause the emergence of double-stranded breaks [101]. MutH can hardly recognize and hydrolyze a completely methylated DNA sequence [139]. Similar to the majority of type II restriction endonucleases, MutH contains a characteristic motif, Asp-(X)$_n$-Glu-X-Lys (DEK-motif, where X is any amino acid). Two Mg^{2+} ions are required for its catalytic activity [140]. The rate of hydrolysis of the DNA by this enzyme is low; however, it increases significantly in the presence of MutS, MutL, and a DNA mismatch [79]. At low ionic strength of the solution, the activity of MutH is stimulated by the MutL protein without the involvement of the MutS protein bound to a mismatch [91].

The crystal structure of the MutH from *Haemophilus influenzae* (61% similarity with MutH from *E. coli*) in complex with DNA and in the absence of the latter has been determined [137, 140]. With respect to folding, the enzyme resembles the type II restriction endonuclease known as PvuII [138]. The MutH apoenzyme is a clamp consisting of two "arms" (N- and C-"arms", *Fig.* 7) separated by a large DNA-binding pocket. The catalytic center is located in the N-"arm." The amino acids responsible for the specific binding to the protein-recognition site, in particular those that form contacts with heterocyclic bases, are located in the C-"arm." When specific DNA binding occurs, the protein undergoes compaction, results in a rotation of both "arms" towards each other by an angle of 6-18° in comparison to the closed apoform of the protein, and the DNA-binding pocket becomes narrower tightly covering the recognition site. The structure of the DNA also undergoes restructuring. This includes the unmethylated recognition site becoming more prominently curved and distorted (the bending angle is approximately 30°) in comparison with the hemimethylated site. Nevertheless, local DNA-protein contacts with recognition sites in the two complexes do not differ. However, hemimethylated

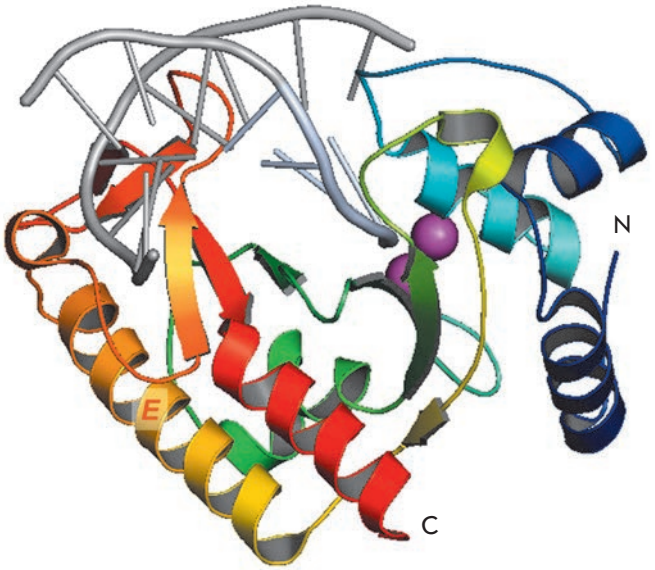

Fig. 7. The crystal structure of the *Haemophilus influencia* MutH-DNA complex (colored in gray) containing a hemimethylated 5′-Gm^{6}ATC-3′/3′-CTAG-5′ site (PDB code 2AOR). The two Ca^{2+} ions coordinated in the complex are shown in magenta. The *E* α-helix of MutH interacting with the MutL protein is indicated

DNA is more tightly gripped by the enzyme than the unmethylated site (the areas of the DNA-protein contact are 2100 and 1850 Å^2, respectively). As a result, the DEK-motif interacts with the DNA more efficiently, which leads to a 10-fold increase in the rate of hydrolysis of a hemimethylated recognition site as compared with the unmethylated one [140]. Therefore, in the case of the MutH protein, the bending degree of the DNA does not correlate with the efficiency of its hydrolysis. Single amino acid substitutions in the DNA-binding pocket have revealed that Tyr212 is important in the determination of the methylated status of the DNA [139].

An important feature of MutH is the increase in its catalytic activity during the MMR process. Up to now the mechanism of stimulation of MutH activity remains unclear. The DNA-binding channel in the crystal structure of the MutH protein apoform is not sufficiently wide to bind the DNA. It is assumed that binding of MutL to MutH widens the DNA-binding channel of the latter, increasing the rate of MutH binding to DNA [140]. As was shown using protein-protein crosslinking, MutL interacts with the C-terminal α-helix *E* located on the surface of MutH globule [141] (*Fig.* 7). Perhaps the formation of protein-protein contacts facilitates the rotational movement of the C-"arm" of MutH; as a re-

sult, the DNA-binding pocket becomes more accessible for binding to the substrate [132, 140].

INTERACTION OF MutS, MutL, MutH AND DNA

As was previously mentioned, a ternary complex consisting of MutS and MutL proteins associated with DNA is the key intermediate in the DNA mismatch repair process. It coordinates all stages of the repair after the recognition of a mismatch (i.e. excision repair including DNA unwinding towards the mismatch) and also participates in the transduction of the signal regarding DNA damage to other systems of the cell that control cell division and the triggering of apoptosis [142]. However, the structure of this complex has not yet been elucidated. Furthermore, the MutL protein itself exhibits a relatively low affinity for DNA, particularly for its short linear fragments. Binding to DNA occurs more efficiently in the presence of MutS, Mg^{2+} ions, and ATP [83, 115].

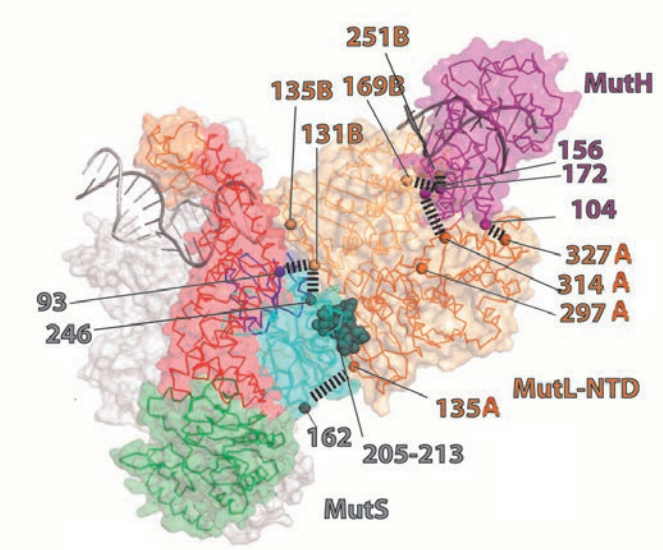

Fig. 8. Structural model of the MutS-MutL-MutH-DNA complex. MutS is shown in gray (the mismatch-binding domain is shown in red, the linker domain – in green). N-Terminal domains (NTD) of the two subunits of the MutL dimer are indicated in dark and light orange. The C-terminal and the linker domains of MutL are not shown. The MutH protein is highlighted in purple. The model is based on the following structures: MutS (PDB code 1E3M), MutL (PDB code 1B63), and MutH with DNA (PDB codes 2AZO, 2AOR). The amino acids involved in protein-protein contacts formation are shown in the figure. Colors of numbers indicate the amino acids residues correspondence to definite proteins

The ternary complex (MutS, MutL and DNA) has a dynamic nature; hence, it is impossible to investigate it using the XRD method. In order to investigate the areas of contact between the MutS and MutL proteins, a mutational analysis and hydrogen/deuterium exchange mass spectrometry were used. It was established that aa of MutS, crucial to the formation of contacts with MutL, are located in its connector domain [143]. The N-terminal and ATPase domains of MutL are involved in the interaction with MutS [133]. In addition, detailed studies were conducted based on site-directed protein-protein crosslinking (using bifunctional chemical agents that react with the cysteine residues of the protein) combined with fluorescent methods [144]. Before, crosslinking mutant forms of the MutS and MutL proteins containing a single cysteine residue in a designated position were produced. On experimental data Winkler *et al.* [144] proposed a model of the structure of the complex comprising MutS, MutL, and MutH bound to a mismatch-containing DNA (*Fig. 8*). In order to build a model of the complex, the authors used a structure of the MutL protein without a C-terminal domain. Previously, it was demonstrated [122] that this domain does not form contacts with the DNA and that the N-terminal domain of MutL is sufficient for the activation of MutH. According to this model, the aa at positions 246 in the MutS and 297 in the MutL (from both protein monomers) are located at a distance of less than 40 Å, and the aa 449 in MutS and 297 in MutL are located at a distance exceeding 50 Å. This model does not describe all the possible interactions of biopolymers; further investigations are required for a deeper understanding of the processes involved. Furthermore, the model does not account for the previously described [95] transition of the DNA from a bent shape into a linear shape following the activation of MutS that precedes the interaction of MutS with MutL.

The model of a complex consisting of the MutS, MutL, MutH proteins and DNA proposed by Winkler *et al.* [144] is based on their previously published model of the interactions between the proteins MutL and MutH [133]. The distances between the two proteins and interaction surfaces have also been determined using mutant forms of MutL and MutH containing a single cysteine residue, as well as thiosulfate reagents and photo-crosslinkers. It was concluded that the existence of the complex is feasible in which all three molecules, MutS, MutL and MutH, are in close proximity to each other. The formation of a DNA loop separating the proteins is not required in this case, which enables the complex to slide along the DNA in search for a signal of discrimination between the parent and daughter DNA strands.

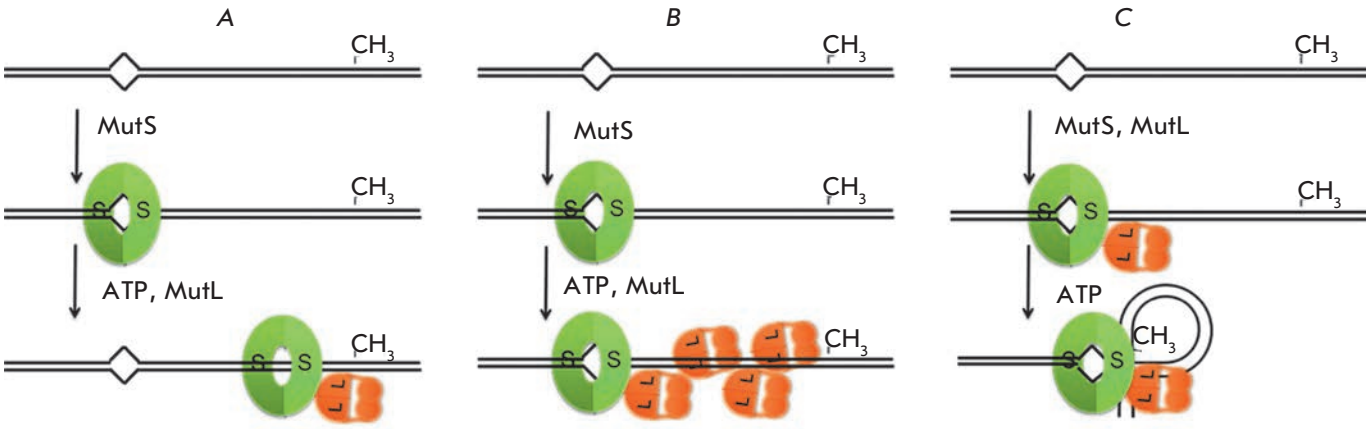

Fig. 9. Models of coordination between a mismatch and the hemimethylated 5′-Gm⁶ATC-3′/3′-CTAG-5′ site: cis- (**A** and **B**) and trans- (**C**) models. With respect to another classification: models of a sliding clamp (**A**), multiple MutL polymerization on DNA (**B**) and DNA looping (**C**)

MODELS OF COORDINATION BETWEEN THE DNA RECOGNITION AND THE CLEAVAGE SITES IN THE MMR SYSTEM

Currently different views exist regarding the processes that occur after the formation of the ultimate recognition complex. A number of articles describe attempts to systematize these models [13, 14, 59, 145]. However, this only complicates the situation as the same phenomena are described using different terminologies and, conversely, the same terms apply to different processes. In the present review we attempted to summarize the existing models of signal transduction from a mismatch to the proteins that perform excision repair basing on the principles of physical interaction of the repair proteins with DNA. The connection between the DNA-binding and the nucleotide-binding functions of the proteins is discussed above and is not considered in order to provide a simplified understanding.

A mismatch and a single-stranded break in *E. coli* cells are separated by significant distances (approaching 2,000 bp) during the stage of signal transduction of the daughter strand detection and subsequent excision repair [146]. The process is bidirectional in nature; i.e., excision occurs in both directions relative to the mismatch [61, 147]. These experimental facts form the basis of all models. Various views regarding the mechanism of initiation of the MMR process are summarized in *Fig. 9*.

Existing trans- and cis-models [13] regarding coordination between the DNA recognition and cleavage sites in the MMR system differ with respect to whether significant conformational rearrangements of the DNA are required (e.g., formation of α-shaped loops) or not, respectively. Examples of the cis-mechanism of action can be found amongst restriction endonucleases (types I and III), and a trans-mechanism can be frequently encountered during the transcriptional regulation of genes [145].

The basis for creating a model also includes another feature – whether MutS (or a MutS–MutL–DNA ternary complex) remains associated with the mismatch or moves away from it. Stationary and sliding clamp models can be distinguished. To date, all of the abovementioned models are supported by experimental evidence. The sliding clamp model is the most popular one [98, 148–150]. According to this model, MutS loses affinity for the mismatch and forms a structure of a unique DNA-clamp in the ultimate recognition complex containing DNA and two molecules of ATP. In this case, the protein dimer has two channels separated by central (mismatch-binding) domains, the larger of which binds to DNA (*Fig. 3*). Significant restructuring occurs within MutS during the formation of a sliding clamp. It is assumed that the central (mismatch-binding) domains from each subunit of the dimer rotated away from each other, and, hence, the channel size in which the DNA is located increases by a factor of 2 as a result of combination of the two channels [44]. However, these assumptions need to be experimentally verified. In the sliding clamp conformation MutS serves as a "turned on" switch capable of translocating along the DNA and activating the functions of other proteins in the MMR system. Hydrolysis of ATP is not required in order for this type of translocation of MutS to occur [104]. "Molecular clamps" perform important functions in the DNA metabolism; e.g., PCNA directs DNA replication and increases the processivity of DNA polymerase. This model is supported by the fact that bacterial MutS proteins and their eukaryotic homologues in the presence

of ATP slide away from the DNA fragment containing a non-canonical base pair, and then from the ends of linear DNA (if they are not blocked by bulky groups or tightly bound proteins) [98, 151]. Recent studies [104] carried out employing fluorescence techniques enabled to estimate the lifetime of a sliding clamp. It was found to be relatively long and was approximately 10 min. The discussed mechanism suggests the possibility of the binding of several molecules of MutS to DNA containing a mismatch, which can improve the efficiency of a repair process [145].

According to other models, MutS must remain bound to the DNA. For instance, Kunkel and Erie [13] suggest that the ATP-dependent translocation of MutS away from the mismatch is not necessary for its functioning, and only conformational changes in the protein are important for the subsequent repair events to occur. This model is supported by the fact that the lifetime of the MutS–MutL–DNA ternary complex bound to ATP in the region containing a mismatch is longer than that for individual MutS molecules activated by a mismatch and bound to ATP [145, 151, 152]. It is highly probable that *in vivo* MutS can translocate away from the mismatch but only for short distances as the results of footprinting [152] and studies performed using the surface plasmon resonance technique [150] demonstrate that the DNA site in the mismatch region is covered by bound proteins. Kunkel and Erie also suggest that DNA bending in the mismatch-containing region or any DNA deformation caused by the MutS protein must be maintained during all phases of the MMR, which will serve as a directing and probably terminating signal during exonuclease degradation of the DNA daughter strand [13]. This is only feasible if the contact between the mismatch and the MutS is preserved.

According to another stationary model, the signal transduction from MutS to MutH (between the mismatch site and the strand discrimination site) occurs as a result of a large number of MutL molecules binding to the DNA (formation of nucleoprotein filaments) until the strand discrimination site is reached (*Fig. 9B*) [153]. Experimental confirmation of this model has been recently obtained. The fluorescence microscopy technique was used on live cells producing fluorescently labeled MutL and MutS proteins; it was demonstrated that in the mismatch region the number of MutL protein molecules exceeds that of MutS by a factor of 3 [154]. However, this number is not sufficiently large to be able to unambiguously confirm the model of polymerization.

There are models suggesting DNA looping out (trans-models, *Fig. 9C*). The first suggestion of such a mechanism was proposed as a result of an investigation of the MutH activation in the presence of MutS and MutL. In the experiment the mismatch was located on one plasmid and the 5'-Gm^{6}ATC-3'/3'-CTAG-5' site – on another. In the control group, both sites were located on the same plasmid. DNA cleavage efficiency in both cases coincided [152]. Moreover, protein-free DNA is rarely encountered within the cell. Typically, almost immediately after replication it becomes structured with the involvement of proteins and as a result MutS sliding along the DNA is hindered [115]. The data obtained using atomic force microscopy also support the model that includes looping out of DNA. These data indicate the importance of MutS tetramerization in the presence of ATP [148, 155]. Two types of MutS-DNA complexes can be identified in the microphotographs. The first type consists of a MutS-DNA dimer, and the other is a DNA loop formed by two protein dimers. Hence, MutS homodimers can be assigned to two groups with respect to the functions where a certain number of molecules remain bound to the mismatch and the other pull the DNA through itself, maintaining contact with the first dimer. The "immobile" group of MutS dimers can result from the hydrolysis of ATP in one of the domains of the dimer. Both the cis- and trans-mechanisms of the MMR process can be explained from the point of view of this "combined" mechanism.

CONCLUSION

Currently, various views regarding the MMR mechanism exist; therefore, extensive ongoing research in this area still continues. The identification of a single mismatch amongst many thousands of canonical base pairs in the DNA is a unique process [155]. The fluorescence resonance energy transfer technique at the single molecule level has enabled to identify many conformations of the MutS protein in the presence of canonical DNA ligands [104]. However, binding of the MutS protein to DNA during the search for a mismatch, which is a key event of the MMR process, has not yet been fully characterized. The pending issues concern not only the short-lived intermediate MutS-DNA complexes but more complicated complexes as well: MutS–MutL–DNA and MutS–MutL–MutH–DNA. In order to characterize these complexes, one can use a combination of various optical [95, 153, 154] and fluorescence [104] techniques associated with crosslinking of proteins to proteins and proteins to DNA [144]. A recently proposed approach to investigating short-lived complexes based on the covalent fixation of MutS to the DNA is considered to be rather promising [156].

Investigations of the MutS structure during DNA scanning are required. It is believed that the mismatch-binding domains of both subunits of the MutS dimer lose affinity for each other: thereby, the protein channel in which the DNA is located undergoes a 2-fold

increase in size [44]. The study of mutual coordination of MMR system proteins is a particularly complicated issue. The same is true for the influences of other cellular proteins on the activity of the abovementioned proteins. It is obvious that further research is required to create a complete picture of the MMR repair system functioning in living cells. ●

This work was supported by RFBR (grant № 13-04-00615-a) and RFBR-DFG "International Research Groups with participation of young scientists" (grant № 11-04-91336-NNIO_a).

REFERENCES

1. Lewin B. Genes. Boston, MA: Jones Bartlett Publ., 2008. 892 p.
2. Futreal P.A., Coin L., Marshall M., Down T., Hubbard T., Wooster R., Rahman N., Stratton M.R. // Nat. Rev. Cancer. 2004. V. 4. P. 177–183.
3. Drake J.W. // Ann. N.Y. Acad. Sci. 1999. V. 870. P. 100–107.
4. Ayala F.J., Kiger J.A. Modern genetics. University of California, Davis. 1984. V. 2. 296 p.
5. Friedberg E.C., Walker G.C., Siede W. DNA repair and mutagenesis. Washington, D.C.: ASM Press, 1995. 698 p.
6. O'Neil N., Rose A. // WormBook. 2006. P. 1–12.
7. Koshland D.E. Jr. // Science. 1994. V. 266. P. 1925.
8. Lavrik O.I. // Biochemistry (Mosc.). 2011. V. 76. P. 3.
9. Buermeyer A.B., Deschênes S.M., Baker S.M., Liskay R.M. // Annu. Rev. Genet. 1999. V. 33. P. 533–564.
10. Hsieh P. // Mutat. Res. 2001. V. 486. P. 71–87.
11. Marti T.M., Kunz C., Fleck O. // J. Cell Physiol. 2002. V. 191. P. 28–41.
12. Barnes D.E., Lindahl T. // Annu. Rev. Genet. 2004. V. 38. P. 445–476.
13. Kunkel T.A., Erie D.A. // Annu. Rev. Biochem. 2005. V. 74. P. 681–710.
14. Iyer R.R., Pluciennik A., Burdett V., Modrich P.L. // Chem. Rev. 2006. V. 106. P. 302–323.
15. Jiricny J. // Nat. Rev. Mol. Cell Biol. 2006. V. 7. P. 335–346.
16. Fukui K. // Journal of Nucleic Acids. 2010. V. 2010. P. 1–16.
17. Goliasnaia N.V., Tsvetkova N.A. // Mol. Biol. (Mosk). 2006. V. 40. P. 211–223.
18. Modrich P. // Annu. Rev. Genet. 1991. V. 25. P. 229–253.
19. Lichten M., Goyon C., Schultes N., Treco D., Szostak J.W., Haber J.E., Nicolas A. // Proc. Natl. Acad. Sci. U.S.A. 1990. V. 87. P. 7653–7657.
20. Reenan R.A., Kolodner R.D. // Genetics. 1992. V. 132. P. 975–985.
21. Modrich P., Lahue R. // Annu. Rev. Biochem., 1996. V. 65. P. 101–133.
22. Kolodner R.D., Marsischky G.T. // Curr. Opin. Genet. Dev. 1999. V. 9. P. 89–96.
23. Branch P., Aquilina G., Bignami M., Karran P. // Nature. 1993. V. 362. P. 652–654.
24. Duckett D.R., Drummond J.T., Murchie A.I.H., Reardon J.T., Sancar A., Lilley D.M.J., Modrich P. // Proc. Natl. Acad. Sci. U.S.A. 1996. V. 93. P. 6443–6447.
25. Ni T.T., Marsischky G.T., Kolodner R.D. // Mol. Cell. 1999. V. 4. P. 439–444.
26. Mazurek A., Berardini M., Fishel R. // J. Biol. Chem. 2002. V. 277. P. 8260–8266.
27. Li G.M., Wang H., Romano L.J. // J. Biol. Chem. 1996. V. 271. P. 24084–24088.
28. Feng W.Y., Lee E.H., Hays J.B. // Genetics. 1991. V. 129. P. 1007–1020.
29. Mu D., Tursun M., Duckett D.R., Drummond J.T., Modrich P., Sancar A. // Mol. Cell. Biol. 1997. V. 17. P. 760–769.
30. Wang H., Lawrence C. W., Li G. M., Hays J. B. // J. Biol. Chem. 1999. V. 274. P. 16894–1690.
31. Mello J.A., Acharya S., Fishel R., Essigmann P. // Chem. Biol. 1996. V. 3. P. 579–589.
32. Pabla N., Ma Z., McIlhatton M.A., Fishel R., Dong Z // J. Biol. Chem. 2011. V. 286. P. 10411–10418.
33. Stojic L., Brun R., Jiricny J. // DNA Repair (Amst). 2004. V. 3. P. 1091–1101.
34. Greig D., Travisano M., Louis E.J., Borts R.H. // J. Evol. Biol. 2003. V. 16. P. 429–437.
35. Sia E.A., Kokoska R.J., Dominska M., Greenwell P., Petes T.D. // Mol. Cell Biol. 1997. V. 17. P. 2851–2858.
36. Wu B.P., Zhang Y.L., Zhou D.Y., Gao C.F., Lai Z.S. // World J. Gastroenterol. 2000. V. 6. P. 902–905.
37. Bechter O.E., Zou Y., Walker W., Wright W.E., Shay J.W. // Cancer Res. 2004. V. 64. P. 3444–3451.
38. Nguyen B., Elmore L.W., Holt S.E. // Cancer Biol. Ther. 2004. V. 3. P. 293–295.
39. Evans E., Alani E. // Mol. Cell. Biol. 2000. V. 20. P. 7839–7844.
40. Schanz S., Castor D., Fischer F., Jiricny J. // Proc. Natl. Acad. Sci. U.S.A. 2009. V. 106. P. 5593–5598.
41. Chahwan R., Edelmann W., Scharff M.D., Roa S. // Biomed. Pharmacother. 2011. V. 65. P. 529–536.
42. Aravind L., Walker D.R., Koonin E. // Nucleic Acids Res., 1999. V. 27. P. 1223–1242.
43. Michailidi C., Papavassiliou A.G., Troungos C. // Curr. Mol. Med. 2012. V. 12. P. 237–246.
44. Qiu R., DeRocco V.C., Harris C., Sharma A., Hingorani M.M., Erie D.A., Weninger K.R. // EMBO J. 2012. V. 31. P. 2528–2540.
45. Jiricny J., Nystrom–Lahti M. // Curr. Opin. Genet. Dev. 2000. V. 10. P. 157–161.
46. Harfe B.D., Jinks–Robertson S. // Annu. Rev. Genet. 2000. V. 34. P. 359–399.
47. Peltomäki P. // J. Clin. Oncol. 2003. V. 21. P. 1174–1179.
48. Reuschenbach M., Kloor M., Morak M., Wentzensen N., Germann A., Garbe Y., Tariverdian M., Findeisen P., Neumaier M., Holinski–Feder E. et al. // Fam. Cancer. 2010. V. 9. P. 173–179.
49. Lahue R.S., Au K.G., Modrich P. // Science. 1989. V. 245. P. 160-464.
50. Balganesh T.S. Lacks S.A. // J. Bacteriol. 1985. V. 162. P. 979–984.
51. Radman M., Wagner R. // Annu. Rev. Genet. 1986. V. 20. P. 523–538.
52. Li G.M. // Cell Res. 2008. V. 18. P. 85–98.
53. Zhao J., Winkler M.E. // J. Bacteriol. 2000. V. 182. P. 5025–5028.
54. Fourrier L., Brooks P., Malinge J.M. // J. Biol. Chem. 2003. V. 278. P. 21267–21275.
55. Lamers M.H., Perrakis A., Enzlin J.H., Winterwerp H.H.K., de Wind N., Sixma T.K. // Nature. 2000. V. 407. P. 711–717.

56. Wildenberg J., Meselson M. // Proc. Natl. Acad. Sci. U.S.A. 1975. V. 72. P. 2202–2206.
57. Wagner R., Meselson M. // Proc. Natl. Acad. Sci. U.S.A. 1976. V. 73. P. 4135–4139.
58. Lyons S.M., Schendel F. // J. Bacteriol. 1984. V. 159. P. 421–423.
59. Duppatla N.J., Rao D.N. // Prog. Nucleic Acid Res. Mol. Biol. 2006. V. 81. P. 1–49.
60. Lu A.–L., Clark S., Modrich P. // Proc. Natl. Acad. Sci. U.S.A. 1983. V. 80. P. 4639–4643.
61. Glickman B.W. // Mutat. Res. 1979. V. 61. P. 153–162.
62. Marinus M.G., Poteete A., Arraj J.A. // Gene. 1984. V. 28. P. 123–125.
63. Gorman J., Chowdhury A., Surtees J.A., Shimada J., Reichman D.R., Alani E., Greene E.C. // Mol. Cell. 2007. V. 28. P. 359–370.
64. Nishant K.T., Plys A.J., Alani E. // Genetics. 2008. V. 179. P. 747–755.
65. Claverys J.–P., Mejean P., Gasc A.–M., Sicard A.M. // Proc. Natl. Acad. Sci. U.S.A. 1983. V. 80. P. 5956–5960.
66. Yamaguchi M., Dao V., Modrich P. // J. Biol. Chem. 1998. V. 273. P. 9197–9201.
67. Mechanic L.E., Frankel B.A., Matson S.W. // J. Biol. Chem. 2000. V. 275. P. 38337–38346.
68. Matson S.W., Robertson A.B. // Nucleic Acids Res. 2006. V. 34. P. 4089–4097.
69. Cooper D.L., Lahue R.S., Modrich P. // J. Biol. Chem. 1993. V. 268. P. 11823–11829.
70. Viswanathan M., Burdett P., Baitinger C., Modrich P., Lovett S.T. // J. Biol. Chem. 2001. V. 276. P. 31053–31058.
71. Han E.S., Cooper D.L., Persky N.S., Sutera V.A. Jr., Whitaker R.D., Montello M.L., Lovett, S.T. // Nucleic Acids Res. 2006. V. 34. P. 1084–1091.
72. Lohman T.M., Ferrari M.E. // Annu. Rev. Biochem. 1994. V. 63. P. 527–570.
73. Bjornson K.P., Blackwell L. J., Sage H., Baitinger C., Allen D., Modrich P. // J. Biol. Chem. 2003. V. 278. P. 34667–34673.
74. Kang J., Huang S., Blaser M.J. // J. Bacteriol. 2005. V. 187. P. 3528–3537.
75. Snowden T., Acharya S., Butz C., Berardini M., Fishel R. // Mol. Cell. 2004. V. 15. P. 437–451.
76. Hollingsworth N.M., Ponte L., Halsey C. // Genes Dev. 1995. V. 9. P. 1728–1739.
77. Culligan K.M., Meyer–Gauen G., Lyons–Weiler J., Hays J.B. // Nucleic Acids Res. 2000. V. 28. P. 463–471.
78. Obmolova G., Ban C., Hsieh P., Yang W. // Nature. 2000. V. 407. P. 703–710.
79. Junop M.S., Obmolova G., Rausch K., Hsieh P., Yang W. // Mol. Cell. 2001. V. 7. P. 1–12.
80. Lamers M.H., Winterwerp H.H.K., Sixma T.K. // The EMBO Journal. 2003. V. 22. P. 746–756.
81. Natrajan G., Lamers M.H., Enzlin J.H., Winterwerp H.H.K., Perrakis A., Sixma T.K. // Nucleic Acids Res. 2003. V. 31. P. 4814–4821.
82. Alani E., Lee J.Y., Schofield M.J., Kijas A.W., Hsieh P., Yang W. // J. Biol. Chem. 2003. V. 278. P. 16088–16094.
83. Lebbink J.H.G., Fish A., Reumer A., Natrajan G., Winterwerp H.H., Sixma T.K. // J. Biol. Chem. 2010. V. 285. P. 13131–13141.
84. Lebbink J.H.G., Georgijevic D., Natrajan G., Fish A., Winterwerp H.H.K., Sixma T.K., de Wind N. // The EMBO J. 2006. V. 25. P. 409–419.
85. Lamers M.H., Georgijevic D., Lebbink J.H., Winterwerp H.H., Agianian B., de Wind N., Sixma T.K. // J. Biol. Chem. 2004. V. 279. P. 43879–43885.
86. Warren J.J., Pohlhaus T.J., Changela A., Iyer R.R., Modrich P.L., Beese L.S. // Mol. Cell. 2007. V. 26. P. 579–592.
87. Jiricny J. // Curr. Biol. 2000. V. 10. P. R788–790.
88. Biswas I., Hsieh P. // J. Biol. Chem. 1997. V. 272. P. 13355–13364.
89. Sixma T. K. // Curr. Opin. Struct. Biol. 2001. V. 11. P. 47–52.
90. Yamamoto A., Schofield M.J., Biswas I., Hsieh P. // Nucleic Acids Res. 2000. V. 28. P. 3564–3569.
91. Junop M.S., Yang W., Funchain P., Clendenin W., Miller J.H. // DNA Repair (Amst). 2003. V. 2. P. 387–405.
92. Hunter W.N., Brown T., Kneale G., Anand N.N., Rabinovich D., Kennard O. // J. Biol. Chem. 1987. V. 262. P. 9962–9970.
93. Skelly J., Edwards K.J., Jenkins T.C., Neidle S. // Proc. Natl. Acad. Sci. U.S.A. 1993. V. 90. P. 804–808.
94. Werntges H., Steger G., Riesner D., Fritz H.J. // Nucleic Acids Res. 1986. V. 14. P. 3773–3790.
95. Wang H., Yang Y., Schofield M.J., Du C., Fridman Y., Lee S.D., Larson E.D., Drummond J.T., Alani E., Hsieh P. et al. // Proc. Natl. Acad. Sci. U.S.A. 2003. V. 100. P. 14822–14827.
96. Hirano M., Hirano T. // EMBO J. 2002. V. 21. P. 5733–5744.
97. Verdon G., Albers S. , van Oosterwijk N., Dijkstra B.W., Driessen A.J., Thunnissen A.M. // J. Mol. Biol. 2003. V. 334. P. 255–267.
98. Gradia S., Subramanian D., Wilson T., Acharya S., Makhov A., Griffith J., Fishel R. // Mol. Cell. 1999. V. 3. P. 255–261.
99. Joshi A., Rao B.J. // Biochemistry. 2002. V. 41. P. 3654–3666.
100. Hess M.T., Gupta R.D, Kolodner R.D. // J. Biol. Chem. 2002. V. 277. P. 25545–25553.
101. Joseph N., Duppatla V., Rao D.N. // Prog. Nucleic Acid Res. Mol. Biol. 2006. V. 81. P. 1–49.
102. Antony E., Hingorani M.M. // Biochemistry. 2004. V. 43. P. 13115–13128.
103. Calmann M.A., Nowosielska A., Marinus M.G. // Nucleic Acids Res. 2005. V. 33. P. 1193–1200.
104. Jeong C., Cho W.K., Song K.M., Cook C., Yoon T.Y., Ban C., Fishel R., Lee J.B. // Nat. Struct. Mol. Biol. 2011. V. 18. P. 379–385.
105. Cheng X., Blumenthal R.M. // Structure. 1996. V. 4. P. 639–645.
106. Bischerour J., Chalmers R. // PLoS One. 2009. V. 4. e6201. doi: 10.1371/journal.pone.0006201.
107. Gradia S., Acharya S., Fishel R. // Cell. 1997. V. 91. P. 995–1005.
108. Fishel R. // Genes Dev. 1998. V. 12. P. 2096–2101.
109. Antony E., Hingorani M.M. // Biochemistry. 2003. V. 42. P. 7682–7693.
110. Martik D., Baitinger C., Modrich P. // J. Biol. Chem. 2004. V. 279. P. 28402–28410.
111. Drotschmann K., Hall M.C., Shcherbakova P.V., Wang H., Erie D.A., Brownewell F.R., Kool E.T., Kunkel T.A. // Biol. Chem. 2002. V. 383. P. 969–975.
112. Kijas A.W., Studamire B., Alani E. // J. Mol. Biol. 2003. V. 331. P. 123–138.
113. Acharya S., Foster P.L., Brooks P., Fishel R. // Mol. Cell. 2003. V. 12. P. 233–246.
114. Bowers J., Sokolsky T., Quach T., Alani E. // J. Biol. Chem. 1999. V. 274. P. 16115–16125.
115. Mukherjee S., Law S.M., Feig M. // Biophysical J. 2009. V. 96. P. 1707–1720.
116. Polosina Y.Y., Cupples C.G. // Mutat. Res. 2010. V. 705. P. 228–238.
117. Zhao N., Zhu F., Yuan F., Haick A.K., Fukushige S., Gu

L., Her C. // Biochem. Biophys. Res. Commun. 2008. V. 370. P. 338–343.
118. Dherin C., Gueneau E., Francin M., Nunez M., Miron S., Liberti S.E., Rasmussen L.J., Zinn-Justin S., Gilquin B., Charbonnier J.B. et al. // Mol. Cell. Biol. 2009. V. 29. P. 907–918.
119. Kanao R., Hanaoka F., Masutani C. // Biochem. Biophys. Res. Commun. 2009. V. 389. P. 40–45.
120. Bende S.M., Grafstrom R.H. // Nucleic Acids Res. 1991. V. 19. P. 1549–1555.
121. Grilley M., Welsh K.M., Su S.S., Modrich P. // J. Biol. Chem. 1989. V. 264. P. 1000–1004.
122. Ban C., Junop M., Yang W. // Cell. 1999. V. 97. P. 85–97.
123. Ban C., Yang W. // Cell. 1998. V. 95. P. 541–552
124. Hu X., Machius M., Yang W. // FEBS Lett. 2003. V. 544. P. 268–273.
125. Guarné A., Ramon–Maiques S., Wolff E.M., Ghirlando R., Hu X., Miller J.H., Yang W. // EMBO J. 2004. V. 23. P. 4134–4145.
126. Pillon M.C., Lorenowicz J.J., Uckelmann M., Klocko A.D., Mitchell R.R., Chung Y.S., Modrich P., Walker G.C., Simmons L.A., Friedhoff P., Guarné A. // Mol. Cell. 2010. V. 39. 145–511.
127. Namadurai S., Jain D., Kulkarni D.S., Tabib C.R., Friedhoff P., Rao D.N., Nair D.T. // PloS One. 2010. 5: e13726-e13726
128. Kosinski J., Steindorf I., Bujnicki J.M., Giron-Monzon L., Friedhoff P. // J. Mol. Biol. 2005. V. 351. P. 895–909.
129. Jones D.T. // J. Mol. Biol. 1999. V. 292. P. 195–202.
130. Jun S.H., Kim T.G. // FEBS J. 2006. V. 273. P. 1609–1619.
131. Sacho E.J., Kadyrov F.A., Modrich P., Kunkel T.A., Erie D.A. // Mol. Cell. 2008. V. 29. P. 112–121.
132. Spampinato C., Modrich P. // J. Biol. Chem. 2000. V. 275. P. 9863–9869.
133. Giron-Monzon L., Manelyte L., Ahrends R., Kirsch D., Spengler B., Friedhoff P. // J. Biol. Chem. 2004. V. 279. P. 49338-49345.
134. Schofield M.J., Hsieh P. // Annu. Rev. Microbiol. 2003. V. 57. P. 579–608.
135. Robertson A., Pattishall S.R. // J. Biol. Chem. 2006. V. 281. P. 8399-8408.
136. Kadyrov F.A., Dzantiev L. // Cell. 2006. V. 126. P. 297–308.
137. Ban C., Yang W. // EMBO J. 1998. V. 17. P. 1526–1534.
138. Yang W. // Mutat. Res. 2000. V. 460. P. 245-256.
139. Friedhoff P., Thomas E., Pingoud A. // J. Mol. Biol. 2003. V. 325. P. 285–297.
140. Lee J.Y., Chang J., Joseph N., Ghirlando R., Rao D.N., Yang W. // Mol. Cell. 2005. V. 20. P. 155–166.
141. Toedt G.H., Krishnan R., Friedhoff P. // Nucleic Acids Res. 2003. V. 31. P. 819–825.
142. Polosina Y.Y., Cupples C.G. // BioEssays. 2010. V. 32. P. 51–59.
143. Mendillo M.L., Hargreaves V.V., Jamison J.W., Mo A.O., Li S., Putnam C.D., Woods V.L. Jr., Kolodner R.D. // Proc. Natl. Acad. Sci. U.S.A. 2009. V. 106. P. 22223-22228.
144. Winkler I., Marx A.D., Lariviere D., Heinze R.J., Cristovao M., Reumer A., Curth U., Sixma T.K., Friedhoff P. // J. Biol. Chem. 2011. V. 286. P. 17326–17337.
145. Kolodner R.D., Mendillo M.L., Putnam C.D. // Proc. Natl. Acad. Sci. U.S.A. 2007. V. 104. P. 12953–12964.
146. Pluciennik A., Modrich P. // Proc. Natl. Acad. Sci. U.S.A. 2007. V. 104. P. 12709–12713.
147. Dzantiev L., Constantin N., Genschel J., Iyer R.R., Burgers M., Modrich P. // Mol. Cell. 2004. V. 15. P. 31–41.
148. Allen D.J., Makhov A., Grilley M., Taylor J., Thresher R., Modrich P., Griffith J.D. // EMBO J. 1997. V. 16. P. 4467–4476.
149. Blackwell L.J., Martik D., Bjornson K., Bjornson E.S., Modrich P. J. // Biol. Chem. 1998. V. 273. P. 32055–32062.
150. Blackwell L.J., Wang S., Modrich P. // J. Biol. Chem. 2001. V. 276. P. 33233–33240.
151. Mazur D.J., Mendillo M.L., Kolodner R.D. // Mol. Cell. 2006. V. 22. P. 39–49.
152. Schofield M.J., Nayak S., Scott T.H., Du C., Hsieh P. // J. Biol. Chem. 2001. V. 276. P. 28291–28299.
153. Modrich P. // Annu. Rev. Biochem. 1987. V. 56. P. 435–466.
154. Elez M., Radman M., Matic I. // Nucleic Acids Res. 2012. V. 40. P. 3929–3938.
155. Jiang Y., Marszalek E. // EMBO J. 2011. V. 30. P. 2881–2893.
156. Heinze R.J., Sekerina S., Winkler I., Biertümpfel C., Oretskaya T.S., Kubareva E., Friedhoff P. // Mol. Biosyst. 2012. V. 8. P. 1861–1864.

Non-Viral Delivery and Therapeutic Application of Small Interfering RNAs

N. A. Nikitenko*, V. S. Prassolov
Engelhardt Institute of Molecular Biology, Russian Academy of Sciences, Vavilova Str., 32, Moscow, Russia, 119991
*E-mail: nanthalia@gmail.com
Received 18.02.2013

ABSTRACT **RNA interference (RNAi) is a powerful method used for gene expression regulation. The increasing knowledge about the molecular mechanism of this phenomenon creates new avenues for the application of the RNAi technology in the treatment of various human diseases. However, delivery of RNA interference mediators, small interfering RNAs (siRNAs), to target cells is a major hurdle. Effective and safe pharmacological use of siRNAs requires carriers that can deliver siRNA to its target site and the development of methods for protection of these fragile molecules from in vivo degradation. This review summarizes various strategies for siRNA delivery, including chemical modification and non-viral approaches, such as the polymer-based, peptide-based, lipid-based techniques, and inorganic nanosystems. The advantages, disadvantages, and prospects for the therapeutic application of these methods are also examined in this paper.**
KEYWORDS **RNA interference; small interfering RNA; non-viral delivery.**
ABBREVIATIONS **RNAi – RNA interference; dsRNA – double-stranded RNA; siRNA – small interfering RNA; shRNA – small hairpin RNA; miRNA – microRNA; dsRNA – double-stranded RNA; RISC – RNA-induced silencing complex; NP – nanoparticle.**

INTRODUCTION

RNA interference (RNAi) is an evolutionarily conserved mechanism of gene expression regulation. Application of interfering RNAs offers opportunities for the development of novel methods for preventing and treating various human diseases [1]. Recent advances in biology and medicine have extended the range of anticipated therapeutic targets. Medicinal agents based on the RNAi principle and intended for use in the treatment of infectious diseases, cancer, and genetic disorders are currently undergoing clinical trials. Such medicinal products as therapeutic ribozymes, aptamers, and small interfering RNAs (siRNAs) are commonly used in various areas of scientific research, as well as in the therapy and diagnosis of human diseases. It should be noted that interfering RNAs possess potential immunogenicity, are characterized by low stability, and require efficient and safe methods for delivery to target cells. Nevertheless, the promising results of clinical trials demonstrate that these barriers can be overcome by improving the synthetic carriers and chemical modifications of RNA [2]. Various methods of non-viral delivery of interfering RNAs, as well as their advantages, disadvantages, and their prospects for application in clinical practice, are discussed in this review. A fairly short review certainly cannon provide a thorough description of each method. Our goal was to highlight the variety of already developed and tested methods of siRNA delivery, which will enable an interested reader to quickly understand the existing problem. We hope that our work will be interesting to a wide circle of readers of *Acta Naturae*.

MECHANISM OF RNA INTERFERENCE

The emergence of exogenous (viral or synthetic, introduced during the experiment) or endogenous (a product of the transcription of a cell's own genes) double-stranded RNA (dsRNA) in a cell induces RNA interference. The minimum size of dsRNA sufficient for the induction of interference is 21 bp. It is most likely that this restriction protects cellular mRNAs containing short intramolecular self-complementary structures against degradation [3, 4].

After the dsRNA penetrates into a cell, the RNase III enzyme Dicer (*Fig. 1*) recognizes and cleaves it [5, 6]. This evolutionarily conserved protein was found in yeast *Schizosaccharomyces pombe*, lower fungus *Neurospora crassa*, and lower and higher plants and animals, including mammals and humans [3, 4].

The Dicer molecule (*Fig. 1*) contains a double-stranded RNA-binding domain (dsRBD) located at the C-terminus, the central domain PAZ that binds to dsRNA with two unpaired nucleotides at the 3'-end,

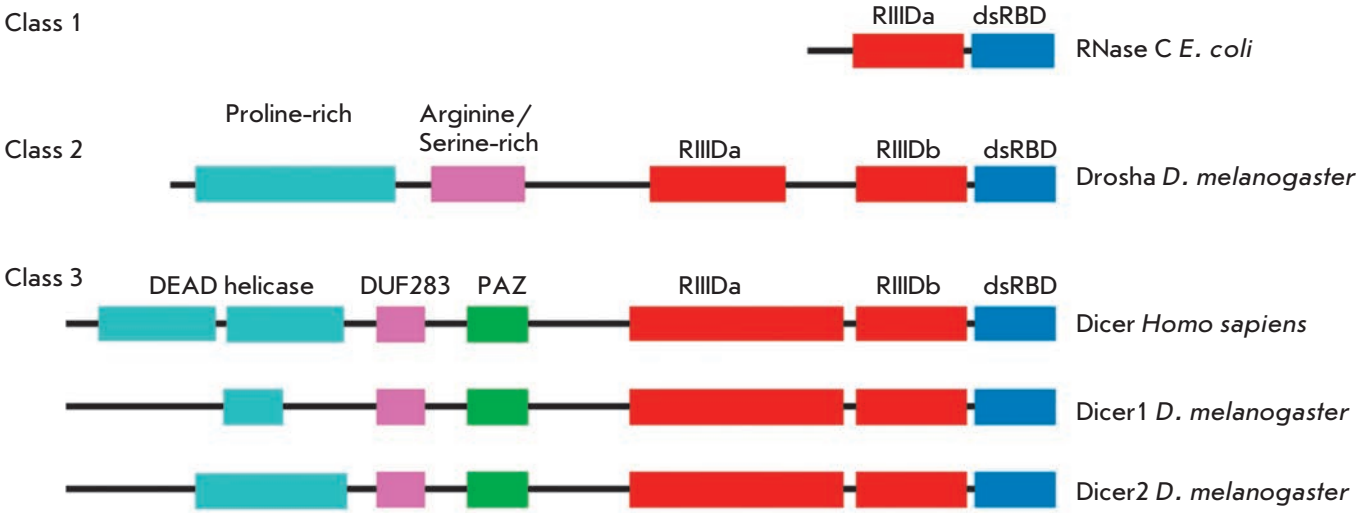

Fig. 1. Domain organization of the RNaseIII gene family [11]

and N-terminal domains – the helicase domain DEAD-box and DUF283 (Domain of Unknown Function 283), which are not crucial for the *in vitro* functioning of the Dicer protein [7, 8].

Dicer also contains two RNase domains (RNase III domain – RIIID) forming an intramolecular pseudodimer in which both catalytic sites localize in close proximity to one another. Each domain cleaves one of the dsRNA strands, yielding duplexes with two unpaired nucleotides at the 3'-ends (*Fig. 2*) [9–11].

In mammals and *Caenorhabditis elegans*, Dicer molecules of the same type are intended for the processing of miRNAs and siRNAs. There are two types of Dicer molecules in Drosophila: Dicer1 – for miRNAs and Dicer2 – for siRNAs. Dicer activity leads to the formation of 21-to 25-nucleotide-long dsRNA (species-specific feature), which has 2-base 3'-overhangs, carries hydroxyl groups at the 3'-ends, and phosphate groups at the 5'-ends [12].

The next phase in the interference process is the formation of the RLC complex (RISC-loading complex) [13]. It consists of the Dicer and TRBP (TAR RNA binding protein) proteins and/or - PACT and dsRNA fragment in humans (in *Drosophila melanogaster* – Dicer1/LOQS and Dicer2/R2D2 for miRNAs and siRNAs, respectively). One of the dsRNA ends is characterized by a higher melting temperature, thus being more thermodynamically stable. Hence, it is believed to bind to the TRBP, while another interacts with Dicer [14]. This arrangement of dsRNA in the RLC complex apparently determines which of the two RNA strands will be the guide strand (complementary to the target mRNA) and which will be the passenger strand (subject to degradation) [15]. RLC transfers dsRNA to the Ago2 protein belonging to the Argonaute family (*Fig. 3*), which is the major protein of the pre-RISC (RISC – RNA-induced silencing complex) complex. Ago2 consists of three major domains (*Fig. 3*): PAZ acting as a binding site for the 3'-end of the siRNA guide strand; MID is a binding site for the 5'-end of the siRNA passenger strand; and PIWI, which is structurally similar to RNase H [16].

The PIWI domain exhibits endonuclease activity [17]. As part of the Ago protein, it cleaves the phosphodiester bond between the nucleotides of the passenger strand complementary to bases 10 and 11 of the guide strand [10]. After the passenger strand is degraded, the pre-RISC complex becomes the functionally active RISC complex (RISC contains only an antisense guide RNA strand complementary to the segment of the target mRNA). The target mRNA molecule is subsequently cleaved (*Fig. 4*) to yield a 21- to 23-nucleotide-long fragments [13]. The mechanism described above is typical of siRNAs (*Fig. 4*). Processing of miRNAs includes several additional phases (*Fig. 4A*).

First, an extended primary transcript – pri-miRNA (which has a hairpin-like structure of the "stem-loop" type) – is synthesized on the miRNA gene with the assistance of RNA polymerase II (or, less frequently, RNA polymerase III) [18, 19]. miRNA genes are typically represented by clusters that are transcribed as single polycistronic units [20]. Meanwhile, the genes of certain miRNAs act as independent transcription units [21]. Processing of pri-miRNAs is carried out in the nucleus with the assistance of a complex consisting of two proteins (RNase type III), Drosha and Pasha (DGCR8 protein is an analog in *D. melanogaster*, *C. elegans* and

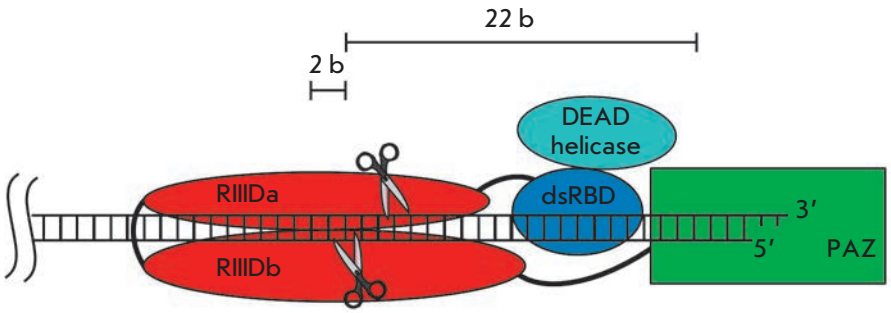

Fig. 2. Model for Dicer catalysis. The PAZ domain binds to the 2 nucleotides 3′ overhang of the dsRNA terminus. Domains RIIIDa and RIIIDb form a pseudo-dimer. Each domain hydrolyzes one strand of the substrate [11]

mammals), carrying two dsRNA-binding domains (dsRBD – double-stranded RNA-binding domain). Pasha interacts with pri-miRNAs, enabling Drosha to cleave the hairpin stem at a distance of 11 bp from its base. This gives rise to pre-miRNA 60–70 nucleotides in length characterized by a hairpin structure, 2-base 3'-overhang, and a 5'-phosphate group. In dipterans, worms, and mammals, certain pre-miRNAs are formed without the involvement of the Drosha enzyme (DGCR8).

Further events depend on the degree of homology between miRNA and the target mRNA. Most of the investigated animal miRNAs are not characterized by complete complementarity between the nucleotide sequence and the target mRNA [3, 4]. However, certain miRNAs in dipterans and mammals are fully complementary to their target mRNAs, resulting in direct mRNA cleavage by endonucleases [22]. Most miRNAs are imperfectly complementary to their target gene. Usually only a short sequence at the 5'-terminal region of miRNA known as the "seed" matches the target mRNA. The "seed" region is one of the factors determining the specificity of the target choice. Due to the small size of the "seed" it is assumed that one miRNA can regulate the expression of hundreds of different genes [23, 24].

PROBLEMS IN APPLICATION AND DELIVERY OF siRNAs

The application of siRNA in therapeutic practice shows significant limitations: sensitivity to serum nucleases [25]; the possibility of non-specific binding; the action of siRNA via the miRNA mechanism, resulting in the suppression of the expression of non-target genes, whose mRNAs are partially complementary to the "seed" region [26]; and activation of the innate immune response [27].

In order to achieve a therapeutic effect during systemic delivery, small interfering RNA molecules need to be in their active form during circulation in the blood stream, and they need to avoid kidney filtration, phagocytosis, formation of aggregates with serum proteins, and degradation by nucleases. Furthermore, siRNAs need to pass through the endothelial barrier to penetrate into the tissues. This barrier retains molecules larger than 5 nm. However, hepatic and splenic blood vessels allow molecules smaller than 200 nm in diameter to pass through, while tumor vessels let through substances with a molecular weight of 40 kDa. This phenomenon is known as the enhanced permeation and retention effect – EPR [28].

After siRNA molecules leave the bloodstream, they have to pass through the extracellular matrix, the network of structural proteins and polysaccharides surrounding the target cells. The extracellular matrix can significantly hinder the cellular absorption of siRNAs, thereby increasing the likelihood of their phagocytosis and digestion [29].

The plasma membrane is the major barrier for siRNA to penetrate into a cell. The hydrophilic nature, high molecular weight, and net negative charge of siRNA molecules result in their absorption being of low efficiency. Several ways to solve this problem have been proposed: for instance, binding of siRNA molecules to

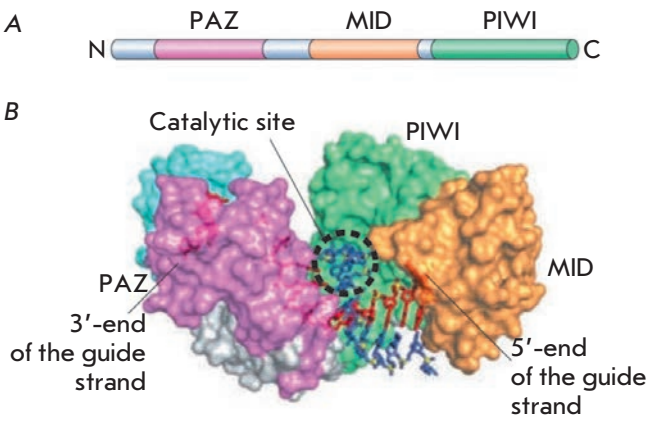

Fig. 3. Argonaute proteins. *A* – Ago-family proteins are composed of three characteristic domains: the PAZ, MID and PIWI domains. *B* – The PAZ domain acts as a docking site for the 3′end of siRNA, whereas the MID domain anchors the 5′ terminal nucleotide [10, 13]

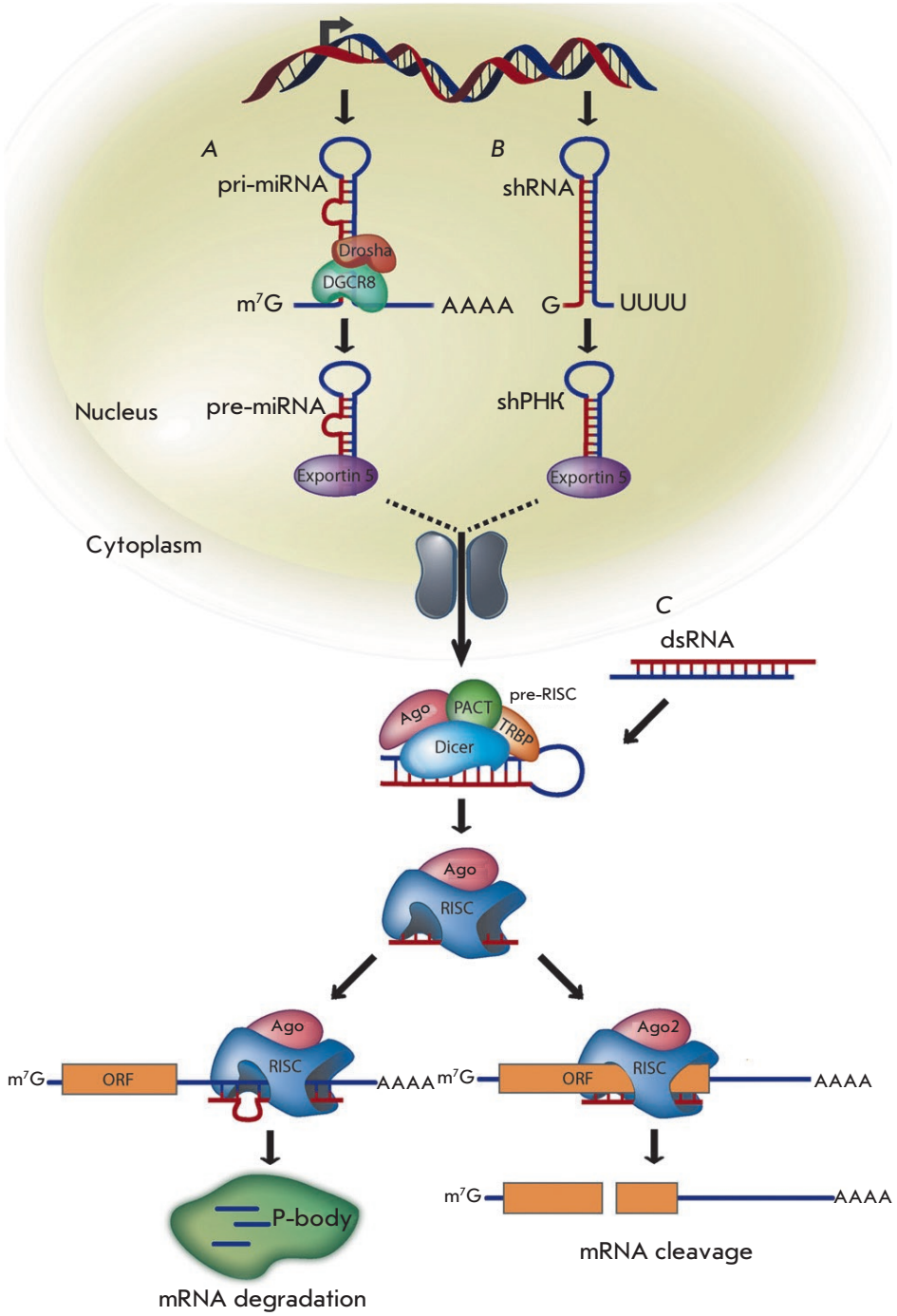

Fig. 4. Mammalian posttranscriptional gene silencing pathway for miRNAs, shRNAs, and siRNAs. *A* – miRNAs are transcribed from DNA as primary miRNAs (pri-miRNAs) and processed into 70 nt stem-loop precursor miRNAs (pre-miRNAs) by Drosha and DGCR8. The pre-miRNAs are transported to the cytoplasm by dsRNA-binding protein exportin 5, where they are processed into 22 nt miRNA duplexes by the Dicer/TRBP complex. The imperfectly complementary miRNA duplexes associated with the AGO protein are loaded into RISC, where the passenger strand is removed and the guide strand remains to target mRNA for silencing. The resulting mature RISC complex may silence gene expression either by inhibiting the initiation of translation or by transporting the complex to cytoplasmic processing bodies (p-bodies), where the mRNA is deadenylated and destroyed. *B* – Identically to miRNAs, shRNAs are transcribed from DNA and undergo similar processing. However, the perfect Watson-Crick base-pairing between the guide strand and the target mRNA triggers AGO2-mediated cleavage of the mRNA target. *C* – In contrast to shRNAs, siRNAs are artificially introduced into the cytoplasm. All steps of siRNA and shRNA are identical after processing by Dicer/TRBP [2]

cationic polymers and lipids results in the neutralization of the negative charge of siRNAs and formation of positively charged complexes [30].

Non-viral carriers have been shown to penetrate into cells via endocytosis. Clathrin-mediated endocytosis, caveolae-mediated endocytosis, macropinocytosis, and clathrin- and caveolae-independent endocytosis have been distinguished [31]. Unlike viruses, synthetic vectors are characterized by low transfection efficiency. One of the approaches to increasing the absorption of carriers by cells is to bind the specific ligands that contribute to the receptor-mediated endocytosis of transport molecules. These ligands are typically targeted at the receptors that mediate the absorption of nutrients: transferrin, folic acid, and low-density lipoprotein receptors [32, 33].

Having penetrated into a cell, siRNA molecules localize in early endosomes. The vacuolar H^+-ATPase activ-

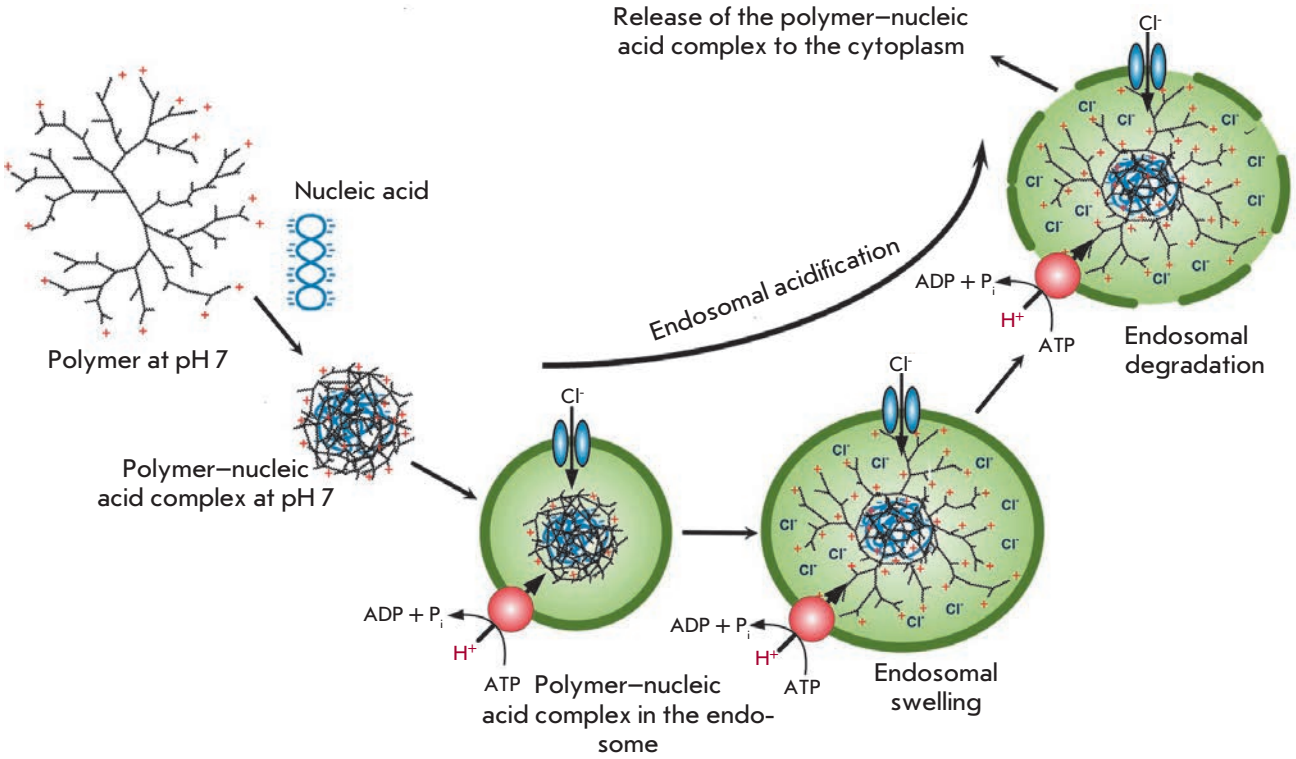

Fig. 5. Schematic representation of the proton sponge and umbrella effect hypothesis. Cationic polymers form a complex with a negatively charged nucleic acid. At lower pH in the endosomes, the complex partially unfolds. Due to the protonation of the terminal amino groups and electrostatic repulsion, the terminal branches of the polymer spread out and adopt the fully extended conformation [40]

ity causes the acidification of the internal environment of early endosomes (a decrease to pH 5–6), resulting in their transformation into late endosomes. The fusion of late endosomes with lysosomes occurs subsequently. The latter are characterized by even lower pH values (approximately 4.5) and contain nucleases that cleave siRNAs. In order to avoid degradation within lysosomes, siRNA molecules (in the unbound form or in complex with a carrier) need to leave the endosomes and enter the cytosol. Leaving the endosome is the key stage that puts limits on the RNA interference process [34, 35].

Efficient siRNA delivery using various cationic polymers is attributed to the high buffering capacity of these compounds (due to the unprotonated secondary or tertiary amines) in a pH range of 5–7. These polymers are believed to act as proton sponges, thus preventing endosomal acidification (*Fig. 5*). This process is accompanied by an increase in the proton influx through the activation of the vacuolar H^+-ATPase, combined with the accumulation of chloride anions Cl^-, as well as an increase in osmotic pressure. This leads to osmotic swelling and endosomal disintegration [36–38].

The umbrella hypothesis, which describes the ability of polymers to undergo voluminous expansion at pH 5–6, has also been proposed (*Fig. 5*). The proton excess in endosomes results in protonation of tertiary amines in the internal part of the polymer. Due to the electrostatic repulsion between the adjacent, charged amino groups, the terminal branches of the polymer are unfolded; the complex is transformed from a folded state to a branched state (provided that there are no steric constraints) [39, 40].

The escape of cationic lipid vectors from the endosomes is predominantly mediated by electrostatic interactions between these molecules and the negatively charged phospholipid membranes of the endosomes, as well as by the ability of lipid structures to transit from the lamellar phase (a bilayer) to the hexagonal phase. The formation of cation-anion pairs destabilizes the lipid bilayers, resulting in the release of a nucleic acid from the complex [41, 42].

CHEMICAL MODIFICATIONS OF RNA

The half-life of unmodified siRNAs in blood serum does not exceed 15 minutes, which significantly impedes

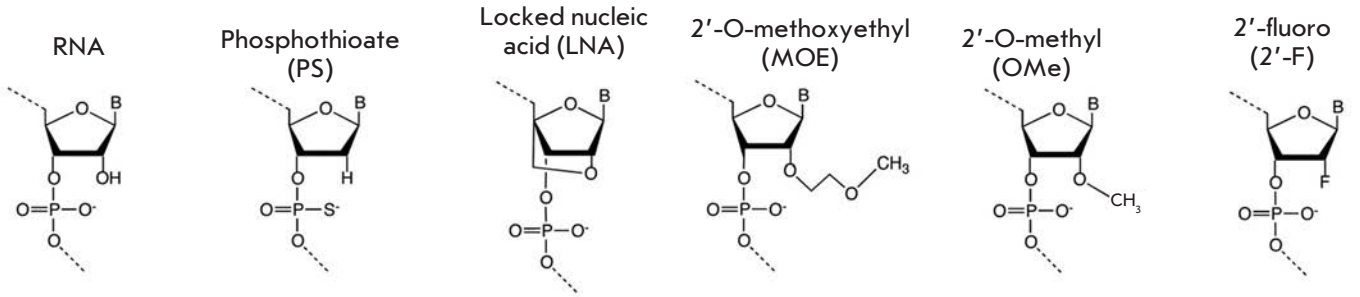

Fig. 6. Chemical modifications of RNA

their clinical use [25, 43]. According to Y. Zou *et al.* [44], the guide strand in rat and human blood serum is to a significant extent affected by exonucleases, while the passenger strand is more affected by endonucleases. Chemical modification is the most common method applied to increase the siRNA stability (resistance to blood serum nucleases) [45, 46]. However, it should be remembered that modification may result in a loss of the biological activity of siRNAs [45].

Selection of the chemical modifications to be effected is determined by the nucleotide sequence of siRNA and their presumed scope of application, as well as the delivery method [26]. Most of the siRNAs that are currently used in scientific, pre-clinical, and clinical studies are synthetic 21 bp RNA duplexes that imitate the structure of natural siRNAs. The 19, 25, and 27 bp RNA duplexes with blunt ends and asymmetric 25/27 or 27/29 bp RNA duplexes are also used in basic research and for drug development [47, 48].

The following types of chemical modifications of siRNAs can be distinguished: modifications of the phosphate backbone of a molecule, a sugar, or bases [49]. Despite the large number of approaches that can be applied to modify the RNA structure, the following modifications are the ones most commonly used (*Fig. 6*): phosphorothioate (PS), 2'-O-methyl (2'-OMe), 2'-fluoro (2'-F), 2'-O-methoxyethyl (2'-MOE), and locked nucleic acid (LNA) [2, 46, 50]. Phosphate backbone modifications entail changes to the phosphodiester bonds of the nucleotides in the RNA molecule. Phosphorothioate results from the replacement of a nonbridging phosphate oxygen atom with a sulfur atom. This modification was first used over 25 years ago; however, it is still commonly used [51]. PS-modification adds the following properties to oligonucleotides: enhanced *in vivo* resistance to nuclease degradation; ability to effect an RNase H-mediated cleavage of the target mRNA; and increased affinity for blood plasma proteins reducing renal clearance and, thus, preventing rapid excretion of oligonucleotides from the organism [2, 52]. Introduction of phosphorothioates reduces the melting point of the siRNA duplexes by approximately 0.5°C per single PS [53]. It should be borne in mind that molecules with a PS-modification can nonspecifically bind to cell membrane proteins, thereby enhancing siRNA cytotoxicity [53]. T. Tuschl *et al.* [53] have reported the cytotoxicity of siRNAs where every second nucleotide contained a PS. It was demonstrated that toxicity can be reduced by decreasing the total PS concentration. The same effect can be achieved by introducing this modification into one siRNA end only. According to Z.Y. Li *et al.* [54], the introduction of PS modifications into positions 3, 5, and 17 at the 5'-end of the passenger strand improves the efficiency of siRNA activity by accelerating the loading of the guide strand into the RISC complex. On the other hand, direct introduction of PS modifications into the guide strand reduces efficiency in the suppression of gene expression with the involvement of siRNA [53, 54].

Modifications at position 2 of the ribose ring are the most commonly used (*Fig. 6*): 2'-O-methyl, 2'-fluoro-, and 2'-O-methoxyethyl [55, 56]. siRNA modified in this way forms a type A thermostable duplex. This is attributed to the fact that 3'-endo- is the preferred conformation of the modified sugar [2, 56]. 2'-O-methyl-RNAs were detected among the ribosomal and transport RNAs of mammals. The introduction of 2'-OMe increases the melting temperature of siRNA duplexes by 0.5–0.7°C per single modification, as well as simultaneously increasing their resistance to nucleases and increasing the efficiency of siRNA activity [53, 56]. It is recommended that 2'-OMe-modifications be introduced into the passenger strand. The introduction of these modifications into the guide strand can reduce the efficiency of RNAi, because binding between the guide strand and the RISC complex becomes impossible [57]. The addition of 2'-OMe, along with PS, increases the affinity of the guide strand for the target mRNA and increases siRNA resistance to nucleases without decreasing the efficiency of RNA interference [56, 57].

The introduction of 2'-fluoro-modifications does not impede the functioning of siRNA and protects the du-

plex from nuclease cleavage. Inclusion of 2'-F- at the pyrimidine positions maintains the *in vitro* and *in vivo* activity of siRNA [58, 59]. 2'-F-modification of the siRNA cleavage site by the Ago2 protein does not affect the efficiency of RNAi [60]. RNA duplexes containing both 2'-F-pyrimidines and 2'-OMe-purines are characterized by an extremely high stability in blood serum, as well as an increased efficiency in the *in vivo* inhibition of gene expression [61]. It has been shown that these siRNAs can function 500 times more efficiently than the unmodified RNAs [59].

2'-Fluoro-β-*D*-arabinonucleotide (FANA) is another important 2'-C-modification of ribose [56, 62, 63]. The introduction of FANA increases the melting temperature of the RNA duplex by approximately 0.5°C per modification [64]. FANA differs from other 2'-C- modifications as it contains arabinose and is structurally similar to DNA (in its 2'-*endo*-conformation). The stereochemistry of FANA is opposite to that of ribose with fluorine at position 2. The introduction of FANA modifications into the RNA duplex inevitably causes distortions in the structure of this molecule. Therefore, this modification should not be introduced into the guide strand. Meanwhile, the efficiency of RNA interference is significantly increased by introducing FANA modifications along the entire length of the passenger strand and at the 3'-end of the guide strand [62, 63].

Ribose modification using 2'-O-methoxyethyl (MOE) is also commonly used. The insertion of MOE results in increased affinity of siRNA for target RNA, increased resistance against the *in vivo* action of nucleases, and reduction of the nonspecific binding of proteins, which can minimize toxic effects. However, this modification should not be introduced into the guide strand. This is associated with the occurrence of steric constraints in the interaction between the side groups of Ago2 and, as a consequence, the inability to load the guide strand into the RISC [55, 65, 66].

It was demonstrated that siRNAs containing both 2'-fluoropyrimidines and 2'-methoxypurines are characterized by extremely high resistance to the action of the nucleases found in the human blood serum (half-life of the guide strand is up to three days) [61]. Locked nucleic acid is a modification in which the 2'- and 4'-positions in the ribose ring are linked to one another via a methylene bridge (*Fig. 6*). The furanose ring is locked in the 3'-*endo*-conformation, which makes it structurally similar to the conventional RNA monomer [67]. The rigidity of the LNA conformation ensures a more efficient organization of the phosphate backbone and the strengthening both of the stacking interactions between the bases and of the hybridization of the guide strand with the target RNA. The high affinity of LNA-modified siRNAs allows one to use shorter sequences (approximately 16 nucleotides instead of 20). The insertion of a single LNA modification can increase the melting temperature of the RNA duplex by 5–10°C. The choice of the position in which to introduce the modification is very important. It was demonstrated that the presence of LNA at positions 10, 12, and 14 of the guide strand results in elimination of the interfering activity in siRNAs. This is attributed to steric and conformational changes when the LNA is inserted near the cleavage site [67, 68]. The presence of LNA at the 3'-end of siRNA protects the duplex against the action of the 3'-exonucleases found in blood serum [69]. Nevertheless, the *in vivo* use of LNA-modified siRNAs is difficult because of their high hepatotoxicity [70].

Modified siRNAs also include spiegelmeres. These molecules are L-oligo-ribonucleotides, the enantiomers of natural *D*-RNAs, originating from the German word "Spiegel" (a mirror). The high resistance of spiegelmeres against nucleases, along with the high affinity of these molecules to target RNA, makes them extremely promising for therapeutic applications [71].

NON-VIRAL DELIVERY SYSTEMS FOR SMALL INTERFERING RNAs

The first studies in the field of delivery of oligonucleotides into cells have been focused on designing synthetic vectors for DNA delivery [72, 73]. Recombinant viral vectors have showed promising results *in vitro*. However, after significant drawbacks and complications during clinical trials were encountered, much attention begun to be focused on non-viral delivery systems, as well [73]. The following types of complexes and nanoparticles (NPs) with a diameter ranging from 1 to 1,000 nm are currently used for interfering RNA delivery: polyplexes, cationic peptides, liposomes, quantum dots, carbon nanotubes, and other inorganic nanoparticles [73].

Polyplexes

Small interfering RNA complexes with cationic polymers are known as polyplexes. These compounds are capable of self-assembly due to ionic interactions between the repetitive, positively charged regions of polymers and negatively charged phosphate groups of siRNAs. The major advantage of polymers is their structural flexibility, which enables them to easily alter the physicochemical properties of the delivery system. Molecular weight, charge density, solubility, and hydrophobicity can be adjusted according to the experimental conditions. Thus, a change in the polymer : siRNA ratio allows one to regulate the neutralization degree of complex charges. Various chemical groups can also be added in order to change the parameters of the polymer molecules and to impart new properties to

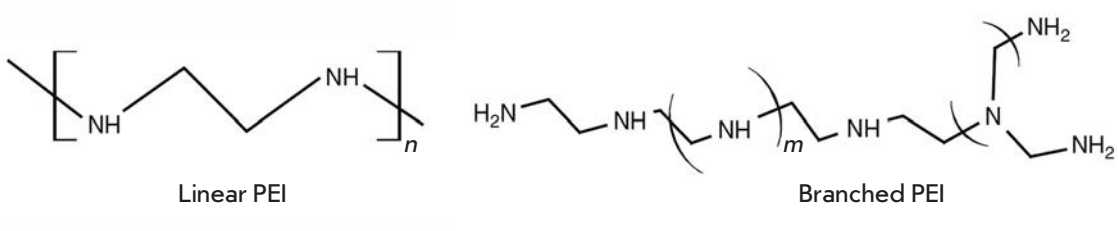

Fig. 7. Polyethylenimine (PEI)

them. Both natural and synthetic polymers are utilized to design polyplex systems for the delivery of nucleic acids into mammalian cells [74–76].

Polyethyleneimine (PEI) (*Fig. 7*) is considered to be one of the most efficient tools to deliver oligonucleotides due to its exceptional ability to undergo endocytosis and exhibit endosomolytic activity. High-molecular-weight PEIs (25 kDa) are commonly applied to deliver small interfering RNAs [77]. The high charge density of the polymer results in the formation of a strong bond between PEI and siRNA and ensures its efficient protection against enzymatic degradation. However, the high cytotoxicity and limited biodegradation of this polymer hinder its clinical application [78, 79]. A low-molecular-weight PEI (< 2 kDa) is less toxic; however, it delivers siRNAs less efficiently. It is considered that PEI and other cationic polymers increase the permeability of the cell membrane by forming short-lived nanoscale holes in it [77, 80]. It is also presumed that the destabilizing effect exerted on the membranes can be the reason for cytotoxicity [80]. Another factor affecting the efficiency and toxicity of PEI is the degree of branching in the polymer structure [60]. A branched PEI contains primary, secondary, and tertiary amines at a 1 : 2 : 1 ratio, while a linear polymer consists of secondary amines only (except for the terminal primary amines) (*Fig. 7*) [81]. A branched PEI is superior to a linear type in terms of the efficiency of nucleic acid delivery [81].

Complexes based on the copolymer of lactic and glycolic acids (poly(lactic-co-glycolic acid) – PLGA) are commonly used as carriers of siRNA and other oligonucleotides. Their advantages are a small size, low cytotoxicity, and ability to undergo prolonged circulation in the blood stream [82]. PLGA·siRNA complexes are prepared in two ways: (1) by inserting siRNA into the complex core and (2) by adsorption of siRNA on the surface of modified cationic PLGA nanoparticles via electrostatic interactions. PLGA protects siRNAs against the action of blood serum nucleases and ensures prolonged release of the substance being delivered [83, 84].

PLGA was employed to deliver siRNA against *TNFα* mRNA (tumor necrosis factor α) in order to suppress inflammatory responses. J774.1 cells (mouse macrophages) exhibited a reduction in the mRNA and TNFα protein levels by 50 and 40 % as compared to the control, respectively. The efficiency of anti-TNFα-siRNA was investigated *in vivo* using the mouse model of collagen-induced arthritis. As a result of injections of PLGA·anti-TNFα-siRNA complexes into the affected knee joints, a local decrease in TNFα expression, as well as a significant reduction in the manifestation of the inflammation symptoms of synovial bursa (according to a histological investigation), was observed. It is important to mention that after these complexes had been injected into the joint cavity, a significant amount of siRNA was detected in the synovial membrane where the cells producing TNFα predominantly localize. The inhibitory effect was recorded for 11 days after the siRNA injection had been administered, since PLGA is characterized by sustained release properties with respect to the transported substance [85].

J. Steinbach *et al.* have successfully used PLGA to deliver siRNAs against mRNAs of the *nectin-1* and *UL29.2* genes, which play the key roles in the development of the herpes simplex virus type 2 infection. Significant suppression of the expression of target genes has been achieved both *in vitro* and *in vivo* (using the mouse model). PLGA nanoparticles were also found to exhibit low cytotoxicity. The feasibility of using PLGA·siRNA complexes during an infection with the herpes simplex virus type 2 is demonstrated in this article [86].

Dendrimers, which are also utilized to deliver therapeutic oligonucleotides, are highly branched polymer molecules 1–5 nm in size. Dendrimer branches are symmetrically arranged around the central part of the molecule. Dendrimers consist of three architectural domains (*Fig. 8*): the inner region including the core, dendrons connected to it, and the surface with a large number of reactive sites [87, 88]. Dendrimeric molecules are characterized by monodispersity and hydrophilicity [89, 90]. The feasibility of functionalizing dendrimers, altering their solubility, and attaching fluorescent probes allows one to use these molecules to deliver various therapeutic agents into target cells, including siRNAs [91]. The transferred substance can be bound to the peripheral groups of dendrimers either through

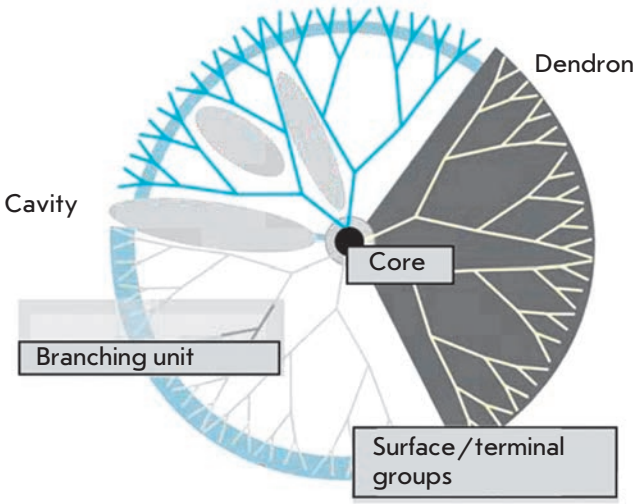

Fig. 8. Dendrimer structure [89]

a covalent bond or by ionic interactions. The transported therapeutic agents can be encapsulated within the dendrimeric particles, thus forming monomolecular micelles [89]. Conjugates derived from dendrimers and transported substances are more stable than liposomes [91]. Highly branched polymers developed in the 1980s, such as polyamidoamine dendrimeric molecules (PAMAM), polypropylenimines (PPI), poly(*L*-lysine) (PLL), and carbon-silane, are now used for siRNA delivery [92].

PAMAM-polymers designed for siRNA delivery are commercially available (Polyfect and Superfect) [93]. PAMAM has been successfully used for *in vitro* and *in vivo* delivery of siRNAs into neurons (intracranial injection to rabbits) and exhibited very low toxicity levels [94].

Y. Tang *et al.* studied *in vitro* and *in vivo* efficiency in the delivery of anti-GFP-siRNA (GFP – green fluorescent protein) using nanoparticles based on PEGylated (bound to polyethylene glycol) PAMAM. A significant decrease in the *GFP* expression level in HEK293 (human embryonic kidney fibroblasts) and Cos7 (green monkey kidney fibroblasts) cells was observed under the action of anti-GFP-siRNA. The transfection efficiency of PAMAM·siRNA nanoparticles was comparable to the efficiency of Lipofectamine 2000 (Invitrogen). Intramuscular administration of these complexes to GFP-transgenic mice also revealed a decrease in the expression level of mRNA of the green fluorescent protein. PAMAM nanoparticles were shown to reliably protect siRNAs against blood serum nucleases [95].

Polypropylenimine (PPI) was specifically designed using PEI for siRNA delivery. O. Taratula *et al.* have studied efficiency in delivering siRNAs targeted at *bcl-2* mRNA using polypropylenimine complexes. PPI nanoparticles were coated with polyethylene glycol (PEG) to make them more stable. The distal end of PEG was bound to a synthetic analog of the releasing factor of the luteinizing hormone to provide targeted delivery of siRNAs into tumor cells. A significant *in vitro* reduction in the expression level of the target gene in A2780 (human ovarian cancer) and A549 (human lung cancer) cells was observed. *In vivo* studies have demonstrated a decrease in the growth rate of xenografts derived from the A549 cells in immunodeficient nude mice. The PPI·siRNA complexes predominantly localized in the tumor tissue; the concentration of the nanovector with siRNA in the liver and kidneys was minimal. The PPI-based nanoparticles were found to be characterized by moderate cytotoxicity; however, it is assumed that the decrease in cell viability (by approximately 20 %) can be attributed to the suppression of the expression of the *bcl-2* gene, which plays an important role in the regulation of cell proliferation [96].

The natural polysaccharide chitosan, which is used for siRNA delivery and consists of glucosamine and N-acetylglucosamine monomers (*Fig. 9*), is obtained by deacetylation of chitin [97, 98]. Chitosan is readily cleaved *in vivo* by lysozymes and chitinases [97]. This polymer is virtually non-toxic to mammals [99]. Chitosan·siRNA complexes are typically not larger than 200 nm, which is an advantage for *in vivo* delivery [97, 98]. Despite the relative safety and biocompatibility of chitosan, few *in vivo* experiments have been conducted. This fact can be attributed to the limited efficiency of the polymer for delivering siRNAs. H. Katas and H.O. Alpar are believed to have used chitosan for *in vitro* siRNA delivery for the first time [100]. The method applied to form chitosan complexes with siRNA was found to significantly affect the efficiency of suppression of gene expression at the posttranscriptional level. It has also been demonstrated that chitosan–tripolyphosphate nanoparticles containing siRNAs are characterized by a number of advantages over siRNA-chitosan complexes: they have a higher binding capacity and high filling factor [100].

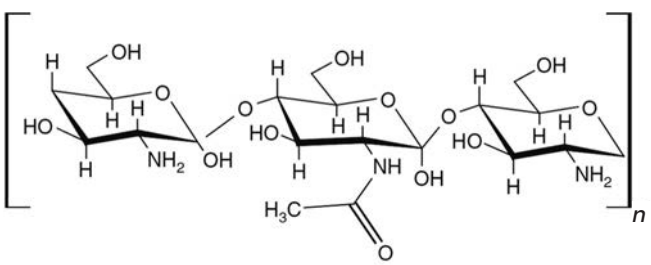

Fig. 9. Chitosan

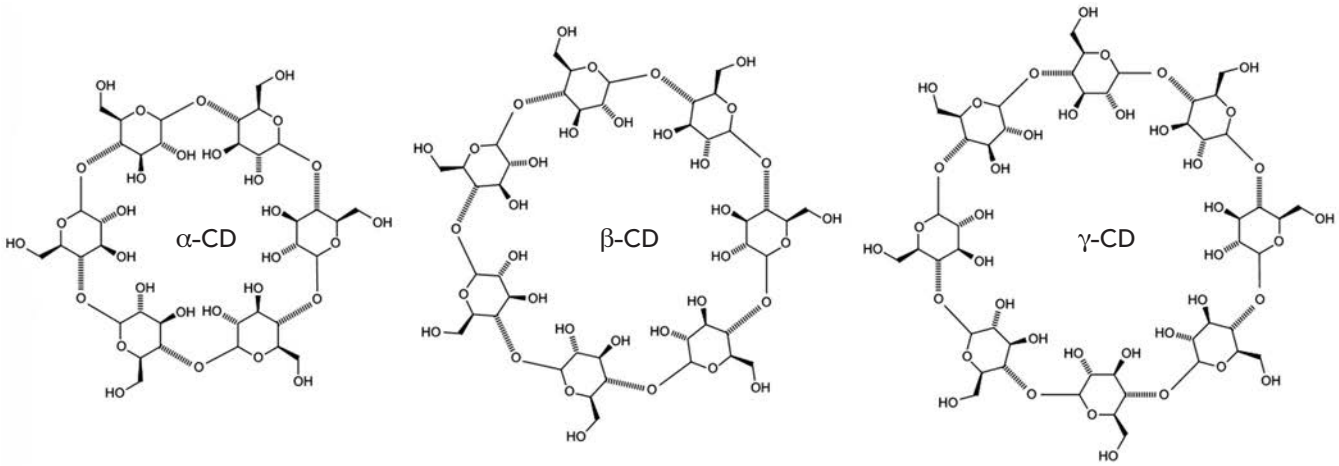

Fig. 10. Chemical structure of cyclodextrins. Cyclodextrins are of three types: α-cyclodextrin (α-CD), β-cyclodextrin (β-CD), and γ-cyclodextrin (γ-CD). α-, β- and γ-cyclodextrins are composed of six, seven, and eight α-(1,4)-linked glycosyl units, respectively

K.A. Howard *et al.* have designed a chitosan-based siRNA delivery system which can be used both *in vitro* and *in vivo*. As a result, ectopic expression of *EGFP* (enhanced green fluorescent protein) in H1299 cells (human non-small cell lung cancer) and mouse peritoneal macrophages was suppressed (reduction in the EGFP fluorescence level by 77.9 and 89.3 %, respectively). It was also demonstrated that chitosan can be used for delivery of anti-EGFP-siRNAs to the bronchiolar epithelial cells of *EGFP*-transgenic mice via intranasal administration. Reduction in the expression of *EGFP* was 37 and 43 % as compared to the mismatch- and negative controls, respectively. These data support the fundamental possibility of using chitosan as a siRNA delivery agent in patients with lesions in mucous membranes [101].

E.J. Nielsen *et al.* [102] have developed a system for delivering anti-EGFP-siRNA to pulmonary epithelium using chitosan nanoparticles in the aerosol form. Transfection of these complexes into H1299 cells reduced the EGFP fluorescence level by 62%. A 68% decrease in EGFP fluorescence as compared to the mismatch control was observed after aerosol nanoparticles had been introduced intratracheally to *EGFP*-transgenic mice. The chitosan·siRNA complexes localized in both alveolar and bronchiolar cells and evenly spread in the entire volume of the lungs. K.A. Howard *et al.* [103] demonstrated that intraperitoneal injection of anti-TNFα-siRNA·chitosan complexes to mice with collagen-induced arthritis reduces the expression of the target gene in peritoneal macrophages by 44% and inhibits the local and general inflammatory responses. Hence, chitosan-based nanoparticles can be used as carriers of therapeutic agents in patients suffering from systemic diseases.

PEGylation of chitosan enhances the stability of siRNA complexes and also increases the half-life of nanoparticles in blood serum [104]. D.W. Lee *et al.* produced chitosan nanoparticles of a specified size by coacervation in the presence of polyguloronate. The diameter of the complexes ranged from 110 to 430 nm, depending on the chitosan : siRNA ratio. These nanoparticles have exhibited high efficiency in the delivery of siRNA into HEK293 (human embryonic kidney fibroblasts) and HeLa (cervical cancer cells) cells, as well as low cytotoxicity [105].

A.M. Ji *et al.* described chitosan·siRNA complexes as irregular, positively charged lamellar and branched structures with a hydrodynamic radius of ~148 nm. These nanoparticles are used for delivery of siRNAs targeted at the mRNA of the gene encoding the FHL2 protein (four-and-a-half LIM-domain protein) expressed in the Lovo cells (colorectal cancer cells). Overexpression of this oncogene has been observed in various types of cancer cells (epithelial ovarian cancer, hepatoblastoma, colon adenocarcinoma, certain types of breast cancer, and the HeLa cell line). A decrease in the expression of the FHL2 gene by 70% was observed; this is comparable to the results obtained after transfection of siRNA using Lipofectamine 2000 (Invitrogen, USA) [106].

Chitosan was also used as a "shell" to enhance the efficiency of other delivery systems. Chitosan-coated particles of polyisohexylcyanoacrylate were utilized to deliver anti-RhoA-siRNA to the cells of breast cancer xenografts in nude mice. Overexpression of the *RhoA* gene (Ras homolog gene family, member A) is associated with poor prognosis in cancer patients, since it accelerates tumor cell proliferation and angiogenesis, as well as invasive tumor growth. Anti-RhoA-siRNA was

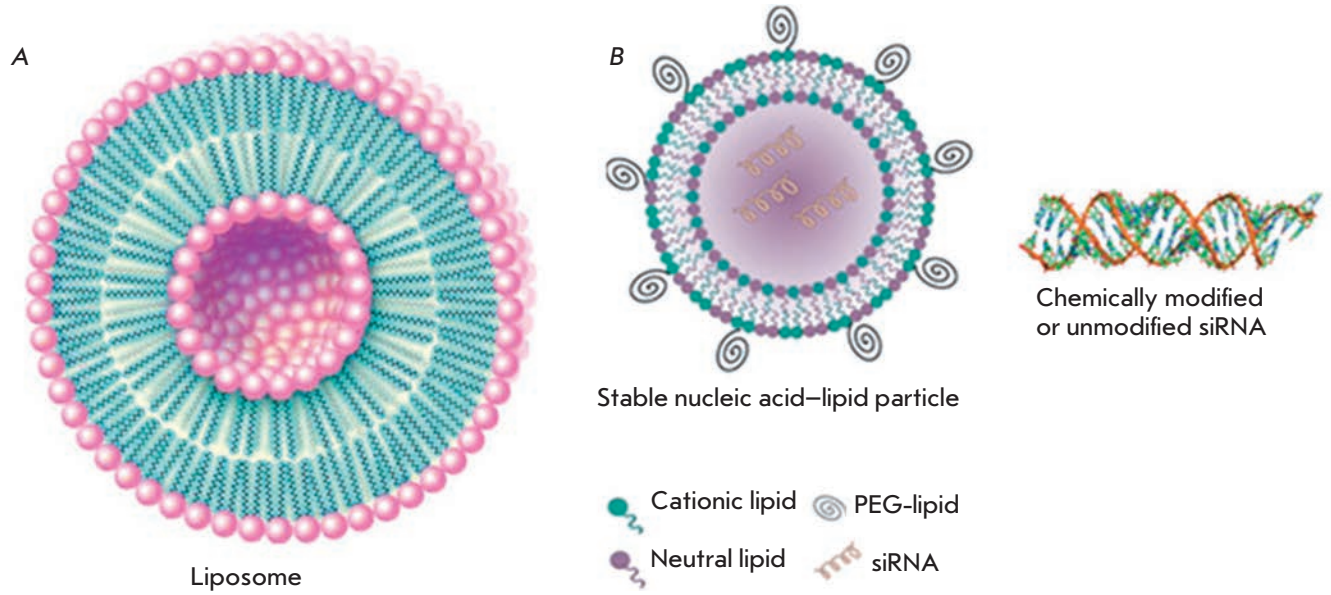

Fig. 11. Lipid-based complexes for siRNA delivery. *A* – Liposome structure (Encyclopaedia Britannica, Inc.). *B* – Structure of the stable nucleic acid lipid particle – SNALP [117]

administered to nude mice every 3 days at a dose of 150 or 1500 μg/kg body weight. As a result of the introduction of this siRNA at a dose of 150 μg/kg, tumor growth was inhibited by over 90%. Introduction of 1500 μg/kg caused partial necrosis of the tumor due to inhibition of angiogenesis. The complexes exhibited no toxic effects [107].

Cyclodextrins are also used for siRNA delivery. They are cyclic (α-1,4)-linked oligosaccharides of β-*D*-glucopyranose. Cyclodextrin molecules are of toroidal shape. They consist of a hydrophobic central cavity and a hydrophilic outer surface (*Fig. 10*) [108, 109]. Cyclodextrins protect siRNAs against degradation by the nucleases found in blood serum and reduce the *in vivo* immunogenicity of siRNA even in the presence of immunostimulatory sequences within the siRNA [109]. Although natural siRNAs are not characterized by immunogenicity, the delivery of double-stranded siRNAs and single-stranded RNAs using liposomes can activate a mammalian immune system. This is accompanied by activation of Toll-like receptors (TLR7, TLR8, and TLR9) in the peripheral mononuclear cells, monocytes, plasmocytoid dendritic cells, and $CD34^+$-precursor cells. The possible reasons for the lack of an immune response associated with the use of cyclodextrins to deliver siRNAs include the antioxidant activity of this delivery system (inhibitors of endosomal oxidation were shown to be capable of blocking the development of an immune response) and the absence of nanoparticle absorption by immunocompetent cells [109].

S. Hu-Lieskovan *et al.* [110] have demonstrated that the use of complex particles formed using cyclodextrin, anti-EWS-FLI1-siRNA, and transferrin (a ligand for targeted delivery) significantly reduces the expression of the target oncogene in Ewing sarcoma cells that express the transferrin receptor.

Patients with solid tumors are currently participating in the first phase of clinical trials of siRNA targeted at mRNA of the *RRM2* gene (Ribonucleoside-diphosphate reductase subunit M2) [111]. *RRM2* encodes a small subunit of the ribonucleotide reductase enzyme that catalyses the conversion of ribonucleotides to deoxyribonucleotides. The inhibitors of ribonucleotide reductase were shown to exhibit an antitumor chemotherapeutic effect. This is attributed to the fact that the reparative capacity of cells depend on the concentration of deoxyribonucleotides [112]. Cyclodextrin-based nanoparticles are used as a system to deliver anti-RRM2-siRNA. Tumor cells in the biopsy material obtained from melanoma patients treated with anti-RRM2-siRNA contain a large number of nanoparticles. A significant decrease in the expression level of mRNA and the RRM2 protein was observed as compared to the levels detected before the therapy [111].

Lipid-based delivery systems

Liposomes are highly organized lipid aggregates (*Fig. 11*). They are formed by one or several closed concentric bilayers made of phospholipids possessing hydrophobic tails and hydrophilic heads, which limit the

inner aqueous phase. Liposomes have been successfully used for delivery of water-soluble substances placed in their hydrophilic core [113, 114].

The widespread use of liposomes for siRNA delivery is associated with their optimal size (approximately 100 nm), good biocompatibility, and the simplicity of the preparation and application procedures [115]. Thus, neutral lipid 1,2-oleoyl-*sn*-glycero-3-phosphocholine (DOPC) can encapsulate up to 65% of siRNAs as a result of mixing the solutions of two components. Liposomes are also prepared from dioleoyl phosphatidylethanolamine (DOPE) (*Fig. 12*), 1,2-distearoyl-*sn*-glycero-3-phosphocholine (DSPC) (*Fig. 12*) , phosphatidylcholine (PC), and other neutral lipids [116].

Liposomes were the first nanoparticles approved for clinical application. These nanoparticles consist of pegylated liposomal doxorubicin complexes. Some 19 out of 53 patients with Kaposi's sarcoma demonstrated a partial response, and one patient exhibited a complete response following administration of doxorubicin within liposomes every 3 weeks. This was accompanied by an increase in the circulation time of doxorubicin in the blood stream, as well as a reduction in its cardiotoxicity [117, 118].

Doxorubicin incorporated in liposomes and used in combination with docetaxel and trastuzumab has been undergoing clinical trials (phase II). A total of 31 patients with metastatic HER2-positive breast cancer participate in the trial. Minimal cardiotoxicity and low incidence of common-side effects have been observed for this drug. Improved prognosis was also recorded in patients with metastatic breast cancer [119].

C.N. Landen *et al.* [120] reported that the expression of *EphA2* (the tyrosine kinase receptor gene associated with poor prognosis in patients with ovarian cancer) in nude mice decreases when using DOPC liposomes as a delivery system. DOPC liposomes were employed to suppress the expression of the PAR-1 receptor gene (protease-activated receptor) in order to halt the growth and metastasis of melanoma due to the reduced angiogenesis. DOPE liposomes were used for delivery of siRNA targeted at *Ubc13* [116, 120].

S.H. Kang *et al.* designed liposomes containing siRNA targeted at *Mcl1* mRNA and the protein kinase MEK inhibitor known as PD0325901. The Raf/MEK/ERK signaling pathway with the MEK kinase involved plays a significant role in the regulation of cell proliferation. Abnormalities in this pathway have been identified for several types of cancer. The *Mcl1* gene product (myeloid cell leukemia sequence 1) belongs to the family of Bcl-2 proteins that regulate apoptosis. Introduction of anti-Mcl1-siRNA into tumor cells enhances their sensitivity to chemotherapeutic agents that induce apoptosis. The antitumor activity of nanoparticles was studied *in vitro*

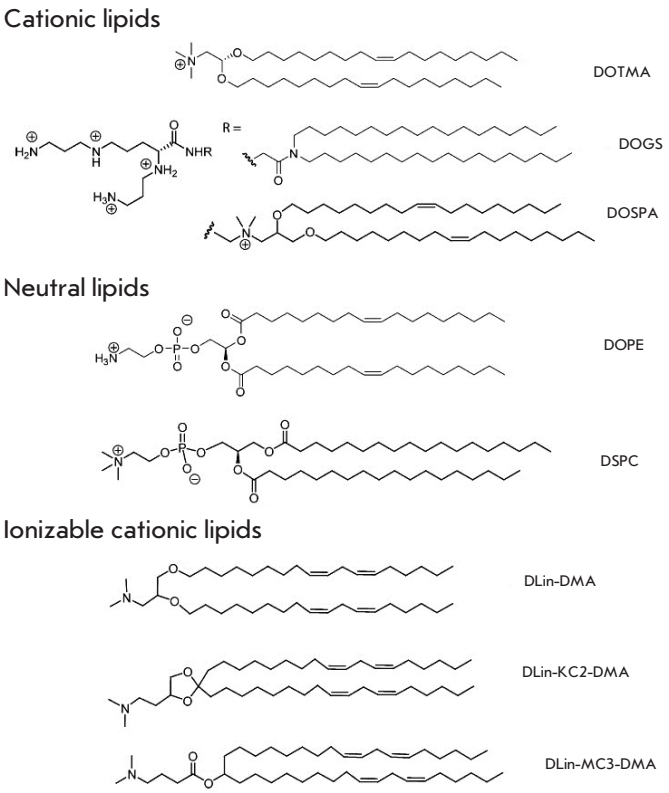

Fig. 12. Cationic, neutral, and ionizable cationic lipids that are important for siRNA delivery [117]

and *in vivo*. Complexes of cationic liposomes based on N,N''-dioleylglutamide with the PD0325901 inhibitor and anti-Mcl1-siRNA were added to KB cells (human nasopharyngeal epidermal carcinoma cells). According to Western blotting data, the amount of Mcl1 and pERK1/2 proteins, as well as the tumor cells survival rate, significantly decreased as compared to the control. These nanoparticles were also administered to BALB/c mice with xenografts derived from the KB cells every 2 days at a dose of 0.7 mg/kg for anti-Mcl1-siRNA and 0.72 mg/kg for the PD0325901 inhibitor. A significant reduction in tumor size (by 79% as compared to the control group) was recorded; the Western blot data were comparable to the results obtained during *in vitro* experiments [121].

Cationic lipid (*Fig. 12*) and nucleic acid complexes are known as lipoplexes. The main advantage of cationic lipids is that they passively interact with negatively charged siRNAs and the cell membrane, which considerably simplifies the internalization process. However, cationic liposomes are more toxic than neutral ones. They are characterized by a lower half-life in blood serum (which can be partly attributed to absorption in the reticuloendothelial system) and increased immu-

nogenicity (attributed to absorption by macrophages) [116].

Lipoplexes based on dimethyl-hydroxyethyl-aminopropane-carbamoyl-cholesterol (DMHAPC-Chol) and dioleoyl phosphatidylethanolamine were successfully applied to deliver siRNA targeted at mRNA of the vascular endothelial growth factor (VEGF) to A431 (human epidermoid carcinoma) and MDA-MB231 (human breast cancer) cells. The introduction of DMHAPC-Chol·DOPE complexes containing anti-VEGF-siRNA reduced the expression of the target gene by over 90 %. These nanoparticles were characterized by higher transfection efficiency as compared to the application of Lipofectamine 2000 (Invitrogen). Transfection of a *GFP*-containing plasmid and anti-GFP-siRNA allowed one to discover that lipoplexes based on DMHAPC-Chol·DOPE are more efficient in transporting siRNA than plasmids [122].

K. Un *et al.* suggested using lipoplexes that are associated with mannose and are sensitive to ultrasound exposure [123–125] for the selective delivery of small interfering RNAs to hepatocytes. This siRNA delivery method combines the advantages of lipofection and sonoporation: a significant amount of the transported nucleic acids can penetrate directly into the cytoplasm due to the pore formation in the cell membrane under ultrasound irradiation. In this article, siRNAs targeted at the mRNA of the intracellular adhesion protein *ICAM-1* gene, whose expression is elevated in liver endothelial cells in the early stages of hepatitis, were used. The expression of *ICAM-1* was significantly lower both *in vitro* in liver endothelial cells and *in vivo* in mouse models of liver inflammation induced by lipopolysaccharides, dimethylnitrosamine, carbon tetrachloride, and ischemia-reperfusion. Furthermore, an *in vivo* anti-inflammatory effect induced by this siRNA was observed. The proposed method for siRNA delivery is considered to be highly promising for treating liver diseases [126].

Stable nucleic acid-lipid particles (SNALPs) have been designed relatively recently by Tekmira Pharmaceuticals Corporation. SNALPs are polymeric nanoparticles ~ 100 nm in size and consisting of ionizable cationic lipids, such as DLin-DMA (1,2-dilinoleyloxy-3-dimethylaminopropane), DLin-KC2-DMA (2,2-dilinoleyl-4-(2-dimethylaminoethyl)-[1,3]-dioxolane) and cholesterol, lipids with a high phase transition temperature (1,2- distearoyl-*sn*-glycero-3-phosphocholine – DSPC), and PEGylated lipids. Complex SNALPs are characterized by a prolonged time of circulation in the blood stream and great potential for modifications, which make it possible to solve various problems associated with siRNA delivery [116, 127].

D.V. Morrissey *et al.* [61] have demonstrated that it is possible to use SNALPs for efficient systemic delivery of siRNAs in a mouse model of viral hepatitis B (HBV). Intravenous administration of SNALPs containing anti-HBV-siRNAs (3 mg/kg) during 3 consecutive days resulted in the inhibition of hepatitis B virus replication. This effect persisted for 7 days after the injection of SNALP·anti-HBV-siRNA complexes.

T.S. Zimmermann *et al.* successfully used SNALPs as a system for delivering siRNAs targeted against apolipoprotein B mRNA (*ApoB*) in Javanese macaque. The liver *ApoB* mRNA levels are reduced by 80–90 % 48 h following a single intravenous administration of 2.5 mg/kg of anti-ApoB-siRNA contained in SNALPs. This is accompanied by a reduction in the concentration of serum cholesterol by 65%. This approach provides a prompt, long-term effect (up to 11 days after the injection of SNALP·siRNA complexes) [128].

SNALPs were successfully utilized to deliver siRNA targeted at PLK1 kinase mRNA. Overexpression of the *PLK1* gene plays an important role in the abnormality in the regulation of the proliferation of tumor cells of different histological origins. Intravenous administration of SNALP·anti-PLK1-siRNA complexes suppressed orthotopic liver tumor growth (Hep3B cells) in mice. SNALPs have also been shown to be not immunogenic [122].

Peptide delivery systems

Peptides can also be used as efficient systems to deliver interfering RNAs [129]. A special class of cationic peptides (cell-penetrating peptides – CPPs) is known as trans-plasma membrane carriers of various macromolecules, including interfering RNAs [130, 131]. HIV-1 Tat protein and INF-1, INF-7 of the influenza virus are the CPPs that were discovered first [116]. Despite their being small in size (5–40 a.a.r.), CPPs can carry substances with a molecular weight 100 times their own [132]. The best-studied CPPs include the basic HIV-1 Tat protein and polyarginine, since basic amino acids (lysine and arginine) participate in the formation of the complex with siRNA [133]. Arginine contains a terminal guanidine group in its side branch, which binds to the cell surface via ionic interactions [134]. CPPs are characterized by a low cytotoxicity level at the concentrations used for the delivery of macromolecules [118, 135].

Two approaches enabling one to use CPPs to deliver interfering RNAs to target cells are currently used [131]. The first approach is based on the formation of a covalent bond between CPPs and siRNAs [136]. The covalent bond between siRNAs and CPP is formed via the disulfide or, less frequently, thioester bond that is degraded in the cytoplasm [137]. It should be mentioned that the use of this strategy can reduce siRNA activity because of incomplete dissociation of the CPP·siRNA complex [131].

Successful *in vitro* application of CPPs penetratin and transportan, which are covalently bound to siRNA targeted at *GFP* mRNA, has been described by A. Muratovska *et al.* Transfection of CPP·siRNA conjugates into *GFP*-expressing CHO (Chinese hamster ovary) cells reduced the GFP fluorescence level by 53 and 63 %, respectively. The use of Lipofectamine 2000 (Invitrogen) resulted in fluorescence reduction by only 36 % [138]. CPP nanoparticles containing penetratin and TAT have recently been tested *in vivo*. siRNA targeted against mRNA of p38 MAP-kinase (this protein is involved in the development of various inflammatory responses) was covalently bound to one of the following carriers: TAT, penetratin, or cholesterol. Incubation of the complexes with mouse fibroblasts resulted in a reduction in the expression of p38 MAP-kinase by 20–36%. However, intratracheal administration of these complexes to mice revealed no significant changes in the expression of p38 MAP-kinase. In addition, penetratin·siRNA complexes increased the levels of TNFα and IL12 immune markers. Thus, it can be assumed that CPPs can activate the immune response [118, 139].

Another approach is based on the formation of complexes between CPPs and siRNAs via the electrostatic interactions associated with positively charged CPPs binding to the negatively charged siRNAs [140, 141]. The latter gives rise to a very stable complex in which siRNA is reliably protected against degradation by blood serum nucleases [131]. However, this approach is associated with the risk of neutralizing the positive charge of CPPs during the electrostatic interactions with siRNAs; hence, binding of CPPs to the plasma membrane and the subsequent absorption of the CPP·siRNA complex becomes impossible [142, 143]. The article by J. Hoyer *et al.* is an illustration of the use of the "noncovalent" approach for the formation of CPP·siRNA nanoparticles [144]. The researchers have synthesized branched derivatives of the truncated form of human calcitonin and evaluated their efficiency as a tool for the delivery of siRNA targeted against mRNA of the human NPY Y_1 receptor gene. This receptor belongs to the family of G-protein-coupled receptors, whose expression increases in the presence of various systemic diseases. Thus, reduction in the expression level of the NPY Y_1 receptor gene is considered to be one of the potential directions for osteoporosis therapy. It has been demonstrated that CPPs can efficiently deliver siRNAs into HEK293 cells without exhibiting any signs of cytotoxicity. The reduction in target gene expression is comparable to the results obtained lipofection.

L. Johnson *et al.* have described the POD peptide (peptide for ocular delivery), which is a CPP designed to deliver macromolecules into eye tissues. POD has been successfully applied to transfer anti-GFP-siRNA into a human retinal embryonic stem cell culture where *GFP* is ectopically expressed. The expression level of transgenic *GFP* decreased by over 50%. It was also shown both *in vitro* and *in vivo* that POD can effectively deliver quantum dots into eye tissues [145].

Inorganic nanoparticles for siRNA delivery

Inorganic nanomaterials (carbon nanotubes, quantum dots, gold nanoparticles, etc.) are an alternative method to deliver interfering RNAs [146–149]. These nanoparticles differ from organic ones in their structure, dimensions, physical, and chemical properties; they can also be functionalized easily. These materials reproduce the structural properties of high-molecular-weight polymers, while possessing a lowmolecular weight [150].

Carbon nanotubes (CNTs) are linear, elongated cylindrical layers graphene. Single-walled carbon nanotubes are composed of one graphene layer, while multi-walled ones consist of several concentric single-walled nanotubes. The diameter of a single-walled nanotube is less than 0.4 nm, while that of a multi-walled one can be ~100 nm. The length of these structures typically ranges from hundreds of nanometers to several dozens of micrometers. The unique feature of carbon nanotubes is the graphene layer that can be easily modified using various biomolecules. CNTs·siRNAs complexes can be formed via a covalent or noncovalent bond. Carbon nanotubes are nontoxic to mammalian cells as they can pass through the cell membrane via the endocytosis-independent pathway without adversely affecting its integrity [146, 151].

I.B. Neagoe *et al.* compared the *in vitro* efficiency of single-walled CNTs to that of the commercial transfection agent siPORT NeoFX, which is manufactured by Ambion and used for delivery of siRNAs targeted at *TNFα* and *VEGF* mRNAs. The expression level (as a percentage of the baseline level) was 53.7 and 56.7% for the *VEGF* and *TNFα*, respectively, when siPORT NeoFX was used. When using single-walled CNTs, the expression level was 47.7 and 46.5%, respectively [152].

X. Wang *et al.* demonstrated that ammonium-modified CNTs can bind to siRNA targeted against A2 cyclin mRNA via electrostatic interactions. The introduction of CNT·anti-cyclin A2-siRNA complexes into K526 (human erythroleukemia) cells causes cell growth inhibition and death [153].

Quantum dots (QDs) are colloidal semiconductor nanoparticles [147]. QDs are typically used as fluorescent probes due to their unique physical and chemical properties that make it possible to overcome the limitations of fluorescent proteins and organic dyes. These nanoparticles have a broad excitation band (which al-

lows one to excite differently colored nanocrystals by a single electromagnetic radiation) and narrow symmetrical fluorescence peaks. In addition, QDs exhibit high photostability [154]. They can be efficient tools to deliver therapeutic oligonucleotides. For instance, QDs have been successfully used for simultaneous visualization and delivery of siRNAs in order to selectively inhibit the expression of the epidermal growth factor receptor III gene in U87 cells (human glioblastoma cells) [155].

High cytotoxicity is the main hurdle for a possible clinical application of QDs as fluorescent probes and delivery tools: most QDs contain highly toxic cadmium (Cd), selenium (Se), or tellurium (Te) [156]. Hence, the application of QDs is currently limited to *in vitro* studies only.

In order to solve the toxicity problem, W.B. Tan *et al.* incorporated QDs in chitosan-based nanoparticles and used these conjugates as carriers of siRNA targeted against mRNA of the human epidermal growth factor receptor (*HER2/neu*). The delivery of siRNA to cells was monitored using flow cytometry techniques. A significant suppression of human *HER2/neu* gene expression was attained [157].

M.V. Yezhelyev *et al.* designed QDs coated with a polymer that absorbs protons (a proton sponge) [158]. The balanced composition of positively and negatively charged functional groups (such as carboxylic acids and tertiary amines) on a QD surface enables to apply these nanoparticles in efficient and safe siRNA delivery. QDs coated with a proton sponge layer increased efficiency in the suppression of cyclophilin B gene expression by 10–20 times, while their cytotoxicity in the MDA-MB231 cells (breast cancer) was decreased by 5–6 times as compared to Lipofectamine 2000 (Invitrogen), TransITTKO (Mirus Bio Corp.), and JetPEI (Qbiogene). Moreover, the QD·siRNA complexes exhibit identical transfection efficiency both in the absence and in the presence of serum in the culture medium, while the best results for other transfection agents can be achieved only in a serum-free medium. The absorption of these nanoparticles by cells can be monitored interactively using the QD fluorescence signal. The localization of complexes in various cellular compartments can be determined using electron microscopy by detecting the presence of semiconductors [158].

A new type of quantum dots has recently been obtained (I-III-VI_2): $AgInS_2$, $CuInS_2$ and $ZnS{\cdot}AgInS_2$. P. Subramaniam *et al.* synthesized a library of $Zn_xS{\cdot}Ag_yIn_{1-y}S_2$ (ZAIS) quantum dots with variable physical properties (photoluminescence). ZAIS quantum dots were shown to exhibit a considerably lower cytotoxicity level as compared to their analogs; thus, they can also be used as multifunctional nanoparticles for simultaneous visualization and siRNA delivery into U87 glioblastoma cells [159].

Gold nanoparticles possess the unique chemical and physical properties required for oligonucleotide transport. They are almost inert and nontoxic; their size varies between 1 and 150 nm [148].

S.T. Kim *et al.* assessed efficiency in the suppression of β-galactosidase (*β-gal*) gene expression in SVR-bag4 endothelial cells by RNA interference. The nanoparticles synthesized by the researchers consisted of a gold core (2 nm in diameter) and polymeric dendrons with terminal triethylenetetramine, and they were used as a delivery system. Positively charged dendrons were bound to the negatively charged siRNA via electrostatic interactions. The suppression of the β-*gal* expression was found to be dependent on the NP:siRNA ratio; maximum reduction in the β-*gal* expression level was 48% at a NP:siRNA ratio = 2. Efficiency in transfection with gold nanoparticles was comparable to that achieved with Lipofectamine 2000 (Invitrogen) [160].

Alternative classification of nanovectors

The dose and biological activity of the substance carried by NPs depends on several factors: the kinetics of the binding to the cell surface and internalization, intracellular processing, final localization of NPs, and the cell cycle stage. The kinetics of cell surface binding and internalization depends on the size, shape, charge, and biological activity of NPs. During cell division, nanoparticles are distributed randomly and unevenly; hence, the nanoparticle concentration in each daughter cell can be different. The metabolic pathway of a NP and its final location in the cell determine the dose and biological activity of the delivered substance [161, 162].

Three main classes can be distinguished (with regard to their functions and features) among a vast variety of delivery systems with different compositions, geometries, and surface modifications.

The first generation of nanovectors is represented by the simplest nanoparticles that are passively delivered to the target sites. These vectors are delivered to tumor cells due to the enhanced penetration and retention (EPR) effect, which is the transfer of substances from blood vessels to the tumor tissue and their accumulation there [163].

Nanovectors of the second generation are more sophisticated than their predecessors; they are an advanced version of first-generation nanoparticles. These delivery systems possess additional functions: binding to the target site via specific interaction between ligands and receptors that are either unique or overexpressed in the tumor tissue, co-delivery of therapeutic agents, and controlled release of the transferred substances [163].

The third generation of nanovectors is represented by multicomponent systems. Since none of the single agents can penetrate through multiple barriers on its way to the target mRNA, these systems are composed of nanoparticles with different properties embedded in a single nanovector. These carriers (known as logic-embedded vectors [164]) are therapeutic multicomponent constructs in which the functions of biological recognition and penetration through biological barriers are performed by different components of the nanovector, ensuring a more efficient and selective delivery. A vector that can pass through the circulatory system due to its geometry can serve as an example of this therapeutic strategy. The vector binds to the capillary wall in the affected area due to specific surface interactions. It subsequently releases various nanoparticles that are synergistically transported from the vessels to the tissue, reach target cells, and deliver therapeutic agents at optimal concentrations with minimal side effects [163].

Biologically active molecular networks consisting of bacteriophages connected to gold nanoparticles and known as nanoshuttles belong to the third generation of nanoparticles. Nanoshuttles combine the ability to exhibit a hyperthermic response near-infrared or radio frequency radiation (which is typical of gold nanoparticles) and the feasibility of targeted delivery of substances [165].

Nanoparticles known as nanocells are another example of third-generation delivery nanosystems. Nanocells have been designed to be used in the field of combined chemotherapy. The outer shell of these nanovectors consists of lipid nanoparticles; the inner core is composed of polymeric nanoparticles [166].

Silicon-based nanoparticles also belong to the third generation of nano-vectors. Nanoparticles based on silicon with medium-sized pores have been successfully used for co-delivery of doxorubicin and siRNA targeted against *bcl-2* gene mRNA. Doxorubicin localized inside the silica pores; anti-bcl-2-siRNA was bound to the dendrimeric shell. The aim of producing this nanovector was to ensure simultaneous delivery of an anticancer drug (to induce apoptosis in tumor cells) and anti-bcl-2-siRNA molecules (to suppress ion pumps mediating the occurrence of multidrug resistance). As a result, a significant increase in doxorubicin cytotoxicity was observed by decreasing the IC_{50} (half maximal inhibitory concentration) 64-fold [167].

CONCLUSIONS

The RNA interference technology holds great promise for treating various human diseases by the targeted suppression of gene expression. Certain therapeutic agents based on the RNA interference principle are currently in clinical trials. Further progress in this therapeutic area depends on the development of safe and efficient carriers for systemic delivery of siRNAs. The general transfection efficiency of non-viral transport agents remains lower than that of viral vectors. Further improvements are required to increase the efficiency and reduce the toxicity of non-viral delivery systems.

This review has attempted to acquaint the reader with currently existing non-viral methods for the delivery of interfering RNAs, as well as the challenges encountered in attempts to implement these technologies in medicine. More thorough information about each of the presented systems can be found in [74–76, 88, 97, 98, 108, 113, 134, 149]. ●

REFERENCES

1. Milhavet O., Gary D.S., Mattson M.P. // Pharmacol. Rev. 2003. V. 55. № 4. P. 629–648.
2. Burnett J.C., Rossi J.J. // Chem. Biol. 2012. V. 19. № 1. P. 60–71.
3. Vilgelm A.E., Chumakov S.P., Prassolov V.S. // Mol. Biol. 2006. V. 40. № 3. P. 339–354.
4. Shrivastava N., Srivastava A. // Biotechnol. J. 2008. V. 3. № 3. P. 339–353.
5. Scherr M., Morgan M.A., Eder M. // Curr. Med. Chem. 2003. V. 10. № 3. P. 245–256.
6. Lima W.F., Murray H., Nichols J.G., Wu H., Sun H., Prakash T.P., Berdeja A.R., Gaus H.J., Crooke S.T. // J. Biol. Chem. 2009. V. 284. № 4. P. 2535–2548.
7. Ma J.B., Ye K., Patel D.J. // Nature. 2004. V. 429. № 6989. P. 318–322.
8. Macrae I.J., Zhou K., Li F., Repic A., Brooks A.N., Cande W.Z., Adams P.D., Doudna J.A. // Science. 2006. V. 311. № 5758. P. 195–198.
9. Zhang H., Kolb F.A., Jaskiewicz L., Westhof E., Filipowicz W. // Cell. 2004. V. 118. № 1. P. 57–68.
10. Kim V.N., Han J., Siomi M.C. // Nat. Rev. Mol. Cell Biol. 2009. V. 10. № 2. P. 126–139.
11. Hammond S.M. // FEBS Lett. 2005. V. 579. № 26. P. 5822–5829.
12. Lee Y.S., Nakahara K., Pham J.W., Kim K., He Z., Sontheimer E.J., Carthew R.W. // Cell. 2004. V. 117. № 1. P. 69–81.
13. Wang Y., Juranek S., Li H., Sheng G., Tuschl T., Patel D.J. // Nature. 2008. V. 456. № 7224. P. 921–926.
14. MacRae I.J., Ma E., Zhou M., Robinson C.V., Doudna J.A. // Proc. Natl. Acad. Sci. USA. 2008. V. 105. № 2. P. 512–517.
15. Miyoshi K., Okada T.N., Siomi H., Siomi M.C. // RNA. 2009. V. 15. № 7. P. 1282–1291.
16. Wang Y., Juranek S., Li H., Sheng G., Wardle G.S., Tuschl T., Patel D.J. // Nature. 2009. V. 461. № 7265. P. 754–761.
17. Nowotny M., Yang W. // Curr. Opin. Struct. Biol. 2009. V. 19. № 3. P. 286–293.
18. Birney E., Stamatoyannopoulos J.A., Dutta A., Guigo R., Gingeras T.R., Margulies E.H., Weng Z., Snyder M., Dermitzakis E.T., Thurman R.E., et al. // Nature. 2007. V. 447.

№ 7146. P. 799–816.
19. Carthew R.W., Sontheimer E.J. // Cell. 2009. V. 136. № 4. P. 642–655.
20. Titov I.I., Vorozheykin P.S. // Vavilov Journal of Genetics and Breeding. 2011. V. 15. № 1. P. 139–147.
21. Makarova J.A., Kramerov D.A. // Biochemistry (Moscow). 2007. V. 72. № 11. P. 1427–1448.
22. Yekta S., Shih I.H., Bartel D.P. // Science. 2004. V. 304. № 5670. P. 594–596.
23. Ameres S.L., Martinez J., Schroeder R. // Cell. 2007. V. 130. № 1. P. 101–112.
24. Selbach M., Schwanhausser B., Thierfelder N., Fang Z., Khanin R., Rajewsky N. // Nature. 2008. V. 455. № 7209. P. 58–63.
25. Kawakami S., Hashida M. // Drug Metabolism and Pharmacokinetics. 2007. V. 22. № 3. P. 142–151.
26. Watts J.K., Deleavey G.F., Damha M.J. // Drug Discovery Today. 2008. V. 13. № 19–20. P. 842–855.
27. Hartmann G. // J. Clin. Invest. 2009. V. 119. № 3. P. 438–442.
28. Fang J., Sawa T., Maeda H. // Adv. Exp. Med. Biology. 2003. V. 519. P. 29–49.
29. Zamecnik J., Vargova L., Homola A., Kodet R., Sykova E. // Neuropathol. Appl. Neurobiol. 2004. V. 30. № 4. P. 338–350.
30. Singh S., Narang A.S., Mahato R.I. // Pharmaceut. Res. 2011. V. 28. № 12. P. 2996–3015.
31. Perez-Martinez F.C., Guerra J., Posadas I., Cena V. // Pharmaceut. Res. 2011. V. 28. № 8. P. 1843–1858.
32. Arias J.L., Clares B., Morales M.E., Gallardo V., Ruiz M.A. // Curr. Drug Targets. 2011. V. 12. № 8. P. 1151–1165.
33. Leucuta S.E. // Curr. Clin. Pharmacol. 2012. V. 7. № 4. P. 282–317.
34. Khatri N., Rathi M., Baradia D., Trehan S., Misra A. // Crit. Rev. Therapeutic Drug Carrier Systems. 2012. V. 29. № 6. P. 487–527.
35. Sakurai Y., Hatakeyama H., Sato Y., Akita H., Takayama K., Kobayashi S., Futaki S., Harashima H. // Biomaterials. 2011. V. 32. № 24. P. 5733–5742.
36. Duan J., Zhang Y., Chen W., Shen C., Liao M., Pan Y., Wang J., Deng X., Zhao J. // J. Biomed. Biotechnol. 2009. V. 2009. P. 149–254.
37. Pack D.W., Hoffman A.S., Pun S., Stayton P.S. // Nat. Rev. Drug Discovery. 2005. V. 4. № 7. P. 581–593.
38. Sonawane N.D., Szoka F.C., Jr., Verkman A.S. // J. Biol. Chem. 2003. V. 278. № 45. P. 44826–44831.
39. Eliyahu H., Barenholz Y., Domb A.J. // Molecules. 2005. V. 10. № 1. P. 34–64.
40. Nguyen J., Szoka F.C. // Accounts Chem. Res. 2012. V. 45. № 7. P. 1153–1162.
41. Zelphati O., Szoka F.C., Jr. // Proc. Natl. Acad. Sci. USA. 1996. V. 93. № 21. P. 11493–11498.
42. Hafez I.M., Maurer N., Cullis P.R. // Gene Therapy. 2001. V. 8. № 15. P. 1188–1196.
43. Chu C.Y., Rana T.M. // RNA. 2008. V. 14. № 9. P. 1714–1719.
44. Zou Y., Tiller P., Chen I.W., Beverly M., Hochman J. // Rapid Comm. Mass Spectrometry: RCM. 2008. V. 22. № 12. P. 1871–1881.
45. Bramsen J.B., Kjems J. // Meth. Mol. Biol. 2011. V. 721. P. 77–103.
46. Chernolovskaya E.L., Zenkova M.A. // Curr. Opin. Mol. Therapeutics. 2010. V. 12. № 2. P. 158–167.
47. Rose S.D., Kim D.H., Amarzguioui M., Heidel J.D., Collingwood M.A., Davis M.E., Rossi J.J., Behlke M.A. // Nucl. Acids Res. 2005. V. 33. № 13. P. 4140–4156.
48. Dore-Savard L., Roussy G., Dansereau M.A., Collingwood M.A., Lennox K.A., Rose S.D., Beaudet N., Behlke M.A., Sarret P. // Mol. Therapy: J. Am. Soc. Gene Therapy. 2008. V. 16. № 7. P. 1331–1339.
49. Deleavey G.F., Watts J.K., Damha M.J. // Curr. Prot. Nucl. Acids Chem. 2009. Suppl. 39. P. 16.3.1–16.3.22.
50. Phelps K., Morris A., Beal P.A. // ACS Chem. Biol. 2012. V. 7. № 1. P. 100–109.
51. Detzer A., Sczakiel G. // Curr. Topics Med. Chem. 2009. V. 9. № 12. P. 1109–1116.
52. Mescalchin A., Detzer A., Wecke M., Overhoff M., Wunsche W., Sczakiel G. // Expert. Opinion Biol. Therapy. 2007. V. 7. № 10. P. 1531–1538.
53. Harborth J., Elbashir S.M., Vandenburgh K., Manninga H., Scaringe S.A., Weber K., Tuschl T. // Antisense Nucl. Acid Drug Devel. 2003. V. 13. № 2. P. 83–105.
54. Li Z.Y., Mao H., Kallick D.A., Gorenstein D.G. // Biochem. Biophys. Res. Commun. 2005. V. 329. № 3. P. 1026–1030.
55. Prakash T.P., Allerson C.R., Dande P., Vickers T.A., Sioufi N., Jarres R., Baker B.F., Swayze E.E., Griffey R.H., Bhat B. // J. Med. Chem. 2005. V. 48. № 13. P. 4247–4253.
56. Gaglione M., Messere A. // Mini Rev. Med. Chem. 2010. V. 10. № 7. P. 578–595.
57. Kraynack B.A., Baker B.F. // RNA. 2006. V. 12. № 1. P. 163–176.
58. Pallan P.S., Greene E.M., Jicman P.A., Pandey R.K., Manoharan M., Rozners E., Egli M. // Nucl. Acids Res. 2011. V. 39. № 8. P. 3482–3495.
59. Allerson C.R., Sioufi N., Jarres R., Prakash T.P., Naik N., Berdeja A., Wanders L., Griffey R.H., Swayze E.E., Bhat B. // J. Med. Chem. 2005. V. 48. № 4. P. 901–904.
60. Muhonen P., Tennila T., Azhayeva E., Parthasarathy R.N., Janckila A.J., Vaananen H.K., Azhayev A., Laitala-Leinonen T. // Chem. Biodiversity. 2007. V. 4. № 5. P. 858–873.
61. Morrissey D.V., Lockridge J.A., Shaw L., Blanchard K., Jensen K., Breen W., Hartsough K., Machemer L., Radka S., Jadhav V., et al. // Nat. Biotechnol. 2005. V. 23. № 8. P. 1002–1007.
62. Ferrari N., Bergeron D., Tedeschi A.L., Mangos M.M., Paquet L., Renzi P.M., Damha M.J. // Ann. N.Y. Acad. Sci. 2006. V. 1082. P. 91–102.
63. Dowler T., Bergeron D., Tedeschi A.L., Paquet L., Ferrari N., Damha M.J. // Nucl. Acids Res. 2006. V. 34. № 6. P. 1669–1675.
64. Watts J.K., Choubdar N., Sadalapure K., Robert F., Wahba A.S., Pelletier J., Pinto B.M., Damha M.J. // Nucl. Acids Res. 2007. V. 35. № 5. P. 1441–1451.
65. Lima W.F., Wu H., Nichols J.G., Sun H., Murray H.M., Crooke S.T. // J. Biol. Chem. 2009. V. 284. № 38. P. 26017–26028.
66. Vickers T.A., Zhang H., Graham M.J., Lemonidis K.M., Zhao C., Dean N.M. // J. Immunol. 2006. V. 176. № 6. P. 3652–3661.
67. Moschos S.A., Frick M., Taylor B., Turnpenny P., Graves H., Spink K.G., Brady K., Lamb D., Collins D., Rockel T.D., et al. // Mol. Therapy: J. Am. Soc. Gene Therapy. 2011. V. 19. № 12. P. 2163–2168.
68. Elmen J., Thonberg H., Ljungberg K., Frieden M., Westergaard M., Xu Y., Wahren B., Liang Z., Orum H., Koch T., et al. // Nucl. Acids Res. 2005. V. 33. № 1. P. 439–447.
69. Mook O.R., Baas F., de Wissel M.B., Fluiter K. // Mol. Cancer Therapeut. 2007. V. 6. № 3. P. 833–843.
70. Swayze E.E., Siwkowski A.M., Wancewicz E.V., Migawa M.T., Wyrzykiewicz T.K., Hung G., Monia B.P., Bennett C.F. // Nucl. Acids Res. 2007. V. 35. № 2. P. 687–700.

71. Hoffmann S., Hoos J., Klussmann S., Vonhoff S. // Curr. Prot. Nucl. Acids Chem. 2011. Suppl. 46. P. 4.46.1–4.46.30.
72. Luo D., Saltzman W.M. // Nat. Biotechnol. 2000. V. 18. № 8. P. 893–895.
73. Paulo C.S., Pires das Neves R., Ferreira L.S. // Nanotechnology. 2011. V. 22. № 49.
74. Jafari M., Soltani M., Naahidi S., Karunaratne D.N., Chen P. // Curr. Med. Chem. 2012. V. 19. № 2. P. 197–208.
75. Xing J., Deng L., Guo S., Dong A., Liang X.J. // Mini Rev. Med. Chem. 2010. V. 10. № 2. P. 126–137.
76. Tros de Ilarduya C., Sun Y., Duzgunes N. // Eur. J. Pharmaceut. Sci.: Official J. Eur. Fed. Pharmaceut. Sci. 2010. V. 40. № 3. P. 159–170.
77. Jere D., Jiang H.L., Arote R., Kim Y.K., Choi Y.J., Cho M.H., Akaike T., Cho C.S. // Expert Opin. Drug Delivery. 2009. V. 6. № 8. P. 827–834.
78. Nimesh S. // Curr. Clin. Pharm. 2012. V. 7. № 2. P. 121–130.
79. Singha K., Namgung R., Kim W.J. // Nucl. Acid Therapeut. 2011. V. 21. № 3. P. 133–147.
80. Hong S., Leroueil P.R., Janus E.K., Peters J.L., Kober M.M., Islam M.T., Orr B.G., Baker J.R., Jr., Banaszak Holl M.M. // Bioconjugate Chem. 2006. V. 17. № 3. P. 728–734.
81. Wightman L., Kircheis R., Rossler V., Carotta S., Ruzicka R., Kursa M., Wagner E. // J. Gene Med. 2001. V. 3. № 4. P. 362–372.
82. Luten J., van Nostrum C.F., De Smedt S.C., Hennink W.E. // J. Controlled Release: Official J. Controlled Release Soc. 2008. V. 126. № 2. P. 97–110.
83. Gary D.J., Puri N., Won Y.Y. // J. Controlled Release: Official J. Controlled Release Soc. 2007. V. 121. № 1–2. P. 64–73.
84. Cun D., Foged C., Yang M., Frokjaer S., Nielsen H.M. // Internat. J. Pharmaceut. 2010. V. 390. № 1. P. 70–75.
85. Presumey J., Salzano G., Courties G., Shires M., Ponchel F., Jorgensen C., Apparailly F., De Rosa G. // Eur. J. Pharmaceut. Biopharmaceut.: Official J. Arbeitsgemeinschaft fur Pharmazeutische Verfahrenstechnik e.V. 2012. V. 82. № 3. P. 457–464.
86. Steinbach J.M., Weller C.E., Booth C.J., Saltzman W.M. // J. Controlled Release: Official J. Controlled Release Soc. 2012. V. 162. № 1. P. 102–110.
87. Svenson S., Tomalia D.A. // Adv. Drug Delivery Rev. 2005. V. 57. № 15. P. 2106–2129.
88. Quadir M.A., Haag R. // J. Controlled Release: Official J. Controlled Release Soc. 2012. V. 161. № 2. P. 484–495.
89. Morgan M.T., Nakanishi Y., Kroll D.J., Griset A.P., Carnahan M.A., Wathier M., Oberlies N.H., Manikumar G., Wani M.C., Grinstaff M.W. // Cancer Res. 2006. V. 66. № 24. P. 11913–11921.
90. Dufes C., Uchegbu I.F., Schatzlein A.G. // Adv. Drug Delivery Rev. 2005. V. 57. № 15. P. 2177–2202.
91. Tomalia D.A., Reyna L.A., Svenson S. // Biochem. Soc. Transactions. 2007. V. 35. Pt 1. P. 61–67.
92. Wang Y., Li Z., Han Y., Liang L.H., Ji A. // Curr. Drug Metabolism. 2010. V. 11. № 2. P. 182–196.
93. Minko T., Patil M.L., Zhang M., Khandare J.J., Saad M., Chandna P., Taratula O. // Meth. Mol. Biol. 2010. V. 624. P. 281–294.
94. Kim I.D., Lim C.M., Kim J.B., Nam H.Y., Nam K., Kim S.W., Park J.S., Lee J.K. // J. Controlled Release: Official J. Controlled Release Soc. 2010. V. 142. № 3. P. 422–430.
95. Tang Y., Li Y.B., Wang B., Lin R.Y., van Dongen M., Zurcher D.M., Gu X.Y., Banaszak Holl M.M., Liu G., Qi R. // Mol. Pharmaceut. 2012. V. 9. № 6. P. 1812–1821.
96. Taratula O., Garbuzenko O.B., Kirkpatrick P., Pandya I., Savla R., Pozharov V.P., He H., Minko T. // J. Controlled Release: Official J. Controlled Release Soc. 2009. V. 140. № 3. P. 284–293.
97. Rudzinski W.E., Aminabhavi T.M. // Internat. J. Pharmaceut. 2010. V. 399. № 1–2. P. 1–11.
98. Saranya N., Moorthi A., Saravanan S., Devi M.P., Selvamurugan N. // Internat. J. Biol. Macromolecules. 2011. V. 48. № 2. P. 234–238.
99. Alameh M., Dejesus D., Jean M., Darras V., Thibault M., Lavertu M., Buschmann M.D., Merzouki A. // Internat. J. Nanomed. 2012. V. 7. P. 1399–1414.
100. Katas H., Alpar H.O. // J. Controlled Release: Official J. Controlled Release Soc. 2006. V. 115. № 2. P. 216–225.
101. Howard K.A., Rahbek U.L., Liu X., Damgaard C.K., Glud S.Z., Andersen M.O., Hovgaard M.B., Schmitz A., Nyengaard J.R., Besenbacher F., et al. // Mol. Therapy: J. Am. Soc. Gene Therapy. 2006. V. 14. № 4. P. 476–484.
102. Nielsen E.J., Nielsen J.M., Becker D., Karlas A., Prakash H., Glud S.Z., Merrison J., Besenbacher F., Meyer T.F., Kjems J., et al. // Pharmaceut. Res. 2010. V. 27. № 12. P. 2520–2527.
103. Howard K.A., Paludan S.R., Behlke M.A., Besenbacher F., Deleuran B., Kjems J. // Mol. Therapy: J. Am. Soc. Gene Therapy. 2009. V. 17. № 1. P. 162–168.
104. Tripathi S.K., Goyal R., Kashyap M.P., Pant A.B., Haq W., Kumar P., Gupta K.C. // Biomaterials. 2012. V. 33. № 16. P. 4204–4219.
105. Lee D.W., Yun K.S., Ban H.S., Choe W., Lee S.K., Lee K.Y. // J. Controlled Release: Official J. Controlled Release Soc. 2009. V. 139. № 2. P. 146–152.
106. Ji A.M., Su D., Che O., Li W.S., Sun L., Zhang Z.Y., Yang B., Xu F. // Nanotechnology. 2009. V. 20. № 40. P. 405103.
107. Pille J.Y., Li H., Blot E., Bertrand J.R., Pritchard L.L., Opolon P., Maksimenko A., Lu H., Vannier J.P., Soria J., et al. // Hum. Gene Therapy. 2006. V. 17. № 10. P. 1019–1026.
108. O'Mahony A.M., Godinho B.M., Ogier J., Devocelle M., Darcy R., Cryan J.F., O'Driscoll C.M. // ACS Chem. Neurosci. 2012. V. 3. № 10. P. 744–752.
109. Alabi C., Vegas A., Anderson D. // Curr. Opin. Pharmacol. 2012. V. 12. № 4. P. 427–433.
110. Hu-Lieskovan S., Heidel J.D., Bartlett D.W., Davis M.E., Triche T.J. // Cancer Res. 2005. V. 65. № 19. P. 8984–8992.
111. Davis M.E., Zuckerman J.E., Choi C.H., Seligson D., Tolcher A., Alabi C.A., Yen Y., Heidel J.D., Ribas A. // Nature. 2010. V. 464. № 7291. P. 1067–1070.
112. Heidel J.D., Yu Z., Liu J.Y., Rele S.M., Liang Y., Zeidan R.K., Kornbrust D.J., Davis M.E. // Proc. Natl. Acad. Sci. USA. 2007. V. 104. № 14. P. 5715–5721.
113. Zhang S., Zhi D., Huang L. // J. Drug Targeting. 2012. V. 20. № 9. P. 724–735.
114. Delong R.K., Risor A., Kanomata M., Laymon A., Jones B., Zimmerman S.D., Williams J., Witkowski C., Warner M., Ruff M., et al. // Nanomedicine (Lond.). 2012. V. 7. № 12. P. 1851–1862.
115. Gavrilov K., Saltzman W.M. // Yale J. Biol. Med. 2012. V. 85. № 2. P. 187–200.
116. Aliabadi H.M., Landry B., Sun C., Tang T., Uludag H. // Biomaterials. 2012. V. 33. № 8. P. 2546–2569.
117. Northfelt D.W., Dezube B.J., Thommes J.A., Levine R., von Roenn J.H., Dosik G.M., Rios A., Krown S.E., DuMond C., Mamelok R.D. // J. Clin. Oncol.: Official J. Am. Soc. Clin. Oncol. 1997. V. 15. № 2. P. 653–659.
118. Gooding M., Browne L.P., Quinteiro F.M., Selwood D.L. // Chem. Biol. Drug Design. 2012. V. 80. № 6. P. 787–809.
119. Venturini M., Bighin C., Puglisi F., Olmeo N., Aitini E., Colucci G., Garrone O., Paccagnella A., Marini G., Crino L.,

et al. // Breast. 2010. V. 19. № 5. P. 333–338.
120. Landen C.N., Jr., Chavez-Reyes A., Bucana C., Schmandt R., Deavers M.T., Lopez-Berestein G., Sood A.K. // Cancer Res. 2005. V. 65. № 15. P. 6910–6918.
121. Kang S.H., Cho H.J., Shim G., Lee S., Kim S.H., Choi H.G., Kim C.W., Oh Y.K. // Pharmaceut. Res. 2011. V. 28. № 12. P. 3069–3078.
122. Briane D., Slimani H., Tagounits A., Naejus R., Haddad O., Coudert R., Charnaux N., Cao A. // J. Drug Targeting. 2012. V. 20. № 4. P. 347–354.
123. Un K., Kawakami S., Higuchi Y., Suzuki R., Maruyama K., Yamashita F., Hashida M. // J. Controlled Release: Official J. Controlled Release Soc. 2011. V. 156. № 3. P. 355–363.
124. Un K., Kawakami S., Suzuki R., Maruyama K., Yamashita F., Hashida M. // Biomaterials. 2010. V. 31. № 30. P. 7813–7826.
125. Un K., Kawakami S., Suzuki R., Maruyama K., Yamashita F., Hashida M. // Mol. Pharmaceut. 2011. V. 8. № 2. P. 543–554.
126. Un K., Kawakami S., Yoshida M., Higuchi Y., Suzuki R., Maruyama K., Yamashita F., Hashida M. // Hepatology. 2012. V. 56. № 1. P. 259–269.
127. Wu S.Y., McMillan N.A. // AAPS J. 2009. V. 11. № 4. P. 639–652.
128. Zimmermann T.S., Lee A.C., Akinc A., Bramlage B., Bumcrot D., Fedoruk M.N., Harborth J., Heyes J.A., Jeffs L.B., John M., et al. // Nature. 2006. V. 441. № 7089. P. 111–114.
129. Laufer S.D., Restle T. // Curr. Pharmaceut. Design. 2008. V. 14. № 34. P. 3637–3655.
130. Herce H.D., Garcia A.E. // J. Biol. Physics. 2007. V. 33. № 5–6. P. 345–356.
131. Fonseca S.B., Pereira M.P., Kelley S.O. // Adv. Drug Delivery Rev. 2009. V. 61. № 11. P. 953–964.
132. Sebbage V. // Biosci. Horizons. 2009. V. 2. № 1. P. 64–72.
133. Stewart K.M., Horton K.L., Kelley S.O. // Organic Biomol. Chem. 2008. V. 6. № 13. P. 2242–2255.
134. Trabulo S., Cardoso A.L., Mano M., De Lima M.C.P. // Pharmaceuticals. 2010. V. 3. № 4. P. 961–993.
135. Vives E., Schmidt J., Pelegrin A. // Biochim. Biophys. Acta. 2008. V. 1786. № 2. P. 126–138.
136. Finstad C.L., Wang C.Y., Kowalski J., Zhang M., Li M.L., Li X.M., Xia W.G., Bosland M.C., Murthy K.K., Walfield A.M., et al. // Vaccine. 2004. V. 22. № 9–10. P. 1300–1313.
137. Pooga M., Langel U. // Meth. Mol. Biol. 2005. V. 298. P. 77–89.
138. Muratovska A., Eccles M.R. // FEBS Lett. 2004. V. 558. № 1–3. P. 63–68.
139. Moschos S.A., Jones S.W., Perry M.M., Williams A.E., Erjefalt J.S., Turner J.J., Barnes P.J., Sproat B.S., Gait M.J., Lindsay M.A. // Bioconjugate Chem. 2007. V. 18. № 5. P. 1450–1459.
140. Morris M.C., Gros E., Aldrian-Herrada G., Choob M., Archdeacon J., Heitz F., Divita G. // Nucl. Acids Res. 2007. V. 35. № 7. P. e49.
141. Crombez L., Charnet A., Morris M.C., Aldrian-Herrada G., Heitz F., Divita G. // Biochem. Soc. Transact. 2007. V. 35. Pt 1. P. 44–46.
142. Liu B.R., Chou J.C., Lee H.J. // J. Membrane Biol. 2008. V. 222. № 1. P. 1–15.
143. Meade B.R., Dowdy S.F. // Adv. Drug Delivery Rev. 2008. V. 60. № 4–5. P. 530–536.
144. Hoyer J., Neundorf I. // J. Controlled Release: Official J. Controlled Release Soc. 2012. V. 161. № 3. P. 826–834.
145. Johnson L.N., Cashman S.M., Kumar-Singh R. // Mol. Therapy: J. Am. Soc. Gene Therapy. 2008. V. 16. № 1. P. 107–114.
146. Cheung W., Pontoriero F., Taratula O., Chen A.M., He H. // Adv. Drug Delivery Rev. 2010. V. 62. № 6. P. 633–649.
147. Qi L., Gao X. // ACS Nano. 2008. V. 2. № 7. P. 1403–1410.
148. Boisselier E., Astruc D. // Chem. Soc. Rev. 2009. V. 38. № 6. P. 1759–1782.
149. Zhang S., Zhao Y., Zhi D. // Bioorganic Chem. 2012. V. 40. № 1. P. 10–18.
150. Son S.J., Bai X., Lee S.B. // Drug Discovery Today. 2007. V. 12. № 15–16. P. 650–656.
151. Liu G., Swierczewska M., Lee S., Chen X. // Nano Today. 2010. V. 5. № 6. P. 524–539.
152. Neagoe I.B., Braicu C., Matea C., Bele C., Florin G., Gabriel K., Veronica C., Irimie A. // J. Biomed. Nanotechnol. 2012. V. 8. № 4. P. 567–574.
153. Wang X., Ren J., Qu X. // ChemMedChem. 2008. V. 3. № 6. P. 940–945.
154. Gao J., Chen K., Xie R., Xie J., Yan Y., Cheng Z., Peng X., Chen X. // Bioconjugate Chem. 2010. V. 21. № 4. P. 604–609.
155. Jung J., Solanki A., Memoli K.A., Kamei K., Kim H., Drahl M.A., Williams L.J., Tseng H.R., Lee K. // Angew Chem. Int. Ed. Engl. 2010. V. 49. № 1. P. 103–107.
156. Bumcrot D., Manoharan M., Koteliansky V., Sah D.W. // Nat. Chem. Biol. 2006. V. 2. № 12. P. 711–719.
157. Tan W.B., Jiang S., Zhang Y. // Biomaterials. 2007. V. 28. № 8. P. 1565–1571.
158. Yezhelyev M.V., Qi L., O'Regan R.M., Nie S., Gao X. // J. Am. Chem. Soc. 2008. V. 130. № 28. P. 9006–9012.
159. Subramaniam P., Lee S.J., Shah S., Patel S., Starovoytov V., Lee K.B. // Adv. Mater. 2012. V. 24. № 29. P. 4014–4019.
160. Kim S.T., Chompoosor A., Yeh Y.C., Agasti S.S., Solfiell D.J., Rotello V.M. // Small. 2012. V. 8. № 21. P. 3253–3256.
161. Duncan R. // Curr. Opin. Biotechnol. 2011. V. 22. № 4. P. 492–501.
162. Summers H.D., Rees P., Holton M.D., Brown M.R., Chappell S.C., Smith P.J., Errington R.J. // Nat. Nanotechnol. 2011. V. 6. № 3. P. 170–174.
163. Serda R.E., Godin B., Blanco E., Chiappini C., Ferrari M. // Biochim. Biophys. Acta. 2011. V. 1810. № 3. P. 317–329.
164. Ferrari M. // Trends Biotechnol. 2010. V. 28. № 4. P. 181–188.
165. Souza G.R., Christianson D.R., Staquicini F.I., Ozawa M.G., Snyder E.Y., Sidman R.L., Miller J.H., Arap W., Pasqualini R. // Proc. Natl. Acad. Sci. USA. 2006. V. 103. № 5. P. 1215–1220.
166. Sengupta S., Eavarone D., Capila I., Zhao G., Watson N., Kiziltepe T., Sasisekharan R. // Nature. 2005. V. 436. № 7050. P. 568–572.
167. Tasciotti E., Liu X., Bhavane R., Plant K., Leonard A.D., Price B.K., Cheng M.M., Decuzzi P., Tour J.M., Robertson F., et al. // Nat. Nanotechnol. 2008. V. 3. № 3. P. 151–157.

AZT 5′-Phosphonates: Achievements and Trends in the Treatment and Prevention of HIV Infection

A.L. Khandazhinskaya*, E.A. Shirokova
Engelhardt Institute of Molecular Biology, Russian Academy of Sciences, Vavilov Str., 32, Moscow, Russia, 119991
*E-mail: khandazhinskaya@bk.ru
Received 18.02.2013

ABSTRACT **Despite the numerous drawbacks, 3'-azido-3'-deoxythymidine (AZT, Zidovudine, Retrovir) remains one of the key drugs used in the treatment and prevention of HIV infection in both monotherapy and HAART. A strategy in searching for new effective and safe AZT agents among latent (depot) forms of AZT has yielded its first positive results. In particular, the sodium salt of AZT 5'-H-phosphonate (Nikavir, phosphazide) has demonstrated clinical advantages over parent AZT: first and foremost, lower toxicity and better tolerability. It can be effectively used for the prevention of vertical transmission from mothers to babies and as an alternative drug for HIV-infected patients with low tolerance to Zidovudine. Preclinical studies of another phosphonate, AZT 5'-aminocarbonylphosphonate, have demonstrated that it releases AZT when taken orally. Pharmacokinetic studies have shown a prolonged action potential. Based on the analysis of both toxicological and pharmacological data, AZT 5'-aminocarbonylphosphonate has been recommended for clinical trials.**
KEYWORDS **anti-HIV therapy; AZT 5'-phosphonates; depot forms; Nikavir; preclinical trials.**
ABBREVIATIONS **HIV RT – human immunodeficiency virus reverse transcriptase; AZT – 3'-azido-3'-deoxythymidine; 3TC – (-)-β-*L*-2',3'-dideoxy-3'-tiacytidine; L-FTC – (-)-β-*L*-2',3'-dideoxy-3'-thia-5-fluoro-cytidine; HAART – high active antiretroviral therapy; LD_{50} – mean lethal dose; AUC – area under the concentration-time curve; MRT – mean residence time; CL – total clearance; V_{ss} – steady state volume of distribution; F – bioavailability.**

INTRODUCTION

In the last quarter of the 20th century, AIDS morphed into one of the main threats to human health. The protracted efforts of researchers yielded a number of agents with anti-HIV activity which can be subdivided into several groups: 1) nucleoside and nonnucleoside reverse-transcriptase inhibitors of HIV (HIV RT); 2) protease inhibitors; 3) integrase inhibitors; and 4) inhibitors of virus binding and penetration into cells. Nucleoside reverse transcriptase inhibitors (NRTI) are the most numerous group of anti-HIV agents used in clinical practice; the most commonly known members include 3'-azido-3'-deoxythymidine (AZT, Zidovudine, Retrovir), (-)-β-*L*-2',3'-dideoxy-3'-thiacytidine (3TC, Lamivudine), (-)-β-*L*-2',3'-dideoxy-3'-thia-5-fluorocytidine (L-FTC, Emricitabine), 2',3'-dideoxyinosine (ddI, Didanosine), etc. [1]. The mechanism of action of these inhibitors includes intracellular triphosphorylation, followed by specific blocking of viral DNA synthesis catalyzed by HIV RT. However, all NRTIs have a number of serious drawbacks. Due to their pharmacokinetic properties and the low efficiency of intracellular conversions (e.g., as little as 0.3% of AZT is converted into the corresponding triphosphate in cells), high doses of the drug are needed, which in turn causes increasing toxicity. Furthermore, the high variability of the virus results in the rapid development of viral resistance [2, 3], which also narrows the range of therapy outcomes.

Among the clinical circumstances of AZT toxicity there are numerous hematological effects, suppression of bone marrow cell functions, liver disorders, myopathies, etc. [4, 5]. Mitochondrial toxicity of AZT causes hyperlactatemia and lipodystrophy in patients with AIDS [6, 7]. Since AZT is eliminated rather fast, this drug needs to be administered three times a day. After long-term therapy, AZT loses its efficiency with the development of viral resistance to it [8, 9]. Nevertheless, despite all the adverse effects, AZT remains the most widely used drug.

The currently used regimens of combined drug therapy (highly active antiretroviral therapy, HAART) allow one to control HIV replication to a more significant

extent, as compared to the drugs taken individually; however, they also require novel components that can be efficient and nontoxic.

One of the ways to enhance the efficacy of an antiviral drug is to synthesize its depot (latent) form; i.e., such a derivative that would release the active substance when undergoing chemical or enzymatic conversion in the organism [10]. Designing depot forms is a good means to reducing NRTI toxicity both by improving the pharmacokinetic parameters and by decreasing their affinity to mitochondrial transport proteins. This approach has been used in many laboratories in the search for novel anti-HIV agents. The following drugs illustrate the successful application of the depot forms of NRTI in practical medicine: Viread® (tenofovir disoproxil fumarate) and Nikavir® (sodium salt of AZT 5'-H-phosphonate, phosphazide) [11, 12].

NIKAVIR (PHOSPHAZIDE), THE FIRST ACHIEVEMENT IN DESIGNING DEPOT FORMS OF AZT

Nikavir was licensed in the Russian Federation in 1999 as an agent to be used for therapy in patients with AIDS and for the prevention of HIV infection [13–15]. Nikavir was designed as a result of lengthy studies devoted to the synthesis and investigation of antiviral agents headed by A.A. Kraevsky at the Engelhardt Institute of Molecular Biology, Russian Academy of Sciences [16, 17]:

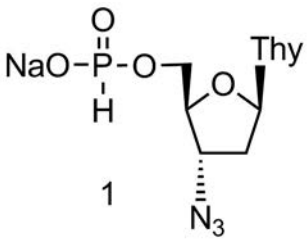

AZT 5'-H-phosphonate was synthesized in 1989 and tested on cell cultures infected with HIV-1 [16]; however, there was a significant discrepancy between the data obtained from the experiments conducted at different laboratories. It was initially reported that phosphazide **1** exhibited moderate anti-HIV activity and lower toxicity in a MT-4 cell culture as compared to AZT [18, 19]. Its selectivity index was higher than that of AZT. However, when phosphazide was later tested on three different cell lines (MT-4, CEM-SS and CEM-X 174), its activity was found to be lower than that of AZT by almost an order of magnitude [20]. It was reported in another paper [21] that the anti-HIV activity of compound **1** in the cell cultures C8 and JM was 10–20 times higher vs. that of AZT. Contrariwise, according to [22], the selectivity indices of H-phosphonate **1** were 1.5 and 15 times higher than those of AZT (IIIB and HXB2 strains of HIV in blood mononuclear cells were used). Despite these discrepant and disputable data, the research into phosphazide was continued, which made it possible to reveal its superiority over AZT in laboratory animal experiments [23].

Pharmacokinetic studies of phosphazide have shown the main difference from AZT: the pharmacokinetic profile of AZT after oral administration of phosphazide was considerably smoother as compared to the case when AZT was administered alone (C_{max} and t_{max} ~ 0.13 mg/l and 2–2.5 h, respectively, vs. 1.2 mg/l and 0.5–0.8 h for AZT). A lower peak concentration of AZT, which was observed after the administration of phosphazide, did not reduce antiviral efficacy but could facilitate a decrease in toxicity. This difference was used in clinical practice: a stable positive therapeutic effect (reduction of viral stress, immunorestoration, and a decrease in the risk of developing concomitant diseases) was observed. Phosphazide is well tolerated in both adults and children. No adverse effects that are typically observed in patients taking AZT (such as vomiting, nausea, headache, diarrhea, myalgia, anemia, thrombocytopenia, and neutrocytopenia) have been detected during phosphazide therapy [17].

A significant therapeutic efficacy and the safety of phosphazide were observed in HIV-infected patients receiving HAART. Various combinations of Nikavir with Didanozine and Nevirapine [24], with Didanozine and Ritonavir/Saquinavir [25], with Lamivudine and Efavirenz or a protease inhibitor (Atazanavir or Lopinavir/Ritonavir) [26], etc. have shown good results. These HAART regimens have demonstrated higher efficacy in patients with concomitant diseases (anemias, chronic hepatitis B and C [27], hepatic cirrhosis, and tuberculosis [28]) as compared to regimens comprising Retrovir or Combivir. The essential advantage of Nikavir is that it is safe for patients with tuberculosis and liver pathologies of viral etiology, since most HIV-infected patients suffer from these opportunistic infections [27, 28].

Another clinical application of phosphazide is the chemoprophylaxis of mother-to-child transmission of HIV during pregnancy, peri- and postnatal periods. Phosphazide does not affect the course of the pregnancy in HIV-infected women, fetal maturity or viability. AZT from phosphazide is capable of efficiently penetrating the placenta; thus, equal AZT concentrations are maintained in the mother's umbilical cord and blood. The use of Nikavir during a pregnancy (combined with Retrovir or Nevirapine during childbirth and the postnatal period) efficiently prevents vertical transmission of HIV [29, 30]. In some cases, Retrovir can be substituted by Nikavir because of a low hemoglobin level in the blood of a pregnant woman. The agent is

well-tolerated; the hematologic indices have been restored in all such cases.

Thus, low toxicity and good tolerance of phosphazide make it a promising component for various examples of HAART. It can be efficiently used to prevent mother-to-child transmission of HIV, to treat HIV infection (in particular, in patients with concomitant chronic viral hepatitis), and to prevent healthcare-worker infections. It is no coincidence that phosphazide has been recommended as a component of the preferred regimens of first-line antiretroviral therapy in the current edition of the Protocols on Treatment of and Care for People with HIV [31].

5'-AMINOCARBONYL PHOSPHONATES AS A TREND IN SEARCHING FOR NEW DEPOT FORMS OF AZT

Following the efforts focused on designing phosphonate depot forms of AZT, various types of compounds have been studied [32–37]. The class of AZT 5'-aminocarbonyl phosphonates substituted at the NH-fragment by various functional groups (C_6H_{13}, $HOCH_2CH_2$, $H_2NCH_2CH_2$, $Me_2NCH_2CH_2$, $Me_3N^+CH_2CH_2$, Me, H, C_4H_9, $PhCH_2CH_2$) has turned out to have the highest potential [38–40].

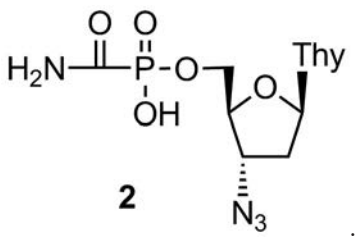

2

Antiviral experiments in HIV-infected MT-4 cells have demonstrated that AZT 5'-aminocarbonyl phosphonates inhibit viral replication with an efficiency an order of magnitude lower than that of AZT. Meanwhile, their toxicity (except for the methylamide derivative) is considerably lower than that of AZT. All the synthesized phosphonates have turned out to be stable in biological fluids (human blood serum, canine whole blood). The preliminary evaluation of the pharmacokinetic parameters after oral administration of AZT 5'-aminocarbonyl phosphonates in dogs has demonstrated that all the compounds can be metabolized to AZT. The shapes of the curves of concentration of the released AZT in blood plasma vs. time have been similar in all amides under study. The peak concentrations (C_{max}) of AZT for phosphonates carrying C_6H_{13}, C_4H_9, $PhCH_2CH_2$ moieties at the NH-fragment, as well as that of nonsubstituted amide **2**, are 2.0, 0.8, 0.9, and 3.7 mg/l, respectively. Thus, AZT 5'-aminocarbonyl phosphate **2** is the most efficient AZT donor within this group. This compound has been studied more thoroughly.

AZT 5'-AMINOCARBONYL PHOSPHONATE

Cell culture experiments

The investigation of the antiviral activity of AZT 5'-aminocarbonyl phosphonate **2** on a human lymphoblastoid cell line MT-4 has shown that its antiviral activity is inferior to that of AZT by about an order of magnitude and 3–4.5 times lower than that of phosphazide. However, its toxicity is considerably lower (by 34–50 and 12.5–15 times, respectively). Therefore, phosphonate **2** is characterized by a higher selectivity index than AZT and phosphazide [38–40].

The efficiency of penetration of phosphonate **2** into cells is 10–100 times lower than that of AZT and approximately 6 times lower than that of phosphazide [23, 39]. This fact gives grounds to hypothesize that the decrease in anti-HIV activity and toxicity in a MT-4 cell culture as compared to the same indicators for AZT and phosphazide is associated with a decrease in the efficiency of its penetration into cells; i.e., there is a direct relationship between the penetration of phosphonate **2**, phosphazide, and AZT into cultured cells and the antiviral properties of these compounds. It should be mentioned that both depot forms are appreciably stable in cell culture experiments, while being efficiently converted into AZT in the organism [39].

Stability studies

The stability of phosphonate **2** in 100% human blood serum has turned out to be comparable to that of phosphazide: the half-life of both compounds is over 6 h [39]. Meanwhile, phosphonate **2** is characterized by a considerably higher stability in canine whole blood at 37°C as compared to phosphazide ($T_{1/2}$ > 24 h vs. 3 h).

PHARMACOKINETIC PARAMETERS AFTER SINGLE-DOSE ADMINISTRATION [41]

Outbred dogs (average weight 22 ± 3.4 kg)

It has been ascertained during a pharmacokinetic study of drug **2** (capsules № 2; 250, 500 and 1000 mg or 10, 20 and 40 mg/kg) that most of it is metabolized into pharmacologically active AZT. *Table 1* lists the pharmacokinetic parameters of AZT released after a single-dose oral administration of phosphonate **2** in dogs.

It was shown by comparing phosphonate **2** with AZT and phosphazide (*Table 2*) that the peak AZT concentration in plasma during the administration of phosphonate **2** is lower, while the accumulation of AZT and the clearance time are longer. The pharmacokinetic parameters of AZT formed from phosphonate **2** were close to those of phosphazide (C_{max} being 2.5 times lower; AUC being twice as low, but t_{max} and other parameters being higher). The maximum concentration of AZT after oral

Table 1. Pharmacokinetic parameters of 5′-aminocarbonyl phosphonate 2 and its major metabolite AZT after a single-dose oral administration of capsules of 5′-aminocarbonyl phosphonate 2 to dogs at doses of 10, 20, and 40 mg/kg body weight

Dose of compound 2, mg	Tested compound	Pharmacokinetic parameters					
		C_{max}, mg/l	t_{max}, h	AUC, mg h/l	$t_{1/2}$, h	MRT, h	C_{max}/AUC, 1/h
10	2	0.31 ± 0.09	1.5 ± 0.25	0.47 ± 0.15	0.62 ± 0.1	2.43 ± 0.04	0.662 ± 0.066
	AZT	0.36 ± 0.24	4.7 ± 1.0	2.87 ± 1.56	4.57 ± 1.46	8.90 ± 5.34	0.119 ± 0.033
20	2	0.51 ± 0.18	1.6 ± 0.2	0.98 ± 0.44	0.81 ± 0.2	2.65 ± 0.16	0.561 ± 0.122
	AZT	0.69 ± 0.49	5.0 ± 1.7	6.0 ± 3.3	9.7 ± 4.3	12.0 ± 2.6	0.107 ± 0.023
40	2	0.51 ± 0.26	1.75 ± 0.27	1.25 ± 0.86	0.59 ± 0.2	2.87 ± 0.49	0.478 ± 0.117
	AZT	0.98 ± 0.56	6.0 ± 1.3	10.4 ± 6.1	7.0 ± 2.5	12.2 ± 1.4	0.100 ± 0.016

Note. Here and in Tables 2, 3: AUC_t – area under the concentration-time curve; MRT – mean residence time; t_{max} – time needed to achieve the maximum concentration; C_{max} – maximum concentration of substance; $t_{1/2}$ – half-life period.

Table 2. Comparison of the pharmacokinetic parameters of AZT after a single-dose oral administration of AZT 5′-aminocarbonyl phosphonate 2, phosphazide 1, or AZT to dogs at doses equivalent to 20 mg of AZT/kg body weight

Compound	C_{max}, mg/l	t_{max}, h	AUC, mg h/l	$t_{1/2}$, h	MRT, h	CL, l/h
2	0.74 ± 0.03	5	9.2 ± 0.2	9.6 ± 0.2	13.9 ± 0.2	27 ± 2.6
1	1.89±0.07	4	16.6 ± 0.3	7.2 ± 0.3	10.4 ± 0.5	15 ± 0.7
AZT	9.77 ± 0.3	2.5	58.8 ± 1.1	5.2 ± 0.5	7.5 ± 0.4	4.2 ± 0.3

administration of phosphonate **2** was attained after 4 h, which is twice as long as that after administration of AZT and 1 h longer than for phosphazide (*Table 2*).

It is noteworthy that the $t_{1/2}$ and t_{max} AZT values in dogs increases in the following order: AZT < phosphazide < AZT 5′-aminocarbonyl phosphonate, which gives grounds for regarding AZT 5′-aminocarbonyl phosphonate **2** as a depot form of AZT with a long-term effect.

No AZT has been detected in the blood plasma of dogs after intravenous administration of phosphonate **2** at a dose of 50 mg (2–5 mg/kg body weight). The pharmacokinetic parameters of **2** were as follows: AUC_t = 2.19 mg·h/l, $t_{1/2}$ = 0.35 h, MRT = 0.74 h, CL = 16.8 l/h, V_{ss} = 12.4 l.

The bioavailability of 5′-aminocarbonyl phosphonate **2** administered orally at specified doses was 4.7%, while the bioavailability of AZT after **2** had been administered orally was 8%, which is twice as low as that of phosphazide. The bioavailability of AZT during oral administration of this drug was six-fold higher than that in the case of phosphonate **2**. However, the high AUC value during the administration of AZT is associated with the excessive peak concentration in plasma, which decreases at a very fast rate. This causes toxicity and rapid emergence of drug-resistant viral strains. In turn, when administering phosphonate **2**, the difference between the maximum and minimum blood concentrations of AZT is significantly less pronounced, and this may reduce toxicity and inhibit the emergence of resistance.

Chinchilla rabbits (average weight 3 ± 0.4 kg) [41]

Studies of the pharmacokinetics of phosphonate **2** (its aqueous solution was intragastrically administrated to rabbits) have also supported the assumption that it is a depot form of AZT. AZT has not been detected in the peripheral blood of rabbits (as well as dogs) that had received phosphonate **2** intravenously. The original phosphonate **2** was the only product detected [17]. This fact confirms the hypothesis that AZT is formed as a result of the absorption of the original compound [17].

A comparison of the pharmacokinetic parameters of AZT and phosphonate **2** after a single-dose oral introduction of phosphonate **2** in rabbits at doses of 7, 70, and 200 mg/kg of body weight has demonstrated that AZT is present in the blood in all the cases. The shape of the concentration–time curves and the ratio between

Table 3. Comparison of the pharmacokinetic parameters of AZT after a single-dose oral administration of AZT 5′-aminocarbonyl phosphonate 2, phosphazide 1, or AZT in rabbits at doses equivalent to 200 mg of AZT/kg body weight

Compound	C_{max}, mg/l	t_{max}, h	AUC, mg h/l	$t_{1/2}$, h	MRT, h	CL, l/h
2	3.75 ± 0.01	3.5	25.12 ± 1.08	3.66 ± 0.74	4.72 ± 0.08	44.22 ± 1.95
1	7.38 ± 3.08	2.0	22.99 ± 10.17	1.42 ± 0.12	3.02 ± 0.12	54.95 ± 22.85
AZT	39.64 ± 4.24	1.0	88.5 ± 25.5	2.13 ± 0.71	2.10 ± 0.30	9.40 ± 2.70

AZT and the original **2** remains virtually unchanged as the dose is altered [39].

The results of a comparison of the pharmacokinetic properties of AZT after oral administration of single doses of AZT, phosphazide **1** or phosphonate **2** to rabbits are listed in *Table 3*. It should be mentioned that the shape of the dependence on the concentration of AZT released from phosphonate **2** was considerably smoother; the C_{max} values of AZT released from phosphazide **1** or phosphonate **2** differs only twofold, while the AUC values of both phosphonates are rather close.

Wistar rats and BALB/c mice

No original phosphonate **2** was detected in the blood plasma after it was taken orally by rats (body weight 200 ± 7 g) at a dose of 20 mg/kg. Only its metabolite AZT (characterized by the following pharmacokinetic parameters: AUC_{0-t} = 2.27 mg·h/l, MRT = 6.54 h, t_{max} = 4 h, C_{max} = 0.4 mg/l, $t_{1/2}$ = 2.45 h and C_{max}/AUC_t = 0.176 h^{-1}) was detectable.

Contrariwise, when phosphonate **2** at a dose of 20 mg/kg was introduced intraperitoneally into rats (body weight 250 ± 10 g), phosphonate **2** was the main compound detected, with trace amounts of its metabolite AZT. The pharmacokinetic parameters of phosphonate **2** were as follows: AUC_{0-t} = 8.02 mg·h/l, MRT = 0.82 h, CL = 0.45 l/h, $t_{1/2}$ = 0.42 h, and V_{ss} = 0.37 l. It is noteworthy that not only the original phosphonate **2**, but also 3.5% AZT were detected in the blood after phosphonate **2** was administered intraperitoneally to mice at a dose of 6 g/kg of body weight.

Thus, AZT 5'-aminocarbonyl phosphonate **2** releases AZT after being administered via different routes (orally, intragastrically or intraperitoneally) to experimental animals (mice, rats, rabbits and dogs) over a wide range of doses (7–6000 mg/kg of body weight) [17]. The pharmacokinetic parameters of phosphonate **2** and the AZT released from it in the blood plasma differ for different animal species. These differences can be attributed to the metabolic features of different animals and/or the route of drug administration.

The linear dependence of the pharmacokinetics of phosphonate **2** with respect to its major metabolite AZT allows one to extrapolate the animal dose to a human dose. Thus, it can be expected for a single-dose oral administration of 600 mg of phosphonate **2** that the AZT concentration in human blood plasma will be 100–115 ng/ml, with an appreciably gentle slope of the pharmacokinetic curve, which is considerably higher than the minimum AZT concentration achieved during regular (200 mg three times a day) oral administration of Zidovudine [42].

PHARMACOKINETIC PARAMETERS DURING MULTIPLE-DOSE ADMINISTRATION OF AZT 5′-AMINOCARBONYL PHOSPHONATE [41]

The results of multiple-dose administration of AZT 5'-aminocarbonyl phosphonate show great promise as well.

Experiments on rabbits have shown a gradual accumulation of phosphonate **2** in blood after a course of oral administration (solution – 1 g in 4–5 ml of water; administered after 6 and 18 h during 5 days) (*Fig.*). Furthermore, after the last dose had been administered (96 h after the onset of the experiment), AZT could be detected in human blood for 66 h (up to 162 h after the onset of the experiment).

Dogs (average weight 10.2 ± 1 kg) received compound **2** orally (600 mg on an empty stomach for 7 days, 24 h intervals). AZT was detected in plasma during the entire interval between the administrations of phosphonate **2**. The identical C_0 (0.17 ± 0.07 mg/l) and C_{min} (0.17 ± 0.07 mg/l) values on day 7 of administration indicate that the steady state was attained. The quasi-stationary concentration was 0.96 mg/l. The plasma levels of AZT at the steady state (2.82 ± 0.26) were characterized by an admissible fluctuation.

On day 7 of oral administration of phosphonate **2** capsules, AZT accumulation in the dog's organism was observed, manifesting itself in an increase in the AUC value (by 1.3 times as compared to day 1 of administration) and C_{min} (by 1.7 times as compared to day 1), as well as in t_{max} (from 2.7 to 4 h) and in C_{max} (from 2.45 to 2.75 mg/l blood plasma).

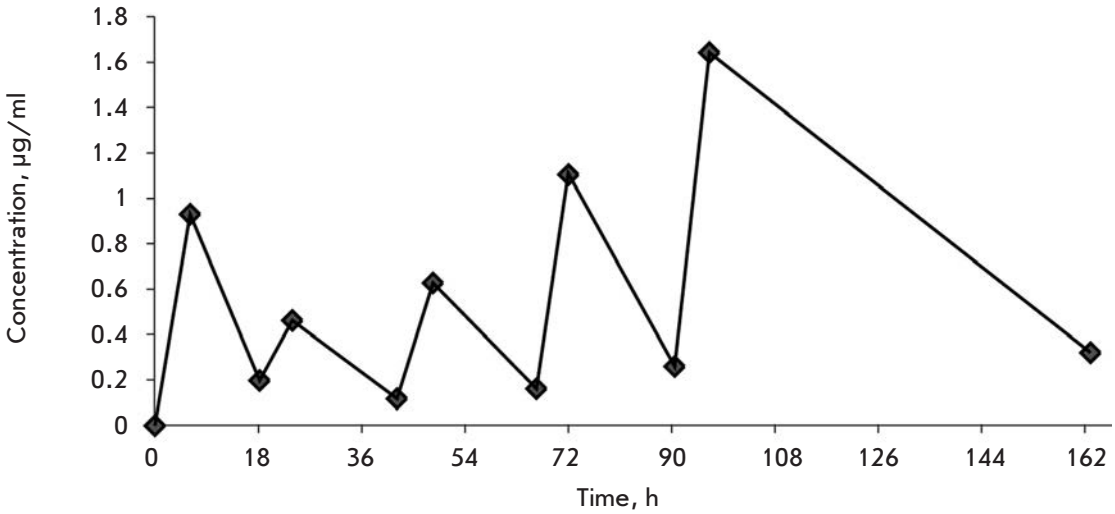

Fig. Concentration of AZT released in rabbit blood after multiple-dose administration of phosphonate **2** [17]

DISTRIBUTION IN TISSUES [41]

The investigation of the tissue availability of novel drugs is an important stage in pharmacokinetic studies. Through distribution processes, a drug is delivered to its zone of action, where the drug interacts with structures that determine its effect. Measuring the tissue availability value allows one to quantitatively assess the intensity of the penetration of an active substance into peripheral tissues and the target organ.

The distribution of AZT, the metabolite of phosphonate **2**, was studied in organs and tissues that differed in terms of blood supply, in the organs ensuring its elimination, and in the organ that is a potential action zone: strongly vascularized (liver, kidneys, spleen, lungs), moderately vascularized (skeletal muscles), and poorly vascularized (mesentery) tissues. AZT was detected in all these organs and tissues; its distribution over the organs was characterized by significant heterogeneity. The threshold of quantitative determination was 10 ng/ml. AZT could be detected in the blood plasma and organs of rats 12 h after a single-dose oral administration of phosphonate **2** at a dose of 100 mg/kg of body weight. Tissue availability of AZT in strongly vascularized organs (liver, spleen, lungs, and kidneys) was considerably higher than that in skeletal muscles and mesentery.

The AZT concentration generally decreased in a monophasic manner. The half-life period of the drug after oral administration was 3.9 h (blood plasma).

After a single-dose oral introduction of phosphonate **2** at a dose of 200 mg/kg, the original substance could not be detected in daily urine and feces, which can be attributed to intense biotransformation of the drug at the absorption stage. Only the major metabolite AZT was detected; it is eliminated as an insignificant percentage (4.11 and 0.04%, respectively) of the introduced dose of the drug.

TOXICITY [41]

The results of toxicity studies conducted in mice have supported the assumption that slow accumulation in the blood and slower elimination of AZT released from phosphonate **2** as compared to AZT administered directly and released after the introduction of phosphazide can decrease toxicity. Indeed, phosphonate **2** is a low-toxicity compound, which has been confirmed by data obtained in experiments measuring acute toxicity (BALB/c mice and Wistar rats) and in chronic experiments (Wistar rats, breedless dogs). A single-dose administration of this substance to mice and rats at tested toxic doses (2000–50000 mg/kg) was accompanied by short-term agitation in animals replaced by distress, inertness and adynamia. The mean lethal dose (LD_{50}) of phosphonate **2** during intraperitoneal administration to mice was ≥ 5 g/kg, against 1.5 and 2.3 g/kg for AZT and phosphazide, respectively. LD_{50} for a single-dose intragastric administration of the substance to rats was higher than 40 g/kg.

The toxicity of phosphonate **2** was studied under chronic experimental conditions in rats that had intragastrically received this substance at doses of 133 and 266 mg/kg daily for 3 months. The tested drug doses were 10- and 20-fold higher than the human daily dosage (13.3 mg/kg body weight). It turned out that compound **2** at tested doses was well-tolerated by animals and had no effect on the functional state of the main organs and systems of the organism (according to the results of biochemical tests) or hematological indicators. The absence of toxic lesions in internal organs and local irritating effects was confirmed in a pathomorphological study conducted after the conclusion of the experiment.

The toxicity of phosphonate **2** in the form of capsules for oral administration, 200 mg, was assessed in dogs which intragastrically received the compound at a dose

of 166 mg/kg (the 12.5-fold maximum recommended therapeutic dose for humans) daily for 4 weeks. It was found to be well-tolerated by the animals and to affect neither the functional state of the internal organs nor their hematological parameters (according to the data of biochemical tests). The absence of toxic lesions in internal organs and local irritating effects of phosphonate **2** in this pharmaceutical form after multiple-dose intragastric administration to dogs was confirmed through pathomorphological studies.

In order to assess the mutagenic properties of phosphonate **2**, its ability to cause gene mutations in indicator strains of *Salmonella typhimurium* (Ames test), to cause chromosomal aberrations in the bone marrow cells of hybrid mice F1(CBAxC57Bl6), and to affect the number of dominant lethal mutations in mouse embryonic cells has been studied. It has been demonstrated that phosphonate **2** at concentrations of up to 1 mg/dish does not increase the number of revertants in the Ames test in any statistically significant way.

When administered at doses 50-fold higher than the maximum recommended therapeutic dose for humans, phosphonate **2** exhibited no mutagenicity in *in vivo* tests: it neither caused an increase in the number of chromosomal aberrations in mouse bone marrow cells nor affected the number of dominant lethal mutations in mouse embryonic cells.

When intragastrically administered at a dose of 133 mg/kg (10-fold maximum recommended therapeutic dose for humans) daily to Wistar rats (for 10 and 2 weeks to males and females, respectively), no effects of compound **2** on the animal reproduction function was detected.

When intragastrically administered at a dose of 133 mg/kg daily to pregnant female rats on days 1–19 of gestation, phosphonate **2** had no effects on the weight gain in pregnant rats, gestation duration, the number of corpus luteum, sites of embryo attachment, embryonic body weight, their craniocaudal dimension, indicators of pre- and post-implantation fetal death, or postnatal development of rat pups. Administration of compound **2** caused neither malformations nor developmental disorders in embryos; in other words, it exhibits neither embryotoxic nor teratogenic effects.

The allergic properties of phosphonate **2** have been studied in guinea pigs. Phosphonate **2** was found to cause no anaphylactic shock when administered as a five-dose series at sensibilizing doses (133 and 266 mg/kg), followed by intragastric administration of an anaphylaxis-provoking dose (266 mg/kg) on days 14 and 21 after the sensibilization. At the doses and sensibilization schemes tested, the agent had no allergic effect in a type III hypersensitivity reaction on guinea pigs. Moreover, phosphonate **2** was shown not to affect the popliteal lymph node reaction in mice.

When administered at doses of 166 and 332 mg/kg (12.5- and 25-fold maximum recommended therapeutic doses for humans), phosphonate **2** affects neither the number of nuclear cells in spleen nor the hypersensitivity of the decelerated type reaction in mice. When administered at the highest of the doses tested (332 mg/kg), phosphonate **2** reduced the primary immune response to a certain extent in F1(CBAxC57BI6) mice.

Thus, AZT 5'-aminocarbonyl phosphonate **2** has been proved to be considerably less toxic as compared to the certified drugs Retrovir and Nikavir, to exhibit neither mutagenic nor allergic properties, to have no immunotoxicity, embryotoxicity or teratogenicity, and to have no effect on the reproductive functions of animals.

CONCLUSIONS

The efforts of numerous researchers have resulted in the synthesis of over 100 novel potential depot forms based on a 5'-phosphonate modification of AZT; their anti-HIV activities have been tested. Nikavir® is the first AZT 5'-phosphonate that has been used as an anti-HIV drug. Preclinical studies of another phosphonate, AZT 5'-aminocarbonyl phosphonate, were completed recently, yielding rather encouraging results. Pharmacokinetic studies conducted on animals have demonstrated that when administered, phosphonate **2** is converted into AZT to a significant degree. The pharmacokinetic parameters of AZT attest to a long-term pharmacological effect.

An analysis of the combination of preclinical toxicological and pharmacological data gives grounds for recommending phosphonate **2** for further clinical studies. The pharmacokinetic properties of this compound will presumably enable the administration of a drug based on it once a day, as opposed to Zidovudine, which is to be administered 2–3 times a day. Due to its lower toxicity, phosphonate **2** can be used not only to prevent vertical HIV transmission, but also in children and HIV-infected patients with liver pathologies.

Thus, AZT 5'-aminocarbonyl phosphonate **2** has an outstanding potential as an alternative to AZT and deserves further study. ●

The authors are grateful to M.K. Kukhanova and S.N. Kochetkov for fruitful discussions and assistance obtained in this work.

This work was supported by the Russian Foundation for Basic Research (grant № 12-04-00581) and the RAS Presidium Program "Molecular and Cellular Biology".

REFERENCES

1. De Clercq E. // Biochim. Biophys. Acta. 2002. V. 1587. P. 258–275.
2. Groschel B., Cinatl J.H., Cinatl J. Jr. // Intervirology. 1997. V. 40. P. 400–407.
3. Antonelli G., Turriziani O., Verri A., Narcisco P., Ferri F., D'Offizi G., Dianzani F.// AIDS Res. Hum. Retrovir.1996. V. 12. P. 223–228.
4. Chariot P., Drogou I., De Lacroix-Szmania I., Eliezer-Vanerot M.C., Chazaud B., Lombès A., Schaeffer A., Zafrani E.S. // J. Hepatol. 1999. V. 30. P. 156–160.
5. Gelmon K., Montaner J.S.G., Fanning M., Smith J. R. M., Falutz J., Tsoukas C., Gill J., Wells G., O'Shaughnessy M., Wainberg M., and Ruedy J. // AIDS. 1989. V. 3. № 9. P. 555–561.
6. Pan-Zhou X.-R., Cui L., Zhou X.-J., Sommadossi J.-P., Darley-Usmar V.M. // Antimicrob. Agents Chemother. 2000. V. 44. P. 496–503.
7. Chiao S.K., Romero D.L., Johnson D.E. // Curr. Opin. Drug Discov. Devc. 2009. V. 12. №1. P. 53–60.
8. Kellam P., Boucher C.A., Larder B.A. // Proc. Natl. Acad. Sci. USA. 1992. V. 89. P. 1934–1938.
9. Ren J., Esnouf R.M., Hopkins A.L., Jones E.Y., Kirby I., Keeling J., Ross C.K., Larder B.A., Stuart D.I. and Stammers D.K. // Proc. Natl. Acad. Sci. USA. 1998. V. 95. P. 9518–9523.
10. Stanczak A., Ferra A. // Pharmacol. Rept. 2006. V. 58. № 5. P. 599–613.
11. Beaumont K., Webster R., Gardner I., Dack K. // Curr. Drug Metab. 2003. V. 4. №6. P. 461–485.
12. Calogeropoulou T., Detsi A., Lekkas E., Koufaki M. // Curr. Top. Med. Chem. 2003. V. 3. № 13. P. l467–1495.
13. Khorlin A.A., Tarusova N.B., Dyatkina N.B., Kraevsky A.A., Bibilashvili R.Sh., Galegov G.A., Korneeva M.N., Nosik D.N., Maiorova S.N., Shobukhov V.M., Zhdanov V.V. 5'-Phosphonates of 2',3'-dideoxynucleosides. RF1548182, 1992; US5043437, 1991; EP0354246, 1994; Japan 0354246 Bl, 1995; Korean 106957. 1996.
14. Yurin O., Kravtchenko A., Serebrovskaya L., Golochvastova E., Burova N., Voronin E., Pokrovsky V. The phase 1 of the clinical trial of 'Phosphazid', the new reverse transcriptase inhibitor [abstract]. 4th International Congress on drug therapy in HIV-infection; Glasgow, UK, 1998. V. 12. № 4. P. 240.
15. Yurin O.G., Krayevsky A.A., Afonina L.Yu., Balaganin V.A., Burova N.V., Voronin E.E., Kolesnik A.N., Molodov I.B., Moshkovich G.F., Pokrovskii V.V. // Epidemiol. Infect. Dis. (Russian). 2001. V. 1. P. 43–45.
16. Tarussova N.B., Khorlin A.A., Krayevsky A.A. Kornylaeva M.N. Nosik D.N., Kruglov N.B. Galegov G.A., Beabealashvili R.Sh. // Mol. Biol. 1989. V. 23. № 6. P. 1716–1724.
17. Khandazhinskaya A., Matyugina E., Shirokova E. // Expert Opinion. Drug Metab. Toxicol. 2010. V. 6. № 6. P. 1–14.
18. Krayevsky A.A., Tarussova N.B., Zhu Q.Y., Vidal P., Chou T.C., Baron P., Polsky B., Jiang X.J., Matulic-Adamic J., Rosenberg I., Watanabe K.A. // Nucleos. Nucleot. 1992. V. 11. № 2–4. P. 177–196.
19. Tarussova N.B., Kukhanova M.K., Krayevsky A.A., Karamov E.V., Lukashov V.V., Kornyalaeva G.V., Rodina M.A., Galegov G.A. // Nucleos. Nucleot. 1991. V. 10. № 1–3. P. 351–354.
20. Gosselin G., Perigaud C., Lefebvre I., Pompou A., Aubertin A.M., Kern A., Azabo T., Stawinski J., Imbach J.L. // Antiviral Res. 1993. V. 22. № 2–3. P. 143–153.
21. McGuigan C., Bellevergue P., Jones B.C.N.M., Mahmood N., Hay A.J., Petrik J., Karpas A. // Antivir. Chem. Chemother. 1994. V. 5. P. 271–277.
22. Machado J., Salomon H., Olivera M., Tsoukas C., Krayevsky A., Wainberg M. // Nucleos. Nucleot. 1999. V. 18. № 4–5. P. 901–906.
23. Skoblov Yu., Karpenko I., Shirokova E., Popov K., Andronova V., Galegov G., Kukhanova M. // Antiviral Res. 2004. V. 63. № 2. P. 107–113.
24. Kravchenko A.I., Salamov G.G., Bogoslovskaya E.V., Serebrovskaya L.V., Sergienko O.G., Pokrovskii V.V. // Epidemiology and infectious diseases. 2001. №4. P. 32–35.
25. Kravchenko A.V., Sitdykova Yu.R., Serebrovskaya L.V., Bogoslovskaya E.V., Ivanova L.A., Pokrovskii V.V. // Infectious diseases. 2003. № 1. P. 14–19.
26. Kravchenko A.V., Kanestry V.G., Gankina N.Yu. // Infectious diseases. 2011. № 4. P. 64–69.
27. Gankina N.Yu., Kravchenko A.V., Kuimova U.A., Kanestry V.G. // Infectious diseases. 2010. V. 8. № 1. P. 14–18.
28. Panteleev A.M., Goliusova M.Yu., Kabanov V.I. // HIV infection and immunosuppression. 2010. № 2. P. 75 –79.
29. Ivanova E.S., Shmagel N.G., Vorobyova N.N. // Challenges in Virology. 2010. V. 55. № 2. P. 31–34.
30. *Ivanova E.S., Shmagel N.G., Vorobyova N.N.* "Nikavir in Chemoprevention Regimens of Vertical HIV Transmission" in "Understanding HIV/AIDS Management and Care - Pandemic Approaches in the 21st Century". Edited by Fyson Hanania Kasenga, Publisher: InTech, DOI: 10.5772/24428.
31. Pokrovskii V.V., Yurin O.G., Kravchenko A. V., Belyaeva V.V., Kanestry V.G., Afonina L.Yu., Ermak T.N., Buravtsova E.V., Shakhgildyan V.I., Kozyrina N.V., Narsia R.S., Zimina V.N., Pokrovskaya A.V., Konov D.S., Goliusova M.A., Efremova O.S., Popova A.A. Protocols of outpatient follow-up and treatment of HIV-infected patients. *Epidemiology and infectious diseases. Topical issues. Supplement.* 2012. № 6. ISSN: 2226-6976.
32. Khandazhinskaya A.L., Shirokova E.A., Karpenko I.L., Zakirova N.F., Tarussova N.B., Krayevsky A.A. // Nucleosides, Nucleotides & Nucleic Acids. 2000. V. 19. № 10–12. P. 1795–1804.
33. Pokrovsky A.G., Pronyaeva T.R., Fedyuk N.V., Khandazhinskaya A.L., Shirokova E.A., Tarussova N.B., Karpenko I.L., Krayevsky A.A. // Nucleosides, Nucleotides & Nucleic Acids. 2001. V. 20. №4–7. P. 767–769.
34. Khandazhinskaya A.L., Shirokova E.A., Jasko M.V., Yanvarev D.V., Ivanov A.V., Pronyaeva T.R., Fedyuk N.V., Pokrovsky A.G., Kukhanova M.K. // Collection Symp. Ser. 2002. V. 5. P. 93–98.
35. Shirokova E.A., Jasko M.V., Khandazhinskaya A.L., Yanvarev D.V., Skoblov Y.S., Pronayeva T.R., Fedyuk N.V., Pokrovsky A.G., Kukhanova M.K. // Nucleosides, Nucleotides & Nucleic Acids. 2003. V. 22. № 5–8. P. 981–985.
36. Shirokova E.A., Jasko M.V., Khandazhinskaya A.L., Ivanov A.V., Yanvarev D.V., Skoblov Yu.S., Mitkevich V.A., Bocharov E.V., Pronyaeva T.R., Fedyuk N.V., Kukhanova M.K., Pokrovsky A.G. // J. Med. Chem. 2004. V. 47. № 14. P. 3606–3614.
37. Kukhanova M. K. // Molecular Biology. 2012. V. 46. № 6. P. 860–873.
38. Shirokova E.A., Khandazhinskaya A.L., Jasko M.V., Kukhanova M.K., Shipitsyn A.V., Pokrovsky A.G. Modified 5'-phosphonate azidothymidine—potential anti-viral preparations. US Patent No: 7,999,099. EP1829885A1.
39. Khandazhinskaya A.L., Yanvarev D.V., Jasko M.V., Shipitzyn A.V., Khalizev V.A., Shram S.I., Skoblov Y.S., Shirokova E.A., Kukhanova M.K. // Drug Metab. Dispos. 2009. V. 37. № 3. P. 494–501.
40. Kukhanova M.K., Jasco M.V., Yanvarev D., Karpenko. I., Shipitzyn A.V., Khandazhinskaya A.L. // Nucleic Acids Symp. Ser. (Oxf). 2008. V. 52. P. 597–598.
41. The results of preclinical studies are provided by "Production and commercial AZT Association" Ltd.
42. Cato A. 3rd, Qian J., Hsu A, Levy B, Leonard J, Granneman R. // Antimicrob. Agents Chemother. 1998. V. 42. № 7. P. 1788–1793.

Clathrin-Mediated Endocytosis and Adaptor Proteins

N.V. Popova*, I.E. Deyev, A.G. Petrenko
Shemyakin-Ovchinnikov Institute of Bioorganic Chemistry of the Russian Academy of Sciences, Miklukho-Maklaya St., 16/10, Moscow, Russia, 117997
*E-mail: n.popova@gmail.com

ABSTRACT **Macromolecules gain access to the cytoplasm of eukaryotic cells using one of several ways of which clathrin-dependent endocytosis is the most researched. Although the mechanism of clathrin-mediated endocytosis is well understood in general, novel adaptor proteins that play various roles in ensuring specific regulation of the mentioned process are being discovered all the time. This review provides a detailed account of the mechanism of clathrin-mediated internalization of activated G protein-coupled receptors, as well as a description of the major proteins involved in this process.**

KEYWORDS **adaptor proteins, clathrin, endocytosis.**

ABBREVIATIONS **EEA1 – Early Endosome Antigen 1; GPCR – G-Protein-Coupled Receptor; GRK – G-protein-coupled Receptor Kinase; LDLR – Low-Density Lipoprotein Receptor; PtdIns(4,5)P2 – phosphatidylinositol-4,5-bisphosphate.**

INTRODUCTION

Endocytosis is a fundamental process that ensures delivery of extracellular or membrane-localized macromolecules to the cytoplasm. Endocytosis is necessary for nutrients to reach the cell, the regulation of the activity of transmembrane receptors, and synaptic vesicle recycling. Clathrin-mediated endocytosis represents the entry of fragments of the cytoplasmic membrane, along with all of their contents, into the cell in the form of vesicles coated on the outside with a lattice consisting of polymerized clathrin. In particular, the clathrin-mediated mechanism is utilized to carry out the endocytosis of activated cell surface receptors. Binding of the receptor molecule to the ligand and activation of the former render possible the subsequent binding of the intracellular part of the receptor to the adaptor proteins. These proteins mediate the interaction between receptors and clathrin molecules, resulting in the formation of the clathrin coat. Several classes of adaptor proteins have been identified.

ENDOCYTOSIS OF G-PROTEIN-COUPLED RECEPTORS AS AN EXAMPLE OF CLATHRIN-MEDIATED ENDOCYTOSIS

The superfamily of G-protein-coupled receptors (GPCR) is considered to be the largest family of membrane proteins involved in intracellular signal transduction [1]. The general structural feature of GPCR is the presence of seven α-helical transmembrane hydrophobic segments each consisting of 25–35 amino acid residues [2]. The N-terminal portion of GPCR and three loops between the transmembrane segments are found outside the cell, and the C-terminal part and the other three loops are found on the cytoplasmic side of the plasma membrane.

The ligands of various GPCR include ions, organic odorants, amines, peptides, proteins, lipids, nucleotides, and photons. Activation of the receptors by their corresponding ligands leads to the formation of complexes consisting of receptors and heterotrimeric G-proteins (consisting of 3 subunits) and the associated exchange of GDP for GTP. This exchange causes the dissociation of a G-protein into a GTP-bound α-subunit and a complex consisting of β- and γ-subunits, as well as the dissociation of all three subunits of the G-protein from the receptor. It is now proven that both the α-subunit and the βγ complex serve as signal transducers by activating or inhibiting enzymes and ion channels [3]. Bound GTP is hydrolyzed following interaction with the effector and re-association of the α-subunit and βγ to form a complex consisting of three subunits with a bound GDP. This complex is again able to interact with the activated receptor [4].

Binding of the ligand to the receptor leads to conformational changes that give rise to the G-protein-mediated signal transduction and conversion of the receptor into the protein kinase GRK substrate (G-protein-coupled Receptor Kinases). The serine or threonine residues of the ligand-activated receptor located in the cytoplasmic domain and/or in the third cytoplasmic loop are phosphorylated. Then, β-arrestins bind to the

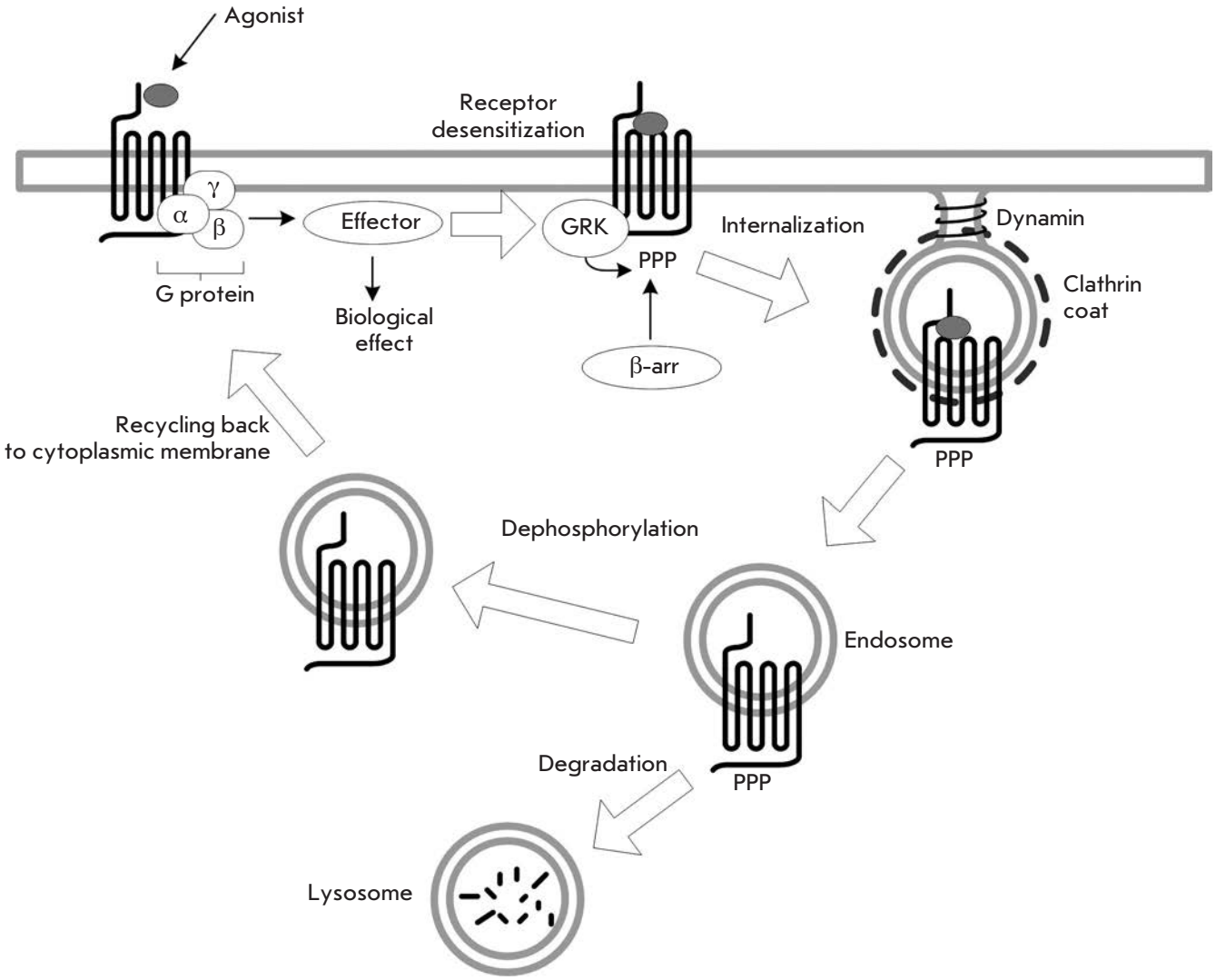

Fig 1. Schematic diagram of clathrin-mediated internalization of a receptor following its activation

activated and phosphorylated receptor [5]. β-Arrestins play a significant role in the process of internalization of GPCR as their binding leads to clathrin-mediated endocytosis of the receptor attributed to interaction with the components of the endocytotic mechanism – clathrin and the AP-2 adaptor protein complex [6, 7].

Newly formed clathrin-coated vesicles containing the receptor detach from the cytoplasmic membrane by means of the protein called dynamin tightening the neck of the forming vesicles [8]. The internalized receptor-ligand complex detached as part of the vesicles further undergoes intracellular transport. The first stage of this pathway is the formation of early endosomes. It is believed that canonical early endosomes contain a small GTPase Rab5 and the early endosome antigen 1 (EEA1). In the majority of cases, the internalized receptor remains accessible to the molecules of the intracellular signaling cascade and, therefore, can continue to participate in the signal transduction as if it was localized on the surface of the membrane [9]. Then, depending on the type of the receptor, one of two scenarios is possible. The receptor either dissociates from the bound ligand and is recycled back to the cell surface (re-sensitization) or is transferred to late endosomes and is subjected to degradation within lysosomes (*Fig. 1*). The fate of specific receptors depends on whether the activation was of a short-term nature or was a prolonged type of activation/reactivation [10]. Thus, for instance, the β2-adrenergic receptor following short-term activation by an agonist recycles back primarily to the cytoplasmic membrane; however, upon prolonged activation it can be transferred to the lysosome for degradation, thereby

reducing the number of receptors on the surface of the membrane (down-regulation) [10].

Recycling to the cytoplasmic membrane can occur via a rapid pathway through Rab4-containing endosomes, and via a slow pathway through Rab11-containing recycling endosomes [11]. It is believed that late endosomes contain receptors intended for degradation. Transition from early to late endosomes is accompanied by the replacement of protein Rab5 with protein Rab7 – the so-called "Rab conversion" [12].

MECHANISM OF CLATHRIN-MEDIATED INTERNALIZATION

Clathrin-coated vesicles have a three-layered structure: the outer layer is formed by clathrin (clathrin lattice), the internal layer is a lipid membrane with protein inclusions, while adaptor proteins are found in between. The adaptor protein complexes interact directly with the lipid bilayer, and clathrin in turn binds to the adaptors [13].

It is presumed that endocytosis begins with the formation of pits on the inner surface of the cytoplasmic membrane containing clathrin, the AP-2 adaptor protein complex, and accessory proteins [14]. The subunits of the adaptor complex trigger the formation of the clathrin lattice at specific sites of the cytoplasmic membrane and mediate the interaction between clathrin and the cargo protein [15]. AP-2 plays an important role in selecting the target for endocytosis by binding either directly to a transmembrane cargo protein containing the necessary sequences or via helper proteins, such as β-arrestins [16]. Binding of AP-2 to the membrane is a two-stage process. First the α-subunit of AP-2 binds weakly to phosphatidylinositol-4,5-bisphosphate (PtdIns(4,5)P2). AP-2 affinity for the corresponding endocytic motifs increases upon phosphorylation of a threonine residue in the μ2-subunit of AP-2 [17] by adaptor-associated kinase, AAK1 [18, 19]. This phosphorylation enables the μ2-subunit to bind to motifs of the cargo protein undergoing endocytosis and to PtdIns(4,5)P2 in the membrane creating the foundation for the formation of a clathrin-coated vesicle. Then, the adaptor complex can bind to the other accessory proteins, such as CALM, required for the formation of a clathrin lattice. Removal of this protein from the cell leads to the formation of large asymmetric clathrin-coated pits [20]. Simultaneously with the polymerization of clathrin, the process involves a variety of other proteins required for the control of the invagination of the cytoplasmic membrane and the formation of the pit on it. It is believed that the bending of the membrane is attributed to the action of several proteins containing BAR-domains (Bin/amphiphysin/Rvs) [21], such as amphiphysin [22] and endophilin [23]. The protein epsin is also able to stimulate the bending of the membrane [24]. Polymerizing clathrin forms the lattice (consisting of hexagons and pentagons) surrounding the emerging pits and, thus, stabilizes the membrane curvature [25].

Subsequent deformation of the membrane and polymerization of clathrin lead to the clathrin-coated vesicle remaining attached to the main part of the membrane via a narrow neck requiring GTPase dynamin for the completion of the detachment of the vesicle. Amphiphysin already being a part of the vesicle contains binding sites for both clathrin and dynamin. It is presumed that it "attracts" dynamin to the forming vesicle and facilitates its oligomerization [26]. According to the two proposed models, after polymerization of dynamin around the neck of the vesicle, a GTP hydrolysis-dependent change in its structure results in the constriction (first model) or stretching (second model) of the neck and detachment of the vesicle from the remainder of the membrane [27].

Removal of the clathrin coat from the surface of the vesicle is necessary for further fusion of the vesicle with the target membrane and delivery of endocytosed "cargo" to the target destination. The primary participants in the process of depolymerization of the clathrin coat include the proteins Hsc70 and auxilin. Auxilin, an homologue of Hsp40, binds to clathrin and attracts Hsc70, which interacts with its J-domain. As a result of interaction with auxilin, the ATPase activity of Hsc70 increases and it binds to clathrin with increased affinity, thus distorting the conformation and contributing to the dismantling of the clathrin lattice into individual molecules [28, 29]. The layer formed by the adaptor complex is removed as a result of dephosphorylation of the AP-proteins by phosphatases, as it was shown for the μ1-subunit of the AP-1 [30]. The proteins synaptojanin and endophilin dephosphorylate membrane phospholipids, thereby reducing the affinity of the adaptors for vesicles [31].

KEY PROTEINS INVOLVED IN CLATHRIN-MEDIATED ENDOCYTOSIS

G-protein-coupled receptor kinases and β-arrestins

A large number of proteins that are capable of direct interactions with the GPCR have been described [32]. However, only two classes of proteins, other than G-proteins, that specifically interact with ligand-activated receptors are known: GPCR kinases (GRK) and β-arrestins [33].

The GRK family comprises products of seven different genes. The expression of GRK1 and -7 is limited to retinal rods and cones, respectively. GRK4 is exclusively expressed in the cerebellum, testis and kidneys. GRK2, -3, -5 and -6, in contrast, are expressed in vari-

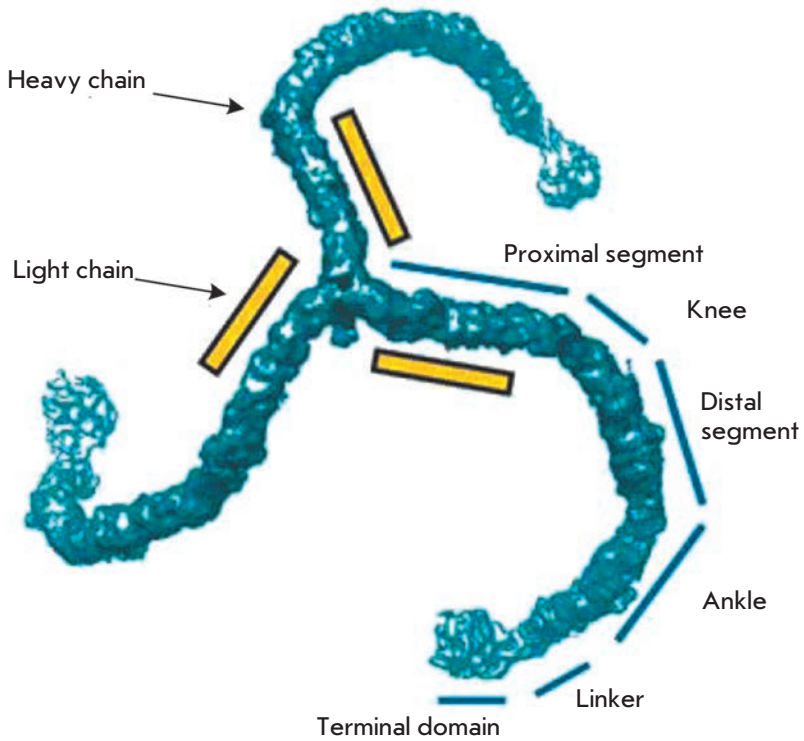

Fig 2. Clathrin molecule (triskelion). Segments of the clathrin heavy chain are indicated. The terminal domain is the N-terminal domain and the C-terminal domains are localized in the center of the molecule. The position of the light chains is shown schematically. Figure adapted from [40]

ous mammalian tissues. Seven kinases are divided into three subfamilies with respect to amino acid sequence homology. GRK1 and -7; GRK2 and -3 contain pleckstrin homology (PH) domain, and association of these kinases with plasma membranes is dependent on the interaction with the $G_{\beta\gamma}$-subunit of the G-proteins and PtdIns(4,5)P2; GRK4–6 proteins are continuously associated with the membrane [34].

Arrestins comprise 4 proteins. Arrestins 1 and 4 (x-arrestin) are expressed in retinal rods and cones, respectively. Arrestins 2 and 3 (also known as β-arrestins 1 and 2) are present in all tissues [5]. GRK and arrestins control GPCR activity at three levels: (1) silencing – functional detachment of the receptor from its G-protein; (2) regulation of transport – removal of the receptor from the cytoplasmic membrane (internalization), recycling back to the membrane and/or degradation; and (3) signal transduction – activation or inhibition of the intracellular signaling pathways independent of G-proteins. The N-terminal portion of arrestin 1 [35] and arrestins 2 and 3 [36, 37] contains the regions responsible for the recognition of agonist-activated phosphorylated GPCR. According to the proposed model, the charged phosphate groups of the receptor destroy the polar core of the arrestin resulting in the release of its C-terminal part, which is responsible for binding to the proteins involved in endocytosis – clathrin and AP-2 [38].

Clathrin

The major protein of clathrin-coated vesicles isolated by Pierce [39] was named clathrin as it was characterized by an ability to form structures with an ordered lattice, or "clathrates." The clathrin molecule resembles a triskelion (derived from Greek. τρισκελης – three-legged – a symbolic mark resembling three running legs that extend from one point) and consists of three heavy and three light chains [40] (*Fig. 2*).

A clathrin heavy chain (HC) isolated from a rat's brain is composed of 1,675 amino acid residues and has a molecular weight slightly exceeding 191 kDa (approximately 180 kDa as determined by denaturing polyacrylamide gel electrophoresis (SDS-PAGE)). The amino acid sequences of the clathrin heavy chain isolated from the brain of a human, rat or bovine are highly conserved (~ 99%) [41]. Clathrin heavy chains have also been isolated from the clathrin-coated vesicles of yeast [42] and plants [43].

Each clathrin heavy chain is in a complex with one of the light chains, LC_a or LC_b, encoded by different genes. The amino acid sequences of the light chains are highly conserved across different species (95-98%). The electrophoretic mobility of light chains consisting of 230–250 amino acid residues in the SDS-PAGE corresponds to a molecular weight of approximately 30–40 kDa. Three domains are identified in the light chain: the conserved C-terminal, the central α-helical,

and the acidic N-terminal. The homology of both chains at the amino acid sequence level reaches 60% [41]. The region consisting of 22 amino acid residues located at the N-terminus, the clathrin heavy chain binding site, the cysteine residues near the C-terminal portion, and the serine residues enriched casein kinase II phosphorylation site of the light chain LC_b are highly conserved [44]. Light chains bind the proximal domains of the clathrin heavy chains [45]; primary binding is provided by the amino acid residues 1267–1522 of the heavy chain, the residues 93–160 of the light chain $LC_{a,}$ and the residues 90–157 of the LC_b [46].

The regions that are necessary for the trimerization of heavy chains, binding of light chains, and formation of the clathrin lattice are located at the intersection of clathrin heavy chains [47, 48]. The domain that ensures the trimerization of heavy chains is localized between the amino acid residues 1488 and 1587.

Two sites for the binding of clathrin to adaptor proteins are located in the N-terminal domain. The first site interacts with peptides containing the "clathrin box" (LØXØ[D/E], where Ø is a large hydrophobic amino acid). Examples of proteins containing such a motif include β-adaptins (the LLNLD sequence is found in β-adaptins 1 and 2, the LLDLD sequence is found in β-adaptin 3), β-arrestins 1 (LIELD) and 2 (LIEFE) and amphiphysins 1 and 2 (LLDLD) [49]. The second site binds proteins containing the W-box motif (PWXXW, where X is any amino acid); e.g., the molecules of the aforementioned amphiphysins 1 and 2 [50].

Clathrin molecules spontaneously self-assemble in weakly acidic Ca^{2+}-containing buffers with a low ionic strength to form a heterogeneous population of closed polyhedral structures resembling a lattice [51, 52]. The vertex of each triskelion is located at the vertex of the lattice. The heavy chain legs and associated light chains extend outwardly from the vertices forming the edges of the lattice (*Fig. 3*).

All heavy chains form the two adjacent edges of a polyhedral lattice. The legs appear to interact via their proximal and distal domains. Each edge consists of two antiparallel proximal domains located above two antiparallel distal domains [53]. The fragments of clathrin obtained by expression in a heterologous system and consisting of a proximal domain and a region necessary for trimerization are able to self-assemble into trimers but cannot form lattices. Formation of the clathrin lattice requires distal domains that are correctly oriented by binding of the terminal domains to adaptor proteins [54]. Terminal domains in the lattice are directed inwardly towards the center and are located under the vertex, which is positioned at a distance of two vertices from the center of the triskelion. Here, the terminal domains assume the shape of hooks-projections providing a points of contact with the inner layer formed by adaptor proteins [55].

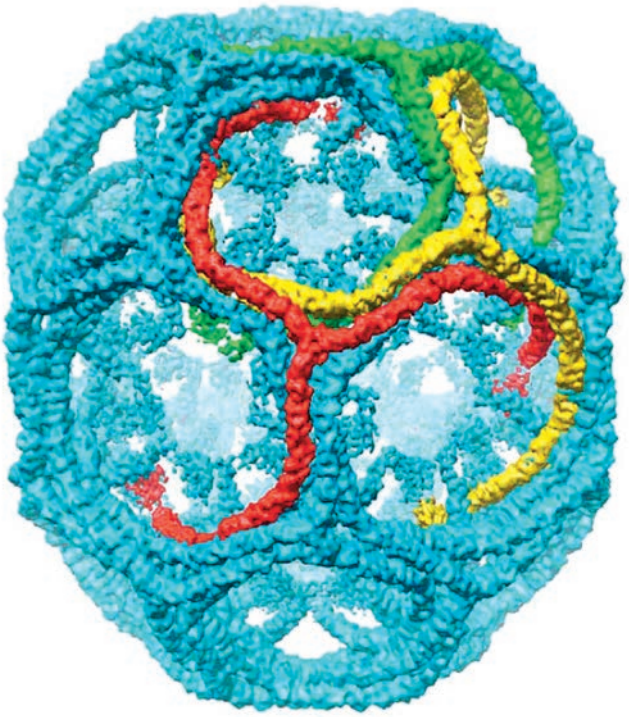

Fig 3. Hexagonal clathrin barrel model (7.9Å resolution). Only the heavy chains of clathrin are indicated. Figure adapted from [40]

It is worth mentioning that clathrin is also involved in mitosis. It is presumed that it is necessary for the stabilization of the microtubules that attach to kinetochores (called K-fibers) [56].

AP adaptor protein complexes

The second major protein of clathrin-coated vesicles is the adaptor protein complex. Its discovery was made possible by its ability to stimulate the assembly of the clathrin lattice under physiological conditions [57]. At least two adaptor complexes – AP-1 and AP-2 – have been extensively researched. These complexes have structural similarities and are composed of two different subunits of high molecular weight ~ 100 kDa (typically called adaptins), two subunits of medium size (47–50 kDa), and two low-molecular-weight subunits (17–19 kDa). The AP-2 complex comprises the following subunits: α and β2 (or β) adaptins, the μ2 subunit (50 kDa) or AP50 and the σ2 subunit (17 kDa) or AP17. The AP-1 complex comprises γ and β1 (or β') adaptins, AP47 (or μ1) and AP19 (or σ1) [58].

The designation that uses the same letters of the Greek alphabet reflects the structural and presumably

functional similarity of the subunits of the AP-1 and AP-2 complexes [59, 60]. α- and γ-adaptins differ most significantly (~ 30% amino acid sequence homology), while the μ- and σ-subunits of the AP-1 complex exhibit high levels (~ 50%) of homology to the corresponding μ- and σ-subunits of the AP-2 complex, and β1- and β2-adaptins are highly homologous (> 90%). AP-3 and AP-4 complexes that are similar in subunit composition have also been identified: δ and β3, μ3, σ3 – in the AP-3 complex; ε and β4, μ4, σ4 – in the AP-4 complex [61, 62].

The complex of subunits forms a structure resembling Mickey Mouse's head (*Fig. 4*), where the center is formed by the μ and δ subunits, and the two "ears" are composed of the C-terminal domains of the two large subunits, α and β, connected to the "head" via a flexible neck [63].

While the assembly of the clathrin lattice occurs on the membrane, it has been established that clathrin itself has no affinity with lipids. It is therefore considered that clathrin is attracted to the membrane by adaptor proteins [64, 65].

AP-2 is the main protein adaptor found on the plasma membrane and is involved in the formation of clathrin-coated vesicles during endocytosis. Immunofluorescence and immunoelectron microscopy demonstrated that AP-1, -3 and -4 are localized in endosomes and the Golgi complex [66]. AP-1 mediates the transport of proteins from the Golgi complex to early or late endosomes.

AP-1 and AP-2 directly interact with the N-terminal domain of the clathrin heavy chain via the clathrin-binding site in the β-chain. In 1998, cryoelectron microscopy was utilized to elucidate the structure of the AP-2 complex with clathrin [55]. It was established that AP-2 forms a shell of continuous density in the center of the lattice. Based on the images obtained, it was also concluded that AP-2 forms contacts with the terminal domains of the clathrin lattice. Subsequently, an X-ray diffraction analysis confirmed that the β-subunits of the AP-1, -2, and -3 containing the clathrin-binding motif interact with the terminal domain of the clathrin heavy chain [49].

In addition to clathrin, AP complexes interact with integral membrane proteins. The YXXØ sequence, located in the intracellular domains of many receptors, is recognized by the μ-subunit of all AP-complexes [67]. [DE]XXXL[LI] motifs, which are also found in the cytoplasmic domain of the receptors, bind to the β-subunits of the AP-complexes, and these subunits exhibit different affinities to different [DE]XXXL[LI] motifs. For instance, AP-1 and AP-2, but not AP-3, interact with the DDQRDLI and NEQLPML sites [68]. The DERAPLI and EEKQPLL signals interact with AP-3, but not AP-1 or AP-2 [69].

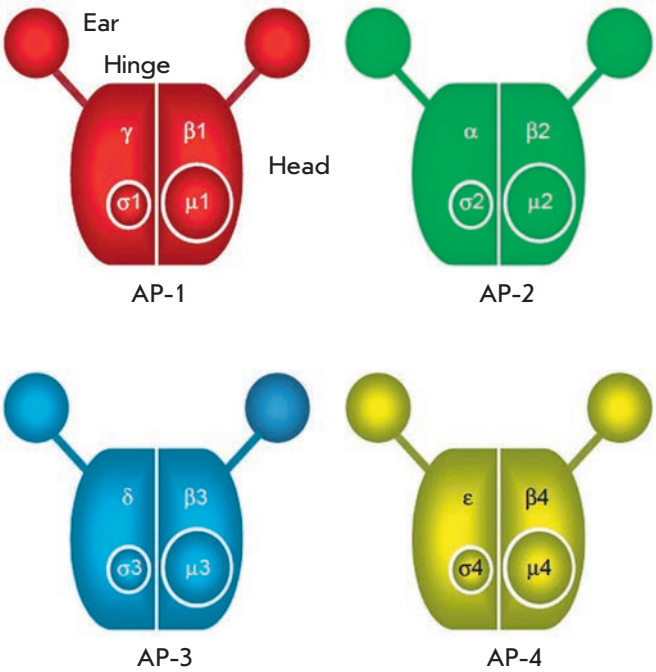

Fig 4. Schematic diagram of the AP complexes. All complexes consist of two large subunits, one medium subunit, and a small subunit. Figure adapted from [63]

Adaptor protein complexes are capable of binding to cell membrane lipids. Two lipid binding sites have been described [70]. The first site is located in the N-terminal part of the α-subunit of AP-2, and the second site is localized on the surface of the μ2 subunit [71]. Binding to the membrane is determined by the interaction of the phosphates PtdIns(4,5)P2 and side chains of the basic amino acid residues of the adaptor protein.

Auxilin

Auxilin is a multi-domain protein with a molecular weight of 100 kDa containing a clathrin-binding domain, a J-domain, and a region homologous to phosphoinositide phosphatase PTEN (*Fig. 5A*) [72, 73]. The N-terminal domain binds to phosphoinositol derivatives and PtdIns(4,5)P2 [74, 75]. The auxilin central domain interacts with clathrin, the AP-2 complex [76], and dynamin [77].

Cryoelectron microscopy at a 20Å resolution was utilized to obtain images of full-sized auxilin [78] and its fragment (549-910) [79] with a clathrin lattice. Auxilin forms a shell of density within the lattice with points of contact with the clathrin terminal domains. Auxilin is capable of interaction with the terminal domain of the clathrin heavy chain via the LLGLE motif comprising the amino acid residues 496-500. It was established that

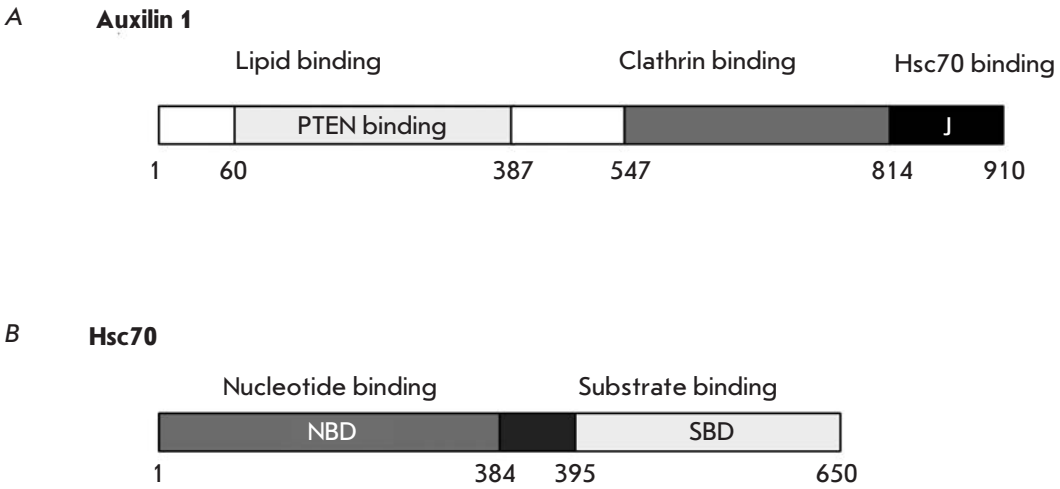

Fig 5. Domain organization of auxilin and Hsc70. Numbers indicate the boundaries of various domains. Figure adapted from [85]

the fragment containing the J- and clathrin-binding domains of auxilin interacts with the two "ankles" of the clathrin heavy chain at their point of intersection and with the subsequent terminal domain. Binding of auxilin to the clathrin lattice causes the terminal domains to twist outwards, which is attributed to a change in the position of the "ankle." This change in the position of terminal domains causes global changes throughout the entire lattice, increasing its diameter. It is believed that auxilin attracts Hsc70 to these areas, which are important for interaction within the lattice [55, 79].

Hsc70

Hsc70 is a constitutively expressed chaperone involved in many cellular processes, including protein folding, degradation, and translocation. Another interesting function of Hsc70 is its ability to "dismount" the clathrin lattice. Thus, addition of ATP and Hsc70 to clathrin-coated vesicles *in vitro* causes disassembly of the clathrin lattice [80]. This is a stoichiometric reaction that requires 3 mol of Hsc70 and ATP for the dissociation of 1 mol of clathrin triskelions [80-82].

Similary to all Hsp70 family members, Hsc70 requires a protein containing a J-domain to "work" with a particular substrate [83]. Auxilin, which binds to clathrin and contains a J-domain, plays that function. The J-domain in the auxilin molecule is positioned in a way that the motif required for the interaction with the Hsc70 protein is exposed on the outside of the lattice. The QLMLT sequence (1638-1642) located in the C-terminal portion of the clathrin heavy chain is also required [84] (*Fig. 5B*). The following model of lattice disassembly is proposed: bending at the location of intersection of "ankles" caused by the interaction with auxilin enables Hsc70 to bind to its site near the C-terminus of the clathrin molecule. It is assumed that one vertex of the triskelion binds one molecule of Hsc70 and for the strong interaction to be achieved hydrolysis of ATP is required. Therefore, deformation of the clathrin lattice which had begun after binding to auxilin is enhanced [85].

Other clathrin-interacting proteins

Apart from the AP-2 adaptor complex, clathrin-coated vesicles also contain other proteins. A vast array of monomeric adaptors that bind to clathrin and are able to interact with integral membrane proteins, PtdIns(4,5)P2 and AP-2, in order to ensure the occurrence of clathrin-mediated endocytosis of transmembrane proteins have been identified (*Fig. 6*). Examples of such adaptors include epsins, the CALM/AP180 protein, HIP1, and HIP1R. The N-terminal domain of these proteins that binds to PtdIns(4,5)P2 is called ENTH (epsin N-terminal homology) or ANTH (AP180 N-terminal homology domain). Another group of monomeric proteins includes Dab2, ARH, and Numb. These proteins bind to AP-2, and some of them interact with clathrin. They all contain a phosphotyrosine-binding domain (PTB) responsible for interaction with membrane lipids and for recognition of the FXNPXY motif localized in the cytoplasmic portions of LDLRs. It was demonstrated that phosphorylation of tyrosine at this motif is not a prerequisite for the binding of monomeric adaptors [71].

In addition to binding to cell membrane lipids, the adaptors recognize the signals localized in the cytoplasmic portion of the receptors. These may include posttranslational modifications (phosphorylation, ubiquitination), short peptide motifs, or both [86]. It is presumed that binding of the adaptor to the cytoplasmic membrane is stabilized upon simultaneous interac-

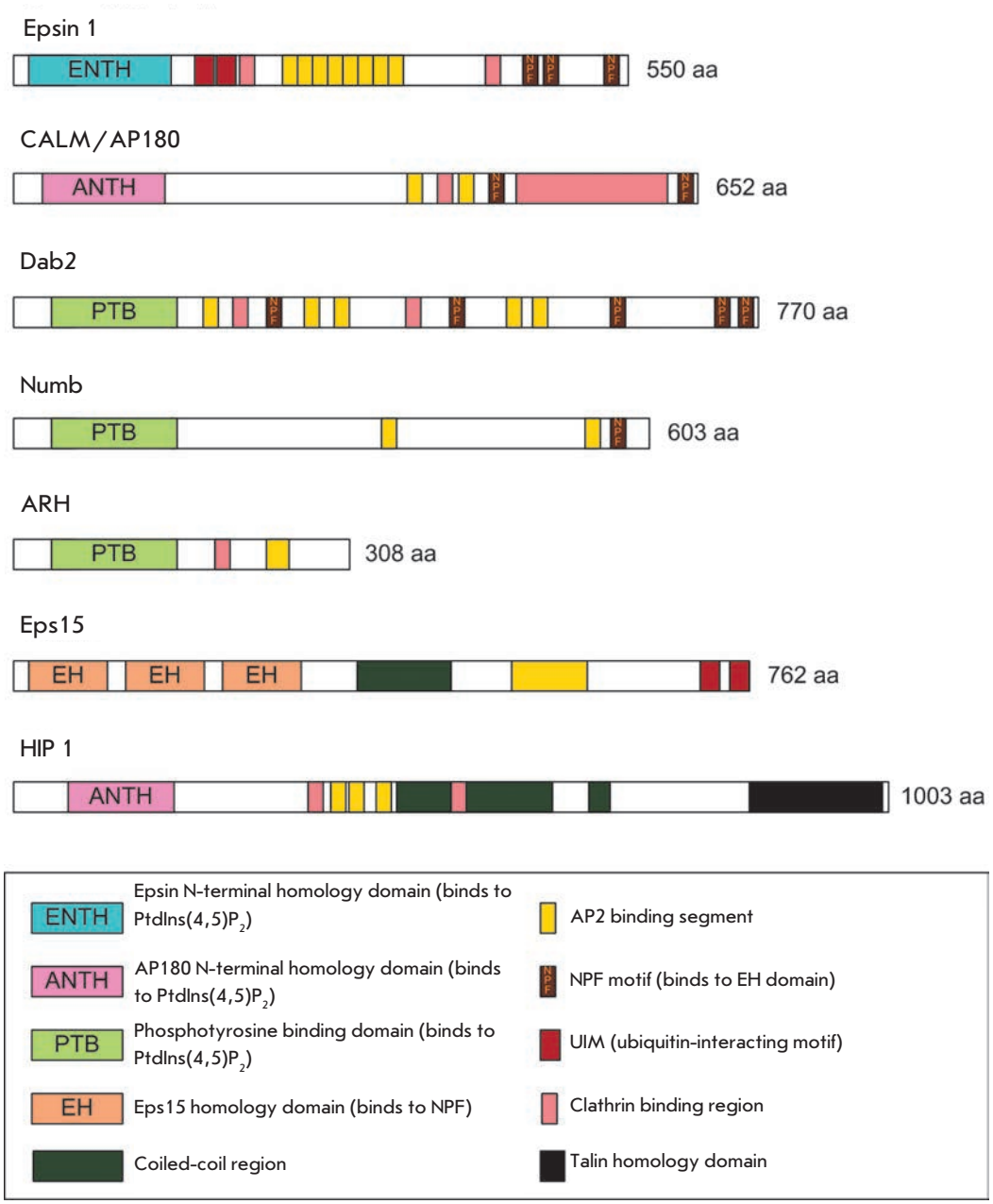

Fig. 6. Monomeric clathrin-binding adaptors. Schematic representation of the overall domain structure. Figure adapted from [70]

tion of the adaptor with PtdIns(4,5)P2 and the receptor [70, 87].

The role of all these adaptor proteins is poorly understood. Perhaps, the use of various proteins enables to avoid simultaneous accumulation of various GPCR in the same clathrin-coated vesicle [88].

Specific recognition of the receptor for its subsequent removal from the membrane is the role of adaptors that has been most researched. This recognition leads to disruption of the delivery of the receptor to the ligand responsible for its activation and often to the transfer of the receptor to lysosomes for degradation. Internalization of the receptor mediated by a specific adaptor may also result in the receptor being directed to another cellular compartment with its own set of signaling molecules [89]. Another consequence of the selective removal of the receptor from the cell surface may be such a cellular development, which is associated with one of the daughter cells receiving a different set of adaptors responsible for the endocytosis of certain receptors. For instance, during the development of Drosophila sense organs, the adaptor Numb is transferred to only one of the two daughter cells. Numb is responsible for the adjustment of the development of

Fig 7. Schematic representation of the protein TRIP8b domain organization

the cell it is located in by inhibiting transduction of signals along the Notch-pathway. Inhibition is attributed to receptor endocytosis; however, it is unclear whether the protein Numb controls the endocytosis of Notch directly or via the transmembrane regulator of Notch – Sandopo [90, 91].

As mentioned above, the proteins Numb, Dab2, and ARH contain a domain that specifically recognizes the FXNPXY sequence in the cytoplasmic portion of the receptors. It was demonstrated that the proteins ARH and Dab2 are involved in the endocytosis of the LDL receptor, and the Numb protein regulates the endocytosis of the integral membrane proteins, including the EGF and Notch receptors [88].

The Epsin protein is involved in clathrin-mediated endocytosis in mammalian cells, where it plays an important role in the cytoplasmic membrane bending attributed to the action of the ENTH domain. The occurrence of this process is associated with the C-terminal portion of the protein binding to clathrin coat components (clathrin and AP-2 N-terminal domains, and EH-domain of the protein Eps15), which leads to the assembly of the clathrin lattice. The UIM-repeats of the epsin protein that acts as an adaptor protein facilitate recognition of the ubiquitinated "cargo": in particular transmembrane proteins [88, 92].

The proteins AP180 and CALM ease the assembly of the clathrin-coated vesicles and regulate their size [20, 93, 94]. It is assumed that AP180 and CALM play an important role in ensuring the polarity and control of the growth of the axons and dendrites of the hippocampal neurons [95].

TRIP8b – novel clathrin-binding protein and a potential endocytosis adaptor

TRIP8b (TPR-containing Rab8b interacting protein) is one of the recently discovered potential adaptors involved in the regulation of endocytosis. Being expressed predominantly in brain tissue, TRIP8b was initially identified as a protein that interacts with the small GTP-ase Rab8b [96]. Six TPR-motifs are located in the C-terminal part of TRIP8b, forming the TPR-domain (*Fig.* 7). TPR-motifs represent repeats consisting of 34 amino acids. These motifs are found in many proteins and are involved in protein-protein interactions [97]. These repeats are often arranged consecutively, resulting in a spatial structure consisting of two antiparallel α-helices connected by a short loop [98]. The N-terminal portion of TRIP8b does not contain sequences homologous to other known proteins and undergoes alternative splicing [99].

It is known that TRIP8b is 40% identical to the Pex5 protein (peroxin protein) and their C-terminal portion containing TPR-domains are 57% identical (other names for the TRIP8b include Pex5Rp, Pex5p related protein) [100]. The Pex5 protein is found in many organisms ranging from yeast to mammals; it is responsible for the recognition and import of peroxisomal proteins containing the C-terminal SKL motif (peroxisome-targeting signal type 1, PTS1) from the cytosol into peroxisomes. Despite the fact that TRIP8b recognizes the PTS1 sequence it has been established that it is not involved in peroxisomal protein import [100].

TRIP8b interacts with the Rab8b protein and also directly with a protein that forms the HCN-channel (Hyperpolarization-activated, Cyclic Nucleotide-regulated channel) [99, 101]. It was found that TRIP8b binds to the CIRL1 receptor [102], which belongs to the GPCR class, and to the transmembrane protein called Caspr [103].

HCN channels belong to the family of voltage-dependent channels [104-106]. These channels are involved in the control of the heart and brain pacemakers' activity, ensuring resting membrane potential and synaptic transmission (see reviews [107] and [108]). Investigations into the interactions between TRIP8b and the HCN channel demonstrated that TRIP8b regulates the functions and surface expression of the channel [99, 101, 109, 110]. It is assumed that TRIP8b acts as an auxiliary adaptor for HCN and that the interaction is mediated by at least two different regions in the TRIP8b and HCN molecules [111, 112].

All of the previously identified interactions of TRIP8b with other proteins were mediated by the TPR-domains localized in the C-terminal part of TRIP8b [96, 99, 100] or a segment located in the conserved central region of the protein [109, 111, 112].

As mentioned above, the N-terminal portion of TRIP8b undergoes alternative splicing. Isoforms of the

protein generated as a result of splicing affect the HCN transport and its localization on the cytoplasmic membrane differently: some isoforms increase the surface expression of HCN1 and others decrease it [109, 110]. It was found that TRIP8b interacts with clathrin and this interaction involves the N-terminal portion of the protein TRIP8b [103, 113]. The clathrin-binding site in the TRIP8b molecule consists of two short motifs reminiscent of the "clathrin box" motif.

In order to investigate the TRIP8b functions two types of knockout mice were obtained. The phenotype of mice lacking certain TRIP8b isoforms was identical to that of wild-type mice [114]. Abnormalities in the motor learning and increased resistance during the behavioral despair test were observed in mice with a complete absence of the protein ($TRIP8b^{-/-}$) [115].

The need to conduct further investigations into clathrin-mediated endocytosis is unquestionable. Internalization of ligand-activated receptors and the functions of various accessory proteins are of significant interest. Interactions between clathrin and numerous adaptor proteins are currently being actively investigated. Clathrin is involved in various processes: endocytosis, intracellular traffic, and segregation of chromosomes. It is assumed that abnormalities in the functioning of clathrin can lead to the development of certain diseases. In this regard, investigations into the structure and functions of clathrin-coated vesicles, as well as the proteins involved in the formation of the latter, is of interest from the point of view of molecular biology and biomedicine. ●

This work was supported by the Russian Foundation for Basic Research (Grant № 11-04-12151-ofi-m-2011, 12-04-01817-a, 12-04-32099 mol_a).

REFERENCES

1. Pierce K.L., Premont R.T., Lefkowitz R.J. // Nat. Rev. Mol. Cell. Biol. 2002. V. 3. P. 639–650.
2. Ovchinnikov Yu.A. // FEBS Lett. 1982. V. 148. P. 179–191.
3. Clapham D.E., Neer E.J. // Nature. 1993. V. 365. P. 403–406.
4. Oldham W.M., Hamm H.E. // Nat. Rev. Mol. Cell. Biol. 2008. V. 9. P. 60–71.
5. Shenoy S.K., Lefkowitz R.J. // Biochem. J. 2003. V. 375. P. 503–515.
6. Goodman O.B., Jr., Krupnick J.G., Santini F., Gurevich V.V., Penn R.B., Gagnon A.W., Keen J.H., Benovic J.L. // Nature. 1996. V. 383. P. 447–450.
7. Laporte S.A., Oakley R.H., Zhang J., Holt J.A., Ferguson S.S., Caron M.G., Barak L.S. // Proc. Natl. Acad. Sci. USA. 1999. V. 96. P. 3712–3717.
8. Doherty G.J., McMahon H.T. // Annu. Rev. Biochem. 2009. V. 78. P. 857–902.
9. Calebiro D., Nikolaev V.O., Persani L., Lohse M.J. // Trends Pharmacol. Sci. 2010. V. 31. P. 221–228.
10. Hanyaloglu A.C., von Zastrow M. // Annu. Rev. Pharmacol. Toxicol. 2008. V. 48. P. 537–568.
11. Stenmark H. // Nat. Rev. Mol. Cell. Biol. 2009. V. 10. P. 513–525.
12. Poteryaev D., Datta S., Ackema K., Zerial M., Spang A. // Cell. 2010. V. 141. P. 497–508.
13. Young A. // Semin. Cell. Dev. Biol. 2007. V. 18. P. 448–458.
14. Ehrlich M., Boll W., van Oijen A., Hariharan R., Chandran K., Nibert M.L., Kirchhausen T. // Cell. 2004. V. 118. P. 591–605.
15. Ohno H., Stewart J., Fournier M.C., Bosshart H., Rhee I., Miyatake S., Saito T., Gallusser A., Kirchhausen T., Bonifacino J.S. // Science. 1995. V. 269. P. 1872–1875.
16. Edeling M.A., Mishra S.K., Keyel P.A., Steinhauser A.L., Collins B.M., Roth R., Heuser J.E., Owen D.J., Traub L.M. // Dev. Cell. 2006. V. 10. P. 329–342.
17. Honing S., Ricotta D., Krauss M., Spate K., Spolaore B., Motley A., Robinson M., Robinson C., Haucke V., Owen D.J. // Mol. Cell. 2005. V. 18. P. 519–531.
18. Lauritsen J.P., Menne C., Kastrup J., Dietrich J., Odum N., Geisler C. // Biochim. Biophys. Acta. 2000. V. 1497. P. 297–307.
19. Ricotta D., Conner S.D., Schmid S.L., von Figura K., Honing S. // J. Cell. Biol. 2002. V. 156. P. 791–795.
20. Meyerholz A., Hinrichsen L., Groos S., Esk P.C., Brandes G., Ungewickell E.J. // Traffic. 2005. V. 6. P. 1225–1234.
21. Blood P.D., Voth G.A. // Proc. Natl. Acad. Sci. USA. 2006. V. 103. P. 15068–15072.
22. Takei K., Slepnev V.I., Haucke V., De Camilli P. // Nat. Cell. Biol. 1999. V. 1. P. 33–39.
23. Farsad K., Ringstad N., Takei K., Floyd S.R., Rose K., De Camilli P. // J. Cell. Biol. 2001. V. 155. P. 193–200.
24. Castillo P.E., Schoch S., Schmitz F., Sudhof T.C., Malenka R.C. // Nature. 2002. V. 415. P. 327–330.
25. McMahon H.T., Boucrot E. // Nat. Rev. Mol. Cell. Biol. 2011. V. 12. P. 517–533.
26. Yoshida Y., Kinuta M., Abe T., Liang S., Araki K., Cremona O., Di Paolo G., Moriyama Y., Yasuda T., De Camilli P., et al. // EMBO J. 2004. V. 23. P. 3483–3491.
27. Ferguson S.M., De Camilli P. // Nat. Rev. Mol. Cell. Biol. 2012. V. 13. P. 75–88.
28. Barouch W., Prasad K., Greene L., Eisenberg E. // Biochemistry (Mosc.). 1997. V. 36. P. 4303–4308.
29. Ungewickell E., Ungewickell H., Holstein S.E., Lindner R., Prasad K., Barouch W., Martin B., Greene L.E., Eisenberg E. // Nature. 1995. V. 378. P. 632–635.
30. Ghosh P., Kornfeld S. // J. Cell. Biol. 2003. V. 160. P. 699–708.
31. Verstreken P., Koh T.W., Schulze K.L., Zhai R.G., Hiesinger P.R., Zhou Y., Mehta S.Q., Cao Y., Roos J., Bellen H.J. // Neuron. 2003. V. 40. P. 733–748.
32. Bockaert J., Fagni L., Dumuis A., Marin P. // Pharmacol Ther. 2004. V. 103. P. 203–221.
33. Lefkowitz R.J., Shenoy S.K. // Science. 2005. V. 308. P. 512–517.
34. Pitcher J.A., Freedman N.J., Lefkowitz R.J. // Annu. Rev. Biochem. 1998. V. 67. P. 653–692.
35. Gurevich V.V., Benovic J.L. // J. Biol. Chem. 1993. V. 268. P. 11628–11638.
36. Gurevich V.V., Richardson R.M., Kim C.M., Hosey M.M., Benovic J.L. // J. Biol. Chem. 1993. V. 268. P. 16879–16882.
37. Gurevich V.V., Dion S.B., Onorato J.J., Ptasienski J., Kim

C.M., Sterne-Marr R., Hosey M.M., Benovic J.L. // J. Biol. Chem. 1995. V. 270. P. 720–731.
38. Gurevich V.V., Gurevich E.V. // Pharmacol. Ther. 2006. V. 110. P. 465–502.
39. Pearse B.M. // J. Mol. Biol. 1975. V. 97. P. 93–98.
40. Fotin A., Cheng Y., Sliz P., Grigorieff N., Harrison S.C., Kirchhausen T., Walz T. // Nature. 2004. V. 432. P. 573–579.
41. Keen J.H. // Annu. Rev. Biochem. 1990. V. 59. P. 415–438.
42. Mueller S.C., Branton D. // J. Cell. Biol. 1984. V. 98. P. 341–346.
43. Wiedenhoeft R.E., Schmidt G.W., Palevitz B.A. // Plant Physiol. 1988. V. 86. P. 412–416.
44. Jackson A.P., Parham P. // J. Biol. Chem. 1988. V. 263. P. 16688–16695.
45. Ungewickell E. // EMBO J. 1983. V. 2. P. 1401–1408.
46. Chen C.Y., Reese M.L., Hwang P.K., Ota N., Agard D., Brodsky F.M. // EMBO J. 2002. V. 21. P. 6072–6082.
47. Blank G.S., Brodsky F.M. // EMBO J. 1986. V. 5. P. 2087–2095.
48. Blank G.S., Brodsky F.M. // J. Cell. Biol. 1987. V. 105. P. 2011–2019.
49. ter Haar E., Harrison S.C., Kirchhausen T. // Proc. Natl. Acad. Sci. USA. 2000. V. 97. P. 1096–1100.
50. Ramjaun A.R., McPherson P.S. // J. Neurochem. 1998. V. 70. P. 2369–2376.
51. Crowther R.A., Finch J.T., Pearse B.M. // J. Mol. Biol. 1976. V. 103. P. 785–798.
52. Kartenbeck J. // Cell Biol. Int. Rep. 1978. V. 2. P. 457–464.
53. Wakeham D.E., Chen C.Y., Greene B., Hwang P.K., Brodsky F.M. // EMBO J. 2003. V. 22. P. 4980–4990.
54. Greene B., Liu S.H., Wilde A., Brodsky F.M. // Traffic. 2000. V. 1. P. 69–75.
55. Smith C.J., Grigorieff N., Pearse B.M. // EMBO J. 1998. V. 17. P. 4943–4953.
56. Royle S.J. // J. Cell. Sci. 2012. V. 125. P. 19–28.
57. Keen J.H., Willingham M.C., Pastan I.H. // Cell. 1979. V. 16. P. 303–312.
58. Schmid S.L. // Annu. Rev. Biochem. 1997. V. 66. P. 511–548.
59. Gallusser A., Kirchhausen T. // EMBO J. 1993. V. 12. P. 5237–5244.
60. Stepp J.D., Pellicena-Palle A., Hamilton S., Kirchhausen T., Lemmon S.K. // Mol. Biol. Cell. 1995. V. 6. P. 41–58.
61. Simpson F., Peden A.A., Christopoulou L., Robinson M.S. // J. Cell. Biol. 1997. V. 137. P. 835–845.
62. DellíAngelica E.C., Mullins C., Bonifacino J.S. // J. Biol. Chem. 1999. V. 274. P. 7278–7285.
63. Robinson M.S., Bonifacino J.S. // Curr. Opin. Cell. Biol. 2001. V. 13. P. 444–453.
64. Aridor M., Traub L.M. // Traffic. 2002. V. 3. P. 537–546.
65. Wilbur J.D., Hwang P.K., Brodsky F.M. // Traffic. 2005. V. 6. P. 346–350.
66. Peden A.A., Oorschot V., Hesser B.A., Austin C.D., Scheller R.H., Klumperman J. // J. Cell. Biol. 2004. V. 164. P. 1065–1076.
67. Bonifacino J.S., Traub L.M. // Annu. Rev. Biochem. 2003. V. 72. P. 395–447.
68. Hofmann M.W., Honing S., Rodionov D., Dobberstein B., von Figura K., Bakke O. // J. Biol. Chem. 1999. V. 274. P. 36153–36158.
69. Honing S., Sandoval I.V., von Figura K. // EMBO J. 1998. V. 17. P. 1304–1314.
70. Maldonado-Baez L., Wendland B. // Trends Cell Biol. 2006. V. 16. P. 505–513.
71. Owen D.J., Collins B.M., Evans P.R. // Annu. Rev. Cell. Dev. Biol. 2004. V. 20. P. 153–191.
72. Ahle S., Ungewickell E. // J. Cell. Biol. 1990. V. 111. P. 19–29.
73. Ungewickell E., Ungewickell H., Holstein S.E. // J. Biol. Chem. 1997. V. 272. P. 19594–19600.
74. Lee D.W., Wu X., Eisenberg E., Greene L.E. // J. Cell Sci. 2006. V. 119. P. 3502–3512.
75. Massol R.H., Boll W., Griffin A.M., Kirchhausen T. // Proc. Natl. Acad. Sci. USA. 2006. V. 103. P. 10265–10270.
76. Scheele U., Kalthoff C., Ungewickell E. // J. Biol. Chem. 2001. V. 276. P. 36131–36138.
77. Newmyer S.L., Christensen A., Sever S. // Dev. Cell. 2003. V. 4. P. 929–940.
78. Smith C.J., Dafforn T.R., Kent H., Sims C.A., Khubchandani-Aswani K., Zhang L., Saibil H.R., Pearse B.M. // J. Mol. Biol. 2004. V. 336. P. 461–471.
79. Fotin A., Cheng Y., Grigorieff N., Walz T., Harrison S.C., Kirchhausen T. // Nature. 2004. V. 432. P. 649–653.
80. Greene L.E., Eisenberg E. // J. Biol. Chem. 1990. V. 265. P. 6682–6687.
81. Barouch W., Prasad K., Greene L.E., Eisenberg E. // J. Biol. Chem. 1994. V. 269. P. 28563–28568.
82. Ma Y., Greener T., Pacold M.E., Kaushal S., Greene L.E., Eisenberg E. // J. Biol. Chem. 2002. V. 277. P. 49267–49274.
83. Hartl F.U., Hayer-Hartl M. // Science. 2002. V. 295. P. 1852–1858.
84. Rapoport I., Boll W., Yu A., Bocking T., Kirchhausen T. // Mol. Biol. Cell. 2008. V. 19. P. 405–413.
85. Xing Y., Bocking T., Wolf M., Grigorieff N., Kirchhausen T., Harrison S.C. // EMBO J. 2010. V. 29. P. 655–665.
86. Robinson M.S. // Trends Cell Biol. 2004. V. 14. P. 167–174.
87. Aguilar R.C., Watson H.A., Wendland B. // J. Biol. Chem. 2003. V. 278. P. 10737–10743.
88. Wolfe B.L., Trejo J. // Traffic. 2007. V. 8. P. 462–470.
89. Polo S., Di Fiore P.P. // Cell. 2006. V. 124. P. 897–900.
90. Le Borgne R. // Curr. Opin. Cell. Biol. 2006. V. 18. P. 213–222.
91. Hutterer A., Knoblich J.A. // EMBO Rep. 2005. V. 6. P. 836–842.
92. Horvath C.A., Vanden Broeck D., Boulet G.A., Bogers J., De Wolf M.J. // Int. J. Biochem. Cell. Biol. 2007. V. 39. P. 1765–1770.
93. Morgan J.R., Zhao X., Womack M., Prasad K., Augustine G.J., Lafer E.M. // J. Neurosci. 1999. V. 19. P. 10201–10212.
94. Zhang B., Koh Y.H., Beckstead R.B., Budnik V., Ganetzky B., Bellen H.J. // Neuron. 1998. V. 21. P. 1465–1475.
95. Bushlin I., Petralia R.S., Wu F., Harel A., Mughal M.R., Mattson M.P., Yao P.J. // J. Neurosci. 2008. V. 28. P. 10257–10271.
96. Chen S., Liang M.C., Chia J.N., Ngsee J.K., Ting A.E. // J. Biol. Chem. 2001. V. 276. P. 13209–13216.
97. Blatch G.L., Lassle M. // Bioessays. 1999. V. 21. P. 932–939.
98. DíAndrea L.D., Regan L. // Trends Biochem. Sci. 2003. V. 28. P. 655–662.
99. Santoro B., Wainger B.J., Siegelbaum S.A. // J. Neurosci. 2004. V. 24. P. 10750–10762.
100. Amery L., Sano H., Mannaerts G.P., Snider J., van Looy J., Fransen M., van Veldhoven P.P. // Biochem. J. 2001. V. 357. P. 635–646.
101. Zolles G., Wenzel D., Bildl W., Schulte U., Hofmann A., Muller C.S., Thumfart J.O., Vlachos A., Deller T., Pfeifer A., et al. // Neuron. 2009. V. 62. P. 814–825.
102. Popova N.V., Plotnikov A., Deev I.E., Petrenko A.G. // Dokl. Biochem. Biophys. 2007. V. 414. P. 149–151.
103. Popova N.V., Plotnikov A.N., Ziganshin R., Deyev

I.E., Petrenko A.G. // Biochemistry (Mosc.). 2008. V. 73. P. 644–651.
104. Santoro B., Grant S.G., Bartsch D., Kandel E.R. // Proc. Natl. Acad. Sci. USA. 1997. V. 94. P. 14815–14820.
105. Ludwig A., Zong X., Jeglitsch M., Hofmann F., Biel M. // Nature. 1998. V. 393. P. 587–591.
106. Santoro B., Liu D.T., Yao H., Bartsch D., Kandel E.R., Siegelbaum S.A., Tibbs G.R. // Cell. 1998. V. 93. P. 717–729.
107. DiFrancesco D. // Annu. Rev. Physiol. 1993. V. 55. P. 455–472.
108. Robinson R.B., Siegelbaum S.A. // Annu. Rev. Physiol. 2003. V. 65. P. 453–480.
109. Lewis A.S., Schwartz E., Chan C.S., Noam Y., Shin M., Wadman W.J., Surmeier D.J., Baram T.Z., Macdonald R.L., Chetkovich D.M. // J. Neurosci. 2009. V. 29. P. 6250–6265.
110. Santoro B., Piskorowski R.A., Pian P., Hu L., Liu H., Siegelbaum S.A. // Neuron. 2009. V. 62. P. 802–813.
111. Han Y., Noam Y., Lewis A.S., Gallagher J.J., Wadman W.J., Baram T.Z., Chetkovich D.M. // J. Biol. Chem. 2011. V. 286. P. 20823–20834.
112. Santoro B., Hu L., Liu H., Saponaro A., Pian P., Piskorowski R.A., Moroni A., Siegelbaum S.A. // J. Neurosci. 2011. V. 31. P. 4074–4086.
113. Popova N.V., Deyev I.E., Petrenko A.G. // J. Neurochem. 2011. V. 118. P. 988–998.
114. Piskorowski R., Santoro B., Siegelbaum S.A. // Neuron. 2011. V. 70. P. 495–509.
115. Lewis A.S., Vaidya S.P., Blaiss C.A., Liu Z., Stoub T.R., Brager D.H., Chen X., Bender R.A., Estep C.M., Popov A.B., et al. // J. Neurosci. 2011. V. 31. P. 7424–7440.

Acadesine Triggers Non-apoptotic Death in Tumor Cells

V. A. Glazunova[1*], K. V. Lobanov[2], R. S. Shakulov[2], A. S. Mironov[2], A. A. Shtil[1]
[1]Blokhin Cancer Center, Russian Academy of Medical Sciences, 24, Kashirskoe shosse, Moscow, Russia, 115478
[2]State Research Institute of Genetics and Selection of Industrial Microorganisms, 1, Dorozhny proezd, Moscow, Russia, 117545
*E-mail: gav-83@mail.ru
Received 27.12.2012

ABSTRACT **We studied the cytotoxicity of acadesine (5-aminoimidazole-4-carboxamide-1-β-D-ribofuranoside) for tumor and normal cells of various species and tissue origin. In tumor cells, acadesine triggered non-apoptotic death; the potency of the compound to normal cells was substantially lower. Acadesine was toxic for tumor cells with multidrug resistant phenotypes caused by the transmembrane transporter P-glycoprotein or lack of pro-apoptotic p53. Activity of adenosine receptors was required for acadesine-induced cell death, whereas functioning of AMP-dependent protein kinase was not required. A more pronounced cytotoxicity for tumor cells, as well as the non-canonical death mechanism(s), makes acadesine a promising candidate for antitumor therapy.**
KEYWORDS **acadesine, cell death, tumor cells.**

INTRODUCTION

Acadesine (5-**aminoimidazole**-4-carboxamide-1-β-*D*-ribofuranoside, AICAR) is currently undergoing clinical trials as an agent for treating chronic lymphocytic leukemia [1, 2]. A very important property of acadesine is its preferential toxicity for tumor cells, while nontumor cells are damaged to a lesser significant extent [2, 3]. It has been demonstrated previously that acadesine can stimulate AMP-activated protein kinase (AMPK), the essential regulator of the cellular energy balance that controls the oxidation of fatty acids, the glucose metabolism, and synthesis of proteins, fatty acids, and cholesterol [4–10]. The mechanism of action of acadesine is determined by its phosphorylation with adenosine kinase, yielding ZMP (5-amino-4-imidazole carboxamide ribotide), an intermediate product of *de novo* synthesis of purine nucleotides [1, 4, 5, 8]. ZMP can activate AMPK by imitating the metabolic effects of AMP. The antitumor effect of acadesine is attributed to apoptosis induction [7, 9, 11, 12]. Meanwhile, data on non-apoptotic cell death and the AMPK-independent mechanism of action of acadesine on tumor cells have also been obtained [12, 13].

The effect of acadesine on mammalian cells was studied in this work. Acadesine was shown to trigger the death of tumor cells of different tissue origins, including those resistant to a number of antitumor agents. The mechanisms of cell death differ from apoptosis; the necessity for adenosine transport turns out to be their crucial feature. The selectivity of the cytotoxic effect and features of the mechanisms of tumor cell death may be significant factors that determine the potential use of acadesine in antitumor therapy.

EXPERIMENTAL

The following human cell lines were used in the experiments: HCT116 (large intestine adenocarcinoma), HCT116p53KO (isogenic p53 knockout subline), K562 (promyelocytic leukemia), K562/4 (subline obtained after selection for survival in the presence of doxorubicine; the multidrug resistance protein (MDR) P-glycoprotein (Pgp) was expressed), MCF-7 (breast adenocarcinoma), MCF-7Dox (subline obtained after selection for survival in the presence of doxorubicine; Pgp-mediated MDR phenotype), passaged human fibroblasts 2 (PHF-2), lymphocytes from healthy blood donors, and murine cells P388 (lymphocytic leukemia) and Sp2/0 (myeloma). The reagents were purchased from PanEco (Russia), except for the specially mentioned cases. The cells were grown in Dulbecco's modified Eagle's medium (DMEM) supplemented with 5% fetal bovine serum (BioWhittaker, Austria), 2 mM *L*-glutamine, 100 AU/ml penicillin, and 100 μg/ml streptomycin at 37°C, 5% CO_2 in a moist atmosphere. Cultures in the logarithmic growth phase were used for the experiments. Lymphocytes were isolated from the peripheral blood from donors via centrifugation in a ficoll–urographin density gradient (d = 1.077 g/cm^3).

Table 1. Acadesine cytotoxicity for mammalian cells

Cells	Acadesine, mM					
	0	0.125	0.25	0.5	1.0	2.0
K562	100*	100	70	46	9	0
P388	100	36	30	20	9	0
Sp2/0	100	34	29	14	0	0
K562/4	100	100	72	42	8	0
MCF-7	100	100	82	50	15	2
MCF-7Dox	100	100	86	48	17	1
HCT116	100	100	50	36	23	0
HCT116p53KO	100	100	54	34	25	0
PHF-2, proliferating	100	100	100	96	96	86
PHF-2, nonproliferating	100	100	100	100	95	92
Donor lymphocytes	100	100	100	98	94	90

Note. MTT assay data of the cells after 72 h of incubation are shown. *The survival rate of the cells incubated without acadesine were taken as 100%. Each value is the average value of five independent experiments; standard deviation ≤ 0%. ** Fibroblast proliferation was terminated by growing cells until the monolayer reached 100% confluency (contact inhibition of cell division).

Acadesine was obtained at the State Research Institute of Genetics and Selection of Industrial Microorganisms via the microbiological procedure using an original recombinant strain [14]. Moreover, the cytotoxicity of acadesine purchased from Sigma was assessed. Dipyridamole (inhibitor of adenosine receptors) [8], 5-iodotubercidine (adenosine kinase inhibitor preventing the conversion of acadesine to ZMP), and zVAD-fmk (carbobenzoxyvalylalanyl-aspartyl-[O-methyl]-fluoromethylketone), a pan-caspase inhibitor, were also purchased from Sigma. All the compounds were dissolved in dimethyl sulfoxide or water (10–20 mM) and stored at –20°C. On the day when the experiment was supposed to take place, dilutions of the sample in the culture medium were prepared. The MTT assay, staining with propidium iodide and Annexin V conjugated to fluorescein isothiocyanate (FITC), determination of the cell cycle by flow cytofluorometry, and electrophoretic analysis of the integrity of genomic DNA were used to assess acadesine cytotoxicity [15, 16]. An apoptosis inductor, alkyl cationic glycerolipid *rac*-N-{4-[(2-ethoxy-3-octadecyloxy)prop-1-yloxycarbonyl] butyl}-N'-methylimidazolium iodide, was used as the control compound in individual experiments [17].

RESULTS AND DISCUSSION

Predominant sensitivity of tumor cells to acadesine

We had ascertained in the preliminary experiments that an acadesine sample obtained microbiologically and commercial acadesine are characterized by identical physicochemical properties, purity, storage stability, and cytotoxicity (data not shown). Acadesine obtained according to the authors' procedure was used for further experiments. *Table 1* lists the cytotoxicity of acadesine for the transformed and non-transformed cells (cultured or freshly isolated) originating from different species and tissues.

It follows from the data listed in *Table 1* that P388 (murine leukemia) and Sp2/0 (murine myeloma) cells exhibit the highest sensitivity to acadesine: ~ 1/3 of the cell population survives at an acadesine concentration of 0.125 mM. Sub-millimolar concentrations of acadesine also cause the death of other transformed cell lines. It is important to note that the acadesine cytotoxicities are almost identical for the K562 leukemia cell line and its subline with Pgp-mediated MDR (K562/4). This is also valid for a MCF-7 breast adenocarcinoma cell line and the MDR subline (*Table 1*). The comparison of

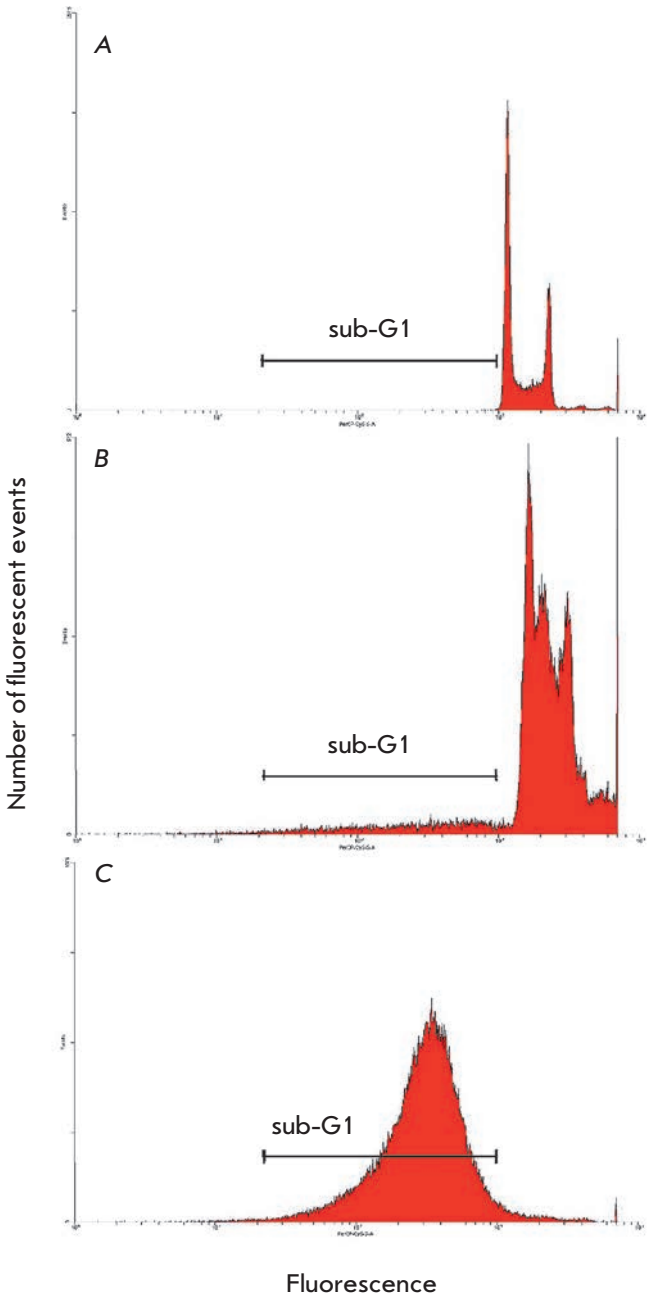

Fig. 1. Cell cycle distribution of HCT116 cells treated with 0.4 mM acadesine. *A* – intact cells; *B* – arrest in S phase after 24 h; *C* – sub-G1 peak after 48 h

the cytotoxicities of acadesine for a HCT116 line and HCT116p53KO subline (resistant to a number of DNA-damaging anticancer drugs) [18] has demonstrated that inactivation of the proapoptotic protein p53 does not increase the survival rate of cells in the presence of acadesine.

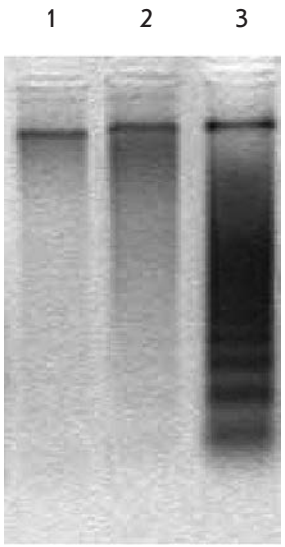

Fig. 2. DNA integrity in HCT116 cells. *1* – intact cells; *2* – acadesine, 0.4 mM, 24 h; *3* – alkyl cationic glycerolipid [17], 6 μM, 24 h (technical control)

The considerably higher survival rate of nontumor cells in the presence of acadesine is also important: death of the donor's lymphocytes and non-transformed fibroblasts was virtually absent even when continuously exposed to acadesine at millimolar concentrations for 72 h (*Table 1*). Thus, acadesine primarily causes the death of transformed cells (suspension and epithelial ones), including the sublines resistant to other anticancer drugs. Nontumor cells are damaged by acadesine to a significantly lesser extent. These features speak to the potential of using acadesine as an antitumor agent. However, the mechanisms that underline the toxicity of acadesine for tumor cells need to be understood.

Acadesine causes non-apoptotic cell death

The effect of acadesine on ploidy distribution in a HCT116 large intestine adenocarcinoma cell line was studied by flow cytofluorometry. Arrest in the S phase and massive cell death (the region to the left of the G1 peak; hypodiploid nuclei) (*Fig. 1*) were observed 24 and 48 h, respectively, after the introduction of acadesine (0.25 mM). Accumulation of fragmented DNA can be indicative of apoptotic cell death if the DNA is split in internucleosomal regions, which can be seen from the formation of a number of 140- to 170-bp-long fragments during electrophoresis. In order to verify this idea, DNA integrity in acadesine-treated HCT116 cells was determined. It turned out that acadesine, as opposed to the control compound (alkyl cationic glycerolipid [17]), does not result in the emergence of a DNA ladder typical of apoptosis (*Fig. 2*).

The results of staining cells with Annexin V-FITC and propidium iodide (*Fig. 3*) argue in favor of a non-apoptotic mechanism of death of HCT116 cells under

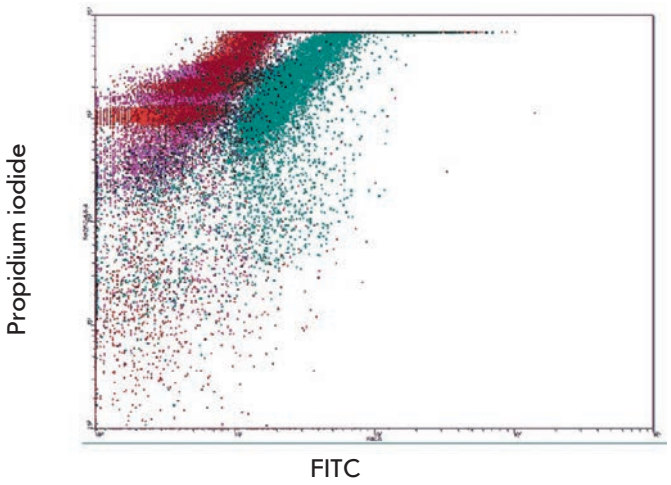

Fig. 3. Staining of HCT116 cells with Annexin V-FITC and propidium iodide. Pseudo colors: red – intact cells; violet – acadesine (0.4 mM, 24 h); blue – alkyl cationic glycerolipid (see legend to *Fig. 2*)

the action of acadesine. Annexin V binds to phosphatidylserine on the plasma membrane (translocation of phosphatidylserine from the inner lipid layer of the membrane to the outer one is considered to be a sign of apoptosis). Propidium iodide is capable of penetrating into cells undergoing necrosis (disrupting the integrity of the plasma membrane). Acadesine-treated HCT116 cells (0.4 mM, 24 h) were not stained with Annexin V-FITC; contrariwise, the cells accumulated propidium iodid (*Fig. 3*), which allows one to hypothesize about a necrotic component of the cell death mechanism. Similar results were obtained when necrotic cells were visualized using trypan blue (data not shown). The disruption of the integrity of the plasma membrane is presumably a late event during acadesine-induced cell death. The control agent, alkyl cationic glycerolipid, caused an increase in the number of Annexin V-positive cells, which is typical of apoptosis (*Fig. 3*). Since apoptotic cell death assumes that caspases play a significant role in it, the effect of the pan-caspase inhibitor zVAD-fmk on acadesine cytotoxicity was studied. HCT116 cells were incubated with 200 μM zVAD-fmk for 30 min; acadesine was then introduced in the cultures, and the incubation was carried out for an additional 24 h. The presence of zVAD-fmk did not reduce cell death, which supports the conclusion about the non-apoptotic mechanism of the cytotoxicity of acadesine.

Interaction with the adenosine receptors is required to ensure the death of tumor cells under the action of acadesine

Acadesine can be transferred from the extracellular space into the cells by adenosine transporters [19]. We have studied the effect of dipyridamole, the inhibitor of these transporters, on acadesine cytotoxicity in a P388 cell line. Cells turned out to be insensitive even to the relatively high (up to 0.8 mM) acadesine concentrations in the presence of dipyridamole (*Table 2*).

In order to shed light on the role of the metabolic pathway acadesine–ZMP–AMPK in the cytotoxicity of acadesine (its phosphorylation by adenosine kinase yielding ZMP and activation by AMPK), cells were incubated with acadesine and the adenosine kinase inhibitor 5-iodotubercidine. The inhibitor had no effect on acadesine cytotoxicity (*Table 2*). Hence, cell death in response to acadesine is not caused by the formation of ZMP or activation of AMPK.

Thus, the investigation into the mechanisms of acadesime cytotoxicity has revealed a number of features indicating a nontrivial nature of the pharmacological effects of this compound. Acadesine triggers death in cultured tumor cells, while its effect on nontumor cells is pronounced to a considerably lesser extent. Acadesine is toxic for cells with molecular determinants of drug resistance: Pgp expression and non-functional p53. It is important to emphasize the non-apoptotic character of the tumor cell death induced by acadesine.

Table 2. Acadesine cytotoxicity in combinations with dipyridamole or 5-iodotubercidine

Effect	Acadesine, mM					
	0	0.08	0.1	0.2	0.4	0.8
Acadesine	100*	79	38	33	20	18
Acadesine + dipyridamole, 5 μM	100	100	99	99	100	101
Acadesine + 5-iodotubercidine, 0.05 μM	100	76	39	31	22	16

*Survival rate (%) of P388 leukemia cells according to the MTT assay data after 72 h of incubation.

These results provide grounds for regarding acadesine as a crucial agent for studying the mechanisms of tumor cell death and a promising drug candidate.

The question regarding the intracellular target of acadesine, the interaction with which causes tumor cell death, remains open. We have demonstrated that the function of adenosine transporters is the criterion for cell death, while no activation of AMPK is required. It is reasonable to assume that tumors expressing the aforementioned adenosine transporters and receptors will exhibit the highest sensitivity to acadesine. The role of the purine nucleotide transport in cell death has yet to be studied sufficiently; an analysis of the differential expression of adenosine carriers and receptors in different types of tumors is required. The enhanced expression of these molecules may turn out to be a novel molecular marker of tumor sensitivity to acadesine and a criterion for the selection of patients for proper therapy. ●

This work was supported by the Ministry of Education and Science of the Russian Federation (state contract 16.N08.12.1010) and in part by the Fund for Non-commercial Programs "Dynasty."

REFERENCES

1. «Acadesine. AICA Riboside, ARA 100, Arasine, GP 1 110» Drugs R D 2008; V. 9 (3). P. 169–175.
2. Jose C, Bellance N, Chatelain EH, Benard G, Nouette-Gaulain K, Rossignol R. // Mitochondrion. 2012. № 12. P. 100–109.
3. Jose C, Hébert-Chatelain E, Bellance N, Larendra A, Su M, Nouette-Gaulain K, Rossignol R. // Biochimica et Biophysica Acta . 2011. № 1807. P. 707–718.
4. Van Den Neste E, Van den Berghe G, Bontemps F. // Expert Opin. Investig. Drugs. 2010. № 19(4). P. 571–578.
5. Javaux F, Vincent MF, Wagner DR, Van den Berghe G. // Biochem. J. 1995. V. 305. P. 913–919.
6. Merrill GF, Kurth EJ, Hardie DG, Winder WW // Endocrinol. Metab. 1997. V. 273. № 6. P. 1107–1112.
7. Su RY, Chao Y, Chen TY, Huang DY, Lin WW. // Mol Cancer Ther. 2007.V. 6(5). P. 1562–1571.
8. Theodoropoulou S, Kolovou PE, Morizane Y, Kayama M, Nicolaou F, Miller JW, Gragoudas E, Ksander BR, Vavvas DG. // FASEB. 2010. № 24. P. 2620–2630.
9. Teresa Whei-Mei Fan et al. (eds.), «The Handbook of Metabolomics», Methods in Pharmacology and Toxicology. 2012. № 17. P. 439–480.
10. Walker J, Jijon HB, Diaz H, Salehi P, Churchill T, Madsen KL // Biochem. J. 2005. № 385. P. 485–491.
11. Campàs C, Santidrián AF, Domingo A, Gil J. // Leukemia. 2005. № 19. P. 292–294.
12. López JM, Santidrián AF, Campàs C, Gil J. // Biochem. J. 2003. № 370. P. 1027–1032.
13. Guigas B, Sakamoto K, Taleux N, Reyna SM, Musi N, Viollet B, Hue L. // IUBMB Life. 2009. V. 61. № 1. P. 18–26.
14. Lobanov K.V., Errais Lopes L., Korolkova N.V., Tyaglov B.V., Glazunov A.V., Shakulov R.S., Mironov A.S. // Acta Naturae 2011. V. 3. № 2 (9). P. 83–93.
15. Lysenkova L.N., Turchin K.F., Korolev A.M., Bykov E.E., Danilenko V.N., Bekker O.B., Trenin A.S., Elizarov S.M., Dezhenkova L.G., Shtil A.A., Preobrazhenskaya M.N. // Journal of Antibiotics (Tokyo). 2012. № 65(8). P. 405–411.
16. Simonova V.S., Samusenko A.V., Filippova N.A., Tevyashova A.N., Lyniv L.S., Kulik G.I., Chekhun V.F., Shtil A.A. // Bul. exp. biol. Med. 2005.V. 4. P. 451–455.
17. Shchekotikhin A.E., Glazunova V.A., Dezhenkova L.G., Shevtsova E.K., Traven' V.F., Balzarini J., Huang H.-S., Shtil A.A., Preobrazhenskaya M.N. // European Journal of Medicinal Chemistry 2011. № 46. P. 213–218.
18. Markova A.A., Plyavnik N.V., Pletneva M.V., Serebrennikova G.A., Shtil A.A. // Clin. Onkogematology. 2012. V. 5. № 2. P. 141–143.
19. Gadalla AE, Pearson T, Currie AJ, Dale N, Hawley SA, Sheehan M, Hirst W, Michel AD, Randall A, Hardie DG, Frenguelli BG. // Journal of Neurochemistry. 2004. № 88. P. 1272–1282.

Cancer Specificity of Promoters of the Genes Involved in Cell Proliferation Control

K. N. Kashkin*, I. P. Chernov, E. A. Stukacheva, E. P. Kopantzev, G. S. Monastyrskaya, N. Ya. Uspenskaya, E. D. Sverdlov
Shemyakin-Ovchinnikov Institute of Bioorganic Chemistry , Russian Academy of Sciences, Miklukho-Maklaya St., 16/10, Moscow, Russia, 117997
*E-mail: kachkine@yandex.ru
Received 08.02.2013

ABSTRACT **Core promoters with adjacent regions of the human genes *CDC6*, *POLD1*, *CKS1B*, *MCM2*, and *PLK1* were cloned into a pGL3 vector in front of the *Photinus pyrails* gene *Luc* in order to study the tumor specificity of the promoters. The cloned promoters were compared in their ability to direct luciferase expression in different human cancer cells and in normal fibroblasts. The cancer-specific promoter *BIRC5* and non-specific CMV immediately early gene promoter were used for comparison. All cloned promoters were shown to be substantially more active in cancer cells than in fibroblasts, while the *PLK1* promoter was the most cancer-specific and promising one. The specificity of the promoters to cancer cells descended in the series *PLK1*, *CKS1B*, *POLD1*, *MCM2*, and *CDC6*. The bidirectional activity of the cloned *CKS1B* promoter was demonstrated. It apparently directs the expression of the *SHC1* gene, which is located in a "head-to-head" position to the *CKS1B* gene in the human genome. This feature should be taken into account in future use of the *CKS1B* promoter. The cloned promoters may be used in artificial genetic constructions for cancer gene therapy.**
KEYWORDS **promoter; cloning; cancer-specific; cancer gene therapy.**
ABBREVIATIONS **TSS – transcription start site.**

INTRODUCTION

The design of genetically engineered vectors that express products that are toxic for tumor cells holds an important position among the topical directions in the development of antitumor agents. These vectors need to contain cancer-specific regulatory elements that can ensure both the expression of the therapeutical gene in the maximum possible number of tumors and the absence of expression in normal tissues. Today, the number of promoters known to have these properties is limited.

While searching for new cancer-specific promoters, we have put forward a hypothesis that many promoters participating in DNA replication may exhibit tumor specificity, since the disturbed regulation of cell division is considered to be the common property of all tumors. In order to verify this hypothesis, we cloned the promoters of several genes participating in DNA synthesis and cell division and assessed the ability of these promoters to direct the expression of the reporter gene in normal and tumor cells of different origins. Promoters of the *CDC6*, *POLD1*, *CKS1B*, *MCM2*, and *PLK1* genes were used for cloning.

The *CDC6* gene product is the homologue of *Saccharomyces cerevisiae* CDC6, a protein essential for the initiation of DNA replication. CDC6 regulates the early stages of DNA replication and helps control the check-point determining the termination of DNA replication before mitosis begins. A disturbed regulation of *CDC6* expression is associated with a high risk of cancer development [1, 2]. The *POLD1* gene encodes the catalytic subunit of DNA polymerase δ, which participates in the replication and reparation of human genomic DNA. This subunit exhibits polymerase (synthesis of DNA) and exonuclease (in the 3'–>5' direction) activities. Moreover, POLD1 participates in the completion of the Okazaki fragments initiated by the DNA polymerase α/primase complex. The frequency of the development of spontaneous tumors is higher in mice with a deficient DNA polymerase δ function [3]. The CKS1B protein is a component of CDC28 protein kinase required for embryogenesis and correct alternation of the phases of the somatic cell cycle [4]. CKS1B forms a complex with the CDC2 protein and regulates the transcription of the *CDC20* gene. The interaction between CKS1B and the SKP2–cyclin E-$p27^{KIP}$ complex ensures ubiquitination and degradation of p27 which is the cell blocker in the G0/G1 phase in response to different signals and unfavorable factors and the regulator of cell mobility and apoptosis [5]. The *CKS1B* gene

localizes head-to-head with the *SHC1* gene and presumably uses the bidirectional promoter shared with this gene [6]. *SHC1* gene products are known to regulate the transfer of mitogenic signals in the cell, to participate in p53-dependent apoptosis under oxidative stress, and to regulat the lifespan. The protein p66Shc plays an important role in carcinogenesis and tumor dissemination [7]. The *MCM2* gene encodes one of the subunits of the MCM2-7 protein complex, which is required for the initiation of DNA replication, formation of the replicative fork, and recruitment of the other proteins that participate in DNA replication. By interacting with the other proteins of the initiation complex, MCM2 regulates its helicase activity [8]. The promoters of the *SHC1* and *MCM2* genes are not characterized yet in detail. PLK1 (polo-like kinase 1) – serine/threonine protein kinase 1 – has several crucial functions during the M-phase of the cell cycle, including centrosome maturation, mitotic spindle assembly, and regulation of mitotic exit and cytokinesis. The PLK1 protein is required for cell restoration after DNA damage and when it enters mitosis [9]. The listed properties of the six genes and their increased expression in a number of human tumors (GeneHub GEPIS, [10]) provide grounds for hoping that the selected promoters could exhibit both tumor specificity and versatility with respect to tumors and would be able to act as regulator elements within genetically engineered anti-tumor constructs.

EXPERIMENTAL

Promoters were amplified from the human genomic DNA using Tersus and Encyclo DNA polymerases (Evrogen, Russia). Promoters were cloned in the given coordinates with respect to the transcription start site (TSS) using the primers listed in *Table*. All the primers were synthesized on an ABI 3900 synthesizer (Applied Biosystems). The amplified DNA fragments were cloned into the vector in pAL-TA (Evrogen, Russia) and re-cloned into the pGL3 Basic Vector (Promega, WI, USA) at the proper restriction sites in front of the *Photinus pyralis* luciferase gene. Plasmid clones containing promoters in the required orientation were selected by restriction analysis and DNA sequencing. The resulting clones with promoters of the *CDC6, CKS1B,* and *PLK1* genes contained no nucleotide substitutions, while the clones with the promoters *POLD1* and *MCM2* contained one and two substitutions with respect to the nucleotide sequences, respectively, which are listed in NCBI GenBank. We used the plasmid clones containing the cloned promoters to transfect the following cell lines: A375 (malignant melanoma, ATCC), A431 (epidermoid carcinoma of the skin, ATCC), A549 (lung carcinoma, ATCC), Calu1 (lung epidermoid carcinoma, ECACC), HepG2 (hepatocellular carcinoma, ATCC), HT1080 (fibrosarcoma, ATCC), Panc-1 (epithelioid pancreatic carcinoma, ATCC), and normal fibroblasts IVL-7C. Fibroblasts IVL-7C were obtained from the morphologically normal tissue of the lung of a patient who had undergone surgical resection of his lung cancer at the Blokhin Cancer Center, Russian Academy of Medical Sciences, using the previously described procedure [11]. Co-transfection with the plasmid pRL-TK (Promega, WI, USA) expressing the *Rluc* gene was used as an internal control of the transfection. Parallel transfection of cells with the vectors pGL3 Basic Vector, pGL3 Promoter Vector (Promega, WI), and pGL3-CMV Pr/Enh containing the AseI/BglII fragment of the promoter of early cytomegalovirus genes from the plasmid pEGFP-N1 (Clontech Laboratories, Inc.) in front of the *Luc* gene was used to standardize the experimental results. In order to compare the tumor specificity of the promoters, the cells were transfected with the 1500-bp-long pGL3-based plasmid containing the promoter of the surviving gene (*BIRC5)* [12]. The cells were transfected by means of Lipofectamine 2000 (Invitrogen, USA) in 24-well plates according to the manufacturer's recommendations. Promoter activity was assessed from the chemiluminescence of cell extracts. The chemiluminescence was measured using a Dual Luciferase Reporter Assay System (Promega, USA) on a GENios Pro plate luminometer (Tecan, Switzerland). The luminescence values of *P. pyralis* luciferase were standardized for the luminescence of *Renilla reinformis* luciferase in each measurement, and a correction for the background activity of the luciferase for the plasmid pGL3 Basic Vector was introduced. The resulting values were averaged for two repeats in each experiment and for a series of three experiments. The data were standardized for the *P. pyralis* luciferase activity under the control of the SV40 promoter within the pGL3 Promoter Vector.

Primers used for promoter amplification

Promoter	Primer (5' –> 3')
POLD1 (–1338; +66)*	GGTACCTGAATACAATCCAGCCCGGAG GGTACCCCTCTACTCACCCGCTTCAAAC
CDC6 (–1539; +238)	GCTAGCGATCATGGCACGGCACTCA GCTAGCTCAGACCTCCAGCGAGCTCA
CKS1B (–910; +106)	GGTACCGGTCCCACAAAGATAAAGCTCC GGTACCTATGATCGCTCGGTTTGCTAG
MCM2 (–1949; +57)	ATCCGAGGTGCATCCTTCAC AGCAGTACCACGATCCTCTCC
PLK1 (–2338; +35)	GCAAGACTCCATCTCAACAACA CAGACCTCGATCCGAGCAG

* Coordinates of promoter with respect to the transcription start site of the gene.

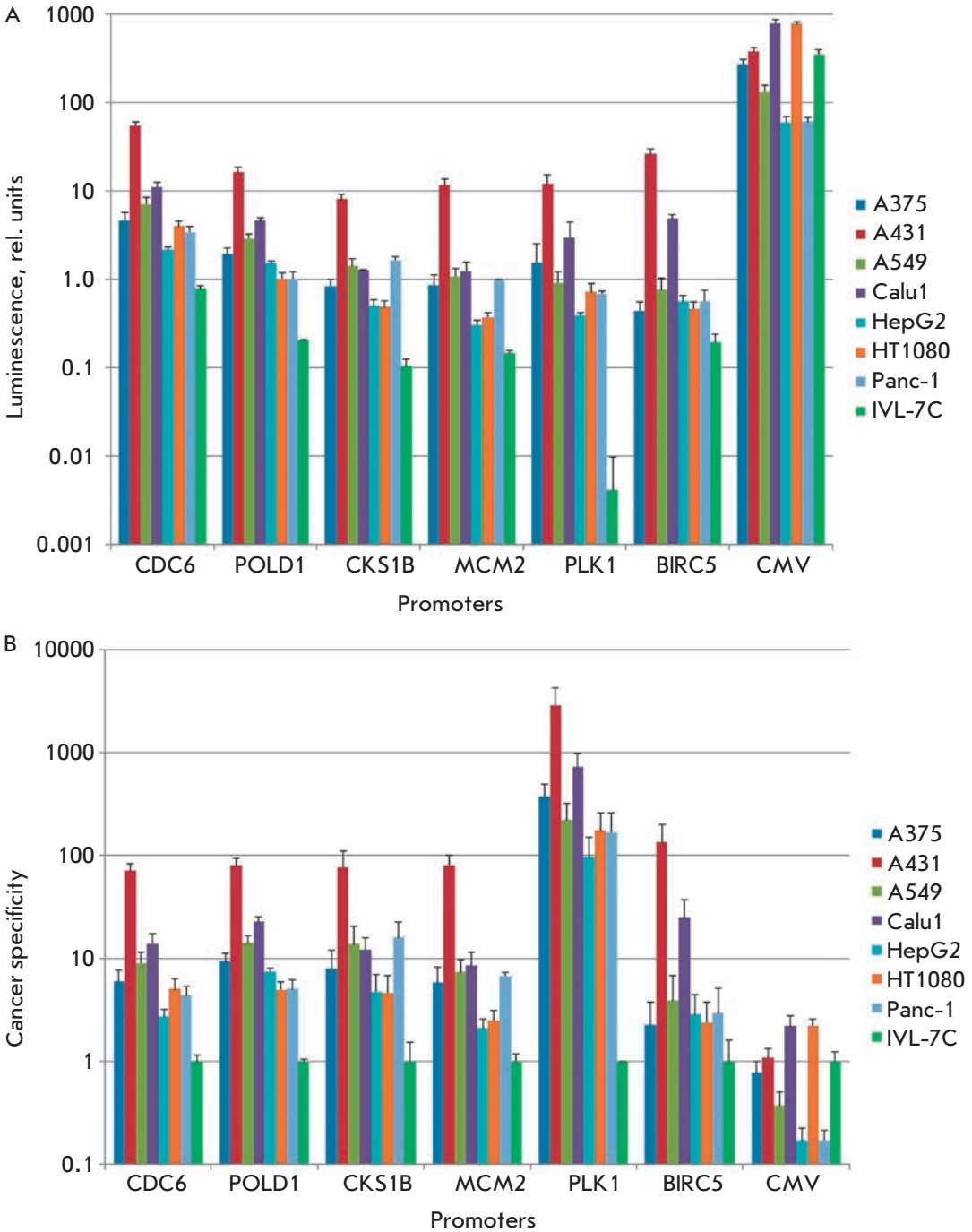

Fig. 1. Activity and cancer specificity of cloned promoters. *A* – Chemiluminescence of lysates of cells transfected with plasmids with the corresponding promoters (logarithmic scale). The mean values and standard errors of the mean (SEM) are presented. *B* – Cancer specificity of promoters expressed as ratios between the chemiluminescence levels of the lysates of cancer cells and fibroblasts for each promoter. *M* – the median of the ratios, generalized index of cancer specificity of promoter

Promoter	CDC6	POLD1	CKS1B	MCM2	PLK1	BIRC5	CMV
M	5.95	9.37	12.19	6.80	220.00	2.94	0.78

RESULTS AND DISCUSSION

It was demonstrated in the transfection experiments that the cloned promoters exhibited activity in all the cell types under study. It should be mentioned that the activity of the cytomegalovirus promoter (CMV) within the construct pGL3-CMV Promotor/Enhancer Vector was 100- to 1,000-fold higher as compared to that of all the other promoters. The activities of promoters of the *POLD1*, *CDC6*, *CKS1B*, *PLK1* and *MCM2* genes in all the human tumor cell lines turned out to be higher than that of the SV40 promoter and were comparable to that of the *BIRC5* gene promoter (*Fig. 1A*). Mean-

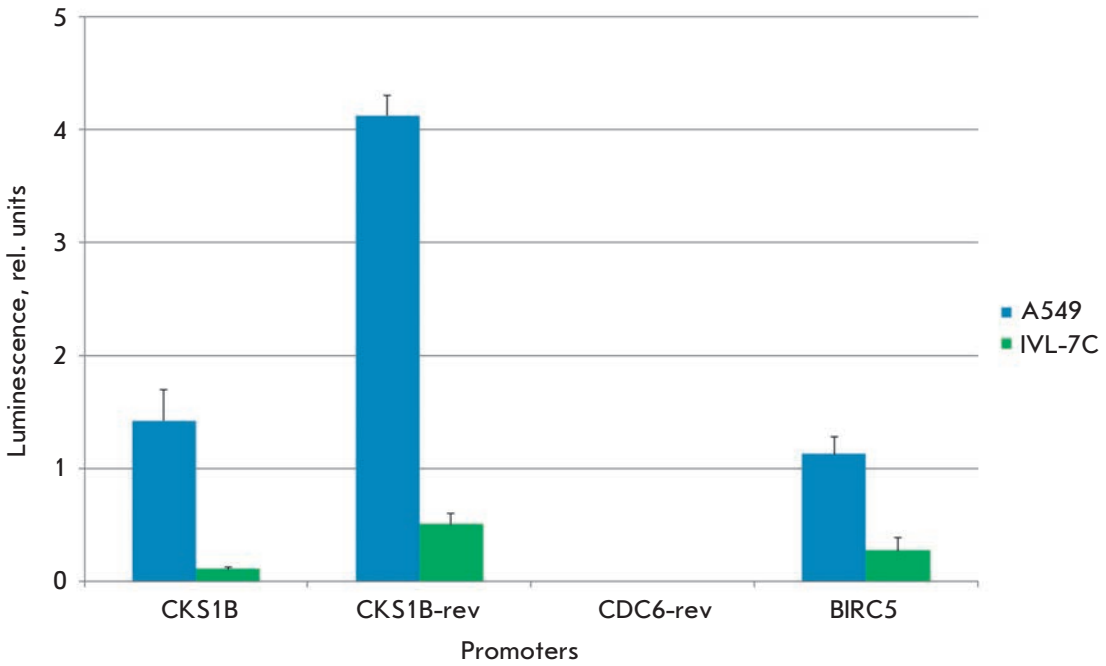

Fig. 2. Chemiluminescence of the lysates of A549 and IVL-7C cells transfected with pGL3-based plasmids with promoters in direct and reverse (rev) orientations. The mean values and the standard errors of the mean (SEM) are presented. See text for explanations

while, the promoters under study (except for the CMV promoter) in normal fibroblasts ensured a considerably lower level of luciferase activity as compared to the SV40 promoter. In order to assess the cancer specificity of each cloned promoter, we calculated the ratio between the chemiluminescence levels of the lysates of tumor cells and fibroblasts transfected with plasmids with the corresponding promoters, and the median value of these ratios as the generalized index of the cancer specificity of the promoter (*Fig. 1B*). The activity exhibited by the *BIRC5* gene promoter, similar to that in the previous study [12], was higher in all the tumor cell lines as compared to that in normal fibroblasts. The activity of five cloned promoters in the tumor cells was also higher than that in normal fibroblasts ($p < 0.01$, Mann–Whitney U test). The CMV promoter exhibited no specificity: its activity in some tumor cells was higher as compared to that in fibroblasts, while in other tumor cells it was lower.

As mentioned previously, the *CKS1B* and *SHC1* genes have a head-to-head orientation and presumably share one bidirectional promoter [6]. Hence, when cloning the *CKS1B* promoter, we additionally selected the pGL3 plasmid clone containing this promoter in reverse orientation. The coordinates of the cloned DNA fragment with respect to the TSS of the *SHC1* gene were (–264; +751). In order to verify the promoter activity of the cloned fragment, we used this clone to transfect A549 cells and normal fibroblasts and measured the chemiluminescence of the cell lysates. The results are shown in *Fig. 2*. The results of determining the activity of the incorporated *CDC6* promoter with the reverse orientation (*CDC6-rev*), which was identical to that of the control vector pGL3-BV, and the *BIRC5* promoter in direct orientation are given here for the sake of comparison. It turned out that the activity of the cloned *SHC1* promoter was higher than that of the *CKS1B* promoter both in the tumor cells and in normal fibroblasts. The activity of the *SHC1* promoter in A549 adenocarcinoma cells was approximately eightfold higher than that in normal fibroblasts, which is lower than the activity of the *CKS1B* promoter but is comparable to the cancer specificity of the *BIRC5* promoter (not shown). Since the range of tumors with an increased expression level of the *SHC1* gene is smaller than that of the tumors with an increased expression level of the other genes that were used in our work (GeneHub GEPIS, [10]), we did not study the *SHC1* promoter using other cells.

Thus, the promoters of five genes that regulate DNA replication and cell division, exhibiting tumor-specific expression, and significantly contribute to carcinogenesis had been cloned. When cells were transfected with plasmid vectors expressing the luciferase gene under the control of these promoters, the promoters exhibited a considerably higher activity in tumor cells of different origins as compared to their activity in normal fibroblasts. The activity and tumor specificity of the cloned promoters, except for the *PLK1* promoter, was comparable to the indices for the *BIRC5* promoter that had been studied previously. The specificity of the promoters slightly decreased for the series *CKS1B*,

POLD1, MCM2, CDC6. The *PLK1* promoter exhibited considerably higher cancer specificity; the expression levels of the reporter gene controlled by the *PLK1* and *BIRC5* promoters in the tumor cells were approximately identical. This makes the *PLK1* promoter superior to other promoters and provides grounds to regard it as the most promising promoter for designing genetically engineered anti-tumor constructs.

We have also demonstrated the bidirectional activity and high cancer specificity of the cloned *CKS1B/SHC1* promoter. One should take these features into account when designing genetically engineered vectors with this promoter, since its bidirectional activity may result in undesirable transcription of the vector sequences in a direction reverse to that of the therapeutical gene. On the other hand, this promoter can be used to simultaneously express two therapeutical genes in tumors or to design anti-tumor constructs that have binary effect with a more complex regulation. Further investigation into the *CKS1B/SHC1* promoter and the genes whose expression it directs in various tissues and tumors is required.

It should be mentioned that only non-tumor control (normal lung fibroblasts) was used in this study. Taking into account the source of the cells (normal tissue obtained from a patient with lung cancer) and the fact that the properties of cells dividing in culture may differ from their properties *in vivo*, one needs to study the cloned promoters in *in vivo* models in order to draw unambiguous conclusions about the cancer specificity of the promoters.

The significant length of the promoters (1016–2373 bp) allows one to put forward a hypothesis that they contain key elements in transcription regulation, such as core promoters and proximal regulatory elements. However, it is entirely possible that there are additional remote regulatory elements, such as enhancers, silencers or repressors, which also participate in the regulation of the activity of these promoters. A comparison of the endogenous activity of the corresponding genes in various cell lines and tissues with the results obtained in our study will allow one to assess the relative contribution of the promoter and additional regulatory elements. ●

This work was supported by the RAS Presidium Program "Molecular and Cell Biology", program "Leading Scientific Schools of the Russian Federation" (NSh1674.2012.4), and the Ministry of Industry and Trade of the Russian Federation (State contract № 11411.1008700.13.084, 2011–2013).

REFERENCES

1. Kawakami H., Katayama T. // Biochem Cell Biol. 2010. V. 88. P. 49–62.
2. Borlado L.R., Mendez J. // Carcinogenesis. 2008. V. 29. P. 237–243.
3. Lange S.S., Takata K., Wood R.D. // Nat Rev Cancer. 2011. V. 11. P. 96–110.
4. Martinsson-Ahlzen H.S., Liberal V., Grunenfelder B., Chaves S.R., Spruck C.H., Reed S.I. // Mol Cell Biol. 2008. V. 28. P. 5698–5709.
5. Krishnan A., Nair S.A., Pillai M.R. // J Cell Mol Med. 2010. V. 14. P. 154–164.
6. Davila Lopez M., Martinez Guerra J.J., Samuelsson T. // PLoS One. 2010. V. 5. P. e10654.
7. Rajendran M., Thomes P., Zhang L., Veeramani S., Lin M.F. // Cancer Metastasis Rev. 2010. V. 29. P. 207–222.
8. Masai H., You Z., Arai K. // IUBMB Life. 2005. V. 57. P. 323–335.
9. Song B., Liu X.S., Liu X. // Cell Div. 2012. V. 7. P. 3.
10. Zhang Y., Luoh S.M., Hon L.S., Baertsch R., Wood W.I., Zhang Z. // Nucleic Acids Res. 2007. V. 35. P. W152–158.
11. Kopantzev E.P., Vayshlya N.A., Kopantseva M.R., Egorov V.I., Pikunov M., Zinovyeva M.V., Vinogradova T.V., Zborovskaya I.B., Sverdlov E.D. // Br J Cancer. 2010. V. 102. P. 1533–1540.
12. Mityaev M.V., Kopantzev E.P., Buzdin A.A., Vinogradova T.V., Sverdlov E.D. // Biochemistry (Mosc). 2010. V. 75. P. 182–191.

Original Nerve Growth Factor Mimetic Dipeptide GK-2 Restores Impaired Cognitive Functions in Rat Models of Alzheimer's Disease

P.Yu. Povarnina*, O.N. Vorontsova, T.A. Gudasheva, R.U. Ostrovskaya, S.B. Seredenin
Zakusov Institute of Pharmacology, RAMS, Baltiyskaya Str., 8, Moscow, Russia, 125315
*E-mail: povarnina@gmail.com
Received 12.01.2013

ABSTRACT **Dipeptide mimetic of the nerve growth factor (NGF) loop 4, hexamethylenediamide bis-(N-monosuccinyl-glutamyl-lysine) (GK-2), was synthesized at the V.V. Zakusov Scientific Research Institute of Pharmacology of the Russian Academy of Medical Sciences. GK-2 exhibited *in vitro* neuroprotective activity at nanomolar concentrations, was efficient in animal models of the Parkinson's disease, ischemic and hemorrhagic stroke, and global cerebral ischemia at doses of 0.01–5 mg/kg (intraperitoneally) and 10 mg/kg (per os). The mnemotropic effects of subchronic intraperitoneal administration of GK-2 on rat models of the Alzheimer's disease are described in this paper. Dipeptide GK-2 at a dose of 1 mg/kg is found to decrease the habituation deficit induced by the septo-hippocampal pathway transsection and, at a dose of 0.5 mg/kg, to significantly prevent spatial memory impairment in Morris water maze induced by intracerebral injection of streptozotocin. Thus, GK-2, an original dipeptide mimetic of NGF, acts on models of the Alzheimer's disease upon systemic administration.**
KEYWORDS **low molecular mimetic of NGF; GK-2; septo-hippocampal transsection; streptozotocin model of Alzheimer's disease; habituation; Morris water maze.**
ABBREVIATIONS **AD – Alzheimer's disease; NGF – nerve growth factor; APP – amyloid precursor protein; i/p – intraperitoneally; EL – escape latency, EOR – exploratory orientation reaction.**

INTRODUCTION

The Alzheimer's disease (AD) is the most common cause of dementia. The number of AD patients is expected to double by 2050 [1]. No pharmacological agents capable of providing long-term neuroprotection to AD patients or limiting the development of cognitive impairment area vailable at the moment [2].

The contribution of the nerve growth factor (NGF) to the pathogenesis of AD has been well documented. The progressive decline in cognitive functions in AD patients is associated with the degeneration of cholinergic neurons in the basal forebrain [3], which are the primary target of this neurotrophin in the central nervous system. This neurotrophin ensures the preservation of the biochemical and morphological phenotypes of the aforementioned neurons and their survival in the presence of damaging factors [4]. NGF inhibits the formation of amyloid plaques and neurofibrillary tangles in the brain – the main pathomorphological characteristics of AD – via the inhibition of amyloidogenic processing of APP [5] and hyperphosphorylation of the tau protein, which is involved in the formation of neurofibrillary tangles [6].

The exact reasons behind sporadic AD still remain unknown; however, evidence is accumulating in support of the hypothesis of the deterioration of trophic maintenance of the cholinergic neurons of the basal forebrain by NGF as a trigger of the disease [7, 8]. It was demonstrated in AD11 transgenic mice (anti-NGF antibodies develop in these mice during the postnatal period) that chronic NGF deprivation causes a cholinergic deficit, loss of neurons and synapses, formation of amyloid plaques and neurofibrillary tangles, a decrease in synaptic plasticity, and memory deficit [8]. Intranasal administration of NGF to AD11 mice prevented the disruption of cholinergic transmission, the accumulation of β-amyloid and the hyperphosphorylated tau protein, and the development of memory deficit [9].

A variety of experimental AD models (such as the destruction of the basal nuclei of Meynert by ibotenic acid, septo-hippocampal transsection and natural aging) have shown that therapeutic intracerebral NGF administration counteracts the degeneration of cholinergic neurons and restores cognitive functions [10–12].

Poor pharmacokinetic properties and the limited ability to penetrate through the blood–brain barrier

and pleiotropy limit the medical application of native NGF. Hence, a number of pharmaceutical companies and research groups are currently in the process of developing low-molecule-weight NGF mimetics [13–15].

Dimeric dipeptide mimetic GK-2 (hexamethylenediamide bis-(N-monosuccinyl-glutamyl-lysine)) was synthesized based on the structure of the β-turn of the NGF loop 4 at the V.V. Zakusov Scientific Research Institute of Pharmacology of the Russian Academy of Medical Sciences [16]. Identically to NGF, GK-2 causes the phosphorylation of specific TrkA receptors and the kinases Akt that participate in the manifestation of the neuroprotective effects mediated by these receptors [17]. GK-2 at nanomolar concentrations exhibited a high NGF-like neuroprotective activity during *in vitro* experiments. However, in contrast to the native protein, GK-2 demonstrated no signs of differentiating activity [18]. GK-2 prevented H_2O_2- or glutamic-acid-induced destruction of immortalized mouse hippocampal neurons in culture (HT-22 line) and protected rat pheochromocytoma PC12 cells from the action of neurotoxin MPTP (1-methyl-4-phenyl-1,2,3,6-tetrahydropyridine) [19]. Dipeptide GK-2 exhibited neuroprotective properties and improved cognitive functions [20–22], and reduced the severity of behavioral symptoms in a number of models of the parkinsonian syndrome [23] in experimental models of acute and chronic cerebral ischemia in rats. Dipeptide GK-2 exhibits low toxicity (LD_{50} = 714 mg/kg upon intravenous administration to male mongrel mice) and shows none of the major side effects typical of NGF. It does not reduce the pain threshold (at doses of 0.5–2 mg/kg i/p in a tail flick test after thermal stimulation, water temperature of 55°C) [24] and does not cause weight loss upon chronic administration to rats (0.5 mg/kg, i/p) [25].

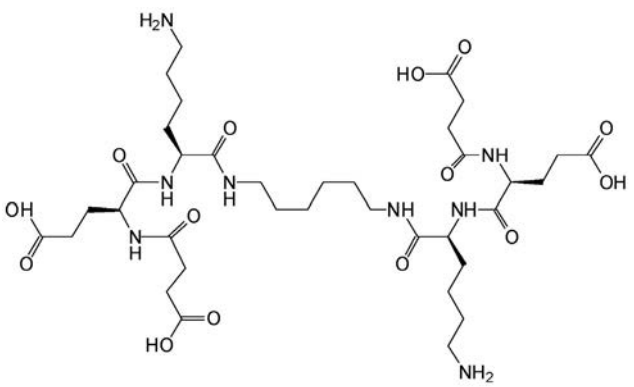

GK-2

The aim of this study was to investigate the mnemotrophic effects of GK-2 on AD models. There are two main approaches to the modeling of the abnormalities typical of AD: surgical and neurotoxic. The former approach entails the transsection of the septo-hippocampal pathway, which is a well-researched and widely used AD model. Deafferentation of the hippocampus attributed to septo-hippocampal transsection results in the development of cholinergic deficiency and the related disorder of cognitive functions [26, 27]. This model has been used by various researchers to study the effects of NGF [28, 29]; hence our decision to use it to evaluate the activity of the NGF mimetic GK-2. A streptozotocin AD model reproducing the major pathological processes in the brain (including the accumulation of β-amyloid and the hyperphosphorylated tau protein, as well as the spatial memory abnormalities [30] that are also typical of AD patients) was used as a neurotoxic model [31].

EXPERIMENTAL

Substances

Dipeptide GK-2 (hexamethylenediamide bis-(N-monosuccinyl-glutamyl-lysine), molecular weight of 835 Da) was synthesized at the V.V. Zakusov Scientific Research Institute of Pharmacology of the Russian Academy of Medical Sciences [16]. Nembutal (Sigma, USA) was used for anesthesia. Memantine (1-amino-3,5-dimethyladamantane hydrochloride, molecular weight of 215 Da) was purchased from the Merck KgaA company (Germany).

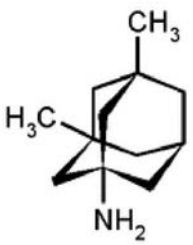

Memantine

Nembutal was administered in the form of a saline suspension, dipeptide GK-2 was dissolved in distilled water, and memantine was administered in the form of a distilled water suspension. All substances (except streptozotocin) were administered i/p at a dose of 2 ml/kg of body weight.

The GK-2 doses (0.5 and 1 mg/kg) were selected as the ones most efficient *in vivo* according to the data obtained in a study of the dose-dependent effect of this compound in the haloperidol catalepsy model in rats used for screening compounds with potential antiparkinsonian activity [23]. The efficacy of these doses was also confirmed in various cerebral ischemia models [20–22].

Animals

The experiments were conducted on 32 male mongrel white rats and 24 male Wistar rats obtained from the animal nursery "Stolbovaya" of the Russian Academy of Medical Sciences. The animals were kept in a vivarium under *ad libitum* feeding and natural light conditions. Behavioral experiments were performed during winter between 10.00 and 14.00 hours, local time. The requirements regarding the use of animals for experimental research specified in the European Council Directives 86/609/EES were abided by during the experiments on the rats.

Investigations into the effects of GK-2 on an AD model with septo-hippocampal pathway transsection [26]

Study design. The Wistar rats (280–400 g) were randomly divided into three groups: rats subjected to sham surgery (n=6); rats subjected to surgery (n=10); and rats that were subjected to surgery and received dipeptide GK-2 (n=8). Dipeptide GK-2 (1 mg/kg) was administered 2 h after the surgery and subsequently every 48 h (a total of seven injections). The "sham surgery" and "surgery" groups received distilled water instead of GK-2, according to the same scheme and in equivalent volumes. The animals were subjected to an open-field test for 48 h after the last injection of GK-2 (or distilled water).

Surgery. A Nembutal-anesthetized (60 mg/kg) and scalped animal was mounted onto a stereotaxic apparatus. Transverse incisions 1 mm wide were made in the cranial bone: the starting point of the incision localized at the level of bregma (AP = 0.0) and 2 mm laterally relative to the latter (L = ± 2.0); the endpoint of the incision localized 2 mm caudally relative to the bregma and 1 mm laterally relative to the latter (AP = −2.0; L = ± 1.0). After the bone had been cut, the dura mater was incised in the area of incisions. A sterile bent needle was placed into the incision to a depth of 6.2 mm from the bone surface (DV = +6.2). Simultaneous manipulation using two stereotaxic screws allowed to relocate the needle almost to the endpoint of the transverse incision. The needle was then slowly lifted from the incision. The procedure was repeated twice on each hemisphere. The sham surgery procedure was similar to that of transsection with one exception: the needle was placed to a depth of 3 mm from the bone surface (DV = +3.0).

Open-field test. This test is commonly used to assess general motor and exploratory activities [32]. The setup consisted of a circular arena made of white PVC. The arena diameter was 90 cm; the walls were 40 cm high. The floor of the arena was divided into 19 squares of approximately equal area with lines. The animal was carefully placed on the floor in the center of the arena; the number of squares and vertical stands crossed by it during 4 min was recorded using the RealTimer software program (Scientific and Production Company "Open science," Russia). Transsection of the septo-hippocampal pathway in rats is known to cause impairment of the extinction of the exploratory orientation reaction (EOR) in the open field test [33, 34]. The EOR extinction coefficient, which represents the ability of rats to exhibit habituation, was calculated according to the equation $C_e = a/b$, where a is the number of squares crossed in the group during the first minute of observation, and b is the number of squares crossed in the group during the last minute of observation.

Investigations into the effects of GK-2 on the AD model associated with the administration of streptozotocin into cerebral ventricles [30]

Study design. The mongrel male rats (330–380 g) were randomly allocated into four groups: those subjected to sham surgery (n = 6); those subjected to surgery (n = 9), those subjected to surgery and treated with dipeptide GK-2 (n = 7), and those subjected to surgery and treated with the reference drug, memantine (n = 6). Dipeptide GK-2 (0.5 mg/kg or 6×10^{-7} mol/kg) was administered 4 h after the surgery and then once daily for 2 weeks (a total of 14 injections). Memantine was administered according to the same scheme at a dose of 10 mg/kg (4.6×10^{-5} mol/kg). This dose was selected as the most effective one according to the published data [35]. Distilled water was administered to the "sham surgery" and "surgery" groups instead of GK-2 or memantine according to the same scheme in equivalent volumes. Three weeks after the surgery, the rats were trained to search for a submerged platform in the "Morris water maze" setup for 5 days. One week after the completion of the training, the rats were tested for retention of this skill.

Surgery. A Nembutal-anesthetized rat (60 mg/kg) was mounted onto a stereotactic apparatus. Streptozotocin in a Ringer's solution at a dose of 3 mg/kg was bilaterally injected into the cerebral ventricles of the animal (5 μl per ventricle) according to the coordinates AP = −1; L = ±1.5; DV = +3.5. A total of 5 μl of the Ringer's solution was injected into the cerebral ventricles of the sham-operated animals. The injections were carried out at a rate of 1 μl/min with a pause after each microliter (1 min). Upon completion of the administration, the needle was left in place for an additional 3 min and then removed.

Morris water maze. This test, first proposed by Morris D. [36], is mainly used to assess spatial memory. Our experimental setup consisted of a pool made of gray plastic (150 cm in diameter, 60 cm high). The pool was filled with water (24–25°C) to a depth of 40 cm. The pool was conventionally divided into four sections. A platform measuring 10 cm in diameter and submerged in water to a depth of 2 cm was located in the center of one of the sections. Various visual stimuli were placed on the walls of the room facing each of the conventional sectors. The rats were taught to find the submerged platform for 5 days. During this period, the animals were placed in water at 4 different starting positions near the pool wall (starting positions were located in the centers of the conventional sectors) four times per day. The sequence of starting positions was identical for all animals during the day and was changed every day. The interval between the placements was 30 s. After a rat reached the platform, it was left on it for 5 s. If an animal could not find the submerged platform within 60 s, it was gently guided to it. After 1 week, the test for retention of the acquired skill of finding the platform was carried out. During the test the animals were again placed in water 4 times at different starting positions. Escape latency (EL) was recorded for each attempt.

Statistical analysis. Statistical processing was carried out using the Statistica 10.0 software. Reduction of the average daily EL during the training period was used as a criterion for spatial learning ability in the Morris water maze setup. The average EL on the day of the test, as well as the EL during the fourth and last test placement, was used as a criterion of safety and effectiveness of reproduction of the acquired skill. In order to carry out the analysis of intergroup differences in the Morris water maze setup, a univariate analysis of variance (one-way ANOVA) and a Fisher's multiple comparison test were utilized. The Wilcoxon test was used for pairwise comparison of the related samples. The data are presented as medians of the samples, lower and upper quartiles. The results were considered statistically significant at $p < 0.05$.

The therapeutic effect (T_e) of dipeptide GK-2 was calculated using the equation:

$$T_e = [(c-d)/(e-d)] \times 100\%,$$

where c is the value of the parameter in the "surgery + treatment" group, d is the value of the parameter in the "surgery" group, and e is the value of the parameter in the "sham surgery" group.

RESULTS AND DISCUSSION

Dipeptide GK-2 counteracts the septo-hippocampal pathway transsection-induced impairment of cognitive functions in rats

No statistically significant intergroup differences in the intensity of horizontal and vertical motor activities were identified. The analysis of the dynamics of the horizontal locomotor activity (number of squares crossed) demonstrated that this parameter in sham-operated animals decreased significantly and 4 minutes into the test was significantly lower than that during the 1st minute (C_e = 2.3). Rodents are characterized by gradual extinction of EOR upon encountering a new situation, which is attributed to addiction or habituation. Transsection of the septo-hippocampal pathway led to impairment of EOR extinction over time, which was reflected at an almost constant level of the horizontal locomotor activity in the rats subjected to surgery over the entire period of testing (C_e = 1). Similar results were also obtained by other researchers using this model [33, 34]. Impairment of the

Table 1. Effect of GK-2 on the impairment of EOR extinction during the open-field test caused by transsection of the septo-hippocampal pathway

Group	min 1	min 2	min 3	min 4	Extinction coefficient
Sham surgery	21(15–32)	14(11–25)	9.5(7–16)*	9(8–13)*	2.3
Surgery	11.5(8–35)	12(9–32)	19(11–24)	11.5(9–29)	1
Surgery + GK-2	12.5(9–21)	11.5(7–14)	15.5(8–17)	6.5(3–8)*	1.9

* $p < 0.05$ as compared to the locomotor activity in the same group during the first minute of the test.
Note. The data are presented as medians of respective samples. The extinction coefficient (C_e) of the EOR reflecting the ability of rats to habituate was calculated using the equation $C_e = a/b$, where *a* is the number of squares crossed in the group during the first minute of observation, and *b* is the number of squares crossed in the group during the last minute of observation.

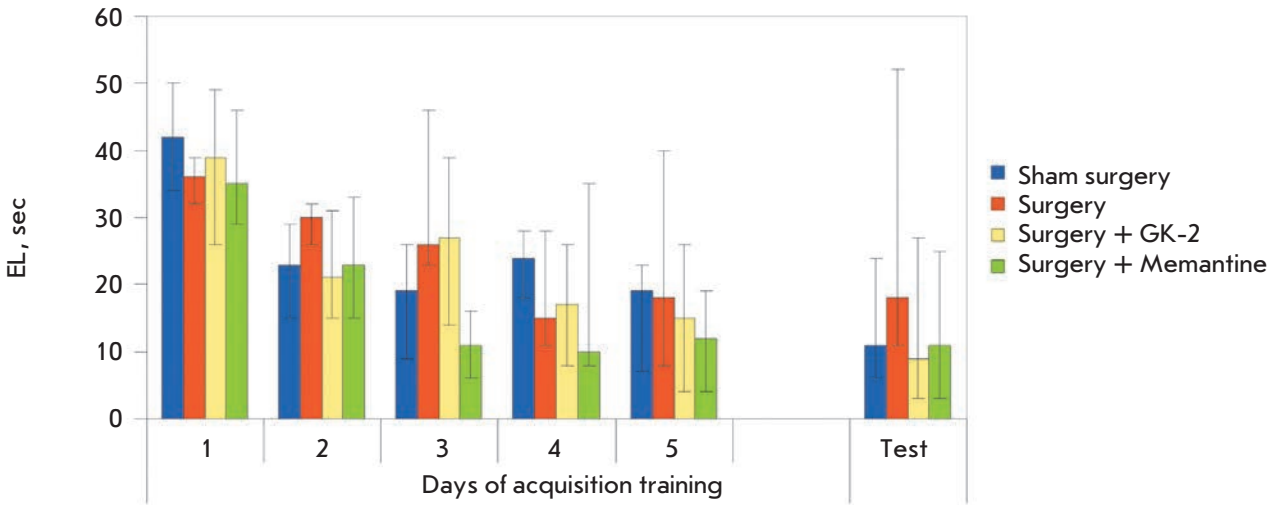

Fig. 1. Spatial learning and skill retention test in the Morris water maze. Sham surgery – bilateral administration of a Ringer's solution into the cerebral ventricles of rats plus subchronic intraperitoneal administration of distilled water.
Surgery – bilateral administration of streptozotocin dissolved in the Ringer's solution into the cerebral ventricles of rats plus subchronic intraperitoneal administration of distilled water.
Surgery + GK-2 – bilateral administration of streptozotocin dissolved in the Ringer's solution into the cerebral ventricles of rats plus subchronic intraperitoneal administration of dipeptide GK-2.
Surgery + memantine – bilateral administration of streptozotocin dissolved in the Ringer's solution into the cerebral ventricles of rats plus subchronic intraperitoneal administration of memantine.
The EL per four placements within 1 day were averaged for each animal. The data are presented as medians and interquartile ranges

extinction of EOR under new conditions caused by the septo-hippocampal transsection was probably associated with abnormalities of the spatial memory [33]. The animals subjected to surgery and treated with GK-2 demonstrated recovery of the ability to habituate (C_e = 1.9) (Table 1). The therapeutic effect of GK-2 was approximately 70%.

Dipeptide GK-2 completely restores the abnormality of spatial memory caused by the administration of streptozotocin into the cerebral ventricles of rats

Intracerebral administration of streptozotocin is known to cause the development of cognitive deficit, which can be detected within 2 weeks after surgery and progresses for several months [30]. In particular, intracerebral administration of streptozotocin causes abnormalities in spatial memory during the Morris water maze test. This disorder correlates with biochemical changes in the hippocampus (decreased activity of choline acetyltransferase [30]), as well as with a significant decrease in the immunoreactivity of the transcription factor CREB, which plays an important role in the regulation of learning and the memory processes participating in the transformation of short-term memory into long-term memory [37].

In this study, the EL decreased during the learning period in all groups; no statistically significant intragroup differences were identified during this period (Fig. 1). Hence, administration of streptozotocin had no effect on the learning ability of animals during the Morris water maze test. This can be attributed to the fact that the training was either conducted 3 weeks after the surgery (the cognitive deficit was probably not sufficiently pronounced during this period) or that mongrel rats were used. Intracerebral administration of streptozotocin in the study conducted by Shingo et al. [37] also had no effect on the ability of Wistar rats to learn in the Morris water maze test 2 weeks after the surgery.

The test for the retention of the acquired skill carried out 1 week after the learning phase had been completed demonstrated that the average (over four placements) EL in the sham-operated rats was characterized by a tendency to decrease as compared to the last day of learning, which is consistent with the data on the increased level of reproduction of long-term spatial memory during later periods after the learning phase [38]. Meanwhile, the EL of the rats subjected to surgery did not decrease as compared to the last day of learning and was higher than that in the "sham surgery" group,

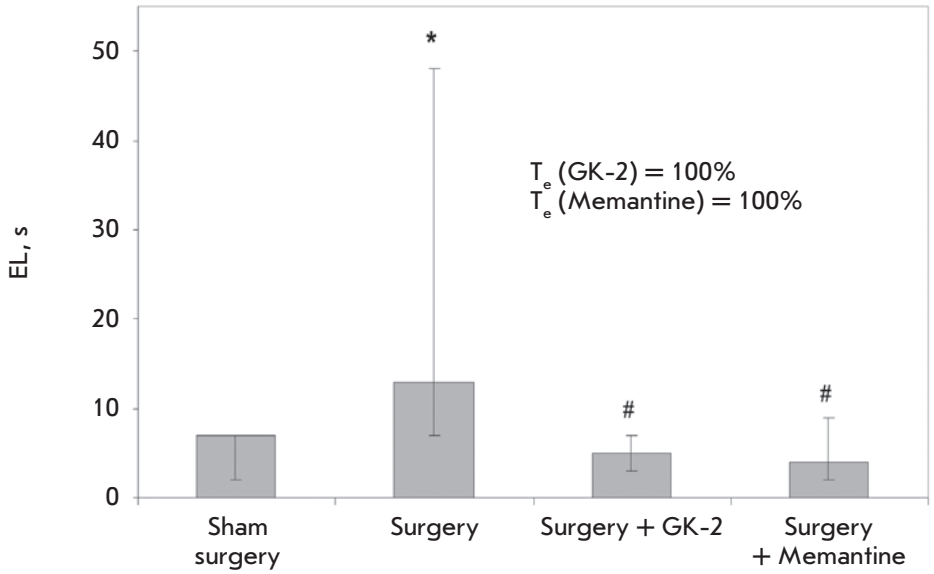

Fig. 2. Effects of GK-2 on the retention of the skill of finding the submerged platform in the Morris water maze setup, which is deficient in rats with experimental AD induced by the injection of streptozotocin into the cerebral ventricles. The data are presented as medians and interquartile ranges. * – $p = 0.017$ in comparison to the "sham surgery" group; # – $p = 0.012$ ("surgery + GK-2") and 0.014 ("surgery + memantine") in comparison with the "surgery" group (one-way ANOVA with subsequent post hoc Fisher test). The therapeutic effect (T_e) of dipeptide GK-2 was calculated using the following equation: $T_e = [(c-d)/(e-d)] \times 100\%$, where c is the EL in the "surgery + treatment" group, d is the EL in the "surgery" group, and e is the EL in the "sham surgery" group

although these results were not statistically significant. The EL among rats receiving GK-2 did not differ from that for the "sham surgery" group (Fig. 1). The analysis of intergroup differences with respect to EL during the last (fourth) placement in the test showed that this parameter in rats subjected to surgery was significantly higher than that in the "sham surgery" group (Fig. 2, Table. 2). NGF mimetic GK-2 fully prevented this abnormality and was equal in terms of its effectiveness to the reference drug memantine (Fig. 2).

Hence, dipeptide GK-2 can counteract the cognitive deficit in rat AD models.

It has previously been established that GK-2 has neuroprotective activity and acts via an NGF-like mechanism [18]. Intracerebral administration of NGF is known to restore cognitive functions in *in vivo* AD models. Thus, administration of mouse NGF into the cerebral ventricles of rats subjected to septo-hippocampal transsection over a period of 14 days significantly improved the spatial memory in the Morris water maze test with a therapeutic effect of approximately 75% [28]. The recovery of cholinergic neurons under the influence of exogenous NGF 1 month after fimbria-fornix transsection in rats was described in [29]. Improvement of the spatial memory in rats treated with NGF 2 weeks after the surgery can be associated with increased survival of cholinergic neurons and/or improvement of cholinergic transmission in the hippocampus [28]. Intracerebral administration of recombinant human NGF to rats for 3 weeks after the destruction of the basal nuclei of Meynert by ibotenic acid partially prevented the impairment of the learning ability in the Morris water maze with a therapeutic effect of approximately 25% [39]. Administration of recombinant human NGF resulted in a decrease in the body weight of rats. In ad-

Table 2. Effects of GK-2 on EL in the Morris water maze in rats with experimental AD induced by administration of streptozotocin into the cerebral ventricles

Group	EL*
Sham surgery	7 (3–7)
Surgery	13 (7–48)
Surgery + GK-2	5 (4–6.5)
Surgery + Memantine	4 (2–8)

* Data are presented as medians; interquartile ranges are given in parentheses.

dition to weight loss, such side effects of NGF as pain syndrome [40, 41], Schwann cell hyperplasia, and multiple sprouting of sympathetic and sensory axons in the medulla and the spinal cord have been observed [42].

Low molecular weight mimetics of NGF exhibiting activity in AD models have been described. A non-peptide mimetic of NGF, the selective agonist of TrkA-receptors known as D3, restored cholinergic deficit and improved spatial memory in aged animals in the Morris water maze upon intracerebral administration (40 μg per rat) [43].

Another low-molecular-weight non-peptide mimetic of NGF known as MT2, which is also a TrkA-receptor agonist, exhibits neuroprotective and antiamyloidogenic activity in cellular AD models at a concentration of 5–30 μmol/ml [44].

No data regarding the systematic application of both NGF and its low-molecular-weight mimetics activating TrkA-receptors in AD models have been obtained. Only a non-peptide agonist of p-75 receptors known as LM11A-31, which demonstrated neuroprotective and antiamnestic activities in a genetic mouse model of AD, has been identified [45].

CONCLUSIONS

Hence, data on the mnemotropic effects of the dipeptide mimetic of NGF causing the phosphorylation of TrkA-receptors and Akt-kinases upon systemic administration in AD models have been obtained for the first time.

Dipeptide GK-2 considerably prevents the abnormalities of habituation caused by septo-hippocampal transsection. Identically to memantine, which is widely used for treatment of AD, GK-2 significantly prevents spatial memory deficit in the Morris water maze in the streptozotocin AD model. The effective dose of GK-2 by weight is 20 times lower than that of memantine; the effective dose by amount of matter is 80 times lower.

The results obtained suggest that further development of GK-2 as a neuroprotective medicinal product that could prevent the development of AD is rather promising. ●

REFERENCES

1. Ubhi K., Masliah E. // J. Alzheimers Dis. 2013. V. 33. Suppl.1. P.185-194.
2. Dunkel P., Chai C. L., Sperlagh B., Huleatt P.B., Matyus P. // Expert Opin. Investig. Drugs. 2012. V. 21. № 9. P. 1267–1308.
3. Gelfo F., Tirassa P., De Bartolo P., Caltagirone C., Petrosini L., Angelucci F. // J. Alzheimers Dis. 2011. V. 25. № 9. P. 213–217.
4. Sofroniew M.V., Howe C.L., Mobley W.C. // Annu Rev Neurosci. 2001. №24. P.1217-1281.
5. Calissano P., Amadoro G., Matrone C., Ciafre S., Marolda R., Corsetti V., Ciotti M.T., Mercanti D., Di Luzio A., Seerini C. // Cell Death Differ. 2010. № 17. P. 1126–1133.
6. Calissano P., Matrone C., Amadoro G. // Dev. Neurobiol. 2010. V. 70. № 5. P. 372–382.
7. Cuello A.C., Bruno M.A. // Neurochem. Res. 2007. V. 32. № 6. P. 1041–1045.
8. Cattaneo A., Capsoni S., Paoletti F. // J. Alzheimers Dis. 2008. V. 15. № 2. P. 255–283.
9. Covaceuszach S., Capsoni S., Ugolini G., Spirito F., Vignone D., Cattaneo A. // Curr. Alzheimer Res. 2009. V. 6. № 2. P. 158–170.
10. Winkler J., Thal L.J. // Exp. Neurol. 1995. V. 136. № 2. P. 234–250.
11. Gu H., Long D., Song C., Li X. // Neurosci. Lett. 2009. V. 453. № 3. P. 204–209.
12. Smith D.E., Roberts J., Gage F.H., Tuszynski M.H. // Proc. Natl. Acad. Sci. USA. 1999. V. 96. № 19. P. 10893–10898.
13. Colangelo A.M., Bianco M.R., Vitagliano L., Cavaliere C., Cirillo G., De Gioia L., Diana D., Colombo D., Redaelli C., Zaccaro L., et al. // J. Neurosci. 2008. V. 28. № 11. P. 2698–2709.
14. Maliartchouk S., Feng Y., Ivanisevic L., Debeir T., Cuello A.C., Burgess K., Saragovi H.U. // Mol. Pharmacol. 2000. V. 57. № 2. P. 385–391.
15. Longo F.M., XieY., Massa S.M. // Curr. Med. Chem. 2005. V. 5. № 1. P. 29.
16. Seredenin S.B., Gudasheva T.A. // Russian Patent. 2010.№ 2410392.
17. Gudasheva T.A., Antipova T.A., Seredenin S.B. // XXII Intern. Symp. on Medicinal Chemistry. Book of Abstracts. Berlin: Chemmedchem. ISMC, 2012.. P. 299.
18. Gudasheva T.A., Antipova T.A., Seredenin S.B. // Dokl Biochem Biophys. 2010. V.434, №4. P. 549–552.
19. Antipova T.A., Gudasheva T.A., Seredenin S.B. // Bull Exp Biol. 2010. V. 150. № 11. P. 537–540.
20. Seredenin S.B., Silachev D.N., Gudasheva T.A., Pirogoc Y.A., Isaev N.K. // Bull Exp Biol Med. 2011. V. 151. № 5. P. 518-521.
21. Seredenin S.B., Romanova G.A., Gudasheva T.A., Shakova F.M., Barskov I.V., Stelmashuk E.V., Antipova T.A. // Bull Exp Biol Med. 2010. V. 150. № 10. P. 406-409.
22. Povarnina P.Yu., Gudasheva T.A., Vorontsova O.N., Nikolaev S.V., Antipova T.A., Ostrovskaya R.U., Seredenin S.B. // Eksp Klin Farmakol. 2012. V. 75. № 9. P. 15-20.
23. Povarnina P.Yu, Gudasheva T.A., Vorontsova O.N., Bondarenko N.A., Seredenin S.B. // Bull Exp Biol Med. 2011. V. 151. № 6 P. 634-638.
24. Konstantinopolsky M.A., Chernyakova I.V., Kolik L.G., Gudasheva T.A. // IV All-Russia Congress of Pharmacologists of Russia «Innovations in modern pharmacology». Moscow. Folium Publishing Company. 2012. P. 94.
25. Povarnina P. Yu., Ozerova I.V., Ostrovskaya R.U., Gudasheva T.A., Seredenin S.B. // Dokl Biochem Biophyz. 2013. V. 449. № 3. P. 364-366.
26. Krugel U., Bigl V., Eschrich K., Bigl M. // Int. J. Dev. Neurosci. 2001. V. 19. № 3. P. 263–277.
27. Lopez-Coviella I., Mellott T.J., Schnitzler A.C., Blusztajn J.K. // PLoS One. 2011. V. 6. № 6. e21166
28. Francis-Turner L., Valouskova V. // Neurosci. Lett. 1996. V. 202. № 3. P. 193–196.

29. Miyamoto O., Itano T., Fujisawa M., Tokuda M., Matsui H., Nagao S., Hatase O. // Acta Med. Okayama. 1993. V. 47. № 3. P. 139–144.
30. Salkovic-Petrisic M., Hoyer S. // J. Neural. Transm. Suppl. 2007. № 72. P. 217–233.
31. Kovacs T., Carris N.J., Lantos P.L. // Neurorept. 2001. № 12. P. 285–288.
32. Buresh, Bureshova O., Houston J.P. Methods and Basic Experiments in Studies of the Brain and Behavior. M.: Higher School, 1991. 399 p.
33. Lamprea M.R., Cardenas F.P., Silveira R., Walsh T.J., Morato S. // Braz. J. Med. Biol. Res. 2003. V. 36. № 2. P. 233–238.
34. Cassel J.C., Kelche C., Peterson G.M., Ballough G.P., Goepp I., Will B. // Neuroscience. 1991. V. 45. № 3. P. 571–586.
35. Filali M., Lalonde R., Rivest S. // Neuropharmacology. 2011. V. 60. № 6. P. 930–936.
36. Morris R. // J. Neurosci. Meth. 1984. V. 11. № 1. P. 47–60.
37. Shingo A.S., Kanabayashi T., Murase T., Kito S. // Behavioural Brain Res. 2012. № 229. P. 378–383.
38. Solnceva S.V., Storozheva Z.I., Nikitin V.P. // 2012. Bull Exp Biol Med. 2012. V. 153. № 5. P. 565–568.
39. Winkler J., Thail L.J. // Exp. Neurol. 1995. V. 136. № 2. P. 234–250.
40. Eriksdotter Jonhagen M., Nordberg A., Amberla K., Backman L., Ebendal T., Meyerson B., Olson L., Seiger, Shigeta M., Theodorsson E., et al. // Dement. Geriatr. Cogn. Disord. 1998. V. 9. № 5. P. 246–257.
41. Apfel S.C., Schwartz S., Adornato B.T., Freeman R., Biton V., Rendell M., Vinik A., Giuliani M., Stevens J.C., Barbano R., et al. // JAMA. 2000. V. 284. № 17. P. 2215–2221.
42. Winkler J., Ramirez G.A., Kuhn H.G., Peterson D.A., Day-Lollini P.A., Stewart G.R., Tuszynski M.H., Gage F.H., Thal L.J. // Ann. Neurol. 1997. V. 41. № 1. P. 82–93.
43. Bruno M.A., Clarke P.B., Seltzer A., Quirion R., Burgess K., Cuello A.C., Saragovi H.U. // J. Neurosci. 2004. V. 24. № 37. P. 8009–8018.
44. Scarpi D., Cirelli D., Matrone C., Castronovo G., Rosini P., Occhiato E.G., Romano F., Bartali L., Clemente A.M., Bottegoni G., et al. // Cell Death Dis. 2012. V. 3. № 7. P. 339.
45. Knowles J.K., Simmons D.A., Nguyen T.V., Vander Griend L., Xie Y., Zhang H., Yang T., Pollak J., Chang T., Arancio O. et al. // Neurobiol Aging. 2013. V. 34. № 8. P.2052-2063.

Kinetic Parameters and Cytotoxic Activity of Recombinant Methionine γ-Lyase from *Clostridium tetani*, *Clostridium sporogenes*, *Porphyromonas gingivalis* and *Citrobacter freundii*

E. A. Morozova[1], V. V. Kulikova[1], D. V. Yashin[2], N. V. Anufrieva[1], N. Y. Anisimova[3], S. V. Revtovich[1], M. I. Kotlov[4], Y. F. Belyi[4], V. S. Pokrovsky[3], T. V. Demidkina[1*]

[1]Engelhardt Institute of Molecular Biology, Russian Academy of Sciences, Vavilova Str., 32, Moscow, Russia, 119991

[2]Institute of Gene Biology, Russian Academy of Sciences, Vavilova St., 34/5, Moscow, Russia, 119334

[3]Blokhin Cancer Research Center, Russian Academy of Medical Sciences, Kashirskoe sh., 24, Moscow, Russia, 115478

[4]Gamaleya Research Institute of Epidemiology and Microbiology, Gamaleya Str., 18, Moscow, Russia, 123098

*E-mail: vadimpokrovsky@yandex.ru, tvd@eimb.ru

Received 04.03.2013

ABSTRACT **The steady-state kinetic parameters of pyridoxal 5'-phosphate-dependent recombinant methionine γ-lyase from three pathogenic bacteria, *Clostridium tetani*, *Clostridium sporogenes*, and *Porphyromonas gingivalis*, were determined in β- and γ-elimination reactions. The enzyme from *C. sporogenes* is characterized by the highest catalytic efficiency in the γ-elimination reaction of *L*-methionine. It was demonstrated that the enzyme from these three sources exists as a tetramer. The N-terminal poly-histidine fragment of three recombinant enzymes influences their catalytic activity and facilitates the aggregation of monomers to yield dimeric forms under denaturing conditions. The cytotoxicity of methionine γ-lyase from *C. sporogenes* and *C. tetani* in comparison with *Citrobacter freundii* was evaluated using K562, PC-3, LnCap, MCF7, SKOV-3, and L5178y tumor cell lines. K562 (IC_{50}=0.4–1.3 U/ml), PC-3 (IC_{50}=0.1–0.4 U/ml), and MCF7 (IC_{50}=0.04–3.2 U/ml) turned out to be the most sensitive cell lines.**

KEYWORDS **kinetic parameters; methionine γ-lyase; pathogenic microorganisms; oligomeric structure; cytotoxicity.**

ABBREVIATIONS **DTT – dithiothreitol; His-tag – poly-histidine fragment; MGL – methionine γ-lyase; MSC – mesenchymal stromal cells; PLP – pyridoxal 5'-phosphate.**

INTRODUCTION

Methionine γ-lyase (MGL) [EC 4.4.1.11] is a pyridoxal 5'-phosphate-dependent enzyme that catalyzes the γ-elimination reaction of *L*-methionine, yielding methyl mercaptan, α-ketobutyric acid, and ammonia:

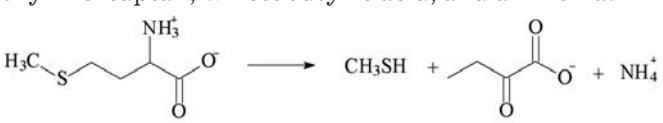

In addition to the physiological reaction, the enzyme catalyzes the β-elimination reaction of *L*-cysteine and its S-substituted derivatives, yielding the corresponding mercaptans, pyruvic acid, and ammonia [1]. The enzyme was isolated from *Pseudomonas putida*, *Aeromonas* sp., *Clostridium sporogenes*, *Porphyromonas gingivalis*, *Brevibacterium linens BL2*, *Citrobacter freundii*, and several others, from eukaryotic protozoa *Trichomonas vaginalis* and *Entamoeba histolytica*, and from fungi *Aspergillus flavipes* [2]. This enzyme is absent in mammalian cells but is present in pathogenic bacteria, such as *Aeromonas* sp. [3], *C. sporogenes* [4], *P. gingivalis* [5], and in pathogenic protozoa *E. histolytica* [6], *T. vaginalis* [7], which allows one to consider the enzyme as a potential target for novel antibiotics.

The enzyme is of interest as an anticancer agent, since the growth of malignant cells of various origins (unlike the growth of normal cells) is accompanied by obligatory methionine utilization [8]. The possibility of development of an anticancer agent based on MGL from *P. putida* has been demonstrated *in vitro* and *in vivo* [9–12]. Antitumor activity of the enzyme from *A. flavipes* with respect to several human tumors was observed *in vivo* [13]. Several kinetic parameters of the recombinant MGL derived from the pathogenic microorganisms *C. tetani* (causative agent of tetanus), *C. sporogenes* (causative agent of gas gangrene and enteritis), and *P. gingivalis* (causative agent of periodontitis) were determined in the present study; the data on the cytotoxic activity of the enzyme from these sources and from *C. freundii* were analyzed.

EXPERIMENTAL

Bacterial cultivation and purification of the enzyme

Escherichia coli BL21 (DE3) cells containing the MGL genes from *C. sporogenes*, *C. tetani*, and *P. gingivalis* in the plasmid pET-28a [14] were cultured in an "inducing" medium [15] at 37°C under stirring (180 rpm) for 24 h. The cells were harvested by centrifugation and stored at −80°C. Cell disruption and the removal of nucleic acids were performed according to [16]. After the separation of nucleic acids, the preparations were transferred to a 50 mM potassium phosphate buffer, pH 8.0, containing 0.05 mM pyridoxal 5'-phosphate (PLP) using a "Centricon-30 ultrafiltration unit" (Amicon, USA). The polypeptide chains of the enzymes isolated from three sources contained the poly-histidine fragment MGSSHHHHHHSSGLVPRGSH at their N-termini. The preparations were purified using affinity chromatography on a column with a Ni^{2+}IMAC −Sepharose sorbent (GE Healthcare, Sweden); a 10–500 mM imidazole gradient in a 50 mM potassium phosphate buffer, pH 8.0, containing 0.05 mM PLP was used for MGL elution. Fractions with the characteristic spectra of pyridoxal 5'-phosphate-dependent enzymes with λ_{max} at 420 nm were obtained at an imidazole concentration of 25–155 mM. Cultivation of the biomass of *E. coli* BL21 (DE3) cells containing a plasmid with the MGL gene from *C. freundii* and purification of the enzyme was carried out as per [17]. The concentrations of the purified preparations were determined using the coefficient $A_{1\%}^{278} = 0.8$ [17]. The purity of the preparations was evaluated using electrophoresis under denaturing conditions according to the Laemmli method [18]. The bands in the electrophoregrams were identified by Coomassie R-250 staining [19] and Western blotting using the poly-histidine fragment HisProbe-HRP reagent (Thermo scientific, Rockford, IL, USA) [20].

The activity of the preparations in the γ-elimination reaction was determined by the rate of formation of α-ketobutyric acid in the coupled reaction with D-2-hydroxy isocaproate dehydrogenase under the conditions described in [17]. One unit of enzyme activity was defined as the quantity of MGL catalyzing the formation of 1.0 μM/min α-ketobutyrate at 30°C. The specific activities of the enzyme from *C. tetani*, *C. sporogenes*, *P. gingivalis* and *C. freundii* were 16.6, 12.8, 5.0, and 10.2 U/mg, respectively.

Cleavage of the His-tag fragment was performed in a reaction with thrombin. The reaction mixture (1 ml) containing 10 mg of the enzyme in a 50 mM potassium phosphate buffer, pH 8.0, 1 mM DTT, 0.05 mM PLP, and 100 units of thrombin were incubated for 24 h at 4°C. The product was then purified by gel filtration on a Superdex 200 column (GE Healthcare, Sweden) equilibrated with a 50-mM potassium phosphate buffer, pH 8.0, containing 1 mM DTT and 0.05 mM PLP. The homogeneity of the preparation was determined by electrophoresis under denaturing conditions.

Determination of the oligomeric composition of MGL from *C. tetani*, *C. sporogenes*, and *P. gingivalis*

The molecular weights of the enzymes from *C. tetani*, *C. sporogenes*, and *P. gingivalis* were determined for the enzymes containing His-tag, and after the thrombin-facilitated cleavage of the tag, followed by gel filtration on a Superdex 200 10/300 GL column (GE Healthcare, Sweden). A 50 mM potassium phosphate buffer, pH 8.0, containing 0.05 mM PLP and 1 mM DTT was used for elution.

Determination of the steady-state kinetic parameters of the γ- and β-elimination reactions

The steady-state parameters of the γ-and β-elimination reactions were determined by the formation rate of α-ketobutyric and pyruvic acids in coupled reactions with D-2-hydroxy isocaproate dehydrogenase and lactate dehydrogenase under the conditions described in [17] by varying the substrate concentrations in the reaction mixtures. The data were processed according to the Michaelis–Menten equation using the Enzfitter software program. The molecular weights of the enzyme subunits with allowance for His-tag (which were equal to 44.04, 44.36, an 44.08 kDa for MGL from *C. tetani*, *C. sporogenes*, *P. gingivalis*, respectively) were used in the calculations.

Evaluation of *in vitro* cytotoxicity

The cytotoxic activity of MGL of various origins was evaluated for the Fisher L5178y lymphadenosis cell line (a collection of tumor strains from the N.N. Blokhin Cancer Research Center), PC-3 and LnCap human

Table 1. Kinetic parameters of MGL from various sources*

Substrate	MGL from *P. gingivalis*			MGL from *C. tetani*			MGL from *C. sporogenes*			MGL from *C. freundii***		
	k_{cat}, s^{-1}	K_m, mM	k_{cat}/K_m, $M^{-1}s^{-1}$	k_{cat}, s^{-1}	K_m, mM	k_{cat}/K_m, $M^{-1}s^{-1}$	k_{cat}, s^{-1}	K_m, mM	k_{cat}/K_m, $M^{-1}s^{-1}$	k_{cat}, s^{-1}	K_m, mM	k_{cat}/K_m, $M^{-1}s^{-1}$,
L-Met	3.9	1.77	2.2×10^3	12	0.947	1.27×10^4	9.86	0.432	2.28×10^4	6.2	0.7	8.85×10^3
S-Et-L-Hcy	3.84	0.93	4.13×10^3	5.89	0.545	1.08×10^4	7.05	0.278	2.54×10^4	6.78	0.54	1.26×10^4
L-Met(SO)	5.05	12.22	4.13×10^2	2.7	7.07	3.82×10^2	6.7	33.51	2.0×10^2	2.52	6.21	4.06×10^2
S-Et-L-Cys	8.05	2.17	3.71×10^3	7.08	0.72	9.83×10^3	6.3	0.358	1.76×10^4	5.03	0.17	2.96×10^4
S-Bzl-L-Cys	5.8	1.47	3.94×10^3	8.5	0.766	1.11×10^4	10	0.348	2.87×10^4	8.16	0.18	4.53×10^4

* The mean squared error of the experiment in the determination of the kinetic parameters did not exceed 10%.
** Data from [16, 17].

prostate cancer cell lines (ATCC, USA), the MCF7 human breast cancer cell line (ATCC , USA), K562 chronic erythroblastic human leukemia cell line (ATCC, USA), and the SKOV-3 human ovarian cancer cell line (a collection of tumor strains from the N.N. Blokhin Cancer Research Center). Cells were cultured at 37°C and 5% CO_2 in the RPMI 1640 medium (PanEco, Russia) containing 10% of fetal bovine serum (HyClone Laboratories, UK), 2 mM *L*-glutamine, and 100 U/ml of penicillin and streptomycin (PanEco, Russia). The cells that reached the logarithmic growth phase were passed into 96-well flat bottom microplates (Costar, USA) – (4-6) × 10^4 cells per well – and pre-incubated for 24 h prior to the addition of the test enzymes under the abovementioned conditions. Light microscopy of the cells was carried out using an AxioVision 4 system (Carl Zeiss, Germany). Cell viability was determined using trypan blue dye exclusion staining (PanEco, Russia). Cell count was determined in the Goryaev chamber.

The MGL preparations in the RPMI 1640 medium in a wide range of progressively decreasing concentrations were added in the wells with the cell culture and co-incubated for 72 h. In addition to MGL, the culture medium contained 5 × 10^{-4} M PLP. The range of enzyme concentrations in the culture medium corresponded to 0.000001–6.2 U/ml. An equal volume of the RPMI 1640 medium with PLP was added in the control wells. The level of cell metabolism following the incubation period was determined using a standard MTT colorimetric assay [21]. The optical absorption of the dimethyl sulfoxide colored solutions was measured using a Multiskan MS plan-table photometer (Labsystems, Finland) at λ = 540 nm. The viability of a cell culture after co-incubation with test substances was evaluated using the following formula: $(N_o/N_c) \times 100\%$, where N_o is the optical absorbance in the test samples and N_c is the optical absorbance in the control sample. The nonlinear regression method was used to calculate the inhibitory concentration of each enzyme in the medium; i.e., the concentration that caused a 50% reduction in the number of viable cells (IC_{50}).

Statistical data analysis

The data were processed using the SPSS 11.5 software package. The relationships between IC_{50} and $K_м$ were studied using the Pearson correlation analysis. The correlation coefficients were calculated for the grouped cytotoxicity data in various cell lines and for the ungrouped data. In the former case, the correlation analysis included the geometric mean of IC_{50} for various cell cultures. In the latter case, the cytotoxicity was individually assessed using each cell line; the data were pre-logarithmized for the symmetrization of the distribution law.

One-way ANOVA test was used to compare the cytotoxicity of the enzymes from *C. freundii*, *C. sporogenes*, and *C. tetani*. An analysis of the logarithmized data was conducted, since the dispersions of IC_{50} in the groups varied considerably. The mean values ± SD – arithmetic mean and standard deviation; geometric mean (antilog of the logarithmic means); $p_{ANOVA} = 0.005$ – statistical significance of the differences according to the data from the analysis of the variance in general were calculated. The statistical significance of the differences in the cytotoxic activity of various enzymes was evaluated using the Tukey method.

RESULTS AND DISCUSSION

Kinetic parameters of MGL from three pathogenic bacteria

We determined the steady-state kinetic parameters of MGL from three sources in the γ-elimination reac-

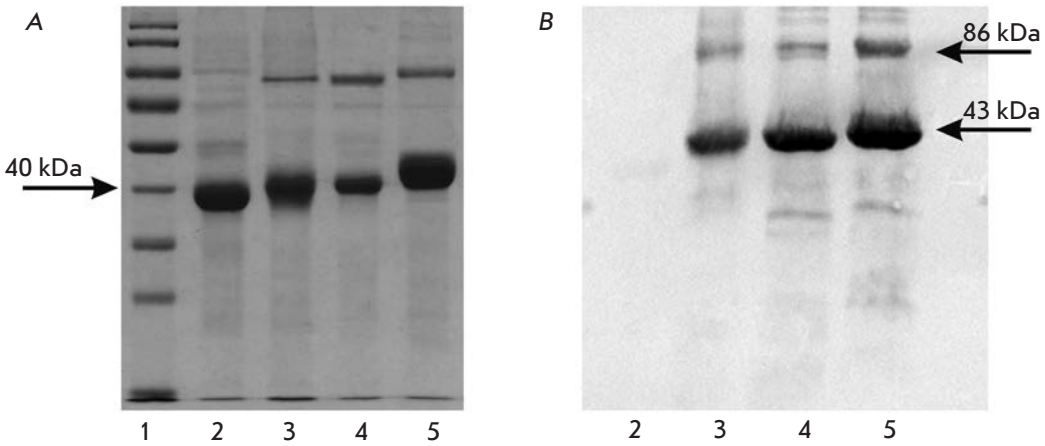

Fig. 1. Electrophoresis (a) and western blot (b) of MGL from various sources. *1* – standard molecular weight markers, *2* – *C. freundii* MGL, *3* – *P. gingivalis*MGL, *4* – *C. sporogenes* MGL, *5* – *C. tetani* MGL

tion for three substrates: *L*-methionine, *L*-methionine sulfoxide, S-ethyl-*L*-homocysteine, and in the β-elimination reaction for two substrates – S-ethyl-*L*-cysteine and S-benzyl-*L*-cysteine. The data are presented in Table 1 in comparison with the parameters for the MGL from *C. freundii.*

In general, the kinetic parameters for the three enzymes and MGL isolated from *C. freundii* were comparable. The enzyme from *C. sporogenes* is characterized by the highest catalytic efficiency in comparison with other enzymes ($\kappa_{cat}/\mathcal{K}_m$ value) in the reaction with the physiological substrate, and the enzyme from *P. gingivalis* is characterized by the lowest catalytic activity. As mentioned above, antitumor activity was previously determined primarily for MGL from *P. putida* [22, 23]. The k_{cat}, K_m, k_{cat}/K_m values for the γ-elimination reaction of *L*-methionine for MGL from this source are equal to 25.39 s^{-1}, 0.92 mmol, and 2.76 × 104 $M^{-1}s^{-1}$, respectively [24]; i.e., the enzyme from *C. sporogenes* is characterized by a higher affinity to *L*-methionine than MGL from *P. putida*, but their catalytic efficiency is virtually identical.

Oligomeric structure of the recombinant proteins

It has previously been demonstrated that MGL from *P. putida* exists in solutions as a tetramer [25]. The X-ray diffraction analysis data for the recombinant MGL from *C. freundii* also indicated that the enzyme exists as a tetramer [26].

Two major bands have been revealed in the electrophoregrams of denatured preparations from *C. sporogenes*, *C. tetani*, and *P. gingivalis*. The first band with respect to the molecular weight corresponds to the MGL subunit; the second band is twice as large as the first one (*Fig. 1A*). Both of these bands interacted with the His-tag reagent (*Fig. 1B*). The bands corresponding to the dimeric form of MGL could form either during the oxidation of the sulfhydryl groups of MGL under the conditions of Laemmli electrophoresis, or their formation could be attributed to the His-tag. In most cases, the presence of the His-tag at the N-or C-terminus of the recombinant proteins did not affect their structure and function [27]; however, data on the influence of the His-tag on the structure and function of proteins are available. Thus, it has been demonstrated [28] that the presence of the His-tag at the C-terminus restores the ability of the mutant form of the DNA binding protein $\pi^{30.5}$ to form dimers, as opposed to the wild-type protein that is incapable of dimerization. The presence of the His-tag at the N-terminus of galactitol-1-phosphate 5-dehydrogenase reduced the enzyme's stability and resulted in aggregation of dimeric molecules [29].

It can be presumed that the presence of the MGSSHHHHHHSSGLVPRGSH sequence at the N-termini of the polypeptide chains of MGL from *C. sporogenes*, *C. tetani* and *P. gingivalis* affects the oligomeric organization of the enzymes.

The molecular weights of the native MGL preparations from the three sources mentioned above and *C. freundii* were determined by gel filtration. It was established that all the enzymes, independent of their source, are characterized by a tetrameric form. Figure 2 shows the data on the gel filtration of MGL from *C. sporogenes.* It was demonstrated that the molecular weights of the preparations from *C. sporogenes*, *C. tetani* and *P. gingivalis* after cleavage of the His-tag by thrombin are all equal approximately to 170 kDa, which corresponds to the tetrameric form. It should be noted that the oligomeric form was identified in the MGL preparation from *C. tetani* (characterized by the physiological activity of MGL) with a molecular weight of approximately 258 kDa. No dimeric forms were detected in the electrophoregrams of any of the preparations (*Fig. 3*), which excludes the aforementioned possibility

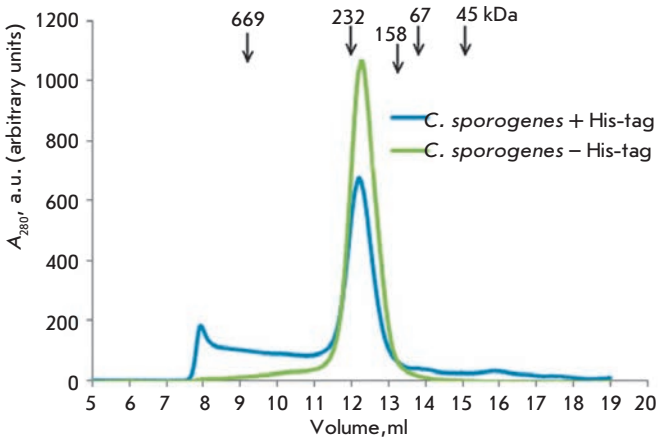

Fig. 2. Gel filtration of *C. sporogenes* MGL. The column was calibrated using standard markers: their molecular weights are shown in the figure

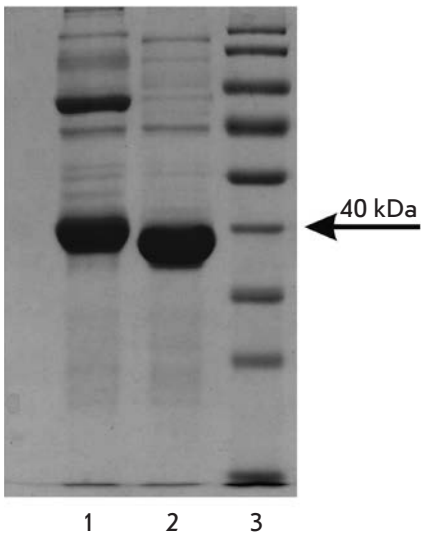

Fig. 3. Electrophoresis of *C. sporogenes* MGL. *1* – enzyme with His-tag fragment, *2* – enzyme after thrombin detachment of His-tag, *3* – standard molecular weight markers

that they form during the oxidation of the sulfhydryl groups of MGL under standard conditions of Laemmli electrophoresis. Therefore, the dimeric form of MGL is observed exclusively during the gel electrophoresis of denatured preparations from three sources containing a His-tag at the N-termini of polypeptide chains.

According to the X-ray diffraction analysis data, a tetrameric molecule of MGL from *C. freundii* consists of two catalytic dimers, each possessing two active sites formed by the residues of two subunits. The N-terminal domains of each subunit participate in the formation of a dimer, generating multiple hydrogen bonds with the residues of the C-terminal domain of the adjacent subunits and in the association of two catalytic dimers as they come into contact with the residues of the two C-terminal domains of the second catalytic dimer (Fig. 4) [26]. It is possible that the N-terminal His-tag present in the molecules of MGL from *C. sporogenes*, *C. tetani* and *P. gingivalis* forms additional bonds with residues of the C-terminal domain of the catalytic dimer and with the C-terminal residues of two subunits of the second catalytic dimer; thus, dimerization of the subunits can occur in denatured preparations.

The specific activity of the MGL preparations from *C. sporogenes*, *C. tetani*, and *P. gingivalis* determined after the cleavage of the His-tag by thrombin in the γ-elimination reaction of *L*-methionine turned out to be 1.5 times higher. The 50% increase in the specific activity of the preparations cannot be attributed exclusively to their minor additional purification after the treatment with thrombin. It is possible that the presence of a His-tag affects MGL activity.

In order to explain the variability in the catalytic efficiency of the enzymes and probable influence of the His-tag localized at the N-terminal regions of the polypeptide chains of the MGL from *C. sporogenes*, *C. tetani*, and *P. gingivalis* on enzyme activity, further investigations involving an X-ray diffraction analysis are required.

Cytotoxicity of methionine γ-lyase from *C. freundii*, *C. sporogenes* and *C. tetani*

The calculated IC_{50} values for MGL of various origins on a panel of cell cultures are presented in Table 2. PC-3 prostate cancer and K562 human chronic erythroblastic leukemia cell cultures were the ones most sensitive to the action of the enzymes; their IC_{50} values were

Table 2. IC_{50} of MGL for several tumor cell cultures

Cell culture	IC_{50} of MGL, U/ml		
	C. freundii	*C. sporogenes*	*C. tetani*
K562	1.3	0.9	0.4
PC-3	0.1	0.4	–
LnCap	> 2.9	> 2.9	>6.2
MCF7	0.5	0.04	3.2
L5178y	1.7	> 2.9	–
SCOV-3	–	–	5.3

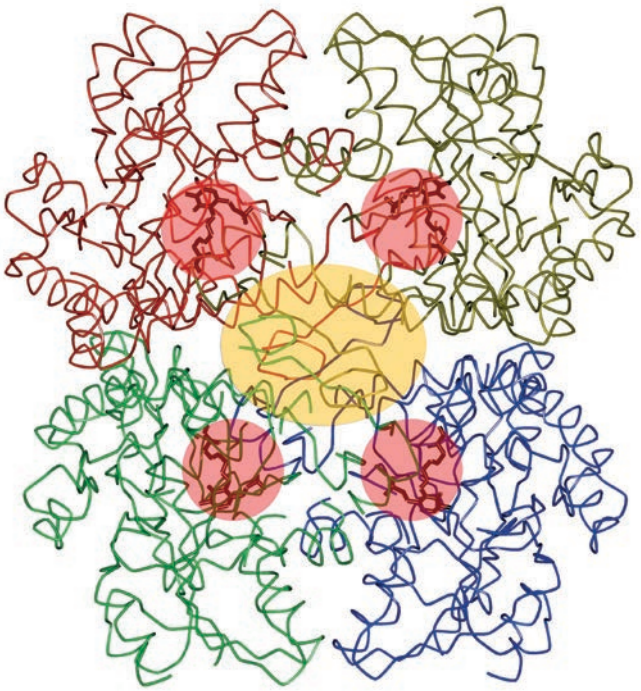

Fig. 4. Tetramer of *C. freundii* MGL. The subunits are marked using different colors, active sites are shown in pink, and the contact region between catalytic dimers is shown in yellow

0.1–0.4 and 0.4–1.3 U/ml, respectively. LnCap prostate cancer cells were the least sensitive: in the investigated concentration range, the IC_{50} value could not be determined for any of the enzymes. The sensitivity of K562 and MCF7 cells to the action of MGL is characterized by a significant variability.

The results obtained are indicative of the relatively high sensitivity of most of the cells that had been investigated to the action of MGL. Thus, the cytotoxicity of MGL is comparable to that of the other known enzymes, in particular, *L*-asparaginase from *E. coli*: with respect to the K562 and MCF7 cell cultures, the IC_{50} values for *L*-asparaginase from *E. coli* are equal to 0.8 and 10.9 U/ml, respectively [30]. The cytotoxicity level closest to that of MGL from *P. putida* was observed for the corresponding enzyme from *C. sporogenes*.

There is a statistically substantiated hypothesis regarding the direct dependence of the antitumor effect of the preparations whose effect is based on the destruction of another amino acid, *L*-asparagine (*L*-Asparaginase) [31, 32]. In connection to this, the contribution of enzymatic activity to the materialiation of the cytotoxic effect of MGL is of considerable interest. A statistical analysis of the grouped data on the dependence of MGL cytotoxicity on K_m for various substrates revealed no relationships between these parameters. However, a tendency has been noted towards a positive relationship between K_m with respect to *L*-methionine and IC_{50} ($r = 0.549$, $p = 0.100$), which indirectly supports the existence of a relationship between enzymatic reduction of the methionine level in the medium and cytotoxic activity.

The identified tendency towards an increase in IC_{50} with increasing K_m may allow one to cautiously assume the probability of an increase in MGL cytotoxicity with increasing affinity to *L*-methionine. This does not contradict the existing concept regarding the enzymes used in oncology as medicinal products, whose antitumor effect is associated with increased sensitivity of cancer cells to the lack of amino acids.

CONCLUSIONS

The determination of the kinetic parameters and cytotoxic activity of MGL from three bacterial sources demonstrated that the enzyme from *C. sporogenes* shows promise and requires further research. It is characterized by a minimal K_m value as compared to the other investigated enzymes and the highest cytotoxicity approaching that of MGL from *P. putida*.

The results obtained for the K562, MCF7, and PC-3 cell cultures allow one to consider further research into the *in vivo* antiproliferative activity of MGL and *in vitro* research into an extended panel of cell cultures as rather promising; there is a possibility of using the enzyme to design a novel antitumor agent. ●

This work was supported by the Russian Foundation for Basic Research (grant № 11-04-12104-ofi-m-2012) and the grant of the President of the Russian Federation for state support of the leading scientific schools (№ 2046.2012.4).

REFERENCES

1. Tanaka H., Esaki N., Soda K. // EnzymeMicrob. Technol. 1985. V. 7. P. 530–537.
2. El-Sayed A.S. // Appl. Microbiol. Biotechnol. 2010. V. 86. P. 445–467.
3. Nakayama T., Esaki N., Lee W.-J., Tanaka I., Tanaka H., Soda K. // Agric. Biol. Chem. 1984. V. 48. P. 2367–2369.
4. Kreis W., Hession C. // Cancer Res. 1973. V. 33. P. 1862–1865.
5. Yoshimura M., Nakano Y., Yamashita Y., Oho T., Saito T., Koga T. // Infection Immunity. 2000. V. 68. P. 6912–6916.
6. Tokoro M., Asai T., Kobayashi S., Takeuchi T., Nozaki T. // J. Biol. Chem. 2003. V. 278. P. 42717–42727.
7. Lockwood B., Coombs G. // Biochem. J. 1991. V. 279. P. 675–682.

8. Cellarier E., Durando X., Vasson M.P., Farges M.C., Demiden A., Maurizis J.C., Madelmont J.C., Chollet P. // Cancer Treat Rev. 2003. V. 29. P. 488–489.
9. Yoshioka T., Wada T., Uchida N., Maki H., Yoshida H., Ide N., Kasai H., Hojo K., Shono K., Maekawa R., et al. // Cancer Res. 1998. V. 58. P. 2583–2587.
10. Miki K., Xu M., An Z., Wang X., Yang M., Al-Refaie W., Sun X., Baranov E., Tan Y., Chishima T., et al. // Cancer Gene Ther. 2000. V. 7. P. 332–338.
11. Miki K., Al-Refaie W., Xu M., Jiang P., TanY., Bouvet M., Zhao M., Gupta A., Chishima T., Shimada H., et al. // Cancer Res. 2000. V. 60. P. 2696–2702.
12. Tan Y., Xu M., Hoffman R.M. // Anticancer Res. 2010.V. 30. P. 1041–1046.
13. El-Sayed A.S., Shouman S.A., Nassrat H.M. // Enzyme Microb. Technol. 2012. V. 51. P. 200–210.
14. Revtovich S.V., Morozova E.A., Anufrieva N.V., Kotlov M.I., Belyi Y.F., Demidkina T.V. // Dokl. Biochem. Biophys. 2012. V. 445. P. 187–193.
15. Studier F.W. // ProteinExpr. Purif. 2005. V. 41. P. 207–234.
16. Manukhov I.V., Mamaeva D.V., Morozova E.A., Rastorguev S.M., Faleev N.G., Demidkina T.V., Zavilgelsky G.B. // Biochemistry (Mosc). 2006. V. 71. P. 454–463.
17. Morozova E.A., Bazhulina N.P., Anufrieva N.V., Mamaeva D.V., Tkachev Y.V., Streltsov S.A., Timofeev V.P., Faleev N.G., Demidkina T.V. // Biochemistry (Mosc). 2010. V. 75. P. 1435–1445.
18. Laemmli U.K. // Nature. 1970. V. 227. P. 680–685.
19. Meyer T.S., Lamberts B.L. //Biochim. Biophys. Acta . 1965. V. 107. P. 144–145.
20. Towbin H., Staehelin T., Gordon J. //Proc.Natl.Acad.Sci. USA. 1979. V. 76. P. 4350–4354.
21. Mossman T. // J. Immunol. Methods. 1983. V. 65. P. 55–63.
22. Xu W., Zhang X., Qian H., Zhu W., Sun X., Hu J., Zhou H., Chen Y. // Exp.Biol.Med. 2004. V. 229. P. 623–631.
23. Tan Y., Xu M., Hoffman R.M. // Anticancer Res. 2010.V. 30. P. 1041–1046.
24. Kudou D., Misaki S., Yamashita M., Tamura T., Esaki N., Inagaki K. // Biosci. Biotechnol. Biochem. 2008. V. 72. P. 1722–1730.
25. Nakayama T., Esaki N., Sugie K., Berezov T.T., Tanaka H., Soda K. // Anal. Biochem. 1984. V. 138. P. 421–424.
26. Mamaeva D.V., Morozova E.A., Nikulin A.D., Revtovich S.V.,Nikonov S.V., Garber M.B., Demidkina T.V. // Acta Cryst. 2005. V. F61. P. 546–549.
27. Chant A., Kraemer-Pecore C.M., Watkin R., Kneale G.G. // Protein Expr. Purif. 2005. V. 39. P. 152–159.
28. Wu J., Filutowicz M. // Acta Biochem. Pol. 1999. V. 46. P. 591–599.
29. Esteban-Torres M., Alvarez Y., Acebrón I., de las Rivas B., Muñoz R., Kohring G.W., Roa A.M., Sobrino M., Mancheño J.M. // FEBS Lett. 2012. V. 586. P. 3127–3133.
30. Pokrovskaya M.V., Aleksandrova S.S., Pokrovsky V.S., Omeljanjuk N.M., Borisova A.A., Anisimova N.Yu., Sokolov N.N. // Protein Expr. Purif. 2012. V. 82. P. 150–154.
31. Sokolov N.N., Zanin V.A., Aleksandrova S.S. // Vopr. Med. Khim.(Aspects of medicinal chemistry). 2000. V. 46. P. 531–548.
32. Krasotkina Y.V, Gladilina Y.A., Borisova A.A., Gervaziev Y.V., Abakumova O.Y., Zanin V.A., Sokolov N.N. // Vopr. Biol. Med. Pharm. Chem. (Aspects of biological, medical and pharmaceutical chemistry). 2008. № 3. P. 18–21.

The Impact of ADH1B Alleles and Educational Status on Levels and Modes of Alcohol Consumption in Russian Male Individuals

S.A. Borinskaya[1,2*], A.A. Kim[1,3], A.V. Rubanovich[1], N.K. Yankovsky[1,3,4]

[1] Vavilov Institute of General Genetics, Russian Academy of Sciences, Gubkina Str. 3, Moscow, Russia, 119991

[2] Moscow State University of Medicine and Dentistry, Delegatskaya Str. 20, Bld. 1, Moscow, Russia, 127473

[3] Moscow Institute of Physics and Technology, Institutsky Lane 9, Dolgoprudny, Moscow oblast, Russia, 141700

[4] Faculty of Biology, Lomonosov Moscow State University, Leninskie Gory 1, Bld. 12, Moscow, Russia, 119234

*E-mail: borinskaya@vigg.ru

Received 05.03.2013

ABSTRACT **Alcohol abuse is one of the main reasons behind the low life span in Russia. Both social and genetic factors affect the alcohol consumption level. The genetic factors are alleles of the alcohol dehydrogenase *ADH1B* and aldehyde dehydrogenase *ALDH2* genes. We have typed and found frequencies for the alleles in a cohort of 642 men, ethnic Russians. The individuals of the cohort were asked to complete a questionnaire in the framework of the Izhevsk Family Study (Leon *et al.*, 2007, 2009) regarding the amount of alcohol consumed and on the type of hazardous alcohol consumption (nonbeverage alcohol consumption and the so-called "*zapoi*" which is a Russian term for a heavy drinking bout lasting for at least 2 days, when an individual is withdrawn from the normal social life). The ADH1B*48His allele was found among heterozygous individuals only (N=68, 10.6% of the cohort). The ALDH2*504Lys allele was also found among heterozygous individuals only (N=2, 0.3%) The effect of *ADH1B* alleles and the influence of the education level on the amount and type of alcohol consumed had not previously been studied in Russians. We have found that the amount of consumed alcohol is 21.6% lower (1733 g of ethanol per year) for *ADH1B*48His* allele carriers in the cohort of Russian men. The amount of consumed alcohol was found to be 9.8% lower (793 g of ethanol per year) in the case when individuals had a higher education as compared to those who had a secondary- or elementary school education level in the same cohort. Hence, the protective effect of the genetic factor (*ADH1B*48His* allele carriage) has proven to be more pronounced than the influence of the social factor (education level) at the individual level in the cohort of Russian men. Both factors have also proven to have a protective effect against hazardous types of alcohol consumption. *Zapoi* was not scored among individuals of the cohort with *ADH1B*48His* allele carriage (*OR*=12.6, P=0.006), as compared to 8.4% of "*zapoi*" individuals who did not carry the *ADH1B*48His* allele (genotype *Arg/Arg*).The percentage of individuals who consume non-beverage alcohol is lower (0.6%) in the subcohort of people with a higher education degree. This percentage is higher (6.0%, *OR*=10.0, P=0.004) in the subcohort of people without a higher education degree.**

KEYWORDS **alcohol consumption level; genetic polymorphisms; *ADH1B* gene; social factors.**

INTRODUCTION

Alcohol abuse is admittedly one of the main causes behind the low life span in Russia. It is responsible, either directly or indirectly, for up to 60% of the deaths occurring to non-elderly males in Russian populations [Nemtsov, 2001; Andreev *et al.*, 2008; Leon *et al.*, 2009; Zaridze *et al.*, 2009].

Exogenous ethanol is metabolized in humans predominantly by liver enzymes, alcohol dehydrogenase (ADH) and aldehyde dehydrogenase (ALDH), which are responsible for the sequential oxidation of up to 90% of consumed alcohol. Another alcohol oxidation route is driven by microsomal cytochrome P450 that converts about 9% of exogenous alcohol; peroxisomal catalase

also has a minor contribution of about 1% [Ostrovsky, Sadovnik, 1984; Halej, Berndt, 1987; Luzhnikov, 1994].

Seven ADH genes characterized by distinct tissue- and age-specific expression patterns have been identified in the human genome [Edenberg, 2000]. The first step of exogenous ethanol oxidation is accomplished predominantly by the *ADH1B*-encoded enzyme. A single nucleotide polymorphism in this gene corresponds to an *Arg48His* amino acid substitution that influences enzyme velocity, so that the histidine-containing isoform (corresponding to *ADH1B*48His*) is 100 times more active than the arginine-containing one (corresponding to *ADH1B*48Arg*) [Jornvall *et al.*, 1984; Matsuo *et al.*, 1989].

Acetaldehyde formed by ADH from ethanol is consequently oxidized to acetate by ALDH. Up to 95% of acetaldehyde is converted into acetate by mitochondrial ALDH encoded by *ALDH2* [Goedde *et al.*, 1987; Hsu *et al.*, 1988]. A single nucleotide polymorphism in this gene corresponds to a *Glu504Lys* substitution, which yields an inactive protein in homozygous individuals. Moreover, since ALDH functions as a homotetramer with one dysfunctional subunit inactivating the entire complex, heterozygous persons possess only about 6% of the ALDH activity characteristic of *504Glu* homozygous humans [Crabb *et al.*, 1989].

The observable toxic effect of consuming large amounts of exogenous alcohol is caused not by alcohol itself but by its primary metabolite, acetaldehyde [Halej, Berndt, 1987]. For *ALDH2*504Lys* carriers, considering his or her low acetaldehyde detoxication rate, a drinking bout may lead to high blood acetaldehyde levels. Hence, the toxic effects of alcohol consumption for these individuals are much more pronounced [Gelernter, 2009]. Therefore, heterozygous carriers of *ALDH2*504Lys* consume less alcohol and are at lower risk of alcohol dependence than those lacking this allele [Wall *et al.*, 2000; Kim *et al.*, 2008]. A similar protective effect, although less pronounced, was shown for the *ADH1B*48His* allele both in combination with *ALDH2*504Lys* for Japanese and Korean populations [Matsuo *et al.*, 2006; Kim *et al.*, 2008] and on its own for white Americans and Australians [Sherva *et al.*, 2009; Macgregor *et al.*, 2009]. For Russian populations, there is still no evidence that these alleles affect the levels of alcohol consumption.

The *ALDH2*504Lys* allele frequency in Asian populations varies from 40% in East Asia to less than 1–2% in Central Asia. The allele is virtually absent in European populations, and among all the examined Russians, only one individual was shown to be an heterozygous carrier of *ALDH2*504Lys* [Li *et al.*, 2009]. The *ADH1B*48His* allele frequency is also very high for East Asia (70%). In Europe it varies between less than 1% and 8–10%. In Russia, *ADH1B*48His* carriers were shown to constitute from 5% to 15%, which corresponds to an allele frequency of 2.5–8% [Borinskaya *et al.*, 2009].

In this study, we focused on specific alcohol consumption patterns characteristic of Russian males with *ALDH2*504Lys* and the *ADH1B*48His* alleles.

MATERIALS AND METHODS

Blood samples of 642 Russian males aged 22 to 59 collected during the 2008–2009 Izhevsk Family Study program [Leon *et al.*, 2007; Andreev *et al.*, 2008] were used as material for this study. The probes were supplemented with biochemical and immunological assay data. The corresponding questionnaire forms (including the fields' ethnicity, educational status, and alcohol consumption habits) were filled out by the individuals and their relatives under the supervision of competent personnel trained for the Izhevsk Family Study program [Leon *et al.*, 2007; Andreev *et al.*, 2008].

The participants were questioned on the amounts of consumed alcoholic beverages and how often they drank them. The individual annual volume of pure ethanol was inferred from data on the periodicity of intake, beverage volume, and alcohol content. The ethanol content of the beverages available in Izhevsk was taken as stated on labels. The alcohol content of the vodka sold in the city was measured independently using conventional laboratory techniques (see Table 1 for specific alcohol consumption characteristics).

Table 1. Alcohol consumption indices among Russian men in Izhevsk 2008-2009

Alcohol consumption	Number of individuals (%)
Total persons	642 (100%)
Abstainers (a year before the survey)	83 (12.9%)
- former consumers	80 (12.5%)
- lifelong abstainers	3 (0.5%)
Alcohol consumed weekly	322 (50.2%)
- including daily consumption	44 (8.9%)
Individuals had at least one *zapoï* episode during the past year	48 (7.5%)
Nonbeverage alcohol consumers*	30 (4.7%)

*Nonbeverage alcohol means an alcohol containing liquid not supposed to be used for drinking purpose (eau-de-Cologne, pharmaceutical alcohol containing tinctures, alcohol containing liquids used for technical needs, etc.).

Genomic DNA from the blood samples was purified with the QIAmp DNA Blood Mini Kit (QIAgen). The genotyping assays for *ADH1B*Arg48His* and *ALDH2*Glu504Lys* were based on the duplex four-primer PCR design [Tamakoshi *et al.*, 2003].

Descriptive statistics and a multiple regression analysis were performed using the STATISTICA 6.0 software. Intergroup variances were estimated by the non-parametric Mann-Whitney test. Odds ratio (*OR*) calculations and the Fisher's exact test for significance were performed using the WinPepi program [available at www.brixtonhealth.com/pepi4windows.html; Abramson, 2004].

The contribution of the genotype (*D*) and other factors (*I*) to alcohol consumption was calculated according to the formula:

$$D = \frac{(\bar{x}_0 - \bar{x}_1)}{\bar{x}_0}$$

$$I = \frac{\bar{x}_0 n_1 - \bar{x}_1 n_1}{\bar{x}_0 n_0 + \bar{x}_1 n_1} = \frac{(\bar{x}_0 - \bar{x}_1) n_1}{(\bar{x}_0 + \bar{x}_1 \frac{n_1}{n_0}) n_0} \approx \frac{(\bar{x}_0 - \bar{x}_1) n_1}{\bar{x}_0 n_0},$$

where D is the relative risk for Arg/Arg genotype carriers, $\bar{x}_i$ is the average level of alcohol consumptions for the i-genotype, n_i is the number of i-genotype carriers, and I is the input of the factor influencing the level of alcohol consumption in the group.

RESULTS AND DISCUSSION

The alcohol consumption indexes for the given sample are presented in Table 1. The average index of pure ethanol consumption is 6765±364 g per individual per year, excluding nonbeverage alcohol consumers. Surprisingly, it is approximately twice as low as the average pure ethanol consumption per individual in Russia [24]. The discrepancy can be explained by at least two factors: *i*) the share of heavy drinkers among young people in the group is rather low; *ii*) The amount of alcohol consumption depends on the type of registration in the questionnaire [25]. The amount of alcohol scored by the period type of registration (over a month) shows a twofold lower level of consumption as compared to the day-by-day type of registration for Russians [26].

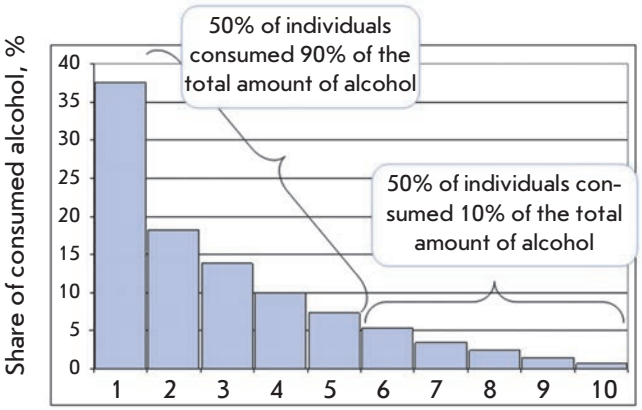

Fig. 1. Share of consumed alcohol in 10 subgroups (53 men in each group) ranked by the alcohol consumption level. Abstainers are excluded; nonbeverage alcohol consumers are excluded

According to the questionnaire-based estimates, one half of the total amount of alcohol drunk is attributed to 14% of the sample. The distribution of individual consumption values (related to the integral sample consumption) in subgroups ranging by consumption level from the maximal to the minimal is presented in Fig.1.

All individuals in the sample were genotyped for the *ADH1B*Arg48His* and *ALDH2*Glu504Lys* polymorphisms. Heterozygous *ADH1B*48His* carriers constituted 10.6% of the sample; no homozygous carriers were identified (Table 2). The distribution of genotype frequencies corresponded to the Hardy-Weinberg equilibrium distribution. The total *ADH1B*48His* allele frequency in the sample (5.2%) corresponded to the data obtained for the previously studied Russian samples [Borinskaya *et al.*, 2009].

Since only two individuals in the sample were identified as *ALDH2*504Lys* heterozygous carriers (0.16% allele frequency), the allele was eliminated from further analysis. The individuals who consumed nonbeverage alcohol were excluded from the analysis, since it was

Table 2. *ADH1B**Arg48His allele and genotype frequencies

Genotype frequencies (Number of individuals)			Allele frequencies (SD)		c2 (p-value)
Arg/Arg	Arg/His	His/His	G	A	
0.894 (574)	0.106 (68)	0	0.947±0.008	0.053±0.008	2.01 (0.157)

Table 3. *ADH1B*48His* carrier frequency and higher education level at different alcohol consumption levels

Alcohol consumption level and style	Total number of individuals	Mean alcohol consumption level (g of ethanol per person per year)	ADH1B*48His carrier frequency % (N)	High education level % (N)
Higher level of alcohol consumption	264	13517	8.7% (23)	22.3% (60)
Lower level of alcohol consumption	265	2162	14.0% (37)	33.6% (89)
Abstainers	83	0	8.4% (7)	9.6% (8)
Nonbeverage alcohol consumers	30	Not determined	3.3% (1)	3.3% (1)
Total:	642	--	10.6%	24.2% (158)
At least one *zapoï* episode during the past year	48	15984	0	18.8% (9)
No *zapoï* episodes during the past year	574	7278	11.8% (68)	24.4% (140)
Total	642			

Note. Number of individuals is given in parentheses.

impossible to estimate the amount of pure alcohol consumed in that case.

The *ADH1B*48His* allele association with the level of alcohol consumption was analyzed using two approaches: between-group comparison of the allele frequency (ranged by consumption values); comparison of consumption values for *ADH1B*48His* and *ADH1B*48Arg* genotyped individuals in the sample stratified by age.

For the first approach, the total sample was subdivided into 4 groups (Table 3). One group included all nonbeverage alcohol consumers (30 individuals); another group included people who reported consuming no alcohol for at least a year (83 individuals). The remaining alcohol consumers (529 individuals) were ranked by the alcohol consumption level and subdivided into two nearly equal subgroups (Table 3): one having a higher consumption level ("heavy drinkers," 264 individuals) and the other having a lower consumption level group ("moderate drinkers," 265 individuals).

The *ADH1B*48His* allele carriage frequency in the "moderate drinkers" subgroup was found to be 13.4% as compared to 8.7% in the "heavy drinkers" subgroup. The result does not contradict the hypothesis on the protective role of the *ADH1B*48His* allele against a high level of alcohol consumption; however, the result is not quite statistically valid (p=0.074, two-tail Fisher test).

Carriers of the *ADH1B*48His* allele in the "no alcohol consumption" group constituted 8.4%. As long as all but three individuals in this group indicated drinking in the past, a plausible cause of drinking cessation at least for part of this group could be related to health problems. This assumption is supported, in particular, by an increased occurrence of *Treponema pallidum* reactive antibodies in the blood samples of this group. The antibodies were detected in 4 of 83 individuals in the "no alcohol" group (4.8%) as compared to 3 of 264 "moderate drinkers" (1.1%) and 5 (1.9%) of 265 "heavy drinkers." A more detailed analysis of individual reasons for the cessation could be of interest.

Only one carrier of the *ADH1B*48His* allele was identified (3.3%) among the non-beverage alcohol consumers.

The groups also differed by the educational status of individuals (Table 3). Among the total sample, 158 individuals (24.6%) possessed a degree in higher education. The percentage of individuals with higher education was 33.6% and 22.3% for "moderate drinkers" and "heavy drinkers," respectively. This difference is statistically significant (OR=1.72, p=0.007 by two-tailed Fisher's test); i.e., a degree in higher education is less frequently accompanied by heavy drinking habits as compared to lack of a degree.

In the abstainer group, the percentage of individuals with a degree in higher education was 9.6% of the group, which was less than in both previous groups (Table 3). This difference is statistically significant (p<0.02). Taking into account the lower probability of heavy drinking for individuals with higher education, the smaller percentage of individuals having a degree in higher education in the "abstinent" group may be regarded as an indirect indication of excessive consump-

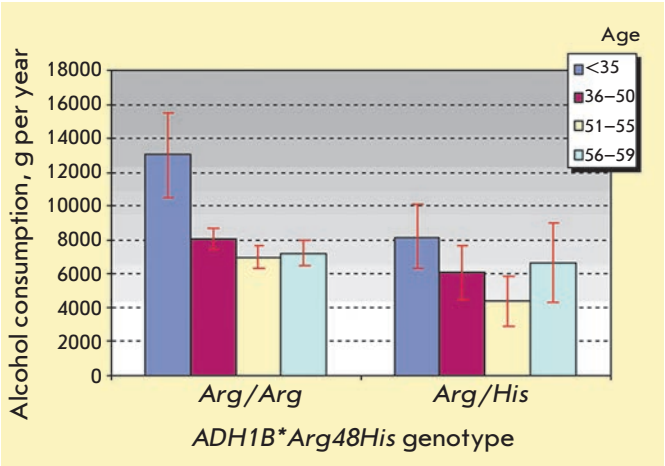

Fig. 2. Mean alcohol consumption level (g per person per year) in age groups for Arg/Arg and Arg/His genotype carriers

tion in the past as one of the reasons for cessation. This consideration is also supported by weaker representation of the *ADH1B*48His* allele carriers in this group (8.4%) that is virtually equal to their representation in the "heavy drinkers" group (8.2%).

In the nonbeverage alcohol consumer group, only one out of 30 individuals (3.3%) declared having a degree in higher education.

Alcohol consumption levels with relation to genotype were determined for the total sample and also separately for different age groups. The *ADH1B*48His* allele carriers consume 1,749 g of ethanol per year less (21.8%) than individuals lacking this allele (*ADH1B*48Arg/Arg* genotype). The differences in alcohol consumption levels were observed for all age groups; however, the statistical significance is compromised (Fig. 2) either due to the inconsistency of the effect or to the small sample size. Since a similar effect of reduced alcohol consumption levels was previously described for other populations on bigger samples (e.g., for Japanese [Matsuo *et al.*, 2006] and for Caucasian groups [Sherva *et al.*, 2009; Macgregor *et al.*, 2009]), it is reasonable to assume that the effect is genuine and statistical significance for Russian males can also be achieved by increasing sample size. The reduced alcohol consumption determined for Russian *ADH1B*48His* carriers in the current study is close to the published data for other populations; e.g., alcohol consumption was reduced by 18% for white American *ADH1B*48His* carriers [Sherva *et al.*, 2009]. For white Australians, the similar effect varied between 20 and 50% depending on the absolute individual alcohol consumption level (more pronounced for heavy drinkers) [Macgregor *et al.*, 2009]. A similar reduction in the amounts of consumed alcohol for Japanese *ADH1B*48His* carriers was found to depend on the *ALDH2*Glu504Lys* background. For the *504Glu/Glu* genotype (normal acetaldehyde detoxication), the presence of *ADH1B*48His* was found to reduce alcohol consumption by 7.1%. For the *504Glu/Lys* genotype (impeded acetaldehyde detoxication), this level was reduced by 48.1% [Matsuo *et al.*, 2006].

We found it interesting to compare the effect of the educational status of an individual with the "protective effect" of the *ADH1B*48His* allele. The analysis included data for the entire year prior to the survey. An analysis of the ratio of standardized regression Beta coefficients (Table 4) has revealed that alcohol consumption in *ADH1B*48His* allele carriers is 1.6-fold lower as compared to the previously described effects of higher education levels.

The average alcohol consumption (calculated as pure ethanol) was 813 g (10%) lower per year for men with a degree in higher education as compared to those without a degree. Individuals consuming nonbeverage alcohol were excluded from the analysis. Meanwhile, the carriers of the "protective allele" *ADH1B*48His* had on average consumed 1,749 g (21.8%) less ethanol per person per year (Table 5). The effects of these factors were similar at the population level. Alcohol consumption was 2.5% lower for the *ADH1B*48His* allele carriers and 2.8% lower for those with a degree in higher

Table. 4. Regression analysis of the association between the alcohol consumption level and the *ADH1B* genotype and education level

Linear regression coefficients	Beta*	SE	B	SE	p-value
Intercept			12864	1260	0.0000
ADH1B genotype (Arg/His vs. Arg/Arg)	-0.073	0.043	-2113	1255	0.0929
Education level (High vs. Low and Medium)	-0.047	0.043	-971	884	0.2722

Note. Abstainers are excluded; nonbeverage alcohol consumers are excluded.
*Regression coefficients for standardized data.

Table 5. Alcohol consumption level in relation to genotype and education level

Mean alcohol consumption (g per person per year)		Differences (*D*)	Contribution of a factor to lower alcohol consumption in the cohort (*I*)
*ADH1B**Arg48His genotype			
Arg/Arg (469 individuals)	Arg/His (60 individuals)	Arg/His vs. Arg/Arg	
8041	6292	21.8%	2.5%
Education level			
Low and Medium (380 individuals)	High (149 individuals)	High vs. Low+Medium	
8071	7259	10.1%	2.8%

Note. Abstainers are excluded; nonbeverage alcohol consumers are excluded.

education (Table 5). However, since the results were not statistically significant for the selected groups, we chose to compare our preliminary data with the results obtained for larger population groups.

The effects of genotype on the pattern of alcohol consumption were assessed by comparing the percentage of individuals with heavy drinking problems and individuals involved in the consumption of nonbeverage alcohol among carriers of the *ADH1B**48Arg and *ADH1B*48His* alleles (Fig. 3). No cases of *zapoï* have been detected and only one person was involved in the consumption of nonbeverage alcohol among the group

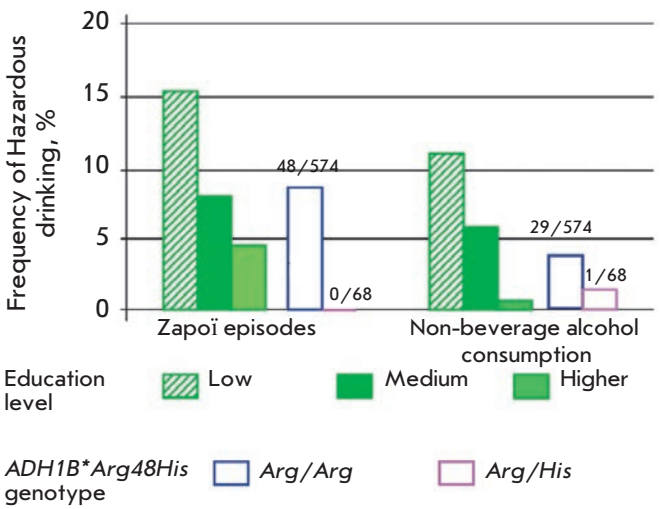

Fig.3. Hazardous drinking in groups with different genotypes and education levels

of 68 Russian males, *ADH1B*48His* allele carriers. On the contrary, these numbers were 8.1% (48 individuals, statistically significant difference, *OR*=12.6, P=0.006) and 5.1% (29 individuals, statistically non-significant), respectively, for the group of 574 *ADH1B**48Arg/Arg genotype carriers. Hence, in this population-based randomly selected sample of Russian men, the *ADH1B*48His* allele carriers appear to be protected against *zapoï*. Our data represent the first piece of evidence of the influence of the *ADH1B*48His* allele on heavy drinking and nonbeverage alcohol consumption behavior among Russian men. A bigger size cohort needs to be studied in order to assess the details of this observation.

The earlier research data involving a group of Russian men of different ethnic backgrounds has indicated that the percentage of individuals with a dangerous pattern of alcohol consumption is lower for individuals with a degree in higher education [2, 21, 27]. The frequency of *zapoï* for Russian men was 5.8% in the higher education subgroup as compared to 8.1% in the secondary and elementary education subgroups.

The higher the education level, the lower the frequency of *zapoï* in the subgroup (Table 6). The result is statistically valid. The conclusion was drawn from an analysis of bigger groups (combined group of 927 men consisting of individuals both with established and not established genotypes). The education level influences the nonbeverage alcohol consumption level as well. The percentage of nonbeverage alcohol consuming persons was higher in the subgroup of individuals without a high education degree (6.0%) as compared to 0.6% in the higher education subgroup (*OR*=10.0, P=0.004) (Fig. 3).

Table 6. Association of the incidence of *zapoï* during the previous year in drinkers and their education level

Did a person have any *zapoï* episodes during the previous year?	Education level (N, %)			Total
	Incomplete secondary	Secondary	Higher	
Yes	5 12.20	62 9.31	9 4.09	76 8.20
No	36 87.80	604 90.69	211 95.91	851 91.80
Total	41 100.00	666 100.00	220 100.00	927 100.00

Note. Pearson $\chi^2 = 6.8939$ Pr = 0.032.

The comparison of the "protective effects" of higher education and presence of the *ADH1B*48His* allele indicates that "genetic protection" is more effective at the individual level, whereas both factors are equally effective at the group level, (Tables 4 and 5).

It has been demonstrated that the *ADH1B*48His* allele is associated with a lower risk of incidence of *zapoï* in Russian males and with lower overall alcohol consumption on average by 1,749 g (2186 ml) of pure ethanol per person per year. This effect is 2–3 times lower than that of the "dry law" campaign practiced in the late 1980s, which had lowered alcohol consumption to 4–6 L per individual per year [28, 29]. The restriction of alcohol sales has an effect on the entire population. The established protective effect of the *ADH1B*48His* allele corresponds only to 10% of Russian males. However, the frequency and significance of this allele may be higher in other ethnic groups of the Russian Federation. Hence, research into the effects of the *ADH1B*48His* allele on alcohol consumption in different ethnic groups in Russia may be important. ●

The authors are grateful to Prof. D.A. Leon (London School of Hygiene and Tropical Medicine) for the materials and valuable contribution to the preparation of the manuscript. This work was partially supported by the Russian Foundation for Basic Research (12-06-00307 (S.A.B.)) and the Basic Research Program of the Presidium of RAS "Basic Sciences for Medicine" (N.K.Y.).

REFERENCES

1. Nemtsov A.V. Alcohol mortality in Russia, 1980–90. Moscow. 2001. 60 p.
2. Andreev E.M., Kiryanov N.A., Leon D.A., McKee M., Tomkins S., Shkolnikov V.M. // Narkologiya. 2008. № 7. P. 38–52.
3. Leon D.A., Shkolnikov V.M., McKee M. // Addiction. 2009. V. 104 (10). P. 1630–1636.
4. Zaridze D., Brennan P., Boreham J., Boroda A., Karpov R., Lazarev A., Konobeevskaya I., Igitov V., Terechova T., Boffetta P., et al. // Lancet. 2009. V. 373. № 9682. P. 2201–2214.
5. Ostrovsky Yu.M., Sadovnik M.N. Ethanol metabolism pathways and their role in alcohol dependance / Moscow. Results of Science and Technology, VINITI. Toxicology.1984. V. 13. P. 93–150.
6. Haley T.J., Berndt W.O. / Handbook of Toxicology. Washington. Hemisphere Publishing Corp. 1987. 365 p.
7. Luzhnikov E.A. / Clinical toxicology. Moscow, Medicine. 1994. 255 p.
8. Edenberg H.J. // Prog. Nucleic Acid Res. Mol. Biol. 2000. V. 64. P. 295–341.
9. Jornvall H., Hempel J., Vallee B.L.,Bosron W.F., Li T.K. // Proc. Nat. Acad. Sci. USA. 1984. V. 81. P. 3024–3028.
10. Matsuo K., Wakai K., Hirose K., Ito H., Saito T., Tajima K. // Cancer Epidemiol Biomarkers Prev. 2006. V. 15 (5). P. 1009–1013.
11. Goedde H.W., Agarwal D.P. // Alcohol Alcohol Suppl. 1987. V. 1. P. 47–54.
12. Hsu L.C., Bendel R.E., Yoshida A. // Genomics. 1988. V. 2. P. 57–65.
13. Crabb D.W., Edenberg H.J., Bosron W.F., Li T.K. // J. Clin. Invest. 1989. V. 83. P. 314–316.
14. Gelernter J., Kranzler H.R. Genetics of alcohol dependence // Hum. Genet. 2009. V. 126. P. 91–99.
15. Wall T.L., Horn S.M., Johnson M.L., Smith T.L., Carr L.G. // J. Stud. Alcohol. 2000. V. 61. P. 13–17.
16. Kim D.J., Choi I.G., Park B.L., Lee B.C., Ham B.J., Yoon S., Bae J.S., Cheong H.S., Shin H.D. // Hum. Mol. Genet. 2008. V. 17. P. 854–858.
17. Sherva R., Rice J.P., Neuman R.J., Rochberg N., Saccone N.L., Bierut L.J. // Alcohol Clin Exp Res. 2009. V. 33 (5) P. 848–857.
18. Macgregor S., Lind P.A., Bucholz K.K., Hansell N.K., Madden P.A., Richter M.M., Montgomery G.W., Martin N.G., Health A.C., Whitfield J.B. // Hum Mol Genet. 2009. V. 18. P. 580–593.
19. Li H., Borinskaya S., Yoshimura K., Kal'ina N., Marusin A., Stepanov V.A., Qin Z., Khaliq S., Lee M.Y., Yang Y., et al. // Ann Hum Genet. 2009. V. 73. P. 335–345.
20. Borinskaya S., Kal'ina N., Marusin A., Faskhutdinova G., Morozova I., Kutuev I., Koshechkin V., Khusnutdinova E.,

Stepanov V., Puzyrev V., et al.// Am J Hum Genet. 2009. V. 84 (1). P. 89–92.
21. Leon D.A., Saburova L., Tomkins S., Andreev E., Kiryanov N., McKee M. Shkolnikov V.M. // Lancet. 2007. V. 369(9578). P. 2001–2009.
22. Tamakoshi A., Hamajima N., Kawase H., Wakai K., Katsuda N., Saito T., Ito H., Hirose K., Takezaki T., Tajima K. // Alcohol Alcohol. 2003. V. 38 (5). P. 407–410.
23. Abramson J.H. //Epidemiol. Persp.Innov. 2004. V. 1. P. 6.
24. http://www.who.int/substance_abuse/publications/global_alcohol_report/profiles/rus.pdf.
25. Midanik L.T. //Br J Addict. 1988. V. 83. P. 1019–1030.
26. Nemtsov A. // Addiction. 2004. V. 99(3). P. 386–387.
27. Tomkins S., Saburova L., Kiryanov N., Andreev E., McKee M., Shkolnikov V., Leon D.A. // Addiction. 2007. V. 102. P. 544–553.
28. Averbakh L.K., Shamota A.Z. // Problemy Narkologii (Problems of Narcology). 1992. № 2, P. 32–37.
29. Nemtsov A.V. // Sotsialnaya i Klinicheskaya Psihiatriya (Social and clinical psychiatry). 1992. V. 2. № 4. P. 46–53.

Transfer of Silver Nanoparticles through the Placenta and Breast Milk during *in vivo* Experiments on Rats

E. A. Melnik[1], Yu. P. Buzulukov[2], V. F. Demin[2], V. A.Demin[2], I. V. Gmoshinski[1]*, N. V. Tyshko[1], V. A. Tutelyan[1]

[1] Federal State Budgetary Institution «Institute of Nutrition» of the Russian Academy of Medical Sciences, 2/14 Ust'inski proezd Moscow, 109240, Russian Federation

[2] National Research Center Kurchatov Institute, 123182, Kurchatov sq. 1, Moscow, Russian Federation

*E-mail: gmosh@ion.ru

Received 18 December 2012

ABSTRACT **Silver nanoparticles (NPs), widely used in the manufacture of various types of consumer products and for medical applications, belong to novel types of materials that pose potential risks to human health. The potential negative effects of the influence of these NPs on reproduction are insufficiently researched. A quantitative assessment of the transfer of metallic silver nanoparticles through the placenta and breast milk was carried out during an *in vivo* experiment. We used 34.9 ± 14.8 nm in size silver NPs that were stabilized by low-molecular-weight polyvinylpyrrolidone and labeled with the ^{110m}Ag radioactive isotope using thermal neutron irradiation in a nuclear reactor. [^{110m}Ag]-labeled NPs preparations were administered intragastrically via a gavage needle to pregnant (20th day of gestation) or lactating (14–16th day of lactation) female rats at a dose of 1.69–2.21 mg/kg of body weight upon conversion into silver. The accumulation of NPs in rat fetuses and infant rats consuming their mother's breast milk was evaluated using a low-background semiconductor gamma-ray spectrometer 24 and 48 hours following labeling, respectively. In all cases, we observed a penetration of the [^{110m}Ag]-labeled NPs through the placenta and ther entry into the mother's milk in amounts exceeding by 100-1,000 times the sensitivity of the utilized analytical method. The average level of accumulation of NPs in fetuses was 0.085–0.147% of the administered dose, which was comparable to the accumulation of the label in the liver, blood, and muscle carcass of adult animals and exceeded the penetration of NPs across the hematoencephalic barrier into the brain of females by a factor of 10-100. In lactating females, the total accumulation of [^{110m}Ag]-labeled NPs into the milk exceeded 1.94 ± 0.29% of the administered dose over a 48 h period of lactation; not less than 25% of this amount was absorbed into the gastrointestinal tract of infant rats. Thus, this was the first time experimental evidence of the transfer of NPs from mother to offspring through the placenta and breast milk was obtained.**

KEYWORDS **pregnancy, lactation, nanoparticles, radioactive tracer, silver, fetoplacental barrier.**

ABBREVIATIONS **FS – food supplement; GIT – gastrointestinal tract; MG – methodological guidelines; MDA – minimum detectable activity; NPs – nanoparticles; NMs – nanomaterials; PVP – polyvinylpyrrolidone; M – sample mean; m – standard error of the mean.**

INTRODUCTION

Advances in the development of nanotechnology and the increase in the volume of production and practical application of artificial nanoparticles (NPs) and nanomaterials (NMs) have led to the belief that in the near future NPs could become a significant source of environmental contamination. Among the most prominent NMs, special attention is focused on the silver NPs that are widely used in various types of consumer products (disinfecting agents, textiles, paint-and-lacquer materials, cosmetics, packaging materials, food supplements) [1, 2] and for a variety of biopharmaceutical applications, including their use as antimicrobial [3, 4], anti-inflammatory agents [5] and as *in vivo* molecular nanodiagnostic tools [6]. However, silver NPs should also be regarded as a particular source of risks because of their potential toxicity to humans [7-15]. This particularly applies to those risks that are associated with the influence of NMs on a child's organism as a result of their possible transfer across the placenta and through breast milk [16]. The possibility of a transfer of the NMs present in a mother's diet or used by her as part of cos-

metic products or household chemical products to her offspring cannot be excluded [17]. A quantitative evaluation of such a transfer of NPs is necessary in order to gauge the potential risks of exposure of offspring to the silver NPs in their mother's body and develop appropriate protective measures, including hygiene regulation of consumer products.

However, the very idea of a natural transfer of the NPs entering a mother's body to her offspring has yet to be sufficiently investigated. This is due to the specific methodological difficulties associated with detecting the presence of NPs in biological objects [18, 19]. An analysis of the methods used to detect NPs in biological samples, including electronic and atomic force microscopy, spectroscopic methods, chromatography, the use of fluorescent, spin, stable-isotope and other labels [18], has enabled to pinpoint the radioactive tracer technique as the optimal method. The latter is strictly quantitative, highly sensitive, and enables a simple and graphic interpretation of the results related to NPs which do not undergo biotransformation and biodegradation in the body – gold, platinum, and silver NPs [20].

The present work contains a quantitative assessment of the transport of silver NPs through the placenta and breast milk on a model of pregnant and lactating female rats using [^{110m}Ag]-labeled NPs preparations.

EXPERIMENTAL

Experiment design

The study was conducted on pregnant and lactating Wistar rats at the clinic of laboratory animals of the Federal State Budgetary Institution "Institute of Nutrition" of the Russian Academy of Medical Sciences. During the preconception period and throughout the pregnancy and lactation, the females received the standard semi-synthetic diet according to [21]. The gestation period of the females was 20 days following conception; lactation period – on average 10–11 days after the birth of offspring. Pregnant rats received [^{110m}Ag]-labeled silver NPs intragastrically through a gavage needle at a dose of 1.69 mg/kg of body weight (three females) and 2.21 mg/kg of body weight (four females) in the form of a dispersion in deionized water containing a non-toxic, non-absorbable in the gastro-intestinal tract (GIT) stabilizer of NPs – polyvinylpyrrolidone (PVP) with a molecular weight of 15-30 kDa. The rats were then placed into individual cages made of polystyrene. Twenty-four hours following the administration of the preparation, the rats were subjected to deep anesthesia using diethyl ether, their abdominal cavities were dissected, the rats were bled from the inferior vena cava, and the uterus with fetuses, the liver, and brain were collected. The fetuses were removed from the uterus and thoroughly washed to get rid of the amniotic fluid. Thereafter, the fetuses, liver, and brain of the females were placed into vials made of high-purity polyethylene for gamma spectrometry. Precaution measures to avoid contamination of the organs and fetuses of the rats with NPs in other internal organs and blood were observed during sampling.

In the experiment on lactating rats, five female species nursing 9 infant rats each were administered a solution of [^{110m}Ag]-labeled silver NPs intragastrically at a dose of 2.11 mg/kg of body weight. The rats were then returned to their individual cages made of polystyrene, where their offspring were located. According to the conditions of the experiment, the possibility of consumption of female excrements (coprophagy) by infant rats was excluded. Forty eight hours after labeling, infant rats nursed by the females were subjected to a lethal dose of diethyl ether by inhalation. They were then thoroughly washed to remove any traces of female excrements from the fur; the skin with subcutaneous fat tissue was removed, and carcasses were placed into vials for gamma spectrometry. The carcasses of the four infant rats were dissected; the gastrointestinal tract, liver, kidneys, spleen, and the remaining carcass were removed. The preparations obtained were placed separately into vials for gamma spectrometry.

Obtaining [^{110m}Ag]- labeled nanoparticles

A preparation of colloidal silver "Argovit" produced by the Scientific and Production Company "Vector-Vita," Co., Ltd. (Russia) was used for the experiments. The preparation is an aqueous dispersion of NPs of metallic silver containing 1.0–1.4% of silver and 18.6–19.0% of PVP by weight. According to electron microscopy data (*Fig. 1*), the average diameter of the NPs was 34.9 ± 14.8 nm; the minimum size was 8.4 nm, and maximum size was 80.9 nm; the particle's shape was close to spherical. The preparation was diluted with deionized water at a ratio of 1:11 or 1:47 and sealed in high-purity quartz vials which were then subjected to thermal neutron irradiation ($0.005 < En < 0.4$ eV) in the vertical experimental canal VEC-9 of the nuclear reactor IR-8. After removal from the reactor, the vials were kept for 48 hours to reduce the background gamma activity of the short-lived silicon isotope in the vial material, followed by their opening. The contents were pooled, sonicated (5 min, 44 kHz, 40 W) to eliminate secondary aggregation of NPs, and adjusted to a fixed volume using deionized water. A total of 0.04 ml of the dispersion of [^{110m}Ag]-labeled NPs was collected, transferred into vials for gamma spectrometry, and adjusted using deionized water to a volume approximately corresponding to the volume of the biological sample (fetus or carcass of the infant rat) immediately prior to the administration

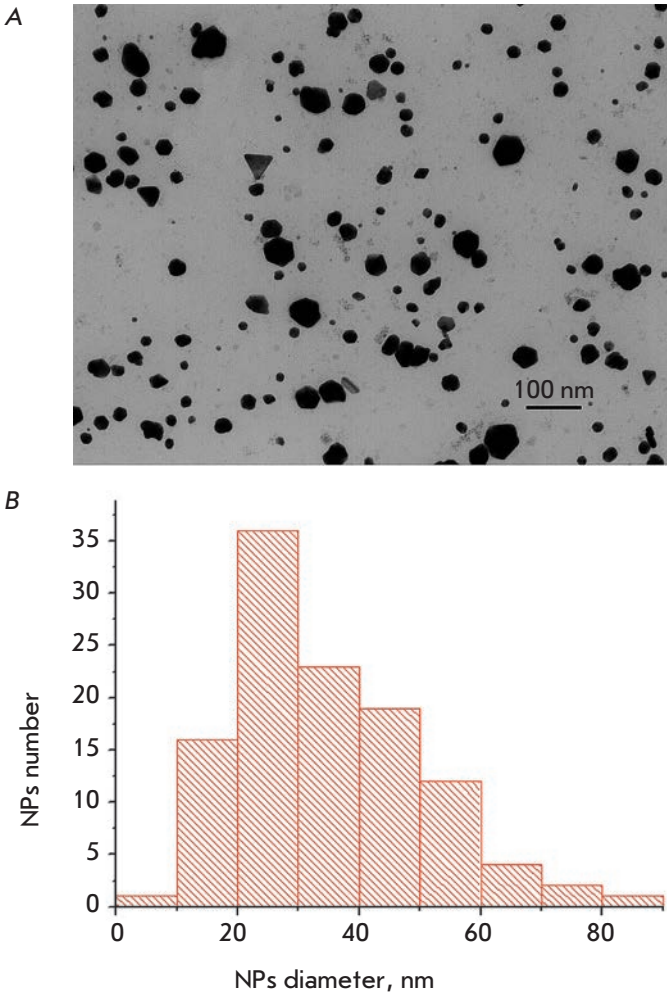

Fig.1. Transmission electronic microscopy of silver NPs preparation Argovit®. NPs image (A) and diameter distribution (B). Electron microscope JEM-100CX ("Jeol", Japan), accelerating voltage 80 kV. Data obtained by prov., D.Sc. Dzantiev B.B., RAS Institute of biochemistry, Moscow

to rats, which accounted for 1% of the amount administered to the rats. The resulting sample was used as a reference in determining the biological activity of the samples.

Analysis of samples

The activity of the biological samples was measured on a gamma-spectrometer manufactured by Canberra company (U.S.) containing a germanium semiconductor detector GC4018, DSA-1000 analyzer, Genie-2000 – Genie S501, and Genie S502 software. The magnitude of the activity expressed in impulses per second in one of the selected energy ranges of the ^{110m}Ag isotope [22] was converted into relative quantities of the radioisotopic label (μ) in % of the injected dose according to the equation:

$$\mu = \frac{A_п}{A_э} \times \left(1/K\right),$$

where A_p is the bioprobe activity, A_r is the activity of the reference sample containing 0.04 cm^3 of the dispersion of the [^{110m}Ag]-labeled NPs, and K is the conversion factor representing the ratio between the individual amount of the dispersion of NPs (cm^3/kg body weight) administered to the females and the average dose obtained by dividing the total volume of the administered dispersion by the total body weight of all female rats in the group.

The concentration of silver NPs in the analyzed samples expressed in ng/g of the sample was calculated with allowance for the individual amount of NMs administered to the female according to the following equation:

$$C = \mu \times D \times \left(F \,/\, s\right) \times 1,$$

where μ is the relative amount of the radioactive label, % of the amount administered to the female rat, D is the administered dose in mg/kg of body weight, F is the female rat body mass in kg, s is the mass of the biological sample in g, and 10^6 is the coefficient of transition from mg to ng.

Application of the relative gamma-spectrometric measurements technique for determining the mass of ^{110m}Ag in the biological samples enabled to exclude the absolute activity (expressed in Bq) from the calculations and use primary raw data of measurements (impulses/sec), thus, eliminating a number of errors that had occured during the transition from the primary raw data to absolute activity. In this situation, the basic error of measurements is determined by the background values in the selected energy range. For this reason, the concept of minimum detectable activity (MDA) in the form of a limit of quantitative determination, L_q, was utilized for assessing the minimum significant level of the ^{110m}Ag counting rate in the samples [23, 24].

Metrological characteristics of the method

For determining the metrological characteristics we utilized the concept of MDA in the form of the limit of quantitative determination, L_q, calculated according to the relation:

$$L_q = 5.66 \times \sqrt{R_b / T},$$

where R_b is the background counting rate equal to 2.64×10^{-3} impulses/sec in the applied gamma-spectrometric devices, T is the average measurement time of

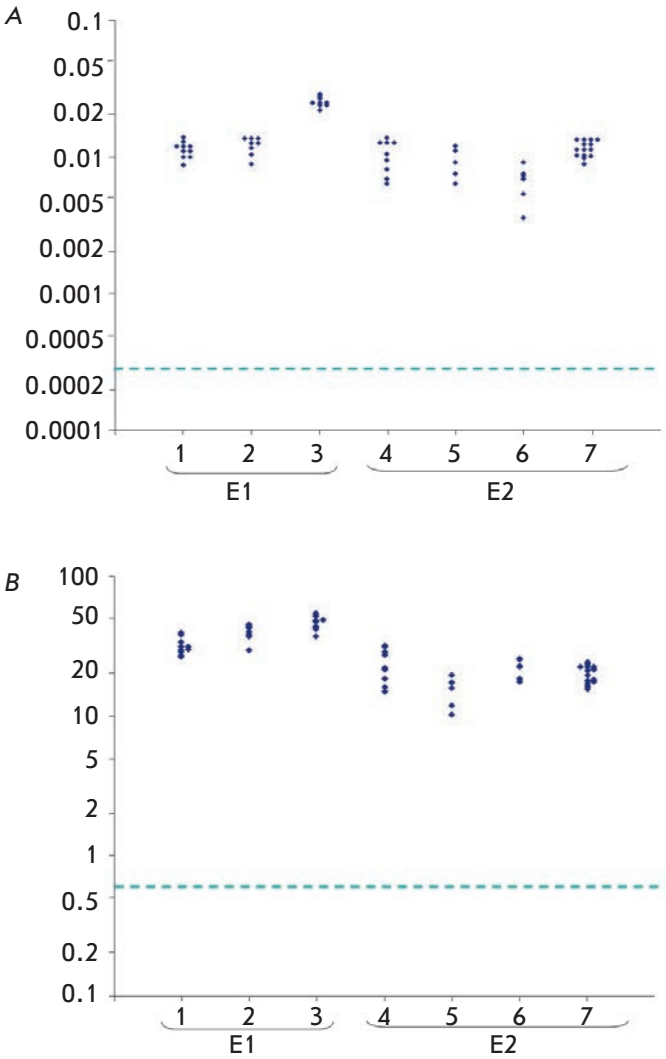

Fig.2. Individual values of total content (A) and concentration (B) of [^{110m}Ag]-NPs in fetuses of rats. Axis of abscises – № of female, № of experiment. Ordinate axis – NPs content, % of dose ingested (A) or concentration, ng/g tissue (B). Dotted line marks the threshold of quantitative determination of [^{110m}Ag]-NPs in samples

the sample equal to 3600 sec, and 5.66 is the coefficient with allowance for the confidence interval of evaluation of $p = 0.95$ and relative statistical uncertainty ± 50%. Accordingly, L_q was equal to 4.8×10^{-3} impulses/sec [23, 24]. With regard to the preparation used, [^{110m}Ag]-NPs corresponds to the minimum limit of quantitative determination of 2.6 ng of silver NPs.

RESULTS

Figure 2 shows the content and the concentration of Ag NPs in rat fetuses 24 hours after intragastric administration of [^{110m}Ag]-labeled NPs to pregnant females, and *Table 1* shows the mean ($M \pm m$) values per each pregnant female rat and for the experiment in general with respect to two utilized doses of NMs. As can be seen from these results, silver NPs were identified in the fetuses of all pregnant females in amounts significantly exceeding the detection limit. The findings are indicative of penetration of silver NPs through the intestinal wall and placenta with subsequent accumulation in the fetuses.

Comparison with data on the absorption and interorgan distribution of [^{110m}Ag]-labeled NPs administered intragastrically to male rats at a comparable dose (0.81 mg of Ag/kg of body weight) [20] shows (*Table 2*) that penetration of Ag NPs through the placenta exceeds the accumulation in the brain by more than 10 times, corresponds to the level in the blood and spleen, and is significantly lower than the accumulation in the liver. The silver NPs content in the liver and brain of pregnant female rats determined in the present experiment (*Table 2*) did not differ significantly from the values obtained previously for adult males [20] under comparable conditions ($P > 0.05$; *t*-Student test).

As can be seen from the data presented in *Fig. 3* and *Table 3*, [^{110m}Ag]-labeled NPs administered intraperitoneally to lactating females were detected in the bodies of all 45 infant rats in the litters of five lactating rats. The concentrations of these NPs significantly (100-100-fold) exceeded the limit of quantitative determination.

According to the experimental conditions, such amounts of [^{110m}Ag]-labeled NPs cannot be explained by ingestion of female feces containing significant amounts of NPs by the offspring, contamination of the cutaneous covering removed prior to carrying out the gamma-ray spectrometry, and ingestion of the mat contaminated with female rat urine, as the total excretion of silver NPs with urine as follows from the data [20] did not exceed 0.032% of the administered dose of the preparation over 2 days, which was 60 times less than the total amount of NPs detected in infant rats.

As can be seen from *Table 4*, the maximum amount of ^{110m}Ag was detected in the gastro-intestinal tract of infant rats; however, significant (well above the limit of quantitative determination) levels of nanoparticles were detected in the internal organs and in the carcasses of the infant rats, which in turn indicates a high level of absorption of NPs in their GIT.

As follows from *Table 3*, the total amount of [^{110m}Ag]-labeled NPs excreted with milk and detected in infant rats was comparable (or exceeded) to the one-time total content of the label in all organs and the carcass of the animal following intragastric administration of the preparation (provided in *Table 2* according to [20]). Therefore, there are grounds to believe that the excre-

tion of Ag NPs with milk during lactation is one of the major ways of excreting these nanoparticles from the body, which is second only to fecal excretion and is far superior to urinary excretion with respect to quantity.

DISCUSSION

Thus, the concentration of NPs in organs and tissues of the offspring is equal to approximately 0.020–0.040 and 0.030–0.070 μg/g of tissue, respectively, upon administration of Ag NPs at doses of approximately 2 mg/kg of body weight to pregnant and lactating female rats. The doses of silver NPs administered to female rats were relatively high upon conversion to average human body weight (70 kg) and were approximately 140 mg. The possibility of exposure of a human to such quantities of NMs at the same time may occur upon consumption of contaminated drinking water, food products, or abuse of Ag-containing FS. The data obtained confirm directly the feasibility of transfer of silver NPs entering the gastrointestinal tract of the mother to her offspring during pregnancy and lactation. The likelihood of such transport of NPs of various types has repeatedly been postulated as a potential source of risks to the development of a fetus and newborn [16, 17], although direct experimental evidence for the occurrence of the process is scarce. It was demonstrated [25] that 14 nm in size silver NPs are absorbed in the gastrointestinal tract of adult rats in limited amounts in the course of multiple intragastric administrations over a period of 28 days and are distributed between organs and tissues, including kidneys and the liver. Data on the penetration of silver NPs through the fetoplacental barrier and mammary gland are unavailable; however, results confirming the transfer of similar, with respect to physical and chemical properties, 12-14 nm in size metal nanoparticles made of gold [26] following their intravenous administration to pregnant female mice have been obtained. Penetration of CdSe quantum dots through the fetoplacental barrier after parenteral administration to female mice was described in [27]; the ability of 50-100 nm in diameter fluorescent polystyrene NPs to penetrate the fetoplacental barrier modeled by a monolayer of human choriocarcinoma cells was demonstrated in [28]. Our data demonstrate that with respect to silver NPs the process is carried out *in vivo* under conditions of natural route of entry of NPs into a mother's body.

The question arises as to how significant are the concentrations of NPs detected in rat fetuses and infant rats and whether they can pose a hazard to the development and health of the offspring. A relatively substantial amount of data has been accumulated on the biological effects of silver NPs given different ways of *in vivo* administration. Thus, colloidal silver was administered to mice intraperitoneally at extremely high doses approaching 1000 mg/kg [12]. Under these deliberately non-physiological conditions, NPs managed to penetrate the hematoencephalic barrier, causing the development of signs of oxidative stress in various regions of the brain. The genotoxic effects of silver NPs administered intraperitoneally at a dose of approximately 1 mg/kg of body weight to mice were demonstrated in [13]. Interpretation of the results of this work was rendered difficult by the presence of toxic surfactants in the NPs preparation – dioctyl sodium sulfosuccinate. The presence of inhalation toxicity by silver

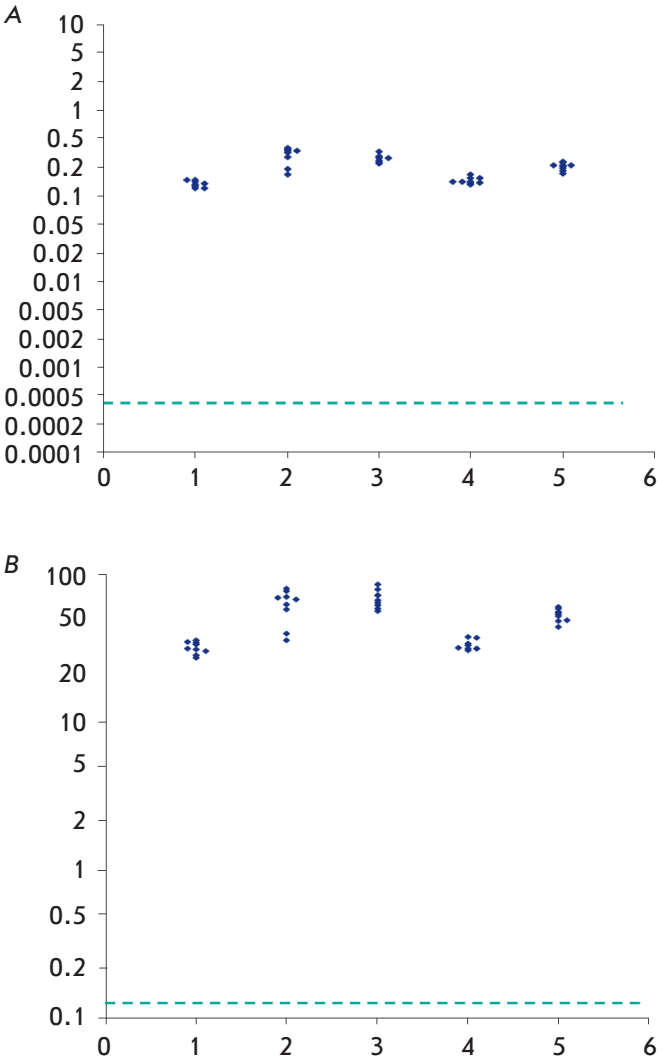

Fig.3. Individual values of total content (A) and concentration (B) of [^{110m}Ag]-NPs in suckling pups of rats. Axis of abscises –№№ of nursing dams, № of experiment. Ordinate axis – NPs content, % of dose ingested (A) or concentration, ng/g tissue (B). Dotted line marks the threshold of quantitative determination of [^{110m}Ag]-NPs in samples

Table 1. Results of silver [^{110m}Ag]-NPs determination in fetuses from pregnant rats after 24 hours of intragastric administration of labeled preparation

№ experiment	Dose mg per kg body mass of female	№№ females	Number of fetuses	Mean, M±m		
				Total NPs content in single fetus, % of ingested dose	NPs concentration in fetus, ng/g of tissue	Mass of fetus, g
1	1.69	1	10	0.0114±0.0005	31.7±1.4	2.66±0.04
		2	8	0.0122±0.0006	40.0±1.8	2.13±0.08
		3	9	0.0254±0.0007	46.7±1.8	4.07±0.08
		Mean of 1-st experiment (N=27)		0.0163±0,013	39.1±1.5	2.97±0.16
		Test of homogenity for rats №№ 1-3 ANOVA, P		<0.001	<0.001	<0.001
2	2.21	4	9	0.0104±0.0009	23.7±2.2	3.91±0.08
		5	5	0.0093±0.0011	15.1±1.8	5.72±0.10
		6	6	0.0067±0.0008	22.2±1.4	3.07±0.23
		7	14	0.0116±0.0004	20.1±0.8	5.26±0.10
		Mean of 2-nd experiment (N=34)		0.0101±0.0005	20.7±.08	4.58±0.18
		Test of homogeneity for rats №№ 4-7 ANOVA, P		<0.001	0.008	<0.001

Table 2. Comparison of mean NPs accumulation in fetuses and in internals of pregnant rats 24 hours after intragastric administration of [^{110m}Ag]-NPs

Experiment №	Dose of ([^{110}mAg]-NPs), mg/kg body mass	Number of rats	Organ/tissue	Content, % of dose ingested
Male rats, experiment from 2011 [11]	0.81	4	Carcass	0.36±0.17
			Liver	0.60±0.18
			Blood	0.126±0.051
			Spleen	0.054±0.020
			Testes	0.016±0.003
			Kidneys	0.014±0.002
			Lungs	0.0094±0.0026
			Brain	0.0029±0.0010
			Pancrestic	0.0079±0.0015
			Heart	0.0042±0.0016
Pregnant females, present study	1.69	3	Fetuses in total	0.147±0.041
			Liver	0.559±0.229
			Brain	0.0035±0.0004
	2.21	4	Fetuses in total	0.085±0.028
		4	Liver	0.324±0.046
		4	Brain	0.0035±0.0006

NPs in rats was established [14, 15]. Oral administration of this nanomaterial at a dose approaching 30 mg/kg of body weight to rats over 28 days resulted in no signs of systemic toxicity or genotoxic effects in the rats, although silver NPs accumulated in the kidneys and liver of the animals [29]. Significantly higher doses of silver nanoparticles (approaching 1000 mg/kg of body weight) administered orally resulted in the emergence of specific biochemical and histopathological changes indicative of toxicity [8, 29].

The toxic properties of silver NPs rendered important the assessment of the likelihood of toxicity in the offspring of animals subjected to exposure to this substance as a result of transplacental transfer or transfer through milk. The data on the *in vitro* cytotoxicity of silver NPs obtained under conditions when the concentration of NPs is precisely determined is without doubt of interest. Thus, it was demonstrated that silver NPs at a concentration of 5–50 μg/cm^3 damage cultured BRL3A rat hepatocytes [30]. The cytotoxic effects of silver NPs identifiable by the release of lactate dehydrogenase in a mitochondrial tetrazolium test were demonstrated at concentrations exceeding 5 μg/cm^3 in experiments on rat spermatogonial cells [31]. Stimulation of apoptosis in mouse fibroblasts was also observed (using caspase-3 activity assay) at a concentration of silver NPs exceeding 3.12 μg/cm^3 [32]. Silver NPs at a concentration exceeding 10 μg/cm^3 impaired the conductivity for Na^+ ions in cultured CA-1 hippocampal neurons [33]. Experiments on mononuclear cells of human peripheral blood [34] demonstrated that silver NPs at a concentration equal to or exceeding 3 μg/cm^3 stimulate the production of the tumor necrosis factor-α. A pronounced cytotoxic effect of silver NPs was observed at concentrations exceeding 15 μg/cm^3. According to [35], silver NPs coated with PVP or citrate are capable of influencing the differentiation of PC12 pheochromocytoma cells of neuroendocrine origin. The minimum effective concentration of NPs was 3 μM by silver (approximately 0.3 μg/cm^3). Finally, the effects of different in size silver NPs in the primary culture of rat cortical neurons were characterized in [36]. A statistically significant increase in the death of cells cultured for 14 days in the presence of 20 nm in size NPs at a minimum concentration equal to or exceeding 5 μg/cm^3 was demonstrated. The toxicity of NPs decreased with a decrease in size. Thus, 40 nm in diameter NPs were only cytotoxic at a concentration exceeding 10 μg/cm^3.

A comparison of the data provided above with the results of our work enables to suggest that the concentration of silver NPs in rat fetuses (not exceeding 50 ng/g of tissue at an administered dose of NPs of approximately 2 mg/kg of body weight, *Table 1*) were 60–300 times lower than the minimum effective concentrations of NPs detected in *in vitro* systems. However, this estimate does not take into account the possibility of a non-uniform distribution of NPs between the organs and tissues of the fetus. It is known that silver NPs accumulate mainly in the liver and kidneys [20, 25]. If we assume that all nanomaterials accumulate in one of these organs, whose mass at this gestational age is 6.0 and 0.9% of the fetal weight, then we obtain an excessive concentration of NPs in the organs – 830 and 5000 ng/g in the liver and kidneys, respectively. The

Table 3. Results of silver [^{110m}Ag]-NPs determination in suckling pups 48 hours after intragastric administration to nursing dams.

№ experiment	Dose mg per kg body mass of female	№№ females	Number of pups	Mean, M±m		
				Amount of [^{110m}Ag]-NPs in one suckling pup, % of ingested dose	Concentration [^{110m}Ag]-NPs in pups ng/g body weight	Mass of pups, g
1	2.11	1	9	0.136±0.004	31.9±1.0	28.9±0.4
		2	9	0.302±0.022	62.5±5.2	29.2±0.4
		3	9	0.272±0.009	68.5±3.2	28.2±0.8
		4	9	0.150±0.004	33.3±0.9	31.4±0.7
		5	9	0.220±0.007	52.9±1.7	28.5±0.2
		Mean of experiment (N=45)		0.216±0.011	49.8±2.6	29.3±0.3
		Test of homogenity for rats №№ 1-5, ANOVA, P		<0.001	<0.001	0.002
		Total content in offspring, % of ingested dose		1.94±0.29		

Table 4. Tissue distribution of [^{110m}Ag]-NPs in suckling pups (N=4) 48 hours after intragastric administration to nursing dams

№№	Organ/ tissue	Mean content of [^{110m}Ag]-NPs , % of amount, detected in the pup, M±m	Mean content of [^{110m}Ag]-NPs , % dose ingested by nursing dams, M±m
1	GIT	73.8±4.4	0.106±0.006
2	Carcass	7.4±1.4	0.0125±0.0011
3	Liver	17.9±3.0	0.0287±0.0033
4	Kidney	0.90±0.18	0.0014±0.0003

latter value is comparable to an *in vitro* determined lower limit of a possible cytotoxic effect equal approximately to 3000–5000 ng/g. It should be noted that the dose of nanomaterials administered to the pregnant female rats of approximately 2 mg/kg of body weight was aggravated by a factor of 2,000 in comparison with the upper tolerable level of silver intake in any form (colloidal particles and ions), which is equal to 70 μg or approximately 1 μg/kg of human body weight. It can, therefore, be concluded that the level of accumulation of silver NPs in the organs of rat fetuses subject to certain conditions can be regarded as safe in the event of intake of silver nanoparticles in physiological amounts (e.g., together with drinking water or food supplements).

The average level of labeled NPs in infant rats receiving milk feeding was 50 ng/g. Seventy-five percent of this value is attributed to the label detected in the gastrointestinal tract. The content of NPs in the liver amounts to 17.9%, and in the kidneys it amounts to 0.9% of the total amount detected in an infant rat. The mass of organs at this age of development is equal to 3.8 and 1.2% of body weight on average, which implies that the concentration of NPs in these organs is approximately 235 and 38 ng/g, respectively. These values are well below the hypothesized level at which cytotoxic effects can be observed and are indicative of the safety of the intake of NPs by lactating females at the above mentioned, deliberately aggravated dose to the development of the offspring.

Therefore, on the basis of the published data it may be concluded that the levels of NPs in the tissues of infant rats and fetuses detected after a single-dose administration of NPs to female rats can be regarded as safe. At the same time, the following must be given due consideration: firstly, the possible accumulation of NPs in the body upon multiple intakes; hence, the level of NPs in the organs and tissues will be higher than upon a single instance of intragastric exposure, and, secondly, partial matching of the conditions during *in vitro* experiments and *in vivo*. In particular, the duration of the exposure to NPs in cell cultures amounts to hours, rarely – 7–14 days, while *in vivo* their effects may last for a lifetime. Therefore, the study of reproductive toxicity must be recommended during a comprehensive assessment of the safety of novel types of NPs and NMs. The transfer of NPs through the placenta and breast milk should be considered during the development of procedures aimed at maximizing the prevention of exposure of a woman's body to NPs and NMs during pregnancy and lactation.

CONCLUSIONS

1. It was established that [^{110m}Ag]-NPs penetrate the placenta and reach breast milk in quantities exceeding the sensitivity of the analytical method used by a factor ranging from 100 to 1,000 upon administration of ^{110m}Ag-labeled silver NPs into the gastrointestinal tract of pregnant and lactating female rats at a dose of approximately 2 mg/kg of body weight.

2. The average level of accumulation of NPs in fetuses was 0.085–0.147% of the administered dose, which was comparable to the accumulation in the liver of female rats (0.3–0.5% of the administered dose) and exceeded the penetration of NPs through the hematoencephalic barrier into the brain of female rats by at least 10-100 times ($3.5.\times 10^{-3}$%).

3. In lactating females the total inflow of [^{110m}Ag]-NPs into the milk was no less than 1.94 ± 0.29% of the administered dose over a 48-hour period of lactation; no less than 25% of the amount was absorbed in the digestive tract of infant rats.

4. Maximum levels of silver NPs were detected in the kidneys of fetuses upon their administration to female rats at a dose multiplied 2,000 times in comparison with an adequate level of intake of this microelement, where they were not significantly higher than the toxic concentrations established during *in vitro* experiments; in other cases, the levels of NPs were significantly lower than the effective concentrations. However, considering the possible effects of an accumulation of NPs in the organs and tissues of offspring upon their prolonged

intake by the mother, it is recommended to conduct an investigation into the reproductive toxicity of NPs in the course of a comprehensive assessment of their safety.

Therefore, for the first time experimental evidence of the transfer of silver NPs from a mother to her offspring through the placenta and breast milk has been obtained. ●

The authors are grateful to S.A. Khotimchenko for a useful discussion of the results of this work.

REFERENCES

1. Vernikov V.M., Gmoshinski I.V., Khotimchenko S.A. Voprosy pitanija (Problems of nutrition). 2009. V. 78. № 6. P. 13–20.
2. Blaser S.A., Scheringer M., Macleod M., Hungerbühler K. // Sci. Total Environ. 2008. V. 390. № 2–3. P. 396–409.
3. Fayaz M.A., Ao Z., Girilal M., Chen L., Xiao X., Kalaichelvan P.T., Yao X. //. Int. J. Nanomedicine. 2012. V. 7. P. 5007–5018.
4. Acosta-Torres L.S., Mendieta I., Nuñez-Anita R.E., Cajero-Juárez M., Castaño V.M. // Int. J. Nanomedicine. 2012. V. 7. P. 4777–4786.
5. Bhol K.C., Schechter P.J. // Dig. Dis. Sci. 2007. V. 52. №. 10. P. 2732–2742.
6. Chrastina A., Schnitzer J.E. //Int. J. Nanomedicine. 2010. V. 5. P. 653–659.
7. Shumakova A.A., Smirnova V.V., Tananova O.N., Trushina E.N., Kravchenko L.V.,Aksenov I.V., Selifanov A.V.,Soto G.S.,Kuznetsova G.G., Bulachov A.V., Safenkova I.V., Gmoshinski I.V., Khotimchenko S.A. // Voprosy pitanija (Problems of nutrition). 2011. V.80. № 6. P. 9–18.
8. Kim Y.S., Song M.Y., Park J.D., Song K.S., Ryu H.R., Chung Y.H., Chang H.K., Lee J.H., Oh K.H., Kelman B.J., Hwang I.K., Yu I.J. Subchronic oral toxicity of silver nanoparticles. // Part Fibre Toxicol. 2010. V. 7, № 1. 20 P.
9. Wijnhoven S.W.P., Peijnenburg W.J.G.M., Herberts C.A., Hagens W.I., Oomen A.G., Heugens E.H.W., Roszek B., Bisschops J., Gosens I., Van De Meent D., Dekkers S., De Jong W.H., Van Zijverden M., Sips A.J.A.M., Geertsma R.E. // Nanotoxicology. 2009. V. 3. № 2. P. 109–138.
10. Onischenko G.G., Archakov A.I., Bessonov V.V., Bokit'ko B.G., Gintsburg A.L., Gmoshinski I.V.,Grigor'ev A.I., Izmerov N.F., Kirpichnikov M.P., Naroditsky B.S., Pokrovsky V.I., Potapov A.I., Rakhmanin Yu.A., Tutelyan V.A., Khotimchenko S.A. // Gigiena i Sanitaria (Hygiene and Sanitation). 2007. № 6. P. 3–10.
11. Onischenko G.G., Tutelyan V.A. // Voprosy pitanija (Problems of nutrition). 2007. V. 76. № 6. P. 4–8.
12. Rahman M.F., Wang J., Patterson T.A., et al. Expression of genes related to oxidative stress in the mouse brain after exposure to silver-25 nanoparticles // Toxicol. Lett. 2009. V. 187, № 1. P. 15–21.
13. Ordzhonikidze C.G., Ramaiyya L.K. , Egorova E.M. , Rubanovich A.V. Genotoxic Effects of Silver Nanoparticles on Mice in Vivo // Acta naturae. 2009. V. 1. № 3. P. 99–101.
14. Sung J.H., Ji J.H., Yoon J.U., et al. Lung function changes in Sprague-Dawley rats after prolonged inhalation exposure to silver nanoparticles // Inhal. Toxicol. 2008. V. 20, №. 6. P. 567–574.
15. Ji J.H., Jung J.H., Kim S.S., et al.Twenty-eight-day inhalation toxicity study of silver nanoparticles in Sprague-Dawley rats // Inhal. Toxicol. 2007. V. 19. №. 10. P. 857–871.
16. Oberdörster G., Maynard A., Donaldson K., Castranova V., Fitzpatrick J., Ausman K., Carter J., Karn B., Kreyling W., Lai D., Olin S., Monteiro-Riviere N., Warheit D., Yang H. // Part. and Fibre Toxicol. 2005. V. 2. №. 1. P. 8–43.
17. Yokel R.A., MacPhail R.C. // J. Occupational Med. Toxicol. 2011. V. 6. № 7. P. 1–27.
18. Raspopov R.V., Gmoshinski I.V., Popov K.I., Krasnoyarova O.V., Khotimchenko S.A. // Voprosy pitanija (Problems of nutrition). 2012. V. 81. № 2. P. 10–17.
19. Tiede K., Boxall A.B., Tear S.P., Lewis J., David H., Hassellov M. // Food Add.Contam. 2008. V. 25. № 7. P. 795–821.
20. Buzulukov Yu.P., Gmoshinski I.V., Raspopov R.V., Demin V.F., Soloviev V.YU., Kuzmin P.G., Shafeev G.A., Khotimchenko S.A. // Medicinskaia Radiologiia i Radiatsionnaia Bezopasnost (Medical Radiol Radiat Safety). 2012. V. 57. № 3. P. 5–12.
21. Tyshko N.V., Zhminchenko V.M., Pashorina V.A., Selyaskin K.E., Melnik E.A., Mustafina O.K., Soto S.G., Trushina E.N., Gapparov M.M.G. // Voprosy pitanija (Problems of nutrition). 2011. V. 80. № 5. P. 30–38.
22. IAEA Database on www.iaea.org/Our Work/Nuclear Data Service.
23. Isaev A.G., Babenko V.V., Kazimirov A.S., Grishin S.I., Ievlev S.M. // Problems of nuclear power stations and Chernobyl safety. Kiev. 2010. V 13. P.103–110.
24. Lochamy J.C. The Minimum Detectable Activity Concept. EG&G ORTEC Systems Application Studies, PSD № 17. September 1981.
25. Loeschner K., Hadrup N., Qvortrup K., Larse A., Gao X., Vogel U., Mortensen A., Lam H.R. Larsen E.H. // Part. Fibre Toxicol. 2011. V. 8. P. 1–18.
26. Yang H., Sun C., Fan Z., Tian X., Yan L., Du L., Liu Y., Chen C., Liang X., Anderson G.J., Keela J.A., Zha Y., Nie G. // Sci.Reports. 2012. V 2. № 11. P. 847–855.
27. Chu M., Wu Q., Yang H., Yuan R., Hou S., Yang Y., Zou Y., Xu S., Xu K., Ji A., Sheng L. // Small. 2010. V. 6. № 5. P. 670–678.
28. Cartwright L., Poulsen M.S., Nielsen H.M., Pojana G., Knudsen L.E., Saunders M., Rytting E. // Int. J. Nanomedicine. 2012. V. 7. P. 497–510.
29. Kim Y.S., Kim J.S., Cho H.S., Rha D.S., Kim J.M., Park J.D., Choi B.S., Lim R, Chang H.K., Chung Y.H., Kwon I.H., Jeong J., Han B.S., Yu I.J. // Inhal. Toxicol. 2008. V. 20. №. 6. P. 575–583.
30. Hussain S.M., Hess K.L., Gearhart J.M., Geiss K.T., Schlager J.J. // Toxicol. in Vitro. 2005. V. 19. № 7. P. 975–983.
31. Braydich-Stolle L., Hussain S., Schlager J.J., Hofmann M.C. // Toxicol. Sci. 2005. V. 88. № 2. P. 412–419. №. 7. P. 975–983.
32. Arora S., Jain J., Rajwade J.M., Paknikar K.M. // Toxicol. Appl. Pharmacol. 2009. V. 236. № 3. P.310–318.
33. Liu Z., Ren G., Zhang T., Yang Z. // Toxicology. 2009. V. 264. № 3. P. 179–184.
34. Shin S.H., Ye M.K., Kim H.S, Kang H.S. // Int.Immunopharmacol. 2007. V. 7. № 13. P. 1813–1818.
35. Powers C.M., Badireddy A.R., Ryde I.T., Seidler F.J., Slotkin T.A. // Environ. Health Perspect. 2011. V. 119. № 1. P. 37–44.
36. Haase A., Rott S., Mantion A., Graf P., Plendl J., Thünemann A.F., Meier W.P,. Taubert A., Luch A., Reiser G. // Toxicol. Sci. 2012. V. 126. № 2. P. 457–468.

Metagenomic Analysis of the Dynamic Changes in the Gut Microbiome of the Participants of the MARS-500 Experiment, Simulating Long Term Space Flight

A.V. Mardanov[1], M.M. Babykin[2], A.V. Beletsky[1], A.I. Grigoriev[3], V.V. Zinchenko[2], V.V. Kadnikov[1], M.P. Kirpichnikov[2], A.M. Mazur[1,2], A.V. Nedoluzhko[1], N.D. Novikova[3], E.B. Prokhortchouk[1,2], N.V. Ravin[1,2], K.G. Skryabin[1,2], S.V. Shestakov[2]*

[1]Centre "Bioengineering", Russian Academy of Sciences, prosp. 60-let Oktyabria, 7/1, Moscow, Russia, 117312.

[2]Biological Faculty, Lomonosov Moscow State University, Leninskie gory, 1/12, Moscow, Russia, 119991

[3]Russian Federation State Research Center Institute of Biomedical Problems RAS (IBMP)

*E-mail: shestakovgen@mail.ru

Received 26.12.2012

ABSTRACT **A metagenomic analysis of the dynamic changes of the composition of the intestinal microbiome of five participants of the MARS-500 experiment was performed. DNA samples were isolated from the feces of the participants taken just before the experiment, upon 14, 30, 210, 363 and 510 days of isolation in the experimental module, and two weeks upon completion of the experiment. The taxonomic composition of the microbiome was analyzed by pyrosequencing of 16S rRNA gene fragments. Both the taxonomic and functional gene content of the microbiome of one participant were analyzed by whole metagenome sequencing using the SOLiD technique. Each participant had a specific microbiome that could be assigned to one of three recognized enterotypes. Two participants had enterotype I microbiomes characterized by the prevalence of *Bacteroides*, while the microbiomes of two others, assigned to type II, were dominated by *Prevotella*. One participant had a microbiome of mixed type. It was found that (1) changes in the taxonimic composition of the microbiomes occurred in the course of the experiment, but the enterotypes remained the same; (2) significant changes in the compositions of the microbiomes occurred just 14-30 days after the beginning of the experiment, presumably indicating the influence of stress factors in the first stage of the experiment; (3) a tendency toward a reversion of the microbiomes to their initial composition was observed two weeks after the end of the experiment, but complete recovery was not achieved. The metagenomic analysis of the microbiome of one of the participants showed that in spite of variations in the taxonomic compositions of microbiomes, the "functional" genetic composition was much more stable for most of the functional gene categories. Probably in the course of the experiment the taxonomic composition of the gut microbiome was adaptively changed to reflect the individual response to the experimental conditions. A new, balanced taxonomic composition of the microbiome was formed to ensure a stable gene content of the community as a whole without negative consequences for the health of the participants.**

KEYWORDS **metagenomics, intestinal microbiota, stressful influences, enterotypes.**

INTRODUCTION

Metagenomic studies of the human microbiome conducted within the framework of large-scale international research programs [1–3] are aimed at shedding light on the role microorganisms play in human life, developing diagnostic techniques, and preventing and treating various diseases. The taxonomic and genetic composition of the microbiota inhabiting the intestines is one of the criteria used to assess human health [4–6]. The intestinal ecosystem is dominated by five phyla of bacteria accounting for over 95% of the entire microbiota; however, the proportion of taxa at the genus and species level is specific to each person [2, 7, 8]. The latter is attributed to the genetic characteristics of every individual, the dominant type of nutrition, and the specifics of the interactions between microbes in a holistic

ecosystem. Meanwhile, every "healthy" individual is characterized by their own balanced and constant metagenomic composition [8–10], which can vary significantly in the presence of various diseases [5, 7, 11, 12] or due to the impact of medicinal products [7, 13, 14]. The interrelation between the condition of the resident microbiota and the type of nutrition [15–17], psychophysiological, and neurohumoral factors [18–20] has been identified. Stressful physical and emotional overloads affect the composition of the microbiota. Deviations from the usual lifestyle (e.g. long trips) can lead to an imbalance in the ratio of various taxa in the microbiota [11], and they are often accompanied by painful symptoms (diarrhea, constipation, etc.). The conditions inherent in space flights may impose both physical and psychological stresses on astronauts [21, 22], influencing the functioning of their intestinal microbiota [23–25].

The "MARS-500" experiment was conducted at the Institute of Biomedical Problems of the Russian Academy of Sciences. It involved the simulation of some of the conditions of a long interplanetary flight. The participants were put into an isolated module for 510 days in order to investigate the possible influence of the conditions of "space flight" on their physiological and psychological states. The composition of the intestinal microbiota of five subjects was assessed during one of the biomedical tests (in the course of the "MARS-500" experiment their feces were periodically sampled). DNA preparations isolated from feces were used for sequencing, with subsequent determination of the taxonomic and genetic composition of the microbiota.

The study established that a prolonged stay in an isolated module leads to changes in the composition of the microbiota. The dynamics of the changes were specific to each participant. Adaptive restructuring of the intestinal ecosystem apparently occurred, reflecting the individual response of each participant to the influence of experimental conditions (psycho-emotional stress, change in type of nutrition, use of probiotics, etc.). These conditions had no significant negative impact on the health of the participants, as evidenced by the results of medical and biological monitoring of each of the participants' condition [26, 27].

EXPERIMENTAL

Collection of samples for the metagenomic analysis

Citizens of four countries (Russia, Italy, France, China) aged 28 to 38 selected for inclusion in the crew subject to approval on the basis of the results of medical and psychological testing participated in the "MARS-500" experiment. In the course of the experiment, their feces were sampled at point zero (immediately prior to entering the isolation module), then after 14, 30, 210, 363, 510 days of stay in the module and 2 weeks after exiting the module (524 days). The samples of feces were stored at −80°C; DNA preparations were isolated using the QIAamp DNA stool Mini Kit (Qiagen, Germany), commonly used for the analysis of microbiota in feces. The quality of the DNA preparations was evaluated by agarose gel electrophoresis. It should be noted that the method used for DNA isolation can lead to an underestimation of the proportion of Actinobacteria and overestimation of the proportion of Bacteroidetes [28]; however, the comparative metagenomic analysis at different stages of the experiment is substantiated, as an identical approach was applied to all samples.

Amplification and pyrosequencing of fragments of 16S ribosomal RNA genes

In order to perform the PCR amplification of the fragment of the 16S rRNA gene comprising the variable V3–V5 regions barcoded "universal," the primers PRK341F (5'-CCTACGGGRBGCASCAG) and PRK806R (5'-GGACTACYVGGGTATCTAAT) were used. PCR was performed in a volume of 50 μl containing 2.5 units of GoTaq-DNA polymerase (Promega), 0.2 mM $MgCl_2$, 0.1 μM of each of the deoxyribonucleoside triphosphates, and 1 μM of each primer and 0.1 μg of the metagenomic DNA. The reaction was carried out using the Eppendorf Mastercycler amplifier (Eppendorf, Germany) according to the following schedule: initial denaturation for 2 min at 96°C, followed by 30 cycles (96°C – 40 s, 58°C – 40 s, 72°C – 1 min), then followed by final elongation for 10 min at 72°C. PCR fragments were purified by agarose gel electrophoresis. The samples were prepared for pyrosequencing according to the standard methodology (excluding the step of DNA fragmentation) using the GS Rapid Library Prep Kit. The GS Titanium LV emPCR Kit (Lib-L) v2 was used for emulsion PCR; pyrosequencing on the GS FLX (Roche) was performed according to the Titanium protocol using the GS Titanium Sequencing Kit XLR70. Reads exceeding 350 nucleotides in length were selected for further analysis. Thus, 549,668 independent sequences of fragments of the 16S rRNA gene were obtained. They were aligned and filtered using the Mothur software package [29] (version 1.23.1). Chimeric sequences were removed using Chimera.uchime [30], which is part of the Mothur package. Reads that did not pass the filtration process amounted to up to 10% of the total number in different samples. Taxonomic classification of the reads that passed the filtration process was performed using the Wang *et al.* method [31] implemented in the RDP Classifier program. Analysis of the results of the re-sequencing of the four DNA preparations obtained from participants № 1 and № 5 at different stages of the experiment demonstrated that the differ-

ences between the parallel samples (with respect to the ratio of fractions of the major taxa) did not account for more than 3% of the total microbial community. This demonstrates the methodological appropriateness of the results shown in the diagrams.

Sequencing of metagenomes using SOLiD technology

Libraries of fragments of metagenomic DNA samples were prepared according to the standard methodology using the SOLiD Fragment Library Construction Kit. The sizes of the libraries were measured using the Agilent BioAnalyzer DNA1000 kit. The length of the fragments varied from 183 to 254 bp. Emulsion PCR was performed according to the standard protocols recommended by Applied Biosystems Company using the EZ Bead System. Determination of DNA nucleotide sequences was carried out using 50 bp reads on the SOLiD 4.0 sequencing machine (Applied Biosystems). The volume of sequencing after the filtration with respect to the quality of a reading ranged from 1.8 to 3.4 billion bp per sample. After filtration the reads were collected and assembled into contigs using a parallel version of Abyss 1.2.5 [32]. The search for genes in the contigs and their functional and taxonomic classification were performed on the MG-RAST server (http://metagenomics.anl.gov/) for automatic annotation and analysis of the metagenomic data. This program predicts genes in the contigs on the basis of FragGeneScan [33] and then conducts a search for their homologues [34] in its own M5NR database using BLAT, which integrates multiple databases – GenBank, KEGG, COG, The SEED [35], and UniProt [36]. During the taxonomic classification each gene was assigned to a family of the closest homologue from the GenBank. Genes containing matches in the KEGG database were assigned several KEGG categories corresponding to different levels of the hierarchy.

The MG-RAST functional and taxonomic classification does not consider a multiplicity of gene readings, and the analysis results were corrected with allowance for the coverage. The nucleotide coverage of the predicted genes was determined by mapping the individual reads onto the assembled contigs using the Bowtie program [37].

RESULTS AND DISCUSSION

Taxonomic composition of the intestinal microbiome on the basis of the results of pyrosequencing of fragments of the 16S rRNA genes

Metagenomics methods using 16S rRNA as a marker revealed more than 40 genera of bacteria in the intestinal microbiota of the participants in the "MARS-500" experiment, the majority belonging to the four phyla: Bacteroidetes, Firmicutes, Proteobacteria and Actinobacteria, which is in agreement with data regarding the composition of the intestinal microbiota in healthy adults [38, 39]. Representatives of certain other phyla, including Fusobacteria, Verrucomicrobia and Synergistia, were also identified. Methanogenic archaea (*Methanobrevibacter* genus) were detected in two participants.

A comparative taxonomic analysis of the microbiota in fecal samples obtained from five participants at point zero of the experiment (prior to entering the isolated module) revealed significant individual differences between the participants with respect to the composition of the microbiota. The results obtained (*Table 1*) allowed to determine the belonging of the microbiota to specific enterotypes according to the classification proposed in 2011 [40, 41]. Specific clusters of microbes with the predominance of a particular taxon are designated as enterotypes. These clusters control the food chains in the microbial community and the interaction of the latter with the host characterized by individual genotypic characteristics.

Participants № 1 and № 3 were characterized by enterotype II dominated by *Prevotella,* combined with Firmicutes *Faecalibacterium*, *Coprococcus*, *Blautia*. Minor groups of *Akkermansia* (Verrucomicrobia) and β-proteobacteria were detected in the intestinal microbiota of participant № 3, while participant № 1 was characterized by a high proportion of γ-Proteobacteria.

The microbiota of participants № 2 and № 5 belongs to enterotype I with the predominance of *Bacteroides* in a cluster with *Parabacteroides*, *Faecalibacterium* and certain groups of Ruminococcaceae and Lachnospiraceae. *Fusobacteria* was also detected in these participants. One of the features of the composition of the microbiota of participant № 5 is a relatively high content of β-Proteobacteria, as well as the prevalence of the *Phascolarctobacterium* genus amongst Negativicutes, while the *Dialister* genus is predominant in participant № 2.

A different picture of the taxonomic composition of the microbial community was found in participant № 4. At point zero of the experiment no pronounced predominance of phylogroups determining enterotypes I and II was identified. A high proportion of Ruminococcaceae (including unclassified phylotypes), Lachnospiraceae, as well as Paraprevotella, was found instead. Amongst Negativicutes the genus *Dialister* was predominant as in participant № 2. The microbiota of participant № 4 was characterized by the presence of archaea *Methanobrevibacter*. Thus, the intestinal microbial community of this participant was different and could belong to a mixed type close to enterotype III [41]. Such a mixed composition could be viewed from the

Table 1. Enterotypes of the microbiota of the participants at point zero of the experiment

Taxonomic affiliation	Participant, №				
	1	2	3	4	5
Firmicutes					
Lachnospiraceae	8.63	12.33	7.59	19.11	15.07
Negativicutes	2.33	4.88	10.35	2.75	7.18
Ruminococcaceae	3.06	19.99	13.66	20.41	5.45
Others	0.6	2.98	3.47	5.60	1.31
Bacteroidetes					
Prevotellaceae	75.25	< 0.01	35.78	9.63	0.03
Rikenellaceae	0.56	1.62	2.77	1.82	1.72
Porphyromonadaceae	0.58	1.23	2.87	5.34	1.31
Bacteroidaceae	2.57	53.36	17.16	28.92	63.82
Others	0.96	0.26	4.62	5.60	0.83
Minor groups					
Proteobacteria	5.09	0.72	1.14	0.15	2.50
Actinobacteria	0.08	0.07	0.02	< 0.01	0.04
Fusobacteriaceae	< 0.01	2.06	< 0.01	< 0.01	0.37
Verrucomicrobia	< 0.01	< 0.01	0.31	0.07	< 0.01
Other microorganisms	0.28	0.5	0.27	0.61	0.36
Number of reads prior to filtration	5450	4883	6253	4929	7882
Number of reads after filtration	5321	4567	5886	4610	7545
Enterotype	II	I	II	III	I

Note. Proportion (%) of the determined 16S rRNA sequences assigned to the respective taxonomic groups.

perspective of the notions regarding the gradient of microbiome composition as opposed to the concept of discrete enterotypes [42, 43].

The results of the metagenomic studies demonstrated that prolonged stay in the isolated module exerted influence on the taxonomic composition of the microbiota of each of the participants (*Fig. 1*). The dynamics of these changes had an individual character reflecting the differences in the initial composition of the microbial communities and the different reactions of the participants to the influence of the conditions/factors of the experiment. As can be seen from *Fig. 1A–D*, a single unidirectional trend in the changes in microbiota composition was absent in the participants from the beginning to the completion of the experiment. The variability of the changes appears to be associated with differences in the conditions at different stages of the experiment. This applies to the administration of the probiotic *Enterococcus faecium* (in the form of tablets during the first 180 days) and Eubikor and Vitaflor during the last months, change in diet, the performance of special types of tasks by certain members of the crew associated with the exit from the main module to the simulated surface of Mars (after 210 days but before sampling after 363 day). All participants received identical probiotics and prebiotics during a single period. Participants № 2, № 3, and № 5 exited the module to the simulated surface of Mars wearing spacesuits.

The individual nature of the response of each participant is reflected in the data regarding the dynamics of the changes in the microbiota at the genus and species level and such indicators as the ratios of the major phyla, Firmicutes (F), and Bacteroidetes (B). With respect to microbiota, the ratio F/B changed significantly in participants № 1, № 2, and № 3 and in participants № 4 and № 5 it remained relatively stable throughout the entire experiment (*Fig. 1A*). The F/B ratio of participant № 1 significantly increased only to the 210th day

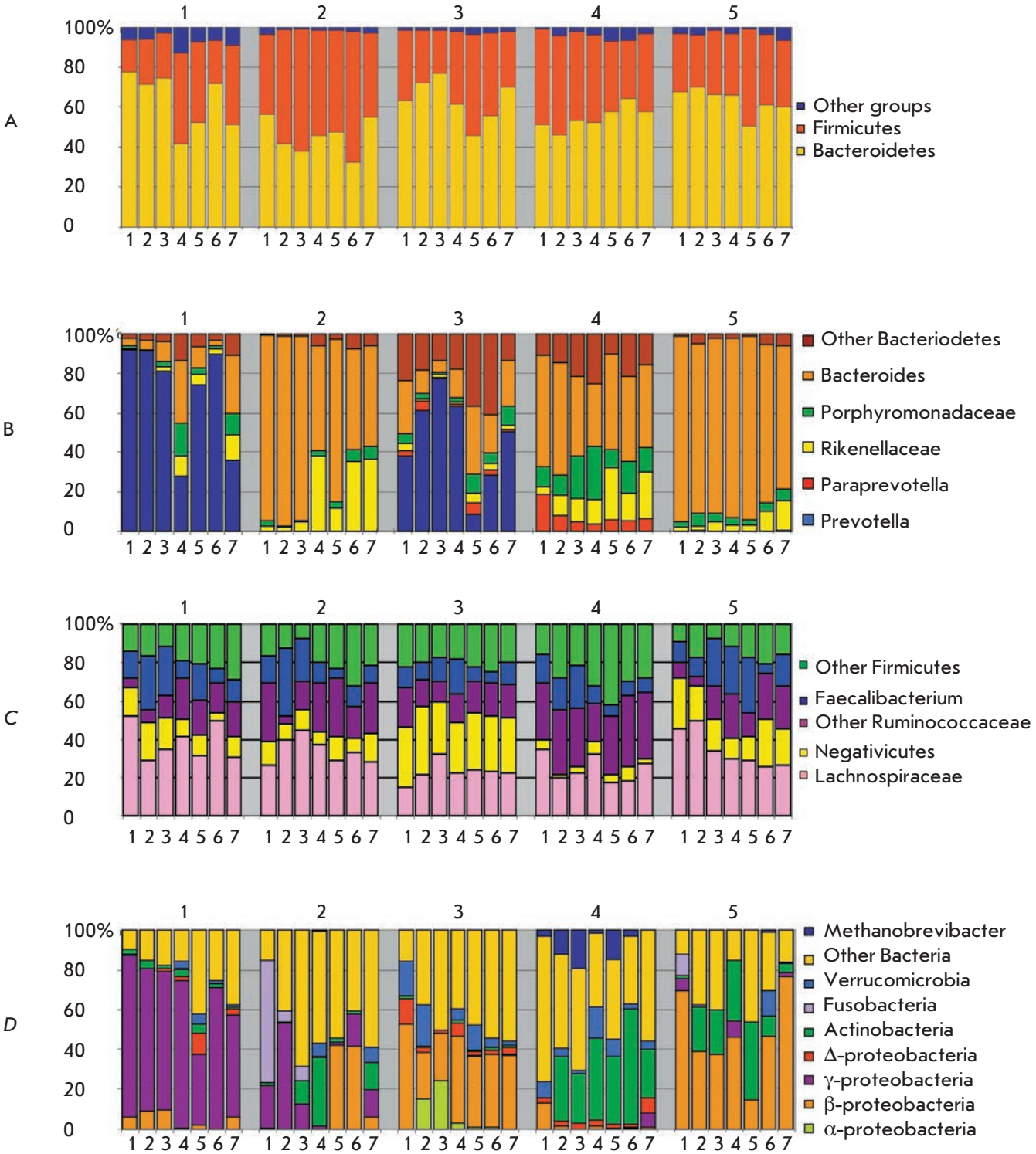

Fig. 1. Dynamic changes in the gut microbiome of participants of the MARS-500 experiment. (A) – main groups of microorganisms, (B) – microorganisms of phylum Bacteroidetes, (C) – microorganisms of the phylum Firmicutes, (D) – minor groups. Fraction of sequences assigned to a particular taxonomic group is shown in vertical axis (%), horizontal axis shows the sample codes (1 – 0 days, 2 – 14 days, 3 – 30 days, 4 – 210 days, 5 – 363 days, 6 – 510 days, and 7 – 524 days). Identification numbers of participants are shown above

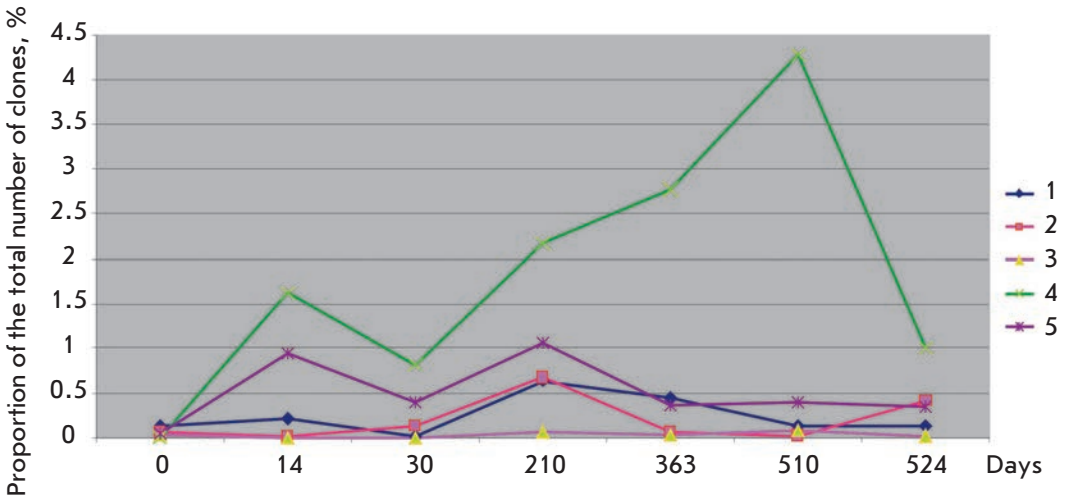

Fig. 2. Dynamic changes in the relative abundances of *Actinobacteria* in the gut microbiome of participants of the MARS-500 experiment

of stay in the module, while an increase in this index was observed after 2 weeks in participant № 2. However, after 210 days it began to decline. On the contrary during the first month the F/B ratio decreased in participant № 3 and then increased once again. Several studies have shown that abrupt changes in the ratio of Firmicutes/Bacteroidetes occur in the presence of certain gastrointestinal [13, 44] and other diseases [45, 46]. However, symptoms of such diseases were not observed in any of the participants of the "MARS-500" experiment during their stay in the module.

Throughout the entire experiment, there were no changes in the basic enterotype, although the fractional content of individual taxa was significantly altered in the microbiota. The proportion of unidentified bacteria, representatives of Firmicutes (*Fig. 1C*), and Proteobacteria (*Fig. 1D*) increased in participant № 1 from the 210th day, while high levels of *Prevotella*, *Faecalibacterium* and *Coprococcus* remained (*Fig. 1B*). In participant № 2 the loss of Fusobacteria was discovered already on the 14th day of the experiment (*Fig. 1D*) and fluctuations in the relative abundance of bacteria from the genus *Bacteroides* defining enterotype II were detected (*Fig. 1B*). During the first weeks, a slight increase in the proportion of *Faecalibacterium* (with a subsequent decline) and a decrease in the proportion of *Roseburia* with an increase in the minor species of *Alistripes* (*Rikkenellaceae*) and representatives of Lachnospiraceae was recorded. An insignificant decrease in the proportion of *Bacteroides* during the first weeks with an accompanying increase in the relative content of Prevotellaceae (*Fig. 1B*) and the proportion of γ-Proteobacteria, as well as *Megamonas* (Negativicutes) and unclassified groups of bacteria, were detected in the microbiota of participant № 3. The history of the changes in the composition of the majority of species and genera of the intestinal microbiota of participant № 4 showed no significant fluctuations (*Fig. 1*). However, an increase in the relative content of *Faecalibacterium prausnitzii* (*Fig. 1C*) during the first weeks of the experiment and *Roseburia* on the 210th day, as well as an increase in the proportion of Actinobacteria, was clearly identified (*Fig. 2*). No significant changes in the microbiota composition (except for Proteobacteria) in participant № 5 (*Fig. 1A*) were detected. However, a trend towards a decrease in the proportion of *Bacteroides* towards the completion of the stay in the module was identified (*Fig. 1B*).

The detailed comparative analysis of the microbiota profiles revealed certain patterns in the dynamics of the content of Actinobacteria and Negativicutes. The Actinobacteria content was minimal in the initial samples of the microbiota of all participants, which could potentially be attributed to the peculiarities of the methods of DNA extraction and/or use of primers, which were ineffective for obtaining fragments of bifidobacteria 16S rRNA. As can be seen from *Fig. 2*, the samples obtained at different stages of the experiment demonstrated an increased relative content of Actinobacteria, especially in the microbiota of participant № 4. This increase in the proportion of Actinobacteria can probably be attributed to the intake of probiotics, as it could stimulate the growth of bifidobacteria. It is possible, however, that this increase in the proportion of Actinobacteria was determined by their more active dissociation from the surface of the epithelium at the sites where colonization occurred. If the composition of Negativicutes at the genus level did not change significantly during the experiment for participants № 2, № 4 and № 5, the microbiota of participant № 3 revealed a consistent replacement of bacteria from the genus *Phascolarctobacter* with bacteria from the genus

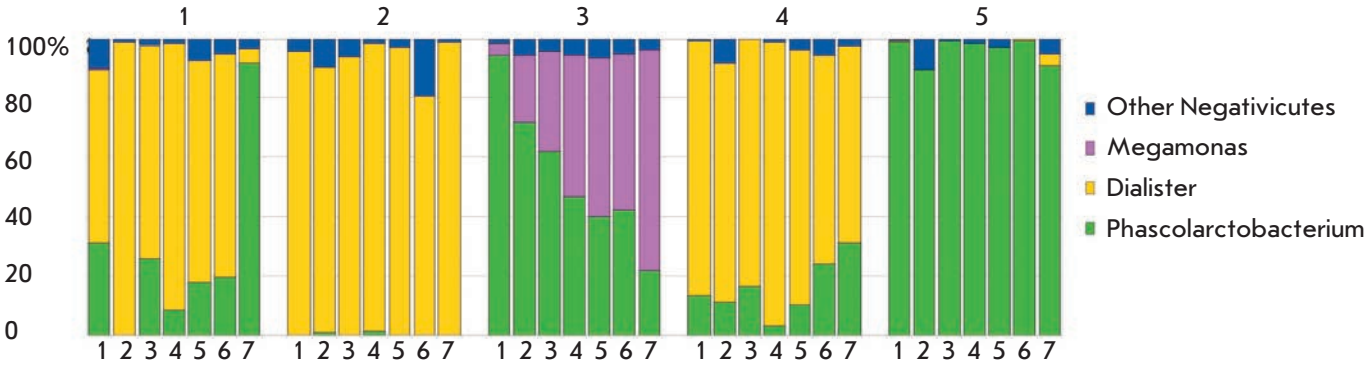

Fig. 3. Dynamic changes in the relative abundances of *Veillonellaceae* in the gut microbiome of participants of the MARS-500 experiment. Fraction of sequences assigned to a particular taxonomic group is shown in vertical axis (%), horizontal axis shows the sample codes (1 – 0 days, 2 – 14 days, 3 – 30 days, 4 – 210 days, 5 – 363 days, 6 – 510 days, and 7 - 524 days). Identification numbers of participants are shown above

Megamonas (*Fig. 3*) without restoration of the initial composition of Negativicutes 2 weeks after exiting the module.

The following trends could be noted during the analysis of the dynamics of the changes in the composition of the intestinal microbiota occurring in the course of the experiment. First, the impact of conditions/factors of the experiment was observed during the first weeks, although to varying degrees for different participants. It is believed that the rapid changes were caused by the initial psychological and emotional reaction to the unusual stressful conditions of containment in the isolated module. Second, there was a tendency toward partial recovery of the initial composition of the microbiota with respect to individual groups of taxa after the completion of the experiment. However, none of the participants demonstrated complete recovery of their initial composition 2 weeks after exiting the module. It is known that the use of antibiotics that cause drastic changes in the composition of the intestinal microbial community is followed by initiation of recovery in the initial composition after discontinuation of the medicinal product [14]. However, even partial recovery of the composition of the indigenous microbiota requires prolonged periods of time [47].

Determination of the gene composition of the microbiota of participant № 2

The results of the analysis of the taxonomic composition of the microbiome with respect to the sequences of 16S rRNA genes presented above did not provide direct information regarding the set of functional genes in the microbial metagenome. Therefore, we determined the gene composition of the samples of the microbiota of participant № 2. This participant demonstrated noticeable changes in the taxonomic composition of microorganisms in the course of the experiment.

During the analysis of the results of the sequencing of samples of metagenomic DNA according to the SOLiD technique (Table 2), one must consider the following: 1) the average length of the contigs for different points did not exceed 200 nucleotides; i.e., it was significantly smaller than the average size of a bacterial gene, and 2) the Bacteroidetes present in the microbiome were represented mainly by the *Bacteroides* genus (complete genomic sequences of many species from this genus had been determined). The bacteria of the phylum Firmicutes were phylogenetically more diverse. Therefore, the taxonomic identification of contigs belonging to Bacteroidetes was relatively more complete, whilst many contigs *de facto* belonging to Firmicutes could not be classified due to the lack of close homologues in the databases. This led to an underestimation of the proportion of Firmicutes in the metagenome compared to the results of the 16S rRNA analysis. Nevertheless, the dynamics of the changes in the ratio between Bacteroidetes and Firmicutes remained the same.

Quantitative representation of the genes of certain functional categories in the metagenome (according to KEGG classification, [34]) and their assignment to various taxonomic groups of bacteria were characterized. In general, significant changes in the microbiota of participant № 2 in the course of the experiment were absent with respect to the major functional categories of genes. Thus, the KEGG category "Carbohydrates metabolism," one of the most important for the functioning of the intestinal microbiota, at various stages of the experiment was represented by 16.7 to 18.6% of the

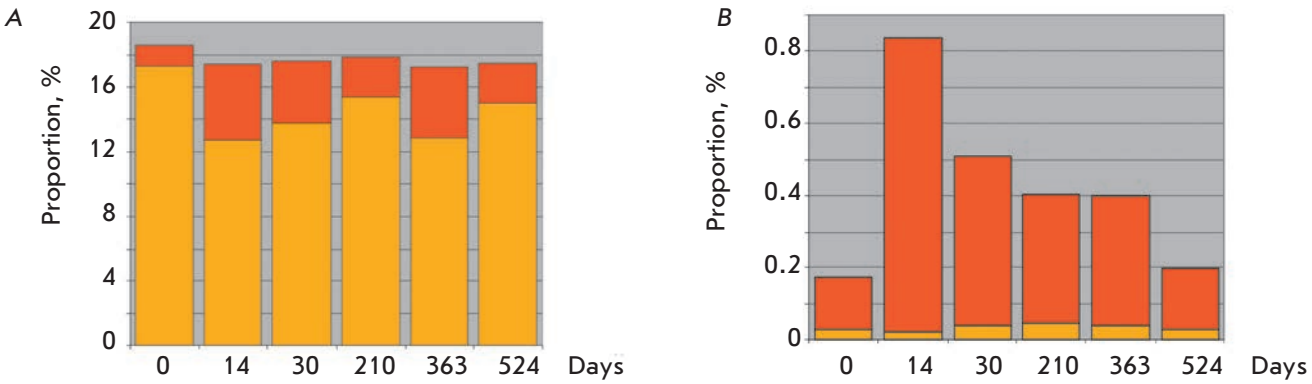

Fig. 4. Dynamic changes in the fractions of genes assigned to KEGG functional categories "Carbohydrates metabolism" (A) and "Cell motility" (B) in the gut microbiome of participant 2. Fraction of genes assigned to a particular category is shown in vertical axis (%), horizontal axis shows the sample codes (1 – 0 days, 2 – 14 days, 3 – 30 days, 4 – 210 days, 5 – 363 days, 6 – 510 days and 7 - 524 days). Fractions of genes taxonomically assigned to *Bacteroidetes* are shown in yellow, those assigned to *Firmicutes*, in orange

identified genes (*Fig. 4A*). However, the relative contribution of various taxa of Bacteroidetes and Firmicutes changed in a significantly wider range as evidenced by the results of the "taxonomic" classification of these genes and the data obtained on the basis of the taxonomic analysis with respect to 16S rRNA. We can assume that the process of restructuring of the taxonomic composition of the microbiome involved the replacement of genes in various representatives of Bacteroidetes and Firmicutes that determine the metabolism of carbohydrates, although the overall proportion of this functional category in the metagenome remained almost unaltered.

A different picture was obtained during the analysis of the dynamics of changes in the proportion of genes of the KEGG category "Cell motility" responsible for cellular motility (*Fig. 4B*). The majority of the genes in this category was assigned to Firmicutes and, accordingly, their proportion in the metagenome varied with changes in the relative content of Firmicutes and, perhaps, Proteobacteria in the community. These data are consistent with a small number of genes that determine cellular motility in the sequenced genomes of members of the genus *Bacteroides*. Cellular motility in Firmicutes and Proteobacteria is controlled by a large number of genes [48]. Flagella not only provide mobility but also perform sensory functions and are involved in intercellular communication in ecosystems [49]. Perhaps the "demand" for cellular motility determined the increase in the proportion of certain phylotypes of Firmicutes in the restructuring of the microbial community in the course of the experiment.

It can be assumed that during the "MARS-500" experiment, adaptive restructuring of the microbial community occurred in response to the stressful condition of prolonged isolation. Likewise, the formation of a new and balanced taxonomic composition of the microbiota occurred, providing maintenance of the normal functioning of the genetic and metabolic networks in the intestinal microbial community and in the system of interactions between the microbiota and the host organism. This adaptive transition to a new combination of taxa with preservation of the optimal gene composition in the entire community can be achieved through redundancy of the majority of categories of genes and functional interchangeability of bacterial phylotypes from different taxonomic groups. An exchange of genes by horizontal gene transfer [50], which is possible with the involvement of viruses, mobile elements and conjugative plasmids that are common in many microbes inhabiting the intestine, can be one of the mechanisms of such interchangeability.

CONCLUSIONS

The results of the metagenomic analysis of the intestinal microbiota of the participants of the "MARS-500" experiment simulating some of the conditions of long interplanetary flights suggest that containment in an isolated module is associated with the microbiota undergoing substantial changes in the composition of the microbial community. These changes were specific to each of the participants, which is attributable to the differences in the initial composition of the microbiota and the different nature of the responses to the influence of the experimental conditions depending on the genetic, physiological, and biochemical characteristics of each participant.

The factors affecting the taxonomic composition of the microbiota include the psychological stress attributed to the change in lifestyle, the switch to a different type of nutrition, and the use of probiotics. Monitoring of the dynamics of the changes in the microbiota demonstrated that (1) significant changes in the taxonomic composition began to appear during the initial stages of the experiment; (2) changes in the enterotypes in the individual taxonomic groups did not occur despite the large variability: i.e., the basic composition of the intestinal ecosystem remained unchanged; and (3) 2 weeks after exiting the module a tendency toward a return to the initial composition of the microbiota was observed; however, none of the participants demonstrated complete restoration of the initial composition of their microbial community. Perhaps, a two-week period of "rehabilitation" was simply insufficient for such recovery to occur.

As during the experiment, none of the participants demonstrated symptoms of diseases associated with considerable changes in the composition of the microbiota [6, 11, 12]: it can be assumed that restructuring of the taxonomic composition occurred in their intestinal ecosystems, reflecting their individual responses to the conditions of the experiment and a new balanced community was formed. This hypothesis is supported by the data on the analysis of the gene composition of the microbiota of participant № 2. The gene composition of the metagenome of the intestinal microbiota of this participant experienced little change throughout the experiment, which could be attributed to a compensatory substitution of certain species/strains with others able to perform functions related to ensuring "normal" interaction between the microbial community and the host organism.

Thus, it can be concluded that the powerful stressful condition of prolonged containment in an isolated module had no "dramatic" effect on the state of the intestinal microbiota and did not lead to significant negative consequences for the health of the participants of the experiment. Obviously, isolation during long space flights is just one of the stress factors that have the potential to affect astronauts. With proper selection and training of a crew, this factor could be rendered moot. Zero gravity, radiation, and certain specific working conditions in a spaceship may be more significant. These factors, which are difficult to reproduce during an experiment on Earth, can increase the likelihood of functional disorders in the gastrointestinal tract, the immune and other systems, potentially leading to the development of dysbiosis manifested as significant changes in the genetic and taxonomic composition of the intestinal microbiota. The data obtained during this experiment regarding the changes in the composition of the intestinal microbiota of the participants of the "MARS-500" experiment should be considered with respect to the possibilities of using methods of metagenomic analysis of the microbiota as one of the approaches to testing the state of health of the participants of real space flights and candidates for performing work under extreme conditions associated with powerful stressful factors. ●

This work was supported by the development program of the Federal State Educational Institution of Higher Professional Education "M.V. Lomonosov Moscow State University" until 2020.

REFERENCES

1. Huttenhower C., Gevers D., Knight R., Abubucker S., Badger J.H., Chinwalla A.T., Creasy H.H., Earl A.M., FitzGerald M.G., Fulton R.S. et al. // Nature. 2012. V. 486. P. 207–214.
2. Methe B.A., Nelson K.E., Pop M., Creasy H.H., Giglio M.G., Huttenhower C., Gevers D., Petrosino J.F., Abubucker S., Badger J.H. et al. // Nature. 2012. V. 486. P. 215–221.
3. Qin J., Li R., Raes J., Arumugam M., Burgdorf K.S., Manichanh C., Nielsen T., Pons N., Levenez F., Yamada T. et al. // Nature. 2010. V. 464. P. 59-65.
4. Kinross J.M., von Roon A.C., Holmes E., Darzi A., Nicholson J.K. // Curr. Gasrtoenterol. Rep. 2008. V. 464. P. 396–403.
5. Shestakov S.V. // Biology Bulletin Rev. 2011. V. 1, № 2. P. 83–93.
6. Blumberg R., Powrie F. // Science Translational Medicine. 2012. V. 4. № 137. 137rv7.
7. Claesson M.J., Cusack S., O'Sullivan O., Greene-Diniza R., de Weerd H., Flannery E., Marchesi J., Falush D., Dinanb T., Fitzgeral G.et al. // Proc. Natl. Acad. Sci. USA. 2011. V. 108 Suppl. 1. P. 4586–4591.
8. Turnbaugh P.J., Quince C., Faith J.J., Yatsunenko T., Niazi F., Affourtit J., Egholm M., Henrissat B., Knight R., Gordon J.I. et al. // Proc. Natl. Acad. Sci. USA. 2010. V. 107. P. 7503–7508.
9. Jalanka-Tuovinen J., Salonen A., Nikkila J. , Immonen Q., Kekkonen R., Lahti L., Palva A., de Vos W. // PLoS One. 2011. V. 6. e23035.
10. Tap J., Mondot S., Levenez F., Pelletier E., Caron C., Furet J-P., Ugarte E., Munoz-Tamayo R., Paslier D.L.E., Nalin R., Dore J., Leclerc M. // Environ. Microbiol. 2009. V.11 (10). P. 2574–2584.
11. Willing B.P., Dicksved J., Halvorson J., Andersson A.F., Lucio M., Zheng Z., Jarnerot G., Tysk C., Jansson J.K., Engstrand L. // Gastroenterology. 2010. V. 139. P. 1844–1854.
12. Frank D.N., St. Amand A.L., Feldman R.A., Boedeker E.C., Harpaz N., Pace N.R. // Proc. Natl. Acad. Sci. USA. 2007. V.104. P. 13780–13785.
13. Dethlefsen L., Huse S., Sogin M.L., Relman D.A. // PLoS Biol. 2008. V. 6. e280.
14. Dethlefsen L., Relman D.A. // Proc. Natl. Acad. Sci. USA.

2011. V. 108. P. 4554–4561.
15. Robinson C.J., Bohannan B.J.M., Young V.B. // Microbiol. Mol. Biol. Rev. 2010. V.74. № 3. P. 453–476.
16. Wu G.D., Chen J., Hoffmann C., Bittinger K., Chen Y.-Y., Keilbaugh S.A., Bewtra M., Knights D., Walters W.A., Knight R. et al. // Science. 2011. V. 334. P. 105–108.
17. Claesson M.J., Jeffery I.B., Conde S. Power S.E., O'Connor E.M., Cusack S., Harris H.M.B., Coakley M., Lakshminarayanan M., O'Sullivan O. et al. // Nature. 2012. V. 488. P. 178–184.
18. Lutgendorff F., Akkermans L.M.A., Soderholm J.D. // Curr. Mol. Med. 2008. V. 8. P. 282–298.
19. Phillips M.L. // Environmental Health Perspectives. 2009. V. 117. P. 199–205.
20. Sharkey K.A., Mawe G.M. // Nature Rev. Gastroenterology, Hepatology. 2012. V. 9. P. 74–76
21. Lebedev V.V. // Herald of the Russian Academy of Sciences. 2010. V. 80 (11). P. 1000–1004.
22. Grigoriev A.I, Egorov A.D. // Airspace biology and medicine. Man in a space flight. M. Science. 1997. V. 3, book 2. P. 368–447.
23. Lizko N.N. // Nahrung. 1987. V. 31. P. 443–447.
24. Lizko N.N. // Vestnik RAMS. 1996. V. 8, P.31–34
25. Ilyin V.K., Batov A.B., Novikova N.D., Mukhamedieva L.N., Poddubko S.V., Gegenava A.V., Mardanov R.G., Solovieva Z.O., Skedina M.A. // Aviakosmicheskaya i Ekologicheskaya Meditsina (Aerospace and Ecological Medicine). 2010. V. 44 (4). P. 52–57.
26. Ushakov I.B. // Abst. Intern. Symp. Results of the experiments simulating manned mission to Mars (MARS-500). Moscow. 2012. P. 64–65.
27. Morukov B.V., Belakovsky M.S., Demin E.P., Suvorov A.V. // Abst. Intern. Symp. Results of the experiments simulating manned mission to Mars (MARS-500). Moscow. 2012. P. 44.
28. Salonen A., Nikkila J., Jalanka-Tuovinen J., Immonen O., Rajilic-Stojanovic M., Kekkonen R.A., Palva A., de Vos W. // J. Microbiol. Methods. 2010. V. 81. P. 127–134
29. Cole R., Wang Q., Cardenas E., Fish J., Chai B., Farris R.J., Kulam-Syed-Mohideen A.S., McGarrell D.M., Marsh T., Garrity G. M., Tiedje J. M. // Nucleic Acids Research, 2009, V. 37, D141–D145
30. Simpson J.T., Wong K., Jackman S.D., Jones S.J.M., Birol I. // Genome Res. 2009. V. 19(6). P. 1117–1123.
31. Rho M., Tang H., Ye Y. // Nucleic Acid Res. 2010. V.38 (20): e191
32. Kent W.J. // Genome Res. 2002. V. 12. P. 656–664.
33. Benson D.A., Karsch-Mizrachi I., D.J.Lipman, J.Ostell, E.W.Sayers. // Nucleic Acid Research. 2011. V. 39. D. 32–37.
34. Kanehisa M., Araki M., Goto S., Hattori M., M. Hirakawa, Itoh M., Katayama T., Kawashima S., Okuda S., Tokimatsu T., Yamanishi Y. // Nucl. Acids Res. 2008. 36 Suppl. 1. D480–D484.
35. Overbeek R., Begley T., Butler R.M., Choudhuri J.V., Chuang H-Y., Cohoon M., de Crecy-Lagard V., Diaz N., Disz T., Edwards R. et al. // Nucl. Acids Res. 2005. V. 33 (17). P. 5691–5702.
36. Apweiler R. , Martin M.J., O'Donovan C., Magrane M., Alam-Faruque J., Antunes R., Barrell D., Bely B., Bimgley M., Binns D. // Nucl. Acids Res. 2011. V. 39. Database issue. D 214–219.
37. Langmead B., Trapnell C., Pop M., Salzberg S.L. Ultrafast // Genome Biol. 2009. V 10. N 3. R25
38. Eckburg P.B., Bik E.M., Bernstein C.N., Purdom E., Dethlefsen L., Sargent M., Gill S.R., Nelson K.E., Relman D.A. // Science. 2005. V. 308. P. 1635–1668.
39. Claesson M.J., O'Sullivan O., Wang Q., Nikkila J., Marchesi J.R., Smidt H., de Vos W.M., Ross R.P., O'Toole P.W. // PLoS One. 2009. V. 4. e6669.
40. O'Toole P.W., Claesson M.J. // Intern. Dairy J. 2010. V. 20. P. 281–291.
41. Arumugam M., Raes. J., Pelletier E., Le Paslier D., Yamada T., Mende D.R., Fernandes G.R., Tap J., Bruls T., Batto J.-M. et al. // Nature. 2011. V. 473. P. 174–180.
42. Huse S.M., Ye Y., Zhou V., Fodor A.A. // PLoS One. 2012. V. 7. e34242.
43. Jeffrey I.B., Claesson J., O'Toole P.W. // Narure Microbiol. Rev. 2012. V. 10. P. 591–592.
44. Frank D.N., Pace N.R. // Curr. Opin. Gastroenterol. 2008. V. 24. P. 4–10.
45. Ley R.E., Turnbaugh P.J., Klein S., Gordon J.I. // Nature. 2006. V. 444. P. 1022–1023.
46. Schwiertz A., Taras D., Schafer K., Beijer S., Bos N.A., Donus C., Hardt P.D. Obesity. 2009. V. 18. P. 190-195.
47. Jerenberg C., Lofmark S., Edlund C., Jansson J.K. // ISME J. 2007. V. 1 P. 55-61.
48. Bratlie M., Johansen J., Sherman B.T., Huang D.W., Lempicki R.A., Drablos F. // BMC Genomics. 2010. V. 11. P. 588
49. Anderson J.K., Smith T.G., Hoover T.R. // Trends Microbiol. 2010. V. 18. № 1. P. 30–37.
50. Smillie C.S., Smith M.B., Friedman J., Cordero O.X., David L.A., Alm E.J. // Nature. 2011. V. 480. P. 241–244.

Stabilization of the Central Part of Tropomyosin Molecule Alters the Ca^{2+}-sensitivity of Actin-Myosin Interaction

D.V. Shchepkin[1], A. M. Matyushenko[2], G. V. Kopylova[1], N. V. Artemova[2], S. Y. Bershitsky[1], A. K. Tsaturyan[3], D. I. Levitsky[2,4,*]

[1] Institute of Immunology and Physiology, Russian Academy of Sciences, Pervomayskaya Str., 106, Yekaterinburg, Russia, 620049

[2] Bach Institute of Biochemistry, Russian Academy of Sciences, Leninsky prosp., 33, Moscow, Russia, 119071

[3] Institute of Mechanics, Lomonosov Moscow State University, Michurinsky prosp., 1, Moscow, Russia, 119992

[4] Belozersky Institute of Physico-Chemical Biology, Lomonosov Moscow State University, Leninskie gory, 1, bld. 40, Moscow, Russia, 119991

*E-mail: levitsky@inbi.ras.ru

ABSTRACT **We show that the mutations D137L and G126R, which stabilize the central part of the tropomyosin (Tm) molecule, increase both the maximal sliding velocity of the regulated actin filaments in the *in vitro* motility assay at high Ca^{2+} concentrations and the Ca^{2+}-sensitivity of the actin-myosin interaction underlying this sliding. Based on an analysis of the recently published data on the structure of the actin–Tm–myosin complex, we suppose that the physiological effects of these mutations in Tm can be accounted for by their influence on the interactions between the central part of Tm and certain sites of the myosin head.**

KEYWORDS **actin-myosin interaction; *in vitro* motility assay; regulation of muscle contraction; tropomyosin.**

ABBREVIATIONS **Tm – tropomyosin.**

INTRODUCTION

Tropomyosin (Tm) is one of the key components of the regulatory apparatus of thin filaments in all types of muscles. According to the 'steric blocking' theory underlying the advanced concept of the regulatory mechanism of contraction of skeletal and cardiac muscles, Tm is capable of opening or closing the sites of actin interaction with myosin heads by shifting over the surface of an actin filament [1]. The Tm molecule is a dimer of α-helices forming a left-handed superhelix ('coiled-coil') [2]. Evidence has recently been obtained showing that the structure of the Tm molecule is not as simple as it has been considered so far. Extraordinary features specific only to Tm, such as the presence of sites with increased conformational mobility (flexibility), were observed. The conserved non-canonical residues Asp137 [3] and Gly126 [4], which disrupt the coiled-coil structure, were found in the central part of the Tm molecule. Replacement of these residues by canonical ones (mutations D137L, G126R and G126A) resulted in the stabilization of this part of the Tm molecule and completely prevented trypsin cleavage of Tm at the nearby Arg133 [3, 4]. Moreover, it was shown in both papers that the stabilizing mutations D137L and G126R (but not G126A) at high calcium concentrations (pCa ≤ 5) cause a significant increase in the actin-activated ATPase activity of myosin heads during their interaction with actin filaments containing Tm and troponin, although having no effect both on the Ca^{2+}-sensitivity of the myosin ATPase and on the Tm affinity for actin [3, 4]. In the present work, a thorough study of the effects of these mutations on the Tm regulatory properties was conducted. An *in vitro* motility assay, a highly sensitive method allowing one to monitor the sliding velocity of the reconstituted thin filaments over the surface covered with immobilized myosin, was used for this purpose for the first time.

EXPERIMENTAL

Recombinant skeletal muscle α-Tms with the mutations D137L and G126R were prepared as described previously [4] using Tm with the mutation C190A in which Cys190 was replaced by Ala as a 'wild type' protein [3]. The experiments and the measuring of the sliding velocities of the regulated thin filaments with the *in vitro* motility assay at different Ca^{2+} concentrations

were performed according to the described method [5]. A flow cell coated on the inside with nitrocellulose was filled with a solution of rabbit skeletal muscle myosin at a concentration of 0.5 μM (0.2 mg/ml); unattached myosin was subsequently washed out, and the regulated thin filaments were added into the cell. The filaments consisted of 10 nM F-actin labeled with rhodamine phalloidin, 0.1 μM troponin, and 0.1 μM Tm in a buffer containing 25 mM KCl, 25 mM imidazole, 2 mM ATP, 4 mM $MgCl_2$, 1 mM EGTA, 20 mM DTT, 3.5 mg/ml glucose, 20 μg/ml catalase, and 0.15 mg/ml glucose oxidase, pH 7.5 (these conditions are optimal for studying the sliding of the reconstituted thin filaments in an *in vitro* motility assay [6]). Free calcium concentrations were set by EGTA/CaEGTA in proportions calculated with the WebMaxC Standard program (http://www.stanford.edu/~cpatton/webmaxc/webmaxcS.htm). The experiments were conducted at 30°C; the sliding velocity of the filaments was measured using the GMimPro software [7].

RESULTS AND DISCUSSION

The results of the experiments indicate that the D137L and G126R mutations, which stabilize the central part of Tm, not only enhance the maximum sliding velocity of the regulated thin filaments in the *in vitro* motility assay at high Ca^{2+} concentrations (Fig. 1A), but also increase the Ca^{2+}-sensitivity of the velocity by shifting the calcium-velocity curve towards lower Ca^{2+} concentrations (Fig. 1B). The pCa_{50} value (i.e. the negative logarithm of the concentration of free Ca^{2+} at which the sliding velocity is half-maximal) was 6.06 ± 0.04 (here and onwards mean ± SEM) for the regulated thin filaments containing the 'reference' Tm with the C190A mutation. The value was equal to 6.36 ± 0.05 for the filaments containing Tm with the mutations D137L/C190A and 6.42 ± 0.03 for the filaments with the Tm mutant G126R/C190A. Thus, we have demonstrated for the first time that the mutations D137L and G126R stabilizing the central part of the Tm molecule significantly increase the Ca^{2+}-sensitivity of the actin-myosin interaction underlying the molecular mechanism of muscle contraction, which is regulated by changes in the Ca^{2+} concentration within muscle fiber. The data on the increase in the filament sliding velocity in the *in vitro* motility assay (Fig. 1A) correlate well with the increase in the myosin ATPase rate in the presence of regulated thin filaments with the mutations D137L and G126R in the central part of Tm at a saturating Ca^{2+} concentration [3, 4].

In order to interpret the results, we chose a new approach based on an analysis of recent data regarding the structure of the actin–Tm–myosin complex obtained using cryo-electron microscopy with a 8 Å resolution [8]. An important feature of this structure is the presence of direct contacts between Tm located on the surface of the actin filament and some areas of the myosin heads. Since this structure was obtained with a non-muscle myosin-I, our model (Fig. 2) was built by replacing the Tm-interacting domain in myosin-I with the corresponding domain of the skeletal muscle myosin-II used in our experiments. In this model, we

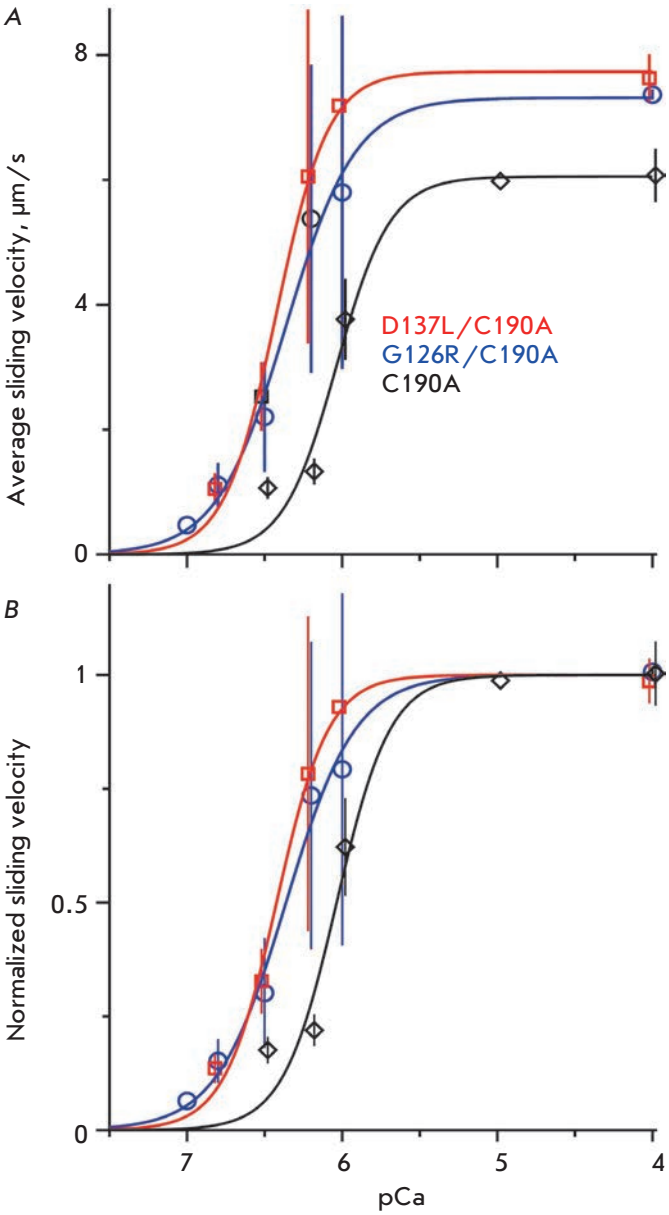

Fig. 1. The average sliding velocity of the thin filaments along the myosin-coated surface as a function of the Ca^{2+} concentration. *A*: average data for 2–3 experiments with each of the Tm mutants. Vertical lines show the standard deviations. *B*: the same data as in *A* normalized for the maximum velocity

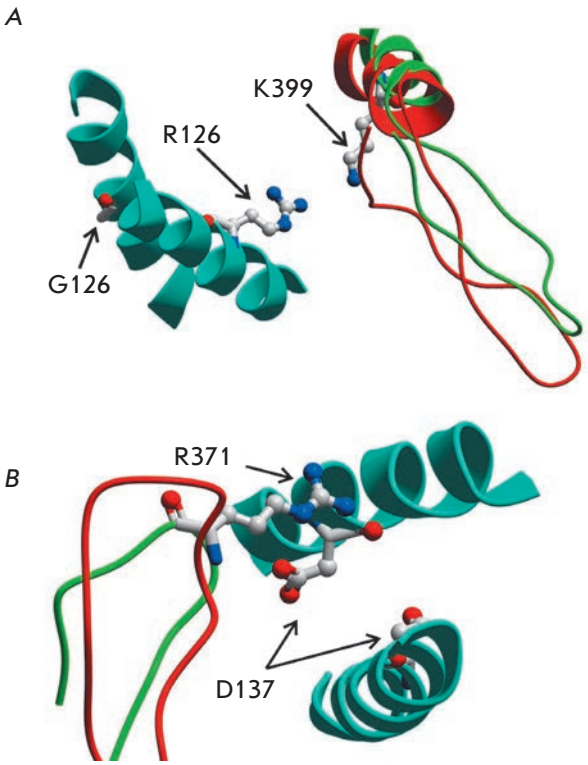

Fig. 2. The structural model of the contact area of a myosin head strongly bound to actin with Tm on the surface of the thin filament. Only some parts of the myosin head adjacent to the amino acid residues 126 (*A*) and 137 (*B*) in the central part of Tm are shown. Actin and other parts of myosin and Tm are not shown. The model was obtained from the structure of the actin–myosin–Tm complex ([8], pdb code 4A7H) by superimposing the upper 50-kDa domain of the myosin head of chicken fast skeletal muscle myosin II (pdb code 2MYS) instead of the same domain of myosin-I used in [8]. Segments of the Tm double α-helix are shown by blue ribbons, the parts of the myosin-I head used in [8] are shown in red, and those of the head of skeletal muscle myosin-II are green. The residue R126 of the Tm G126R mutant (*A*) and a 'non-canonical' Tm residue D137 (*B*), which was replaced with Leu in the Tm mutant D137L/C190A, as well as the charged myosin residues K399 (*A*) and R371 (*B*) located in close proximity to these Tm residues are shown in a 'ball-and-stick' atomic representation. The distance between the charged atoms of myosin residue K399 and Tm residue R126 (*A*) in the model was 8.8 Å, and that between myosin R371 and Tm D137 (*B*) was 4.7 Å. The model and the picture were prepared using ICM-Browser (MolSoft, CA, USA)

searched for the residues in the myosin head that are sufficiently close to the residues at the positions 126 and 137 in the central part of Tm in order to be able to interact with them. The results of the search are shown in Fig. 2. It turned out that a small Gly126 is incapable of any interaction with myosin. However, due to the G126R mutation, the side chain of Arg126 in Tm is in the vicinity of that of residue Lys399 in the myosin head, so that an electrostatic repulsion emerges between the positively charged atoms of these residues (Fig. 2A). Such interpretation is supported by the fact [3] that the replacement of Gly126 in Tm with a small hydrophobic Ala, not charged Arg, did not affect the ATPase activity of myosin in the presence of regulated actin filaments. On the other hand, the negative charge of Asp137 is close to the positive charge of Arg371 of the myosin head and electrostatically interacts with it (Fig. 2B). This interaction is violated by replacing the charged residue Asp137 with a neutral Leu residue in the D137L mutant.

Thus, the investigated mutations in the central part of the Tm molecule in both cases should lead to a decrease in the energy of interaction between Tm and the myosin head strongly bound to actin. The magnitude of the energy reduction is small compared to the energy of the strong myosin binding to actin [8] but is comparable to the energy required to move Tm over the surface of the actin filament. According to the steric blocking theory [1, 9], in the absence of Ca^{2+} troponin keeps Tm on the actin filament at a position in which it covers the myosin binding sites on actin. When the Ca^{2+} concentration increases, troponin detaches from actin and Tm moves aside, slightly opening the myosin binding areas. The myosin heads first attach to actin 'weakly' and not tightly, and then go into the 'strongly'-bound state and shift the Tm chain further away, thus opening the neighbor myosin binding sites on the adjacent actin monomers. According to our data, the explored mutations which stabilize the central part of Tm facilitate its displacement over the surface of the actin filament by strongly bound myosin heads and accordingly allow a greater number of neighboring myosin heads to bind actin and to produce mechanical work. This can probably explain the noticeable effect of such mutations in the Tm molecule on the sliding velocity of regulated thin filaments and the Ca^{2+}-sensitivity of their sliding in the *in vitro* motility assay. ●

This work was supported by the Russian Foundation for Basic Research (grants 12-04-00411, 11-04-00750, 11-04-00908, 12-04-31328, 13-04-40099, 13-04-40100, and 13-04-40101) and the Program "Molecular and Cell Biology" of the Russian Academy of Sciences

REFERENCES
1. McKillop D.F.A., Geeves M.A. // Biophys. J. 1993. V. 65. P. 693–701.
2. Nevzorov I.A., Levitsky D.I. // Biochemistry (Moscow). 2011. V. 76. № 13. P. 1507–1527.
3. Sumida J.P., Wu E., Lehrer S.S. // J. Biol. Chem. 2008. V. 283. P. 6728–6734.
4. Nevzorov I.A., Nikolaeva O.P, Kainov Y.A., Redwood C.S., Levitsky D.I. // J. Biol. Chem. 2011. V. 286. P. 15766–15772.
5. Shchepkin D.V., Kopylova G.V., Nikitina L.V., Katsnelson L.B., Bershitsky S.Y. // Biochem. Biophys. Res. Commun. 2010. V. 401. № 1. P. 159–163.
6. Homsher E., Kim B., Bobkova A., Tobacman L.S. // Biophys. J. 1996. V. 70. № 4. P. 1881–1892.
7. Mashanov G.I., Molloy J.E. // Biophys. J. 2007. V. 92. № 6. P. 2199–2211.
8. Behrmann E., Müller M., Penczek P.A., Mannherz H.G., Manstein D.J., Raunser S. // Cell. 2012. V. 150. № 2. P. 327–338.
9. Lehman W., Craig R. // Adv. Exp. Med. Biol. 2008. V. 644. P. 95–109.

GENERAL RULES

Acta Naturae publishes experimental articles and reviews, as well as articles on topical issues, short reviews, and reports on the subjects of basic and applied life sciences and biotechnology.

The journal is published by the Park Media publishing house in both Russian and English.

The journal *Acta Naturae* is on the list of the leading periodicals of the Higher Attestation Commission of the Russian Ministry of Education and Science

The editors of *Acta Naturae* ask of the authors that they follow certain guidelines listed below. Articles which fail to conform to these guidelines will be rejected without review. The editors will not consider articles whose results have already been published or are being considered by other publications.

The maximum length of a review, together with tables and references, cannot exceed 60,000 symbols (approximately 40 pages, A4 format, 1.5 spacing, Times New Roman font, size 12) and cannot contain more than 16 figures.

Experimental articles should not exceed 30,000 symbols (20 pages in A4 format, including tables and references). They should contain no more than ten figures. Lengthier articles can only be accepted with the preliminary consent of the editors.

A short report must include the study's rationale, experimental material, and conclusions. A short report should not exceed 12,000 symbols (8 pages in A4 format including no more than 12 references). It should contain no more than four figures.

The manuscript should be sent to the editors in electronic form: the text should be in Windows Microsoft Word 2003 format, and the figures should be in TIFF format with each image in a separate file. In a separate file there should be a translation in English of: the article's title, the names and initials of the authors, the full name of the scientific organization and its departmental affiliation, the abstract, the references, and figure captions.

MANUSCRIPT FORMATTING

The manuscript should be formatted in the following manner:

- Article title. Bold font. The title should not be too long or too short and must be informative. The title should not exceed 100 characters. It should reflect the major result, the essence, and uniqueness of the work, names and initials of the authors.
- The corresponding author, who will also be working with the proofs, should be marked with a footnote *.
- Full name of the scientific organization and its departmental affiliation. If there are two or more scientific organizations involved, they should be linked by digital superscripts with the authors' names. Abstract. The structure of the abstract should be very clear and must reflect the following: it should introduce the reader to the main issue and describe the experimental approach, the possibility of practical use, and the possibility of further research in the field. The average length of an abstract is 20 lines (1,500 characters).
- Keywords (3 – 6). These should include the field of research, methods, experimental subject, and the specifics of the work. List of abbreviations.
- INTRODUCTION
- EXPERIMENTAL PROCEDURES
- RESULTS AND DISCUSSION
- CONCLUSION

  The organizations that funded the work should be listed at the end of this section with grant numbers in parenthesis.
- REFERENCES

  The in-text references should be in brackets, such as [1].

RECOMMENDATIONS ON THE TYPING AND FORMATTING OF THE TEXT

- We recommend the use of Microsoft Word 2003 for Windows text editing software.
- The Times New Roman font should be used. Standard font size is 12.
- The space between the lines is 1.5.
- Using more than one whole space between words is not recommended.
- We do not accept articles with automatic referencing; automatic word hyphenation; or automatic prohibition of hyphenation, listing, automatic indentation, etc.
- We recommend that tables be created using Word software options (Table → Insert Table) or MS Excel. Tables that were created manually (using lots of spaces without boxes) cannot be accepted.
- Initials and last names should always be separated by a whole space; for example, A. A. Ivanov.
- Throughout the text, all dates should appear in the "day.month.year" format, for example 02.05.1991, 26.12.1874, etc.
- There should be no periods after the title of the article, the authors' names, headings and subheadings, figure captions, units (s – second, g – gram, min – minute, h – hour, d – day, deg – degree).
- Periods should be used after footnotes (including those in tables), table comments, abstracts, and abbreviations (mon. – months, y. – years, m. temp. – melting temperature); however, they should not be used in subscripted indexes (T_m – melting temperature; $T_{p.t}$ – temperature of phase transition). One exception is mln – million, which should be used without a period.
- Decimal numbers should always contain a period and not a comma (0.25 and not 0,25).
- The hyphen ("-") is surrounded by two whole spaces, while the "minus," "interval," or "chemical bond" symbols do not require a space.
- The only symbol used for multiplication is "×"; the "×" symbol can only be used if it has a number to its right. The "·" symbol is used for denoting complex compounds in chemical formulas and also noncovalent complexes (such as DNA·RNA, etc.).
- Formulas must use the letter of the Latin and Greek alphabets.

- Latin genera and species' names should be in italics, while the taxa of higher orders should be in regular font.
- Gene names (except for yeast genes) should be italicized, while names of proteins should be in regular font.
- Names of nucleotides (A, T, G, C, U), amino acids (Arg, Ile, Val, etc.), and phosphonucleotides (ATP, AMP, etc.) should be written with Latin letters in regular font.
- Numeration of bases in nucleic acids and amino acid residues should not be hyphenated (T34, Ala89).
- When choosing units of measurement, SI units are to be used.
- Molecular mass should be in Daltons (Da, KDa, MDa).
- The number of nucleotide pairs should be abbreviated (bp, kbp).
- The number of amino acids should be abbreviated to aa.
- Biochemical terms, such as the names of enzymes, should conform to IUPAC standards.
- The number of term and name abbreviations in the text should be kept to a minimum.
- Repeating the same data in the text, tables, and graphs is not allowed.

GUIDENESS FOR ILLUSTRATIONS

- Figures should be supplied in separate files. Only TIFF is accepted.
- Figures should have a resolution of no less than 300 dpi for color and half-tone images and no less than 500 dpi.
- Files should not have any additional layers.

REVIEW AND PREPARATION OF THE MANUSCRIPT FOR PRINT AND PUBLICATION

Articles are published on a first-come, first-served basis. The publication order is established by the date of acceptance of the article. The members of the editorial board have the right to recommend the expedited publishing of articles which are deemed to be a priority and have received good reviews.

Articles which have been received by the editorial board are assessed by the board members and then sent for external review, if needed. The choice of reviewers is up to the editorial board. The manuscript is sent on to reviewers who are experts in this field of research, and the editorial board makes its decisions based on the reviews of these experts. The article may be accepted as is, sent back for improvements, or rejected.

The editorial board can decide to reject an article if it does not conform to the guidelines set above.

A manuscript which has been sent back to the authors for improvements requested by the editors and/or reviewers is reviewed again, after which the editorial board makes another decision on whether the article can be accepted for publication. The published article has the submission and publication acceptance dates set at the beginning.

The return of an article to the authors for improvement does not mean that the article has been accepted for publication. After the revised text has been received, a decision is made by the editorial board. The author must return the improved text, together with the original text and responses to all comments. The date of acceptance is the day on which the final version of the article was received by the publisher.

A revised manuscript must be sent back to the publisher a week after the authors have received the comments; if not, the article is considered a resubmission.

E-mail is used at all the stages of communication between the author, editors, publishers, and reviewers, so it is of vital importance that the authors monitor the address that they list in the article and inform the publisher of any changes in due time.

After the layout for the relevant issue of the journal is ready, the publisher sends out PDF files to the authors for a final review.

Changes other than simple corrections in the text, figures, or tables are not allowed at the final review stage. If this is necessary, the issue is resolved by the editorial board.

FORMAT OF REFERENCES

The journal uses a numeric reference system, which means that references are denoted as numbers in the text (in brackets) which refer to the number in the reference list.

For books: the last name and initials of the author, full title of the book, location of publisher, publisher, year in which the work was published, and the volume or issue and the number of pages in the book.

For periodicals: the last name and initials of the author, title of the journal, year in which the work was published, volume, issue, first and last page of the article. Must specify the name of the first 10 authors. Ross M.T., Grafham D.V., Coffey A.J., Scherer S., McLay K., Muzny D., Platzer M., Howell G.R., Burrows C., Bird C.P., et al. // Nature. 2005. V. 434. № 7031. P. 325–337.

References to books which have Russian translations should be accompanied with references to the original material listing the required data.

References to doctoral thesis abstracts must include the last name and initials of the author, the title of the thesis, the location in which the work was performed, and the year of completion.

References to patents must include the last names and initials of the authors, the type of the patent document (the author's rights or patent), the patent number, the name of the country that issued the document, the international invention classification index, and the year of patent issue.

The list of references should be on a separate page. The tables should be on a separate page, and figure captions should also be on a separate page.

The following e-mail addresses can be used to contact the editorial staff: vera.knorre@gmail.com, actanaturae@gmail.com, tel.: (495) 727-38-60, (495) 930-87-07

INNOVATION RUSSIA

Discussion club

We form a dialogue between all the socially active groups of people: students, scientists, lecturers, businessmen, managers, innovators, investors, designers, art critics, architects, photographs.

Learn more at WWW.STRF.RU

Everyone who has something to say and some ideas to share is welcome to visit our events

Tel.: +7 (495) 930-87-07, 930-88-50
E-mail: seminar@strf.ru